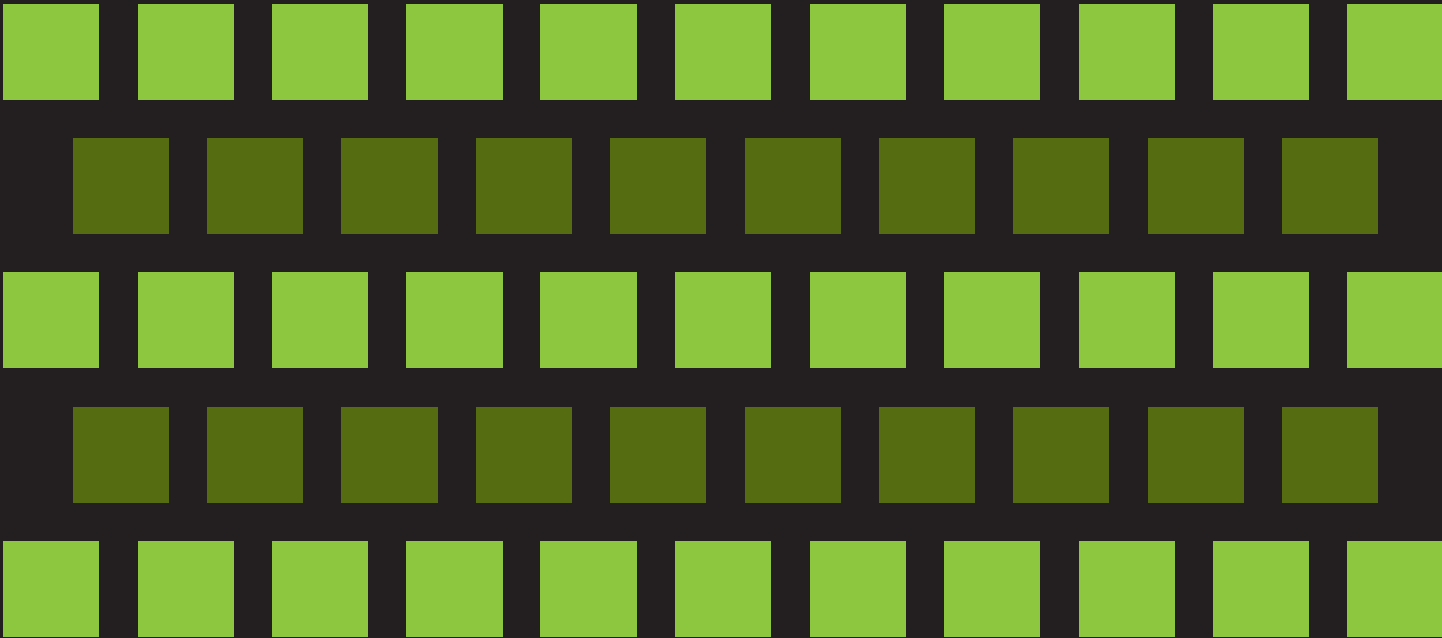


BRANCH LEG STUDY FOR BIOPROCESSING EQUIPMENT



STP-PT-065

BRANCH LEG STUDY FOR BIOPROCESSING EQUIPMENT

Contributing Authors and Editors:

Ethan Babcock, URI Mechanical Engineering Graduate
Mallory Corbin, Stevens Institute, Applied Chemistry Graduate
Randy Cotter, Sr., Cotter Brothers Corporation
Matthew Deane, URI Environmental Science Graduate Student
Bo Boye Busk Jensen, Ph.D., Alfa Laval
Dan Mathien, Behringer Corporation
Phil Paquette, P.E.
Marc Pelletier, CRB Engineering
Joe Serdakowski, AutoSoft Systems
James Dean Vogel, P.E. The BioProcess Institute
Deborah Botham, Cotter Brothers Corporation
Jay Ankers, M+W U.S., Inc.



Date of Issuance: December 19, 2013

This report was prepared as an account of work sponsored by ASME Pressure Technology Codes & Standards and the ASME Standards Technology, LLC (ASME ST-LLC).

Neither ASME, ASME ST-LLC, the author, nor others involved in the preparation or review of this report, nor any of their respective employees, members or persons acting on their behalf, makes any warranty, express or implied, or assumes any legal liability or responsibility for the accuracy, completeness or usefulness of any information, apparatus, product or process disclosed, or represents that its use would not infringe upon privately owned rights.

Reference herein to any specific commercial product, process or service by trade name, trademark, manufacturer or otherwise does not necessarily constitute or imply its endorsement, recommendation or favoring by ASME ST-LLC or others involved in the preparation or review of this report, or any agency thereof. The views and opinions of the authors, contributors and reviewers of the report expressed herein do not necessarily reflect those of ASME ST-LLC or others involved in the preparation or review of this report, or any agency thereof.

ASME ST-LLC does not take any position with respect to the validity of any patent rights asserted in connection with any items mentioned in this document, and does not undertake to insure anyone utilizing a publication against liability for infringement of any applicable Letters Patent, nor assumes any such liability. Users of a publication are expressly advised that determination of the validity of any such patent rights, and the risk of infringement of such rights, is entirely their own responsibility.

Participation by federal agency representative(s) or person(s) affiliated with industry is not to be interpreted as government or industry endorsement of this publication.

ASME is the registered trademark of the American Society of Mechanical Engineers.

No part of this document may be reproduced in any form,
in an electronic retrieval system or otherwise,
without the prior written permission of the publisher.

ASME Standards Technology, LLC
Two Park Avenue, New York, NY 10016-5990

ISBN No. 978-0-7918-6916-1

Copyright © 2013 by
ASME Standards Technology, LLC
All Rights Reserved

TABLE OF CONTENTS

Foreword.....	v
Acknowledgments.....	vi
1 PURPOSE AND USE	1
2 INTRODUCTION.....	3
2.1 Dead Leg.....	3
2.2 Standard and Short Outlet Tee.....	4
3 LITERATURE REVIEW	5
4 EXPERIMENT.....	6
4.1 System Description.....	6
4.2 Testing Procedure.....	8
4.3 Experimental Technique.....	8
4.3.1 Flow Rate Increase (FRI) Test.....	8
4.3.2 Flow Rate Maintain (FRM) Test.....	8
4.3.3 Pressure Increase (PI) Test.....	8
4.3.4 Pressure Maintain (PM) Test.....	9
4.4 Explanation of Rotation/Slope.....	9
4.5 Data Collected.....	9
4.6 Evaluation Method.....	9
5 THE FITTING TEST SPECIMEN	12
5.1 Variables Evaluated.....	14
5.1.1 Pipe Style.....	14
5.1.2 Flow Direction.....	16
5.1.3 Pipe Slope.....	16
5.1.4 Branch Rotation.....	16
5.1.5 Back Pressure.....	17
5.1.6 Temperature.....	17
6 RESULTS AND DISCUSSION.....	18
6.1 Variables Evaluated.....	18
6.2 Impact of L/D Ratio on Flow Rate Required to Achieve Air Removal State.....	18
6.2.1 Impact of Rotation Angle on Flow Rate Required to Achieve Air Removal State....	18
6.2.2 Parameters for Predicting Air Removal States.....	18
6.2.3 Influence Flow Startup.....	19
6.2.4 Horizontal T-pieces Straight Through (L/D = 2).....	19
6.2.5 Vertical T-pieces Straight Through (L/D = 2).....	20
6.2.6 Horizontal T-pieces Straight Through (Short Outlet Tee).....	20
6.2.7 Elbow on the Wall.....	20
6.2.8 Influence of Temperature.....	22
6.2.9 Influence of Back Pressure.....	22
7 CONCLUSIONS & RECOMMENDATIONS	23
7.1 Considerations When Evaluating Existing Designs.....	23
References.....	25
Appendices	
Appendix A: Test Schematic	
Appendix B: Properties for PP-R Pipe	
Appendix C: Measure data for PP-R Pipes used in Experiments	
Appendix D: Flow Rate, Velocity and Reynolds Numbers	

Appendix E: Overview of Combinations of Configurations, Slopes and Rotations Tested for Straight Through Flow and Elbow Flow
Appendix F: Test Results
Appendix G: Representative Test Graphs
Appendix H: Literature

LIST OF FIGURES

Figure 1-1: Cotter’s Test Fixture Used in the Pre-Study 2
Figure 2-1: Principle Sketch of Branches 3
Figure 4-1: Test Schematic for Horizontal Runs 7
Figure 4-2: Example Images of a Visual Air Grade 10
Figure 4-3: Example Image of Air Grade 1 10
Figure 4-4: Evaluation Scheme for Including Time for Clearing Air into the Evaluation of Data-Developed During the Project 11
Figure 5-1: Justification of the Designation Given to the Polypropylene (PP-R) and PVC Piping 12
Figure 5-2: Principle Sketches of Manufactured Test Pieces 13
Figure 5-3: T- designation, the True L/D and for Reference the L/D Achieved by the Dimension of ASME BPE Tees 14
Figure 5-4: BPE Hygienic Clamp Joint: Short Outlet Tee (BPE 2012 Table DT-4.1.2-5) and Straight Tee (Table DT-4.1.2-4 BPE 2012) 14
Figure 5-5: PP-2 Inch Straight Geometry L/D = Short (left) and L/D = 2 (right) 15
Figure 5-6: PP-2 Inch Elbow Geometry L/D = 2 (left) and L/D = Short (right)..... 15
Figure 5-7: Branch Rotation Designation 17
Figure 6-1: Data for Upward Pointing Branch (0°) on a Horizontal Line at Ambient Temperature Plotted with Reynolds Number, Velocity and Flow Rate 19
Figure 6-2: Velocity Required to Reach Certain State..... 20
Figure 6-3: Results from the Elbows Configurations Test for L/D =2 21
Figure 6-4: Results from the Elbow Configurations Test for SO tee..... 22

FOREWORD

Industry standards for dead legs in biopharmaceutical processing equipment have been in place for over a decade. A dead leg is defined as an area of entrapment in a vessel or piping run that could lead to contamination of the product (ASME BPE 2012 GR-8). While an L/D (ratio of length leg over diameter of leg) of six may have been the historical maximum acceptable ratio, multiple studies promote designing to an L/D less than two. The drivers for reducing the L/D ratio are cleanability and the fact that today's technology renders the L/D target of two or less achievable.

The prevailing opinion was that optimum cleaning of process piping was achieved with a tangential turbulent flow rate of 5 feet/sec, and that solution passing through a pipe at this velocity would be sufficient to clean-un-place the piping with branches having an L/D less than two.

The purpose of this document is to provide information on the flow conditions required to displace air from piping branches in a timely manner. When air is displaced from the branched fitting, the cleaning solution comes in contact with the branched piping components being cleaned-in-place (CIP'ed) and effective cleaning can occur. Without contact of CIP solutions, there is no cleaning. This document is a study on the flow conditions required to ensure contact of the cleaning solution with the branched fittings – a key requirement for cleaning.

Established in 1880, the American Society of Mechanical Engineers (ASME) is a professional not-for-profit organization with more than 135000 members and volunteers promoting the art, science and practice of mechanical and multidisciplinary engineering and allied sciences. ASME develops codes and standards that enhance public safety, and provides lifelong learning and technical exchange opportunities benefiting the engineering and technology community. Visit www.asme.org for more information.

The ASME Standards Technology, LLC (ASME ST-LLC) is a not-for-profit Limited Liability Company, with ASME as the sole member, formed in 2004 to carry out work related to new and developing technology. The ASME ST-LLC mission includes meeting the needs of industry and government by providing new standards-related products and services, which advance the application of emerging and newly commercialized science and technology and providing the research and technology development needed to establish and maintain the technical relevance of codes and standards. Visit www.stllc.asme.org for more information.

ACKNOWLEDGMENTS

ASME greatly appreciates the many contributors from the ASME BioProcess Equipment Standards Committee who participated in this study. They are named below, along with their role in this study. Special thanks go to Randy Cotter Sr. and Cotter Brothers Corporation, for their efforts in preparing the final report.

- Ethan Babcock, URI Mechanical Engineering Graduate – *Experiments*
- Mallory Corbin, Stevens Institute, Applied Chemistry Graduate – *Data Analysis*
- Randy Cotter, Sr., Cotter Brothers Corporation - *Contributor*
- Matthew Deane, URI Environmental Science Graduate Student – *Experiments*
- Bo Boye Busk Jensen, Ph.D., Alfa Laval - *Contributor*
- Dan Mathien, Behringer Corporation - *Contributor*
- Phil Paquette, P.E. - *Design Review*
- Marc Pelletier, CRB Engineering - *Contributor*
- Joe Serdakowski, AutoSoft Systems - *Data Analysis*
- James Dean Vogel, P.E. The BioProcess Institute - *Project Director*
- Deborah Botham, Cotter Brothers Corporation – *Contributing Editor*
- Jay Ankers, M+W U.S., Inc. – *ASME BPE Committee Chair*

Additionally, the following companies provided goods and services to support this study:

- Polypropylene Test Pieces - Arkema (through George Fisher)
- Hoses - AdvantaPure
- Valves - ITT, Gemu, Crane/Saunders, PBM
- Instruments - Anderson
- Fittings - VNE
- Seals - Parker
- Hangers - Behringer
- Pump - Fristam
- Spool Pieces - Cotter Brothers

1 PURPOSE AND USE

Industry standards for dead legs in biopharmaceutical processing equipment have been in place for over a decade. A dead leg is defined as an area of entrapment in a vessel or piping run that could lead to contamination of the product (ASME BPE 2012 GR-8). While an L/D (ratio of length leg over diameter of leg) of six may have been the historical maximum acceptable ratio, multiple studies promote designing to an L/D of less than two. The drivers for reducing the L/D ratio to less than two, are cleanability and the fact that today's technology renders the L/D target of two or less achievable.

The prevailing opinion was that optimum cleaning of process piping was achieved with a tangential turbulent flow rate of 5 feet/sec, and that solution passing through a pipe at this velocity would be sufficient to clean-in-place the piping with branches having an L/D of less than two.

The purpose of this document is to provide information on the flow conditions required to displace air from piping branches in a timely manner. When air is displaced from the branched fitting, the cleaning solution comes in contact with the branched piping components being cleaned-in-place (CIP'ed) and effective cleaning can occur. Without contact of CIP solutions, there is no cleaning. Note: The actual cleaning of process piping is more complicated than simply supplying an adequate flow rate (it involves many other factors such as the reagent concentration, temperature, contact time, etc.) and cleaning processes are outside of the scope of this document. The focus of this document is on the flow conditions required to ensure contact of the cleaning solution with the branched fittings – a key requirement for cleaning.

The desire to minimize the L/D of branches in piping systems to facilitate cleaning is intuitive. The original $L/D \leq 6$ specification was driven mostly by technology limitations in the pre-1997 (1st edition of the ASME BPE) era. As fabrication methods improved making smaller L/D ratios achievable, the $L/D \leq 2$ became the standard. This requirement for L/D of < 2 created new challenges in equipment, components, and process piping design; however Mr. Randy Cotter Sr. questioned whether the L/D of ≤ 2 target was valid. Until now, there was no scientific basis for the new standard.

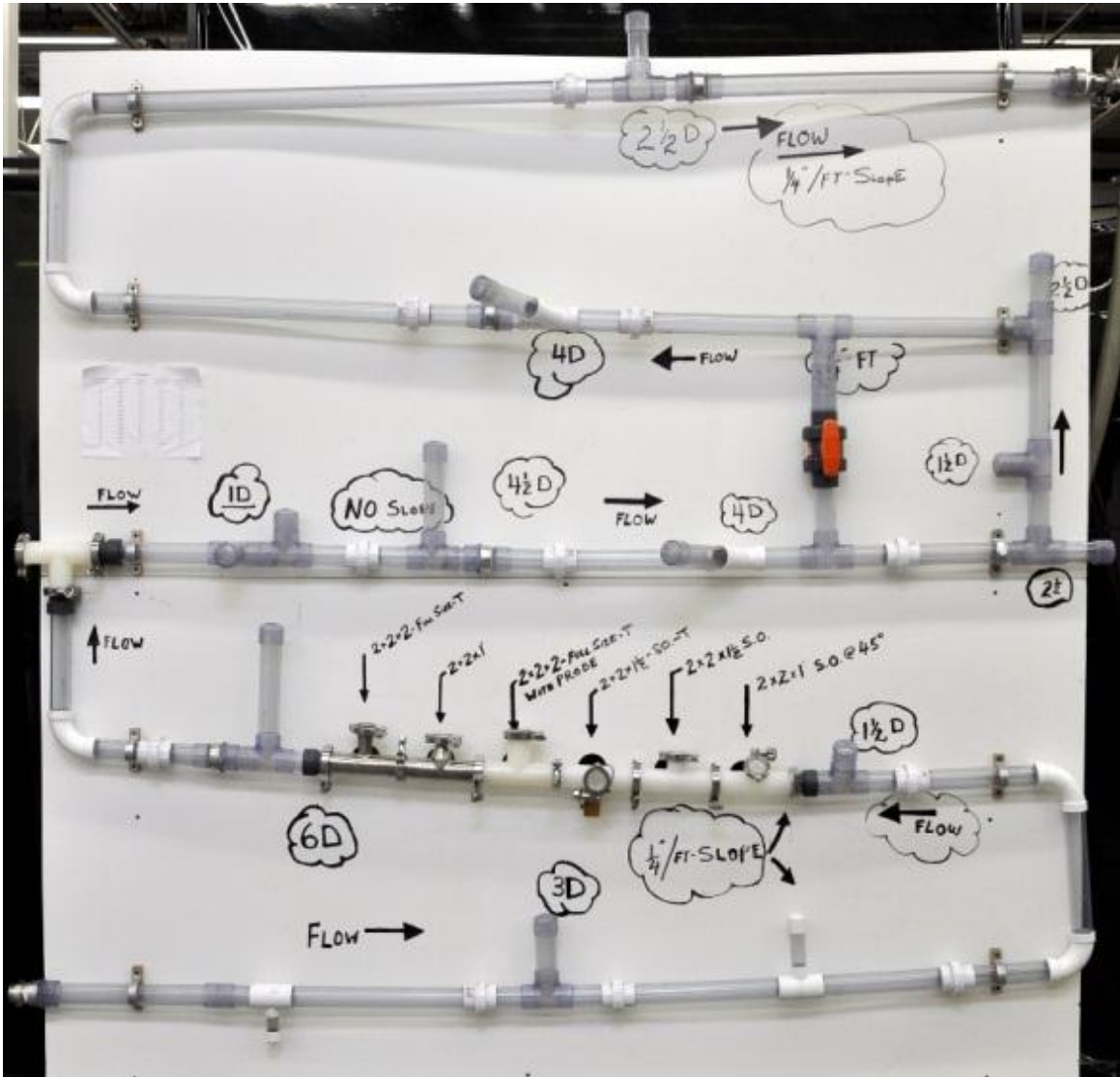
In 2010, Cotter fabricated a serpentine test fixture from 1½ inch Sch. 40 clear PVC tubing with a 1.610 inch ID (see next page for Figure 4-1) to model a typical biopharmaceutical piping system and typical CIP conditions. The test fixture incorporated various branch connections with different L/D ratios (L/D = 1, 2, 3, 4, and 6), oriented 90° vertical upward, 45° upward, and 90° vertical downward. Testing was performed with water at ambient temperature with flow rates ranging from 10 to 80 gpm, and back pressure ranging from 5 to 80 psig.

Initial test results indicated that for both the 45° and 90° vertical upward tee installations, regardless of flow or pressure, entrapped air could not be fully expelled from the branches. Further testing performed using red dye indicated that the turbulence created by the tangential flow of water across a downward oriented branch (L/D ratio of > 4) was insufficient to evacuate the red solution in a timely manner. The tests were performed at a variety of flow rates.

Cotter also had a series of discussions with collaborators who had developed CFD models. The CRD models had not included the presence of air in their evaluation.

Cotter Brothers Corporation presented their data complete with videos of the tests to the ASME BPE Committee. The Committee decided that further research was required. The ASME BPE commissioned a study that was executed in 2011-2012. This report provides the data from the study and includes conclusions and recommendations.

Figure 1-1: Cotter's Test Fixture Used in the Pre-Study



2 INTRODUCTION

BioProcess equipment is primarily used for the manufacture of products which are either generated by a biological process or contain biochemicals, e.g. biopharmaceuticals. Bioprocess equipment and systems typically house aqueous-based processes that are prone to bioburden. These systems are designed to be cleaned, sanitized and or sterilized to mitigate the risk of contamination from the environment and/or from carryover/crossover contamination as a result of inadequate removal of soils post-processing. The ASME BPE Standard provides requirements for systems and components that are subjected to cleaning and sanitization and/or sterilization. This includes systems that are cleaned in place (CIP) and/or steamed in place (SIP) and/or other suitable processes.

Effective removal of air during CIP and SIP operations is critical for effective cleaning and sanitization. Removal of air is difficult requiring:

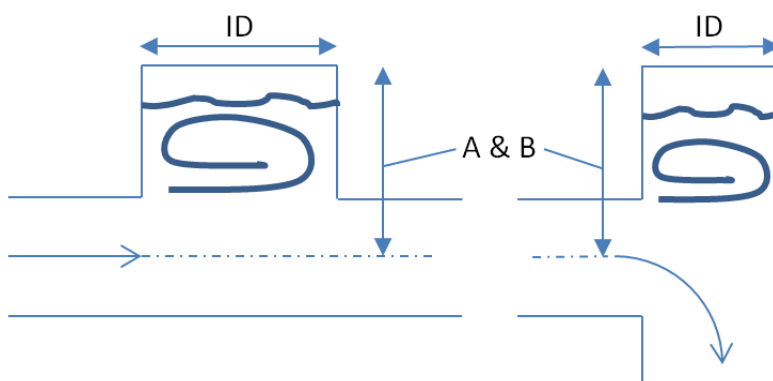
- Detailed piping design to many of the ASME BPE Standards requirements
- Effective process conditions (i.e. flow rates, pressures, temperatures)
- Proper sequence of operations (e.g. valve sequencing, venting, draining)

2.1 Dead Leg

Branch tee connections that are capped and/or closed off are routinely referred to as dead legs. The ASME BPE Standard defines a dead leg as “an area of entrapment in a vessel or piping run that could lead to contamination of product.”

Dead legs are no-flow or limited-flow process fluid regions usually formed at process tubing branch connections (typically at 90° to tangential flow). Typical examples include instruments or components that are attached using tee style fittings such as to provide an insertion location into the process flow path. Examples are analytical probes, rupture disks, diaphragm pressure gauges, thermowells, etc. The geometry of some of these branches may be slightly different than a flat-capped end due to the shape of the component or configuration. Tee fitting sizes most widely used in biotechnology processes and clean-in-place piping systems are ½, ¾, 1, 1 ½, and 2 inch. Both straight-through and right-angle tee configurations are used in piping systems. Both are examined in this study.

Figure 2-1: Principle Sketch of Branches



**Left side: An upward pointing branch on a horizontal line.
Right side: An upward pointing branch in an elbow.**

A branch is defined in the 2012 ASME BPE Standard (Tables SD-1, SD-2) as the process length, L, measured from the inside diameter of the main run line to the closure device on the branch (a flat cap or a valve weir). The ratio of this L dimension to the inside diameter, ID, of the branch is referred to as the L/D. The ASME BPE Standard recommends a target L/D ratio not exceed 2:1. It should be noted that early industry practice was to measure the L dimension from the centerline of the main flow line, not the inside diameter. Some countries still use this centerline dimension when discussing dead legs; it is therefore important to define term when presenting and comparing testing information.

The “L” dimension is not readily obtainable from vendor literature as they have long provided fitting dimensions from the centerline to the edge. (Vendors and the BPE Standard refer to this centerline dimension with the letter designation A or B.) Both piping designers and detailers need these centerline dimensions to accurately develop design drawings and models.

The ASME BPE Standard has established a “benchmark” set of these centerline-based dimensions (see Part DT) for stainless steel tube and fittings to permit designers and detailers to have uniform dimensions available regardless of individual manufacturers. The “L” is a process dimension, calculated as:

$$L = (A \& B) - \frac{1}{2} ID$$

2.2 Standard and Short Outlet Tee

The introduction of short outlet (SO) tee fittings where the A and B dimensions are significantly reduced (thus reducing the process dimension L), has greatly enhanced the ability of piping designers and detailers to achieve the target L/D of < 2:1. Not all short outlet branched fittings yield an L/D ratio less than the recommended two value when used as is. The addition of a standard valve versus a cap would increase the L and resultant L/D ratio. This study will examine both the L/D ratio obtained from using a standard short outlet tee fitting and a fixed L/D ratio equal to two. (See Figure 5-3 in Section 5).

3 LITERATURE REVIEW

Most of the prior articles covered the mixing within dead legs, with a focus on achieving effective cleaning in the branch leg. No reference was found which focused on the removal of air, and only a few references even mentioned it.

Gaerke's study [3] on the flow rate required to displace the air/flood sections of straight piping (without branched fittings) of different diameters of transparent schedule 40/80 PVC piping fabricated with socket joints in a variety of installation configurations (horizontal, sloped, and vertical) with different outlet configurations (open on the end and liquid sealed) indicated the following:

- The piping configuration that required the highest flow rate to displace the air was a vertical pipe with the flow directed downward that was open on the end.
- The addition of backpressure had no impact on the flow rate required to displace the air from the piping systems evaluated.

Although it was not the primary focus of the study, Gaerke looked briefly at transparent PVC branched tees fabricated with socket joints and determined that liquid velocities as high as 7 feet/sec were insufficient to displace air from a 2 inch branched tee directed upward to an L/D ratio of 2.

Young's study [4] discusses air removal in the effective SIP of a system. Air is heavier than steam at routine SIP conditions. The primary issue is to displace the air with the steam. They concluded:

- L/D values do not provide a general guideline which can be used to predict sterilization. Tubes with similar L/Ds, but different diameters, showed sterilization times varying up to 250%
- SIP of dead legs with saturated steam is dependent on tube diameter, length and orientation with respect to the gravitational vector
- Saturated steam sterilization did not occur at any location above the initial steam-air interface

Young stresses that the proper sizing of the tube diameter had the greatest effect on sterilization as it increased the ratio of buoyant forces to viscous dissipation forces. They effectively showed how a small tube of 40mm ID and 88mm long, L/D of 22, exhibited little buoyant driven convective flows, and the minimal air displacement observed was due primarily to diffusion.

These buoyant forces are in reverse in CIP where the process liquid is heavier than the air. Even with proper tube diameter the air requires more than gravity to remove it from a branch sloped above the horizontal centerline.

Grasshoff [5][6] verified that flows into the dead leg, rather than away from the dead leg, provided better mixing in the dead leg, but their work did not mention the removal of air.

They showed that if the L/D is large enough, a secondary recirculation zone is formed at the end of the dead leg reducing exchange of mass (liquid or air) from the dead leg to the main pipe. They also showed that the net velocities in the primary recirculation zone were as low as one-eighth of the bulk velocity. These results were confirmed in Jensen's Computational Fluid Dynamic (CFD) and experimentation. Seven Helium (He) experimented with a flow diverter to improve cleaning.

Sassanami [8] noted that the soil removal rate would be much lower in the dead space area than the pipe because the fluid mechanics involved in this area are significantly different, reducing the ability to clean this area. This study showed that for a dead space with an L/D value of 1, there was a significant advantage to operating at Reynolds numbers above 70,000 since this caused a significant increase in cleaning. For dead zones with an L/D of 4, the cleaning rate becomes independent of the Reynolds number.

4 EXPERIMENT

Experiments for estimating the removal of air were conducted using a translucent test spool system by recirculating liquid in the system. Removal of air was recorded on video to estimate the time for removal with various configurations. A series of experiments were conducted over a wide range of flow rates, different geometrical configurations, two different temperatures, and different back pressures. A grade system was developed for quantification of air removal. The following sections provide detail on the experimental set-up and data analysis, ending with the configurations investigated.

4.1 System Description

The system (Figure 4-1) consisted of a manually operated liquid reservoir tank, pump, recirculation piping, instrumentation, and hand valves. The system was reconfigured as needed to allow for different arrangements. Most of the system piping was comprised of two inch stainless steel and silicone hose. Experiments for estimating the removal of air were done in translucent natural polypropylene (PP-R) test spool pieces while recirculating liquid in the system. The major system components are:

- Centrifugal Pump, maximum 155 gpm, (flow energy)
- Turbine Flow Meters, two, ranges 1.75-150 gpm, (flow rate)
- Digital Temperature Gauge, 0-100 °C, (fluid temperature)
- Analog Pressure Gauges, two, 0-100 psig, (inlet/outlet pressure)
- Digital Pressure Gauge, 0-100 psig, (outlet pressure)
- 2 inch Diaphragm Valves, three, (feed control, bypass control, backpressure control)
- 2 inch Ball Valves, three, (feed on/off, bypass on/off, feed outlet on/off)
- ½ inch Ball Valves, two (air bleed valve, pump drain valve)
- 1 inch Ball Valve (spool drain valve)
- 250 gallon Tank, natural polypropylene (system sump)
- 500 liter Tank , stainless steel (system sump)
- Heat Exchanger (heat energy)
- Pipe Fittings, stainless steel and polypropylene
- Piping, stainless steel, mostly 2 inch
- Hoses, 2 inch, stainless steel end crimped silicone

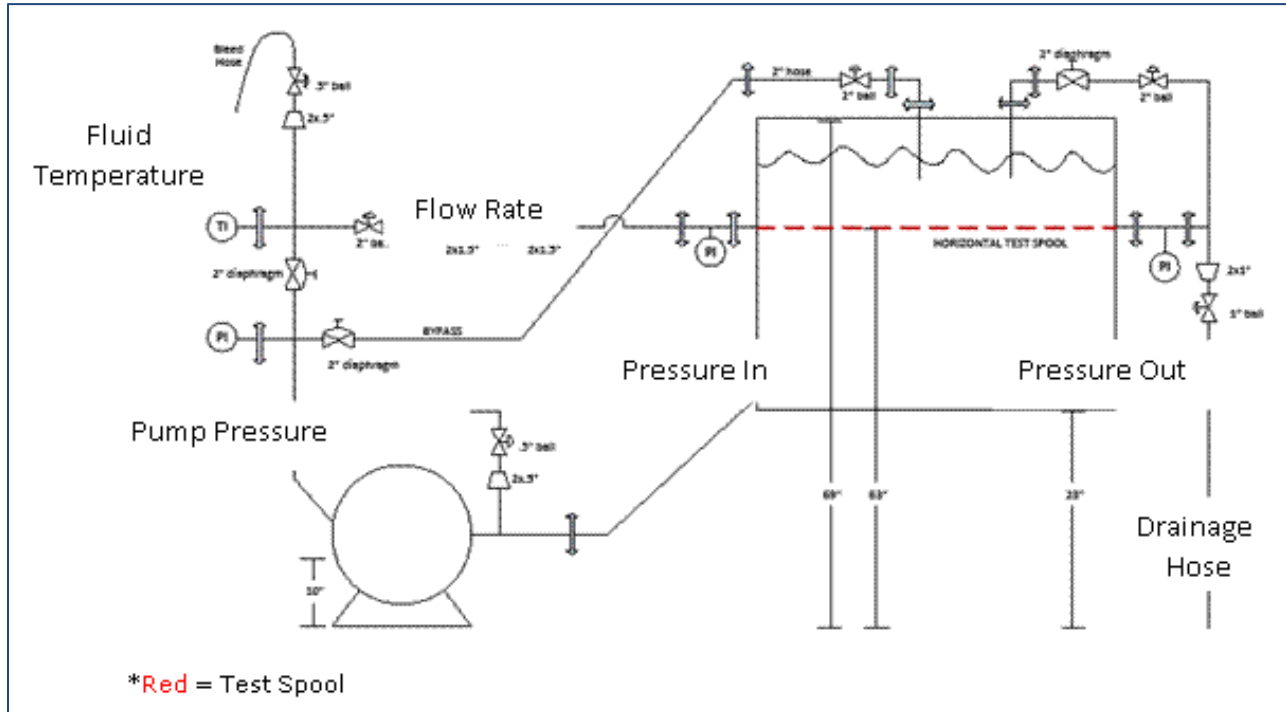
The central system consists of a 250 gallon feed tank that serves as the liquid reservoir, in which gravity feeds the centrifugal pump. The pump drives the water at the desired flow rate and is adjusted by varying the opening of the diaphragm valve at the beginning of the feed line. Opening this valve allows a higher flow rate through the line, while closing it decreases the flow rate through the line. The bypass diaphragm valve allows the operator to divert some amount of flow from the main line so as to more easily find the correct flow rate through the main line.

The water next moves in ascending order through:

- the pump pressure gauge
- the fluid temperature gauge
- the flow meter
- the inlet pressure gauge
- the test spool
- outgoing pressure gauge

It is then directed back into the tank, using flexible hosing, to be recirculated.

Figure 4-1: Test Schematic for Horizontal Runs



Note: The rest spool is the milk white section in the top part of the picture. Schematic for the other configurations can be seen in Appendix A.



The remaining valves are used to prepare the system for tests, e.g. drain the system. An air bleed ball valve, which can be opened to allow air into the system and out of the test spool, is located above the feed control diaphragm valve. A back pressure diaphragm valve is located on the return line just before the

water re-enters the feed tank. Closing this valve will increase the pressure on the line to test effects of increasing back pressure on the test spools. A heat exchanger is added to the return line and the tank is changed to the smaller stainless steel tank during runs which require heating.

4.2 Testing Procedure

1. Start up the pump in order to run water through the pipeline.
2. Adjust the flow rate using the diaphragm valve until the desired BPI Visual Air Grade is reached. A low flow rate is suggested to begin, so that immediate flooding of the branch leg does not occur.
3. Once the desired visual air grade is reached
 - (a) Photograph the result.
 - (b) Record the flow rate, pump pressure, water temperature, incoming pressure, outgoing pressure, and visual air grade.
 - (c) Close the test spool using the two ball valves on either side.
 - (d) Photograph the still spool.
 - (e) Remove the cap from the branch leg, and pour water into it from a graduated cylinder.
 - (f) Record the volume of water needed to fill the branch leg, as that is the volume of air that was left in the branch leg.
4. Drain and repeat two subsequent times for this amount of air, and then repeat the procedure for each individual visual air grade (from 0-5 – see Section 5.6).

This experiment will also be repeated for a test spool with its branch leg rotated from the vertical position to an angle of 45°, (from 1-4). This, however, does require one to rotate the test spool back into the vertical position once the photos have been taken. This allows the experimenter to safely measure the amount of air using the above method with a graduated cylinder without losing water and contaminating the results.

4.3 Experimental Technique

For each configuration, four different tests were performed to collect data. Each test was repeated three times to ensure redundancy of results. These four tests are as follows:

4.3.1 Flow Rate Increase (FRI) Test

Increase flow incrementally (minimal back pressure). This test is a quick screening to assess the high level performance characteristics of the configuration.

- Record temperature, flow rate, air quality, and pressures at each flow increment
- Take photos of branch leg at each flow increment
- Determine what flow rates to run Flow Rate Maintain tests

4.3.2 Flow Rate Maintain (FRM) Test

Maintain a certain flow rate over time (minimal back pressure). This test simulates most process conditions, including CIP.

- Record temperature, flow rate, air quality, and pressures at regular time increments
- Record video (whether real time or 2 second snapshots) of branch leg at regular time increments
- Determine flow rate needed to clear branch leg at 1 min and 5 minutes

Anything over 5 minutes is considered unacceptable.

4.3.3 Pressure Increase (PI) Test

Increase pressure incrementally while maintaining a certain flow rate. This test is a quick screening test to assess if increasing the pressure will assist in air elimination.

- Record temperature, flow rate, air quality, and pressures at each pressure increment, and with pump shut off

- Take photos of the branch leg at each pressure increment, and when pump is shut off
- Determine what pressures and flow rates to run Pressure Maintain tests

4.3.4 Pressure Maintain (PM) Test

Maintain a certain pressure and flow rate over time. This test simulates some process conditions where pressure is maintained.

- Record temperature, flow rate, air quality, and pressures at regular time increments
- Record video (whether real time or 2 second snapshots) of branch leg at regular time increments
- Determine flow rate needed to clear branch leg at 1 min and 5 minutes.

Anything over 5 minutes is considered unacceptable.

4.4 Explanation of Rotation/Slope

A digital level that measured in tenths of degrees was used for the different slopes and rotations. For the slopes, it was calculated that 1/8 by 12 inches is about 0.6 degrees; that set point was employed to find the correct slopes. For the rotations, the level was placed on the dead leg until the correct rotation in degrees for that orientation was achieved.

4.5 Data Collected

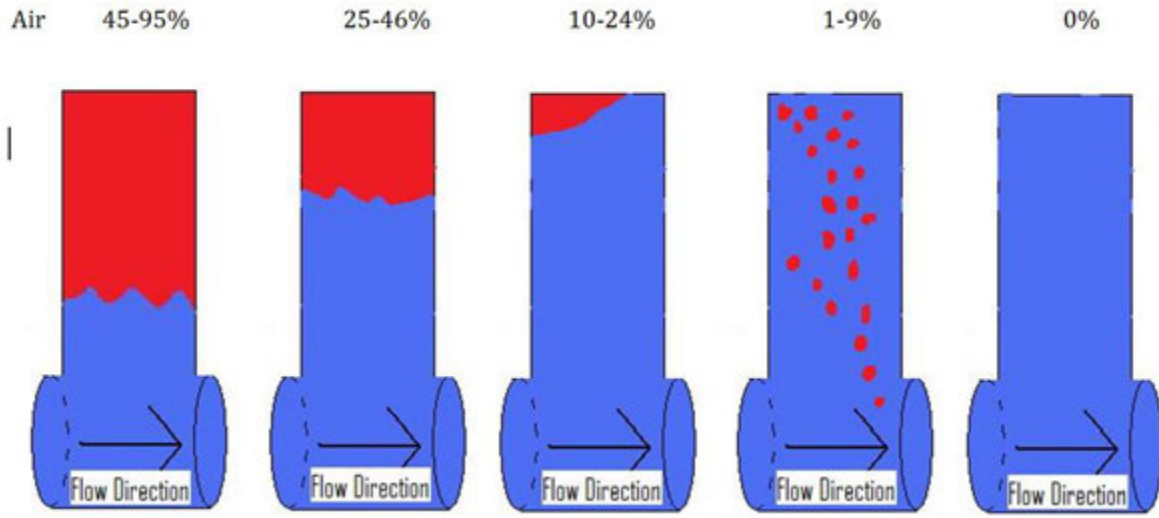
Visual observations, such as the amount of air left in the branch leg, were recorded with the test spools. Flow rate, temperature, time, and pressure data were all recorded where applicable.

4.6 Evaluation Method

A qualitative scale to judge the amount of air still trapped in the branch leg was used to assess the level of air elimination in the system. This scale ranged from 0 to 5, making it possible to record how much air was still left in the dead leg for different configurations (see Figure 4-2).

0. No water in the branch
1. Less than 1/2 full of water (more than 1/2 full of air)
2. 1/2 to 3/4 full of water (1/4 to 1/2 full of air)
3. 3/4 to completely full of water (clear to 1/4 full of air), there is always a standing bubble of air
4. Completely full of water, many bubbles remain throughout the branch leg (nearly clear of air)
5. Completely full of water (clear of air)

Figure 4-2: Example Images of a Visual Air Grade



From left to right, the Air Grade is 1,2,3,4 and 5 respectively

Figure 4-3: Example Image of Air Grade 1



Left: No rotation with the pump off and the spool closed. Right: No rotation with the pump running and the spool open.

By performing this experiment, a quantitative standard has been introduced in which the amount of air can be measured in a branch leg. This is important to the BioProcess Equipment (BPE) community, as a standard will help when determining how quickly a leg reaches a 4 or 5 when cleaning the equipment.

Figure 4-4: Evaluation Scheme for Including Time for Clearing Air into the Evaluation of Data-Developed During the Project

Time to Clear	All Air Removed (5)	All Surfaces Wetted Some Bubbles Present (4)
<1 minute	Preferred	Acceptable
5 minutes	Acceptable	Borderline
> 5 minutes	Unacceptable	Unacceptable

Removal of air is not only flow rate dependent, but time dependent as well. Therefore, an additional scale for simultaneous evaluation of time and flow rate was proposed (see Figure 4-4).

5 THE FITTING TEST SPECIMEN

In order to conduct an experiment and analysis of a fluid's performance in a dead leg, it was necessary to view the internals of the tubing system. In the industry, the majority of the tubing is made of stainless steel with dimensions per the ASME BPE standard (see Table DT-4-1 on page 87 of the BPE 2012) with a smooth surface roughness of Ra 25µin or smoother.

As the evaluation basis for this study was visual, a transparent/translucent material with a surface roughness similar to that of stainless steel pipes was required to simulate standard conditions. Natural Polypropylene (PP-R) was selected as the material to replicate the BPE Standard's stainless steel fittings because of its optical characteristics, heat tolerance, smooth interior surface and existing industry use (see Appendix B for PP-R material data). Suitable material was available from the Georg Fischer Company (PROGEF Natural) in piping sizes 20 mm < OD < 90 mm (16.2 mm < ID < 79.8 mm). The roughness of this material is Ra 63 µin.

Since there is not a direct correlation between pipe and tube dimensions, the PP-R pipe's inside diameters were reviewed and a pipe size was selected to match up with the equivalent ASME BPE tube size (see Figure 5-1). The inside dimensions matched within 15%.

Figure 5-1: Justification of the Designation Given to the Polypropylene (PP-R) and PVC Piping

	Nominal size – original. Outside Diameter [mm]	Inner Diameter Average measured [inch]	Inner Diameter nearest ASME BPE pipe [inch]	Nominal Size - ASME BPE pipe [inch]	Designation in Report [inch]
Polypropylene pipe	20	0.61	0.62	0.75	pp - 0.75
	25	0.78	0.87	1	pp - 1
	40	1.25	1.37	1.5	pp - 1.5
	50	1.56	1.87	2	pp - 2
PVC	Sch. 40 SW	1.57	1.87	2	pvc - 2
Stainless steel	2"	1.86	1.87	2	ss - 2

Note: Actual measured data in inch and mm can be found in Appendix C.

There was no a match for the ASME BPE ½ inch tube in the available piping sizes, so it was not fabricated in PP-R for testing.

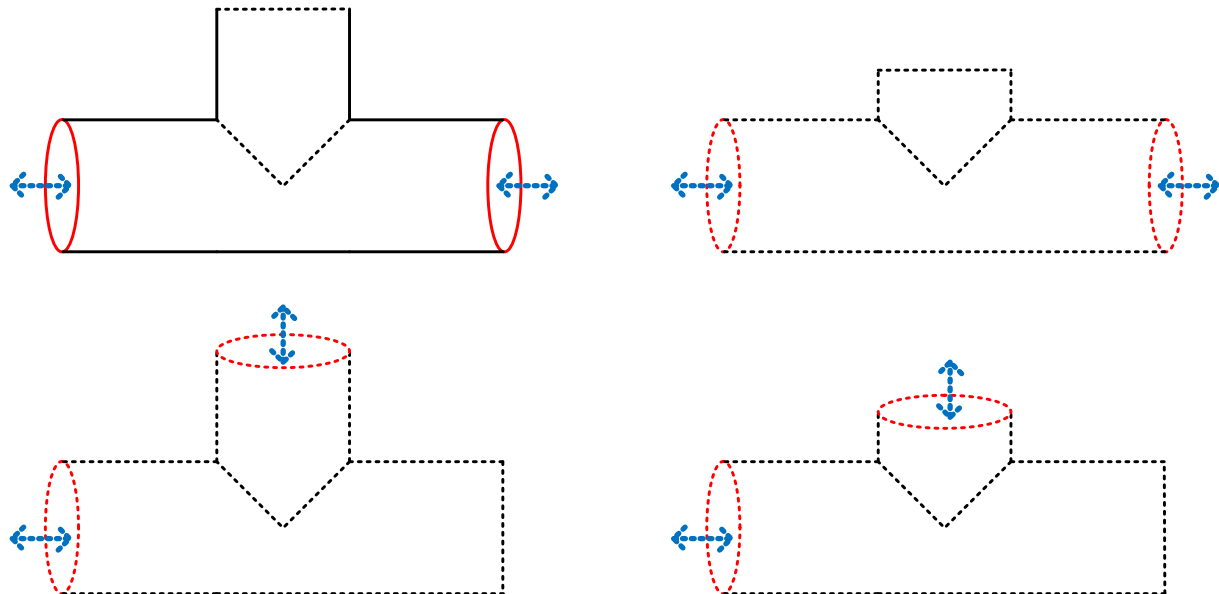
The PVC system was used in the pre-experiment done by Cotter and was a correlation/comparison to the current 2 inch stainless steel test skid. The PVC was transparent, which provided a clearer view of the internals, but it contained socket welds, which were not representative of typical flush welded stainless steel systems. In the new test skid, stainless steel fittings with clear end caps were used to provide visibility of the branch interior.

Five feet per second (5 fps) represents the typical average velocity used in CIP operations. This velocity is well into the turbulent regime (see Appendix D for Reynolds number at different flow rates and velocity at different GPM for the four sizes of pipes used in these experiments). All sizes but the smallest (pp-0.75") are in the fully developed range, meaning that flow patterns are unaffected by flow rate. For

pp-0.75” the flow is just below the $Re = 40,000$ normally considered as the limit where flow patterns become independent of flow rate.

For each nominal pipe size, four different test configurations were assembled (a total of 16 test pieces): one set with a long branch and one set with a short branch, both sets with either straight through flow path (straight) or 90° flow path (elbow) (see Figure 5-2).

Figure 5-2: Principle Sketches of Manufactured Test Pieces



Top row: Straight flow path (Straight). Bottom row: 90° flow path (Elbow)

Fabrication of a hygienic-clamped end on the branches was not possible by the piping manufacturer due to tooling tolerances, so fixed end caps were used.

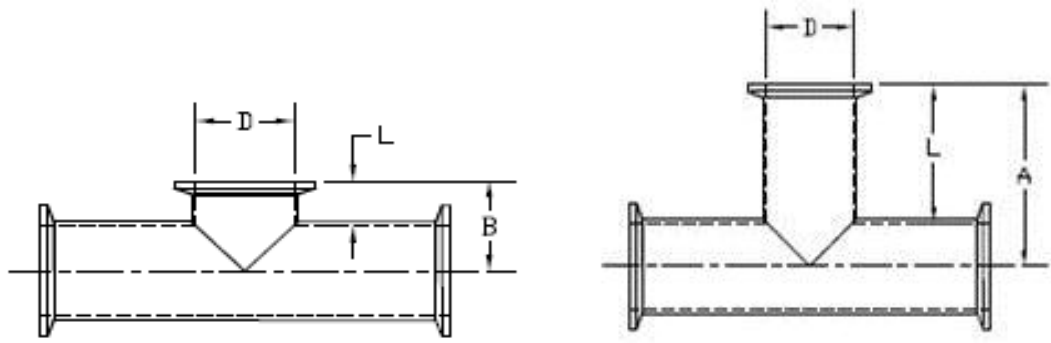
Figure 5-2 shows only the geometry around the branch. A minimum length of 3 straight feet of piping was provided to the supply side of a branch to mitigate the possible effect of flow path perturbations. A minimum of 1 foot was also provided after the study branch. Straight fittings had one foot after the branch (Figure 5-5), and 90° degree fittings had 3 feet after the branch (Figure 5-6) to allow for reverse flow mounting.

The PP-R piping test specimen's inside dimensions (see Figure 5-1) were used to back calculate the required L dimension of the branch to yield the same branch leg L/D ratios as the equivalent tubing size for both a 2:1 (L/D) branch leg and the short outlet (SO) branch leg from BPE Table DT-4.1.2.4 and DT-4.1.2.2. Figure 5-3 shows the L/D 's based on the measured dimensions of the final pieces.

Figure 5-3: T- designation, the True L/D and for Reference the L/D Achieved by the Dimension of ASME BPE Tees

	T-designation	Inner Diameter (D) [inch]	Distance from center line to top of dead-end (A) [inch]	Depth of dead-end ($L = A-D/2$) [inch]	L/D of Test samples	ASME BPE L/D for nominal sizes
pp - 0.75"	L/D = 2	0.61	1.598	1.293	2.12	3.33
pp - 1"	L/D = 2	0.78	2.011	1.621	2.08	2.23
pp - 1.5"	L/D = 2	1.25	3.213	2.588	2.07	1.23
pp - 2"	L/D = 2	1.56	4.012	3.232	2.07	0.77
pp - 0.75"	SO - L/D = 1.8	0.61	1.157	0.852	1.40	1.31
pp - 1"	SO - L/D = 1.5	0.78	1.043	0.653	0.84	0.79
pp - 1.5"	SO - L/D = 0.7	1.25	1.291	0.666	0.53	0.50
pp - 2"	SO - L/D = 0.4	1.56	1.394	0.614	0.39	0.37

Figure 5-4: BPE Hygienic Clamp Joint: Short Outlet Tee (BPE 2012 Table DT-4.1.2-5) and Straight Tee (Table DT-4.1.2-4 BPE 2012)



5.1 Variables Evaluated

During the experimentation phase, the influence of different parameters on the removal of air from the branch was investigated. The choice of variables was based on literature review and prior experience with the test setup (pre-experiments by Cotter and pre-experiments by the group). The following variables were evaluated:

- Pipe style
- Flow direction
- Branch orientation
- Pipe slope
- Back pressure
- Temperature

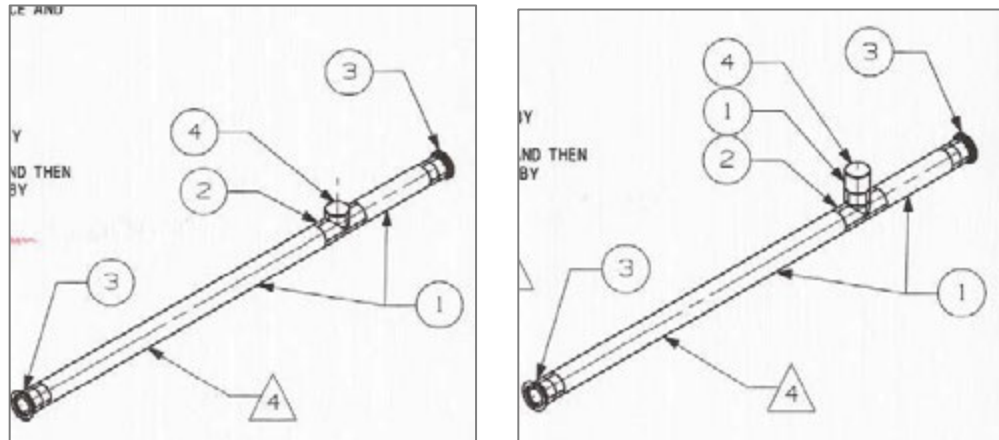
5.1.1 Pipe Style

Six different types of pipe were tested as follows (see Figure 4-1 for sketches of branch section).

STP-PT-065: Branch Leg Study for Bioprocessing Equipment

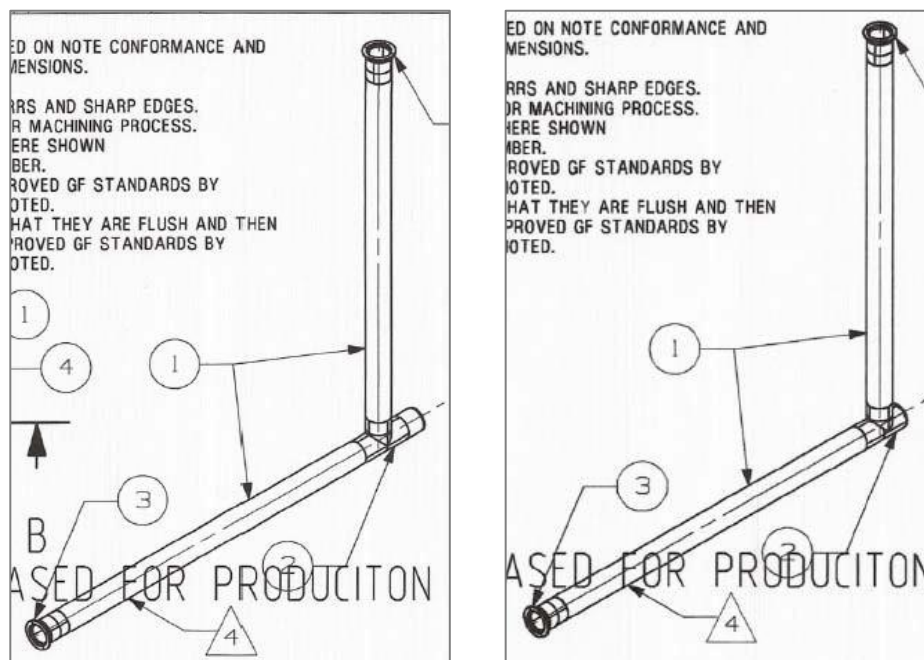
1. Polypropylene (PP-R) Straight Tee (L/D of 2) – *PP-straight-2:1*
 - Defined as a 4 foot long straight tube with a branch whose length is twice the diameter of the tube. The branch’s centerline is 1 foot from one end of the tube.
2. Polypropylene (PP-R) Straight Tee (SO) – *PP-straight-SO*
 - Defined the same as above, with a short outlet branch as opposed to an L/D of 2.

Figure 5-5: PP-2 Inch Straight Geometry L/D = Short (left) and L/D = 2 (right)



3. Polypropylene (PP-R) Elbow Tube (L/D of 2) - *PP-Elbow-2:1*
 - Defined as two 3-foot long straight tubes attached at a 90 degree angle at their ends, with a branch whose length is twice the diameter of the tube. The branch is off the connection, with it being parallel to one tube and perpendicular to the other.
4. Polypropylene (PP-R) Elbow Tube (SO) - *PP-Elbow-SO*
 - Defined the same as above, with a short outlet branch as opposed to an L/D of 2.

Figure 5-6: PP-2 Inch Elbow Geometry L/D = 2 (left) and L/D = Short (right)



STP-PT-065: Branch Leg Study for Bioprocessing Equipment

5. PVC Straight Tee
 - Defined as a 9 inch pipe and a 34 inch pipe attached at opposite ends to a tee, with a branch capped at a length that is twice its pipe diameter.
6. Stainless Steel Straight Tee
 - Defined as a 24 inch pipe and 16 inch pipe attached to a standard tee at opposite ends, with its other branch capped with a clear end cap.

The majority of the experiments were performed in the PP-R pipes. The PVC and stainless pieces were used mainly for verification purposes.

5.1.2 Flow Direction

Eleven different flow directions were tested: Three for the tees on the straight lengths, and eight for the elbow (see Appendix E for sketches of geometry and flow direction- *underlined words in the appendix are the terms used in the Excel data sheet for raw data and those used to reference the combination in the results section of the report*):

Straight through flow:

- Main pipe horizontal
- Main pipe vertical
 - Bottom-to-top
 - Top-to-bottom

Elbow flow:

- Pipes are horizontal (on the floor)
 - Parallel
 - Perpendicular
- Pipes are vertical (on the wall)
 - Flow up to horizontal – branch up
 - Flow up to horizontal – branch horizontal
 - Flow horizontal to up – branch horizontal
 - Flow horizontal to down – branch up
 - Flow horizontal to down – branch horizontal
 - Flow down to horizontal – branch horizontal

5.1.3 Pipe Slope

The straight tee was evaluated in the horizontal direction with slopes of 0° , $+0.6^\circ$ (+1/8 inch per foot), and -0.6° (-1/8 inch per foot). The horizontal runs of the elbow tubes also were configured with slope of tangential pipe.

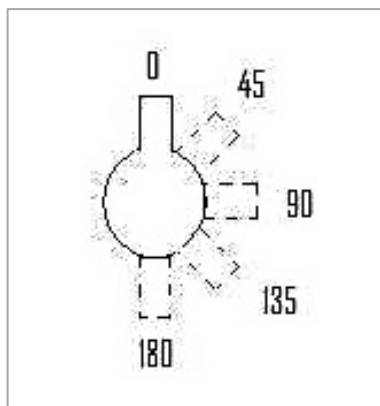
Slope description: For every 12 inches that the pipe is long, one end of the pipe will be 1/8 inch higher than the other. For example, the four feet long pipe will rise 1/2 inch from one end to the other.

(See Appendix E for sketches of geometry and flow direction - *Underlined words in the appendix are those terms used in the Excel data sheet for raw data and that are used to reference the combination in the results section of the report.*)

5.1.4 Branch Rotation

The straight tee was evaluated in the horizontal direction with branch rotations of 0, 45, 90, 135, and 180 degrees from the vertical.

Figure 5-7: Branch Rotation Designation



5.1.5 Back Pressure

The impact of back pressure on the filling of the branch leg was evaluated. Testing was performed with negligible back pressure up to 60 psig back pressure, and only on 2 inch and $\frac{3}{4}$ inch horizontal lines.

5.1.6 Temperature

First tests were performed at ambient temperatures. Subsequent tests were performed at 65°C to mimic typical CIP conditions. The 65°C tests were performed only on 2 inch and $\frac{3}{4}$ inch lines.

Test Plan

- (a) 2 inch piping, all configurations, ambient temperature
- (b) Horizontal comparison with standard stainless steel tee, ambient temperature
- (c) Horizontal comparison with Cotter Brothers tee, ambient temperature
- (d) $\frac{3}{4}$ inch piping, most configurations, ambient temperature
- (e) 1 and 1 1/2 inch piping, some configurations (chosen from experience with 2 and $\frac{3}{4}$ inch lines), ambient temperature
- (f) 2 inch and $\frac{3}{4}$ inch piping, some configurations, 65 °C
- (g) Standard stainless steel tees with clear end caps, 65 °C

6 RESULTS AND DISCUSSION

This section contains a case by case discussion of the results presented earlier. An overall discussion of all the results is provided in the next chapter on recommendations for the industry.

6.1 Variables Evaluated

During this testing the following variables were evaluated (See Section 5 for further details):

- Pipe diameter (3/4" – 2" nominal)
- Tee rotation angle – reference 0° = vertical (0°, 45°, 90°, 135°, 180°)
- L/D ratio (L/D = 2 and L/D = equivalent to that of ASME-BPE short outlet tee for that size)
- Temperature (only evaluated for 2" and 3/4" size)
- Back pressure (only evaluated under 2" and 3/4" horizontal conditions)

During each study, the flow rate required to achieve the desired air removal state (e.g., air removal ranking of 2, 3, 4 and 5) within the allotted time duration was recorded. The corresponding velocities and Reynolds numbers were calculated for the flow rates. All were plotted versus pipe diameter for the following:

- Preferred – Complete air removal from the branch within one minute. 2D only.
- Acceptable – Complete air removal from the branch within 5 minutes. 2D and SO.
- Borderline – Completely wetted within 5 minutes. Some moving air bubbles remained in the branch. 2D only.

6.2 Impact of L/D Ratio on Flow Rate Required to Achieve Air Removal State

With the larger diameters, as the L/D ratio is decreased, the flow rate required to achieve a given air removal state for a given pipe configuration also decreased. The smaller diameters' similar flow rates were required to remove the air from the branch.

6.2.1 Impact of Rotation Angle on Flow Rate Required to Achieve Air Removal State

As one would expect, it is easiest to displace the air from a tee installed in a horizontal line when it is rotated so that the branched portion is directed straight downward (180° rotation angle) and it becomes more and more difficult to displace the air as the branched portion is directed straight upward (0° rotation angle).

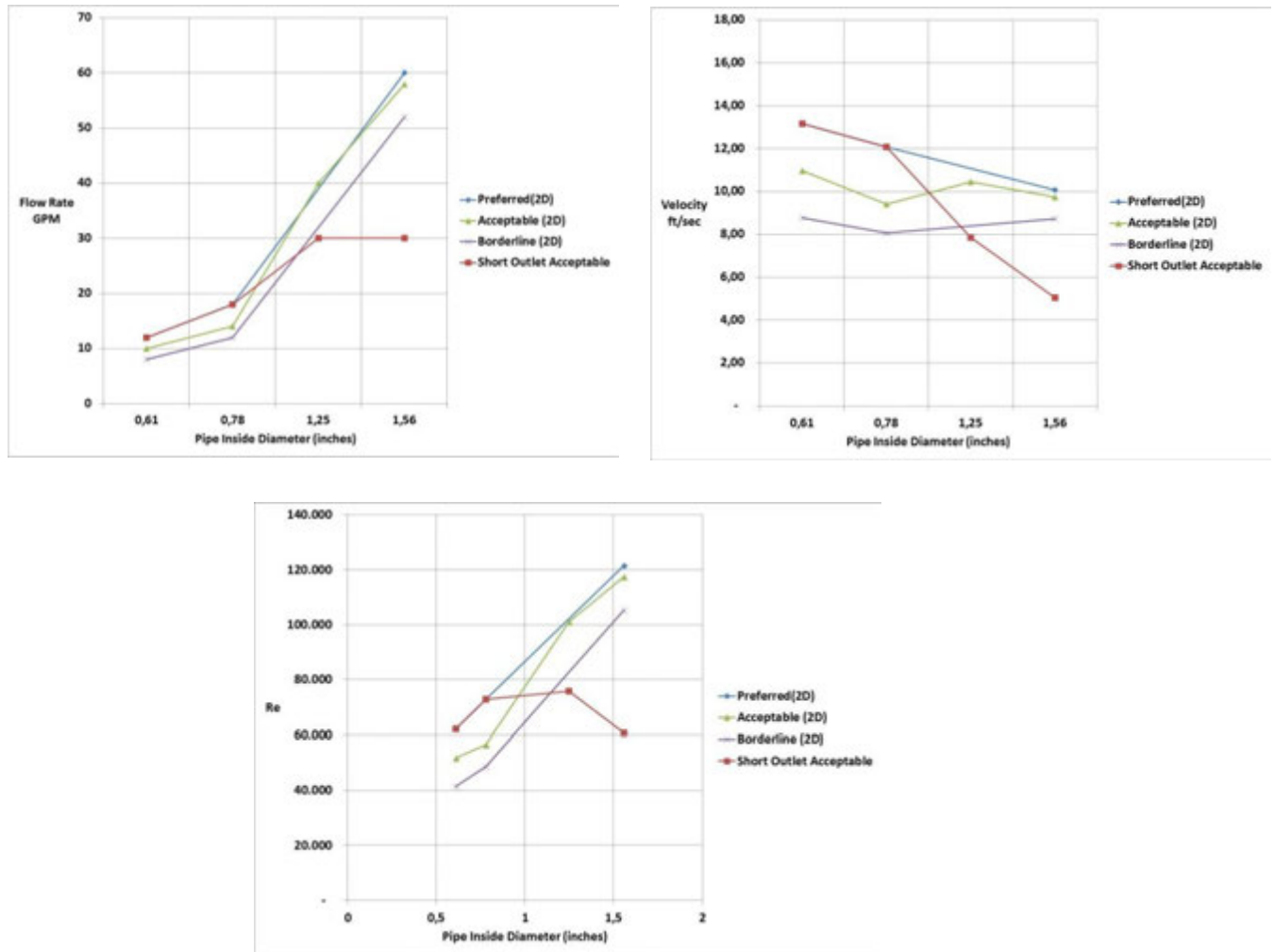
6.2.2 Parameters for Predicting Air Removal States

With the data obtained for different flow rates and different pipe dimensions, it is possible to evaluate if reaching a certain air removal state (preferred or acceptable) is best related to Reynolds number, velocity or flow rate for the different conditions evaluated. The test results indicate that the best parameter to predict an air removal state for different pipe diameter branches with a constant L/D ratio of two is the velocity in the main pipe, as this gives an almost constant velocity to reach an air removal state independent of pipe diameter. With Reynolds number and flow rate, a parabolic to linear relationship is seen between the required Reynolds number and flow rate to reach a certain state.

For the short outlet tee, the Reynolds number would be the best parameter as it appears to be independent of pipe dimension, while it has an almost linear relationship with flow rate and velocity (see more in the discussion on short outlet tees).

The velocities appeared to be linear across the diameters and ranged between 8 and 13 feet/sec to clear air out of the 2D branches. The velocities were similar for the short outlet of 3/4 and 1 inch and were as low as 6 feet/sec for the 2 inch size.

Figure 6-1: Data for Upward Pointing Branch (0°) on a Horizontal Line at Ambient Temperature Plotted with Reynolds Number, Velocity and Flow Rate



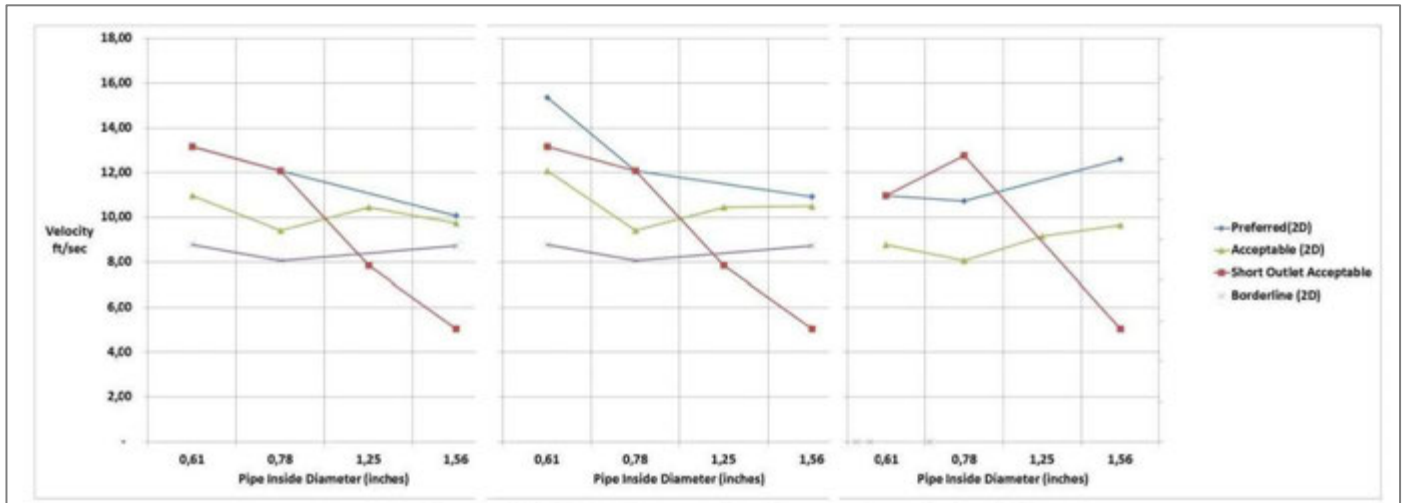
6.2.3 Influence Flow Startup

Experiments were performed increasing the flow rate to obtain a certain grade (4 or 5), and experiments were performed with a constant flow rate starting immediately from $t = 0$ s, recording the time to reach a certain grade. A certain grade was reached in a similar time frame when flow was increased compared to when flow was maintained at a predefined flow rate.

6.2.4 Horizontal T-pieces Straight Through ($L/D = 2$)

For the five configurations tested, air was most easily removed from the two with the downward pointing branch, as gravity and density differences assisted in air removal. In all the situations tested with a downward pointing branch, less than 5 feet/sec was needed to immediately remove air to a grade 5.

Figure 6-2: Velocity Required to Reach Certain State



From Left To Right: 0° Branch (Upward Pointing), 45° and 90° T-Pieces Straight Through Ambient Temperature

For the configuration with a horizontal branch (90°) the velocity required to reach the acceptable state (grade 4 in 1 min) was approximately 9 feet/sec and the preferred state (grade 5 in 1 min) was approx. 12.5 feet/sec.

For the configuration with a branch angled 0° and 45°, the velocity required to reach the acceptable state was approximately 12 feet/sec and the preferred state was approximately 13 feet/sec. For all cases, there were no significant differences when sloping the pipe line from +/-0.6°.

6.2.5 Vertical T-pieces Straight Through (L/D = 2)

A considerable difference was seen for an upward going flow compared to a downward going flow. For the upward flow, a velocity of 12.9 feet/sec was needed to reach preferred state; for a downward flow, the velocity was approximately 9.6 feet/sec.

6.2.6 Horizontal T-pieces Straight Through (Short Outlet Tee)

For the short outlet tee there was a decrease in the velocity required for reaching the acceptable state with increasing diameter, starting from approximately 13 feet/sec at the smallest diameter to roughly 5 feet/sec for the largest inner diameter.

The decrease in velocity for increasing diameter is likely for two reasons: the influence of surface tension on retaining the bubbles in the branch is greater in the smaller ID as the surface to liquid ratio is larger and/or the L/D for the short outlet tee actually decreases with increasing pipe size (See Figure 5-3). Studies by Jensen have shown that very short outlet tees change the flow pattern in the dead-end dramatically, as the recirculation zone seen in larger branches (L/D ~ 2) no longer exists if the branch has significantly reduced L/D. This could explain why an L/D of 1.4 and 0.8 need velocity above 12 feet/sec, while L/D 0.5 and 0.4 require velocity below 8 feet/sec.

6.2.7 Elbow on the Wall

Flows *into* the branch result in significantly lower velocities required to clear the air than passing the branch at an elbow. This is a way to overcome the high velocity rates.

Figure 6-3: Results from the Elbows Configurations Test for L/D = 2
Velocity to reach grade 4 in less than 1 minute

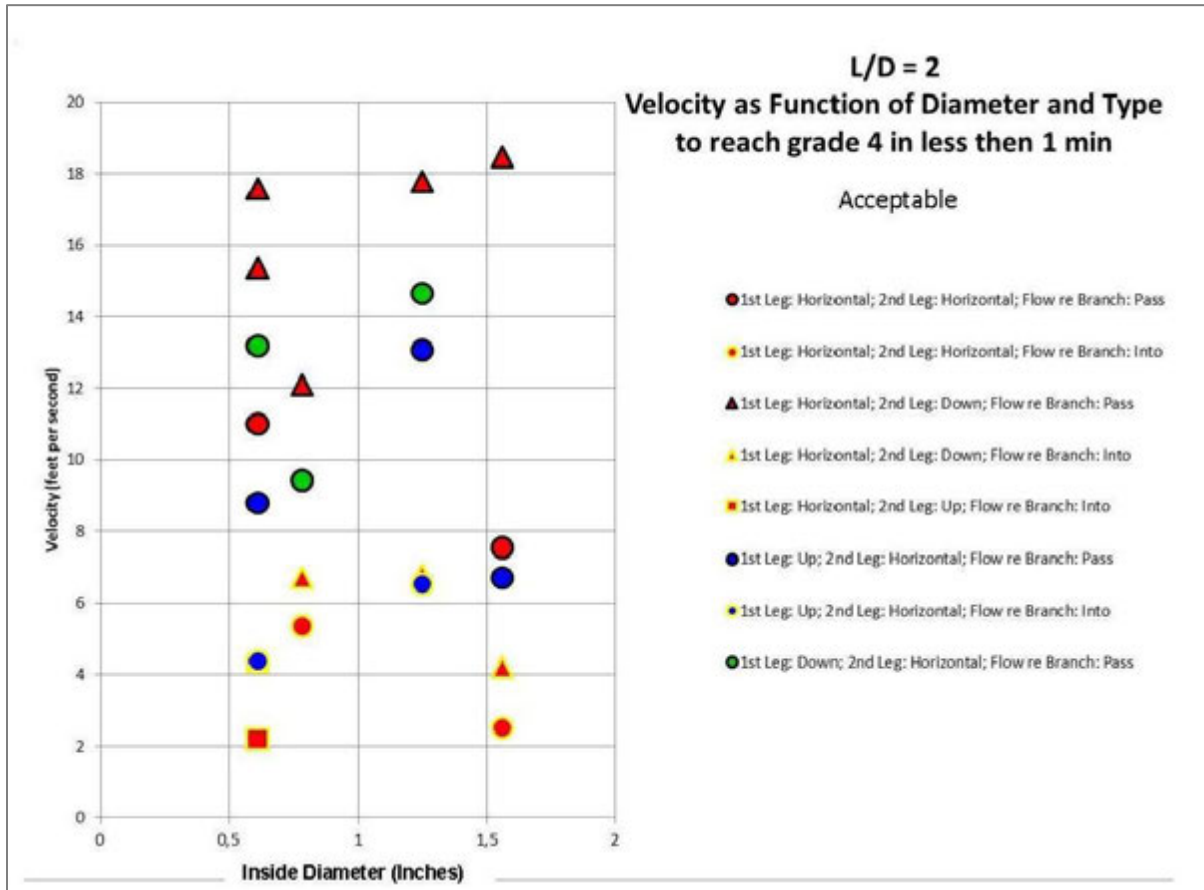
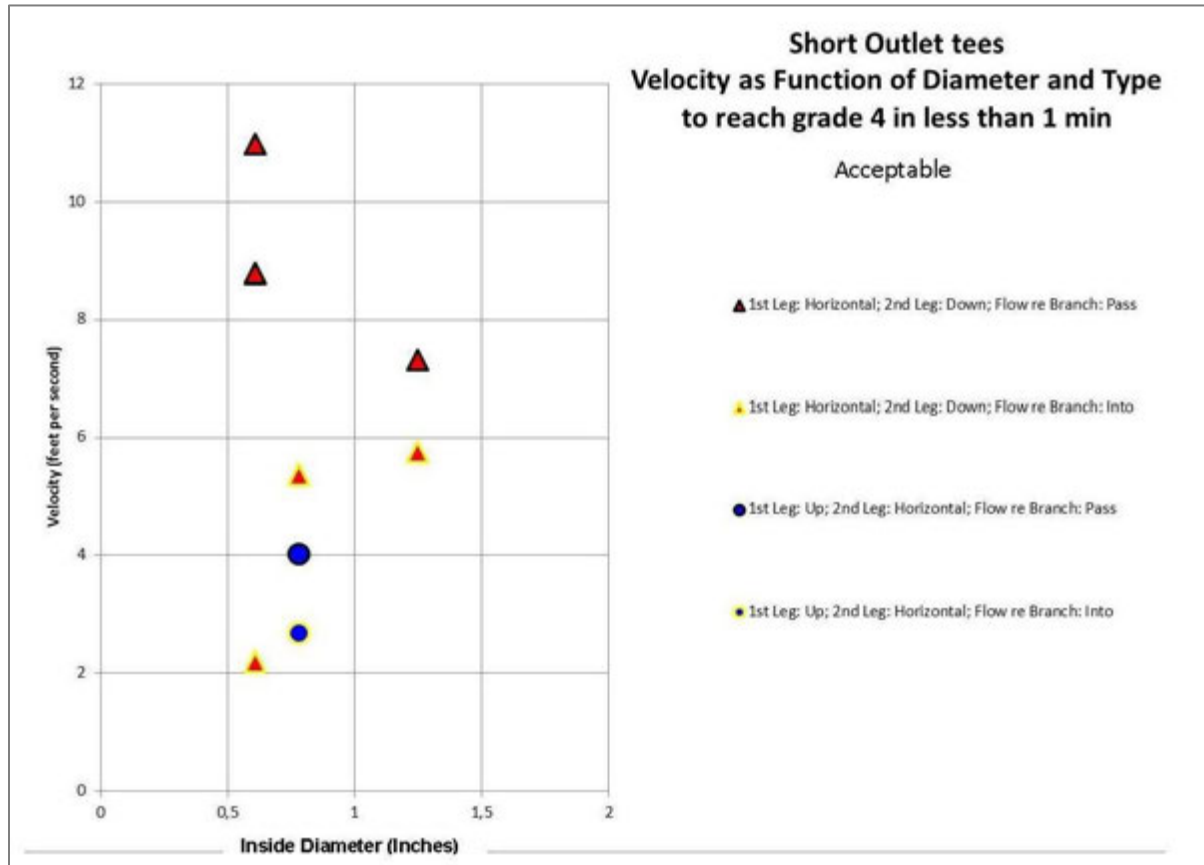


Figure 6-4: Results from the Elbow Configurations Test for SO tee
Velocity to reach grade 4 in less than 1 minute



6.2.8 Influence of Temperature

Increasing the temperature decreases the rate at which the air is removed from the branch. Hence, a higher velocity is required to remove air from a hotter solution within the same amount of time. (Note: This can be significant for those who typically perform CIP at 65° or hotter)

For the horizontal T-pieces with straight through flow, the velocity increase is approximately 2 feet/sec. For the vertical T-pieces, data support these findings, but is not sufficient to conclude on the velocity increase needed.

6.2.9 Influence of Back Pressure

Back pressure had little to no effect on the clearance of the air. The air bubble volume decreased due to increased pressure, and returned to its original size when the pressure was relieved.

7 CONCLUSIONS & RECOMMENDATIONS

This study confirmed that a high flow rate is the driving factor for optimized removal of air in BioProcess piping systems, specifically it confirmed that flow rates much greater than the traditional 5 feet/second would be required. Direction of flow and orientation also have some influence. The following trends were noticed:

- Pressure increases provide little improvement to the removal of air.
- Vertical runs require lower flow rates to remove air.
- Short Outlet Tees require lower flow rates to remove air.
- Rotation of the branch leg influences its ability to clear.
- Minor effects were seen with elevated temperatures, mainly due to the physical property changes in the fluid.
- Configuration of the fittings has an effect

The buoyant forces between the two phases are very much in play. The fluid transfer momentum from the higher flow rates provides turbulence. When high enough, they can displace the air which is lighter at the top of the fittings. The stagnant zone was witnessed where bubbles would remain in the branch for extended periods of time.

As such, this study proposes the following recommendations for optimizing air removal from the system (not taking into account other aspects of cleaning and sterilization):

- (1) Design piping systems with only downward pointing branches (Note: This is not good for sterilization or an acceptable practice in the BPE)
- (2) If branches are needed, put them on vertical lines
- (3) Branches (regardless of orientation and position) should be SOT as short as 0.4 (this requires only 5 feet/sec to remove air) – only proven for 2 inch pipe
- (4) If branches of any kind are unavoidable, refer to Figure 6-1 for design velocities
- (5) Removal of air should be done with liquid at ambient temperature rather than hotter temperatures
- (6) Removal of air should be done by steadily increasing the flow to the desired flow rate or by instantly increasing the flow to the desired flow rate
- (7) Elbows should be oriented for the flow to enter the branch rather than passing by them

7.1 Considerations When Evaluating Existing Designs

The goal of this report is to share the results of the test data obtained to better understand the flow conditions required to displace air from tees in a variety of different pipe sizes, L/D ratios, installation orientations, and flow directions. Although this testing was conducted in a thorough and robust manner, the results of this testing should not be used to definitively determine if the air is being removed from a specific process application.

As an example, assume that an existing process application involves CIP cleaning of a horizontal section of 2 inch stainless steel tubing with a tee with an L/D ratio of two directed vertically upward that contains a conductivity sensor which protrudes into the process line. This line is CIP cleaned at a flow rate which corresponds to a linear velocity of 5 feet/sec. In reviewing the results of the testing, one would expect to need a much higher flow rate to displace the air from the system in a timely manner and ensure adequate contact between the cleaning reagents and the process residue. Even though the flow rate is significantly less than the value listed in this report, the air may be easily displaced from the tee (e.g. due to interaction with the conductivity sensor, pulsing that occurs during the CIP operation, rinsing lasting more than one minute).

STP-PT-065: Branch Leg Study for Bioprocessing Equipment

The guidance set forth in this document should be used as a starting point for additional study and dialogue, but it should not be implied that air is not being displaced from applications that do not meet this criteria. Successful displacement of air from each application will be determined by the specific installation and process conditions.

REFERENCES

- [1] ASME BioProcess Equipment, BPE, Standard, 2009 and 2012.
- [2] Deadleg Studies Presented to the ASME BPE Committee, 2009, 2010, and 2011, Cotter Brothers, Danvers, MA.
- [3] Testing to Determine Flowrates Required to Flood Piping, Jeff J. Gaerke, P.E., Eli Lilly, 06 June 2011.
- [4] Parameters Governing Steam Sterilization of Deadlegs, Young, Ferko, and Gaber, Penn State University, Pharm. Sci. Tech, 1994, may Jun, 48 (3): 140-7.
- [5] Flow characteristics in dead spaces in CIP-pipeline systems Grasshoff, A., 1982: Flow characteristics in dead spaces in CIP-pipeline systems. XXI International Dairy Congress Vol. 1, Book 1: 228...
- [6] Flow behavior of liquids in cylindrical dead spaces of pipeline systems Grasshoff, A., 1980: Flow behavior of liquids in cylindrical dead spaces of pipeline systems. Kieler Milchwirtschaftliche Forschungsberichte 32(4): 273-298...
- [7] Cleaning mechanism Study for bioPharmaceutical Plant Design, Murakami, Haga, Ostrove and Weiss, Pharmaceutical Engineering, September/October 1997, vol. 17, No5,
- [8] Facility Design and construction suitable for Cleaning Validation, Sasanami and Watanbe, PDA Asian Symposium and Exhibit, 14-16 November, 1994.
- [9] Characteristics of flow field and water concentration in a horizontal Deadleg, Habib, Badr, Said, Mokheimer, Hussaini, Al-Sanaa, Heat Mass transfer, 2005, 41:315-326.
- [10] Experimental Work, Bo Jensen, Alfa Laval, 2011.

APPENDICES

APPENDIX A: TEST SCHEMATIC

<p>Horizontal w. Branch</p>	<p>See Figure 4-1 in report</p>
<p>Vertical w. branch</p>	<p style="text-align: center;">*Red = Test Spool</p>
<p>Elbow Vertical</p>	

APPENDIX B: PROPERTIES FOR PP-R PIPE

The PROGEF material used in these experiments is the PROGEF Natural.

General Properties (Polypropylene)

Material Data

The following table lists typical physical properties of Polypropylene thermoplastic materials. Variations may exist depending on specific compounds and product.

Mechanical

Properties	Unit	PROGEF Standard PP-H	PROGEF Natural PP-R	PPro-Seal Natural PP-R	ASTM Test
Density	lb/in ³	0.0325	0.0325	0.0327	ASTM D792
Tensile Strength @ 73°F (Yield)	PSI	4,500	3,625	4,350	ASTM D638
Tensile Strength @ 73°F (Break)	PSI	5,600	4,500	5,000	ASTM D638
Modules of Elasticity Tensile @ 73°F	PSI	188,500	130,500	150,000	ASTM D638
Compressive Strength @ 73°F	PSI	6,500	5,500	5,500	ASTM D695
Flexural Modulus @ 73°F	PSI	181,250	130,500	130,000	ASTM D790
Izod Impact @ 73°F	Ft-Lbs/In of Notch	11.3	8.0	8.0	ASTM D256
Relative Hardness @ 73°F	Shore	70	70	70	ASTM D2240

Thermodynamics

Properties	Unit	PROGEF Standard	PROGEF Natural	PPro-Seal Natural	ASTM Test
Melt Index	gm/10min	0.25	0.30-0.40	0.40-0.80	ASTM D1238
Melting Point	°F	320	316	316	ASTM D789
Coefficient of Thermal Linear Expansion per °F	in/in/°F	0.5 x 10 ⁻⁴	0.5 x 10 ⁻⁴	0.61 x 10 ⁻⁴	ASTM D696
Thermal Conductivity	BTU-in/ft ² /hr/°F	1.6	1.6	1.2	ASTM D177
Maximum Operating Temperature	°F	176	176	176	
Heat Distortion Temperature @ 264 PSI	°F	125	125	130	ASTM D648

Other

Properties	Unit	PROGEF Standard	PROGEF Natural	PPro-Seal Natural	ASTM Test
Water Absorption	%	<0.1%	<0.1%	<0.03%	ASTM D570
Poisson's Ratio @ 73°F		0.38	0.38	0.38	
Industry Standard Color		7032	Neutral	Neutral	RAL 9005
Food and Drug Association (FDA)		YES	YES	YES	CFR 21.177.1520
United States Pharmacopeia (USP)		YES	YES	YES	USP 25 Class VI

Note: This data is based on information compiled from multiple sources.

APPENDIX C: MEASURE DATA FOR PP-R PIPES USED IN EXPERIMENTS

Table A3.1: Size designation, dimension and corresponding ASME BPE pipe inner diameter for the different pipe materials and pipe sizes used in this study. Results from similar designation size cannot be directly compared as inner diameter may be different depending on material of pipe.						
Spool Component	Size designation in report	Outside Diameter		Inside Diameter		Corresponding ASME BPE pipe inner diameter
		(inch)	(mm)	(inch)	(mm)	
Polypropylene parts (20 mm)	pp - 0.75"	0.79	20.19	0.61	15.61	0.62
Polypropylene parts (25 mm)	pp - 1"	0.99	25.15	0.78	19.89	0.87
Polypropylene parts (40 mm)	pp - 1.5"	1.57	39.90	1.25	31.69	1.37
Polypropylene parts (50 mm)	pp - 2"	1.98	50.23	1.56	39.64	1.87
PVC straight tube	pvc - 2"	1.90	48.27	1.57	39.95	1.87
PVC Tee	pvc - 2"	2.24	56.78	1.83	46.51	
Stainless Steel Pipe	ss - 2"	2.00	50.89	1.86	47.32	1.87

Nominal dimensions of polypropylene parts are not comparable to Nominal dimensions of stainless steel parts as per ASME BPE – Table A3.1 shows the real Nominal size depending of pipe material (Polypropylene, PVC or Stainless steel).

APPENDIX D: FLOW RATE, VELOCITY AND REYNOLDS NUMBERS

Table A4.1: fps and Reynolds number for four Polypropylene pipe sizes used in this study as a function of the GPM used

GPM	pp-0.75"		pp-1"		pp-1.5"		pp-2"	
	fps	Re @ 20C	fps	Re @ 20C	fps	Re @ 20C	fps	Re @ 20C
2	2.20	10579	1.34	6470	0.52	2519	0.34	1618
4	4.39	21158	2.69	12940	1.05	5039	0.67	3235
6	6.59	31737	4.03	19411	1.57	7558	1.01	4853
8	8.78	42316	5.37	25881	2.09	10077	1.34	6470
10	10.98	52895	6.71	32351	2.61	12597	1.68	8088
12	13.17	63474	8.06	38821	3.14	15116	2.01	9705
14	15.37	74053	9.40	45291	3.66	17635	2.35	11323
15	16.47	79343	10.07	48527	3.92	18895	2.52	12132
16	17.56	84633	10.74	51762	4.18	20155	2.69	12940
18	19.76	95212	12.08	58232	4.71	22674	3.02	14558
19	20.86	100501	12.76	61467	4.97	23934	3.19	15367
20	21.95	105791	13.43	64702	5.23	25193	3.36	16176
22	24.15	116370	14.77	71172	5.75	27713	3.69	17793
24	26.34	126949	16.11	77642	6.27	30232	4.03	19411
25	27.44	132238	16.78	80878	6.54	31492	4.20	20219
26	28.54	137528	17.46	84113	6.80	32751	4.36	21028
28	30.74	148107	18.80	90583	7.32	35271	4.70	22646
30	32.93	158686	20.14	97053	7.84	37790	5.04	24263
35	38.42	185134	23.50	113229	9.15	44088	5.87	28307
40	43.91	211581	26.85	129404	10.46	50387	6.71	32351
42	46.10	222160	28.20	135874	10.98	52906	7.05	33969
45	49.40	238029	30.21	145580	11.76	56685	7.55	36395
50	54.89	264477	33.57	161755	13.07	62984	8.39	40439
52	57.08	275056	34.91	168225	13.59	65503	8.73	42056
54	59.28	285635	36.25	174695	14.12	68022	9.06	43674
55	60.37	290924	36.92	177931	14.38	69282	9.23	44483
56	61.47	296214	37.60	181166	14.64	70542	9.40	45291
58	63.67	306793	38.94	187636	15.16	73061	9.73	46909
60	65.86	317372	40.28	194106	15.68	75580	10.07	48527
62	68.06	327951	41.62	200576	16.21	78100	10.41	50144
66	72.45	349109	44.31	213517	17.25	83138	11.08	53379
68	74.64	359688	45.65	219987	17.78	85658	11.41	54997
75	82.33	396715	50.35	242633	19.61	94475	12.59	60658
90	98.79	476058	60.42	291159	23.53	113370	15.11	72790
95	104.28	502506	63.78	307335	24.83	119669	15.94	76834
100	109.77	528953	67.14	323510	26.14	125967	16.78	80878
110	120.75	581849	73.85	355861	28.76	138564	18.46	88965

Appendix continues on next page.

STP-PT-065: Branch Leg Study for Bioprocessing Equipment

Table A4.2: Reynolds number and flow rates based on average velocity for evaluating flow characteristics of experimental set-up

		at Laminar Flow Re 2000				at 2.5 fps				at 5 fps				at 7.5 fps			
		20 C		66 C		20 C		66 C		20 C		66 C		20 C		66 C	
SS Tube Size	OD. in	GPM	Vel fps	GPM	Vel fps	GPM	Re	GPM	Re	GPM	Re	GPM	Re	GPM	Re	GPM	Re
		1/2"	0.39	0.42	0.17	0.18	2.35	11952	2.35	27271	4.71	23903	4.71	54543	7.06	35855	7.06
3/4"	0.55	0.30	0.24	0.13	4.63	16771	4.63	38268	9.26	33542	9.26	76536	13.90	50312	13.90	114804	
1"	0.87	0.19	0.38	0.08	11.49	26409	11.49	60261	22.97	52818	22.97	120522	34.46	79227	34.46	180783	
1 1/2"	1.19	0.14	0.52	0.06	21.40	36048	21.40	82254	42.80	72095	42.80	164508	64.21	108143	64.21	246762	
2"																	
PPn Pipe Size																	
Nom. in																	
20 mm	0.39	0.42	0.17	0.18	2.31	11846	2.31	27029	4.62	23691	4.62	54059	6.93	35537	6.93	81088	
25 mm	0.50	0.33	0.22	0.15	3.75	15099	3.75	34452	7.51	30197	7.51	68904	11.26	45296	11.26	103356	
40 mm	0.79	0.21	0.35	0.09	9.52	24048	9.52	54873	19.05	48095	19.05	109745	28.57	72143	28.57	164618	
50 mm	0.99	0.17	0.43	0.07	14.90	30081	14.90	68640	29.81	60163	29.81	137280	44.71	90244	44.71	205921	

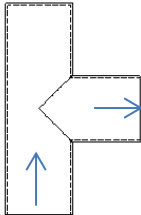
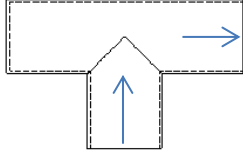
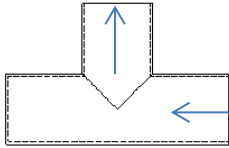
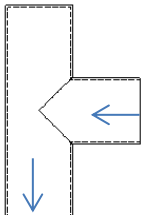
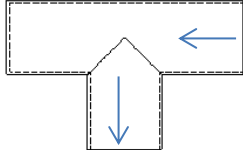
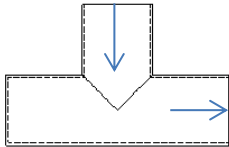
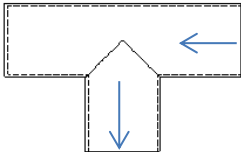
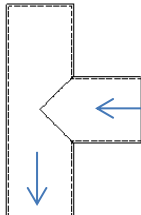
Note 1: All flows 2.5 fps and above are in the turbulent regime (4000 < Re < 40,000)

Note 2: Fully developed flow, where flow rate no longer affects the flow pattern is approx. Re = 40,000

APPENDIX E: OVERVIEW OF COMBINATIONS OF CONFIGURATIONS, SLOPES AND ROTATIONS TESTED FOR STRAIGHT THROUGH FLOW AND ELBOW FLOW

<u>Orientation</u>	<u>Slope</u>	<u>Rotation</u> 0°	<u>Rotation</u> 45°	<u>Rotation</u> 90°	<u>Rotation</u> 135°	<u>Rotation</u> 180°
Horizontal	0°					
	0.6° Up					
	0.6° Down					
	<u>Flow direction</u>	<u>Slope</u> Straight up/down	<u>Slope</u> 0.6° Down	<u>Slope</u> 0.6° Up		
Vertical	Bottom-to-top					
	Top-to-bottom					

Table D2: Orientation and flow direction of elbows
 Underlined words are those that can be found in the results section.

<u>Orientation</u>	<u>Flow direction</u> : Up to horizontal <u>Branch</u> : up	<u>Flow direction</u> : Up to horizontal <u>Branch</u> : horizontal	<u>Flow direction</u> : Horizontal to up <u>Branch</u> : horizontal
Vertical (on the wall)			
	<u>Flow direction</u> : Horizontal to down <u>Branch</u> : up	<u>Flow direction</u> : Horizontal to down <u>Branch</u> : Horizontal	<u>Flow direction</u> : Down to horizontal <u>Branch</u> : Horizontal
Vertical (on the wall)			
	<u>Branch</u> : Parallel	<u>Branch</u> : Perpendicular	
Horizontal (on the floor) Also with slope up and down as seen in table A5.1 for			

APPENDIX F: TEST RESULTS

The material in this and the subsequent appendices, documents experiments conducted by The BioProcess Institute as well as papers referenced within the body of this report.

The following tables are the committee's test results:

- Sorted Data reference visual grade
- Ambient Tests
- Hot Tests
- Tee Plus Spool Test
- Air Scale Test
- Sorted Data per various configurations
- Spool Pieces

Experiment	Date	Run	Description	Branch Size (in) (measured from outer wall of tube)	Piece	Spool Size (in)	Orientation	Flow Direction	Branch Leg Position	Slope (in)	Rotation (deg)	Material	Temperature (°C)	Velocity (ft/s)	Reynolds Number	BPI Visual Grade (FI)		BPI Visual Grade (FM)		BPI Visual Grade (PI)		BPI Visual Grade (PM)		Notes
																4 (gpm)	5 (gpm)	4 (min)	5 (min)	4 (psig)	5 (psig)	4 (min)	5 (min)	
793	111228	2	Flow Maintain (45)	3	Straight	1.5	Vertical	Bottom-Top	NA	0	0	PP	14.7	11.65	1.1331E+05	NA	NA	Imm	4	NA	NA	NA	NA	Mid-test Flow Drop
794	111228	3	Flow Maintain (45)	3	Straight	1.5	Vertical	Bottom-Top	NA	0	0	PP	14.9	11.65	1.1331E+05	NA	NA	Imm	3.5	NA	NA	NA	NA	
795	111228	1	Flow Maintain (35)	1.375	Straight	1.5	Vertical	Bottom-Top	NA	0	0	PP	15.4	9.18	8.8693E+04	NA	NA	Imm	0.5	NA	NA	NA	NA	
796	111228	2	Flow Maintain (35)	1.375	Straight	1.5	Vertical	Bottom-Top	NA	0	0	PP	15.4	9.18	8.8693E+04	NA	NA	Imm	0.5	NA	NA	NA	NA	
797	111228	3	Flow Maintain (35)	1.375	Straight	1.5	Vertical	Bottom-Top	NA	0	0	PP	15.5	9.18	8.8693E+04	NA	NA	Imm	0.5	NA	NA	NA	NA	
798	111228	1	Flow Maintain (25)	3	Elbow	1.5	Vertical	Up, Horizontal	Parallel to Flow	0	0	PP	16.0	6.44	6.2799E+04	NA	NA	DNR	0.5	NA	NA	NA	NA	
799	111228	2	Flow Maintain (25)	3	Elbow	1.5	Vertical	Up, Horizontal	Parallel to Flow	0	0	PP	16.0	6.44	6.2799E+04	NA	NA	DNR	0.5	NA	NA	NA	NA	
800	111228	3	Flow Maintain (25)	3	Elbow	1.5	Vertical	Up, Horizontal	Parallel to Flow	0	0	PP	16.1	6.44	6.2799E+04	NA	NA	DNR	0.5	NA	NA	NA	NA	
801	111228	1	Flow Maintain (50)	3	Elbow	1.5	Vertical	Up, Horizontal	Perp to Flow	0	0	PP	16.7	12.89	1.2560E+05	NA	NA	Imm	2	NA	NA	NA	NA	
802	111228	2	Flow Maintain (50)	3	Elbow	1.5	Vertical	Up, Horizontal	Perp to Flow	0	0	PP	16.9	12.89	1.2560E+05	NA	NA	Imm	2	NA	NA	NA	NA	
803	111228	3	Flow Maintain (50)	3	Elbow	1.5	Vertical	Up, Horizontal	Perp to Flow	0	0	PP	17.1	12.89	1.2560E+05	NA	NA	Imm	2	NA	NA	NA	NA	
804	111228	1	Flow Maintain (30)	1.375	Elbow	1.5	Vertical	Up, Horizontal	Perp to Flow	0	0	PP	17.4	7.67	7.5060E+04	NA	NA	DNR	Imm	NA	NA	NA	NA	
805	111228	2	Flow Maintain (30)	1.375	Elbow	1.5	Vertical	Up, Horizontal	Perp to Flow	0	0	PP	17.5	7.67	7.5060E+04	NA	NA	DNR	Imm	NA	NA	NA	NA	
806	111228	3	Flow Maintain (30)	1.375	Elbow	1.5	Vertical	Up, Horizontal	Perp to Flow	0	0	PP	17.5	7.67	7.5060E+04	NA	NA	DNR	Imm	NA	NA	NA	NA	
807	111228	1	Flow Maintain (20)	1.375	Elbow	1.5	Vertical	Up, Horizontal	Parallel to Flow	0	0	PP	17.8	5.11	5.0040E+04	NA	NA	DNR	Imm	NA	NA	NA	NA	
808	111228	2	Flow Maintain (20)	1.375	Elbow	1.5	Vertical	Up, Horizontal	Parallel to Flow	0	0	PP	17.8	5.11	5.0040E+04	NA	NA	DNR	Imm	NA	NA	NA	NA	
809	111228	3	Flow Maintain (20)	1.375	Elbow	1.5	Vertical	Up, Horizontal	Parallel to Flow	0	0	PP	17.8	5.11	5.0040E+04	NA	NA	DNR	Imm	NA	NA	NA	NA	
810	111230	1	Flow Maintain (20)	1.375	Elbow	1.5	Vertical	Up, Horizontal	Parallel to Flow	0	0	PP	20.2	5.11	5.0040E+04	NA	NA	DNR	Imm	NA	NA	NA	NA	Metal Tank Confirmation Tests
811	111230	2	Flow Maintain (20)	1.375	Elbow	1.5	Vertical	Up, Horizontal	Parallel to Flow	0	0	PP	20.4	5.11	5.0040E+04	NA	NA	DNR	Imm	NA	NA	NA	NA	Metal Tank Confirmation Tests
812	111230	3	Flow Maintain (20)	1.375	Elbow	1.5	Vertical	Up, Horizontal	Parallel to Flow	0	0	PP	19.6	5.11	5.0040E+04	NA	NA	DNR	Imm	NA	NA	NA	NA	Metal Tank Confirmation Tests
813	111230	4	Flow Maintain (20)	1.375	Elbow	1.5	Vertical	Up, Horizontal	Parallel to Flow	0	0	PP	20.7	5.11	5.0040E+04	NA	NA	DNR	Imm	NA	NA	NA	NA	Metal Tank Confirmation Tests
814	111230	1	Flow Maintain (25)	3	Elbow	1.5	Vertical	Up, Horizontal	Parallel to Flow	0	0	PP	21.0	6.44	6.2799E+04	NA	NA	Imm	0.5	NA	NA	NA	NA	Metal Tank Confirmation Tests
815	111230	2	Flow Maintain (25)	3	Elbow	1.5	Vertical	Up, Horizontal	Parallel to Flow	0	0	PP	21.2	6.44	6.2799E+04	NA	NA	DNR	0.5	NA	NA	NA	NA	Metal Tank Confirmation Tests
816	111230	3	Flow Maintain (25)	3	Elbow	1.5	Vertical	Up, Horizontal	Parallel to Flow	0	0	PP	21.4	6.44	6.2799E+04	NA	NA	DNR	0.5	NA	NA	NA	NA	Metal Tank Confirmation Tests
817	111230	1	Flow Maintain (50)	3	Elbow	1.5	Vertical	Up, Horizontal	Perp to Flow	0	0	PP	22.6	12.89	1.2560E+05	NA	NA	Imm	2	NA	NA	NA	NA	Metal Tank Confirmation Tests
818	111230	2	Flow Maintain (50)	3	Elbow	1.5	Vertical	Up, Horizontal	Perp to Flow	0	0	PP	23.1	12.89	1.2560E+05	NA	NA	Imm	2	NA	NA	NA	NA	Metal Tank Confirmation Tests
819	111230	3	Flow Maintain (50)	3	Elbow	1.5	Vertical	Up, Horizontal	Perp to Flow	0	0	PP	24.8	12.89	1.2560E+05	NA	NA	Imm	2	NA	NA	NA	NA	Metal Tank Confirmation Tests
1031	120301	1	Flow Maintain (90)	4	Straight	2	Horizontal	NA	NA	0	45	PP	13.5	14.34	1.7778E+05	NA	NA	Imm	NA	NA	NA	NA	NA	
1032	120301	2	Flow Maintain (90)	4	Straight	2	Horizontal	NA	NA	0	45	PP	14.1	14.34	1.7778E+05	NA	NA	Imm	NA	NA	NA	NA	NA	
1033	120301	1	Flow Maintain (95)	4	Straight	2	Horizontal	NA	NA	0	45	PP	15.5	15.14	1.8766E+05	NA	NA	Imm	NA	NA	NA	NA	NA	
1034	120301	2	Flow Maintain (95)	4	Straight	2	Horizontal	NA	NA	0	45	PP	16.6	15.14	1.8766E+05	NA	NA	Imm	NA	NA	NA	NA	NA	
1035	120301	1	Flow Maintain (100)	4	Straight	2	Horizontal	NA	NA	0	45	PP	18.3	15.94	1.9754E+05	NA	NA	Imm	1	NA	NA	NA	NA	
1036	120301	2	Flow Maintain (100)	4	Straight	2	Horizontal	NA	NA	0	45	PP	18.8	15.94	1.9754E+05	NA	NA	Imm	1	NA	NA	NA	NA	
1037	120301	3	Flow Maintain (100)	4	Straight	2	Horizontal	NA	NA	0	45	PP	19.4	15.94	1.9754E+05	NA	NA	Imm	1	NA	NA	NA	NA	
1038	120301	1	Flow Maintain (75)	4	Straight	2	Horizontal	NA	NA	0	90	PP	20.2	11.95	1.4815E+05	NA	NA	Imm	1	NA	NA	NA	NA	
1039	120301	2	Flow Maintain (75)	4	Straight	2	Horizontal	NA	NA	0	90	PP	20.6	11.95	1.4815E+05	NA	NA	Imm	1	NA	NA	NA	NA	
1040	120301	3	Flow Maintain (75)	4	Straight	2	Horizontal	NA	NA	0	90	PP	21.1	11.95	1.4815E+05	NA	NA	Imm	1	NA	NA	NA	NA	

Experiment	Date	Run	Description	Branch Size (in) (measured from outer wall of tube)	Piece	Spool Size (in)	Orientation	Flow Direction	Branch Leg Position	Slope (in)	Rotation (deg)	Material	Temperature (°C)	Velocity (ft/s)	Reynolds Number	BPI Visual Grade (FI)		BPI Visual Grade (FM)		BPI Visual Grade (PI)		BPI Visual Grade (PM)		Notes
																4	5	4	5	4	5	4	5	
																		(min)	(min)					
820	120102	1	Flow Maintain (40)	4	Elbow	2	Vertical	Up, Horizontal	Parallel to Flow	0	0	PP	63.7	6.68	8.0884E+04	NA	NA	f	2.5	NA	NA	NA	NA	
821	120102	2	Flow Maintain (40)	4	Elbow	2	Vertical	Up, Horizontal	Parallel to Flow	0	0	PP	63.8	6.68	8.0884E+04	NA	NA	1	2.5	NA	NA	NA	NA	
822	120102	3	Flow Maintain (40)	4	Elbow	2	Vertical	Up, Horizontal	Parallel to Flow	0	0	PP	63.9	6.68	8.0884E+04	NA	NA	1	2.5	NA	NA	NA	NA	
823	120102	1	Flow Maintain (45)	4	Elbow	2	Vertical	Up, Horizontal	Parallel to Flow	0	0	PP	59.6	7.52	9.0994E+04	NA	NA	DNR	1	NA	NA	NA	NA	
824	120102	2	Flow Maintain (45)	4	Elbow	2	Vertical	Up, Horizontal	Parallel to Flow	0	0	PP	59.6	7.52	9.0994E+04	NA	NA	DNR	0.75	NA	NA	NA	NA	
825	120102	3	Flow Maintain (45)	4	Elbow	2	Vertical	Up, Horizontal	Parallel to Flow	0	0	PP	59.5	7.52	9.0994E+04	NA	NA	Imm	0.75	NA	NA	NA	NA	
826	120102	1	Flow Maintain (50)	4	Elbow	2	Vertical	Up, Horizontal	Perp to Flow	0	0	PP	58.5	8.35	1.0110E+05	NA	NA	2	DNR	NA	NA	NA	NA	
827	120102	1	Flow Maintain (55)	4	Elbow	2	Vertical	Up, Horizontal	Perp to Flow	0	0	PP	62.0	9.19	1.1121E+05	NA	NA	1	DNR	NA	NA	NA	NA	
828	120102	1	Flow Maintain (60)	4	Elbow	2	Vertical	Up, Horizontal	Perp to Flow	0	0	PP	62.9	10.02	1.2133E+05	NA	NA	Imm	DNR	NA	NA	NA	NA	
829	120102	1	Flow Maintain (65)	4	Elbow	2	Vertical	Up, Horizontal	Perp to Flow	0	0	PP	64.6	10.85	1.3144E+05	NA	NA	Imm	1.5	NA	NA	NA	NA	
830	120102	2	Flow Maintain (65)	4	Elbow	2	Vertical	Up, Horizontal	Perp to Flow	0	0	PP	65.2	10.85	1.3144E+05	NA	NA	Imm	1.5	NA	NA	NA	NA	
831	120102	3	Flow Maintain (65)	4	Elbow	2	Vertical	Up, Horizontal	Perp to Flow	0	0	PP	65.2	10.85	1.3144E+05	NA	NA	Imm	1.5	NA	NA	NA	NA	
832	120104	1	Flow Maintain (3)	1.5	Elbow	0.75	Vertical	Up, Horizontal	Parallel to Flow	0	0	PP	63.3	3.24	1.5427E+04	NA	NA	0.5	1	NA	NA	NA	NA	
833	120104	2	Flow Maintain (3)	1.5	Elbow	0.75	Vertical	Up, Horizontal	Parallel to Flow	0	0	PP	63.1	3.24	1.5427E+04	NA	NA	0.5	1	NA	NA	NA	NA	
834	120104	3	Flow Maintain (3)	1.5	Elbow	0.75	Vertical	Up, Horizontal	Parallel to Flow	0	0	PP	62.9	3.24	1.5427E+04	NA	NA	0.5	1	NA	NA	NA	NA	
835	120104	1	Flow Maintain (10)	1.5	Elbow	0.75	Vertical	Up, Horizontal	Perp to Flow	0	0	PP	64.0	10.80	5.1424E+04	NA	NA	Imm	DNR	NA	NA	NA	NA	
836	120104	1	Flow Maintain (12)	1.5	Elbow	0.75	Vertical	Up, Horizontal	Perp to Flow	0	0	PP	63.7	12.96	6.1708E+04	NA	NA	Imm	1	NA	NA	NA	NA	
837	120104	2	Flow Maintain (12)	1.5	Elbow	0.75	Vertical	Up, Horizontal	Perp to Flow	0	0	PP	63.6	12.96	6.1708E+04	NA	NA	Imm	1	NA	NA	NA	NA	
838	120104	3	Flow Maintain (12)	1.5	Elbow	0.75	Vertical	Up, Horizontal	Perp to Flow	0	0	PP	63.5	12.96	6.1708E+04	NA	NA	Imm	1	NA	NA	NA	NA	
839	120105	1	Flow Maintain (10)	1.5	Straight	0.75	Vertical	Bottom-Top	NA	0	0	PP	65.3	10.77	5.1340E+04	NA	NA	Imm	DNR	NA	NA	NA	NA	
840	120105	1	Flow Maintain (12)	1.5	Straight	0.75	Vertical	Bottom-Top	NA	0	0	PP	64.9	12.91	6.1608E+04	NA	NA	Imm	1.5	NA	NA	NA	NA	
841	120105	2	Flow Maintain (12)	1.5	Straight	0.75	Vertical	Bottom-Top	NA	0	0	PP	64.8	12.91	6.1608E+04	NA	NA	Imm	2	NA	NA	NA	NA	
842	120105	3	Flow Maintain (12)	1.5	Straight	0.75	Vertical	Bottom-Top	NA	0	0	PP	64.8	12.91	6.1608E+04	NA	NA	Imm	2	NA	NA	NA	NA	
843	120105	1	Flow Maintain (60)	4	Straight	2	Vertical	Bottom-Top	NA	0	0	PP	65.2	9.56	1.1852E+05	NA	NA	1	DNR	NA	NA	NA	NA	
844	120105	2	Flow Maintain (60)	4	Straight	2	Vertical	Bottom-Top	NA	0	0	PP	64.1	9.56	1.1852E+05	NA	NA	1	DNR	NA	NA	NA	NA	
845	120105	1	Flow Maintain (72)	4	Straight	2	Vertical	Bottom-Top	NA	0	0	PP	58.6	11.47	1.4223E+05	NA	NA	Imm	DNR	NA	NA	NA	NA	Limited by Configuration, Cavitation occurred
846	120106	1	Flow Maintain (60)	4	Straight	2	Horizontal	NA	NA	0	0	PP	65.9	9.56	1.1852E+05	NA	NA	5	DNR	NA	NA	NA	NA	
847	120106	2	Flow Maintain (60)	4	Straight	2	Horizontal	NA	NA	0	0	PP	66.4	9.56	1.1852E+05	NA	NA	5	DNR	NA	NA	NA	NA	
848	120106	1	Flow Maintain (70)	4	Straight	2	Horizontal	NA	NA	0	0	PP	67.7	11.16	1.3827E+05	NA	NA	2	DNR	NA	NA	NA	NA	
849	120106	2	Flow Maintain (70)	4	Straight	2	Horizontal	NA	NA	0	0	PP	67.7	11.16	1.3827E+05	NA	NA	2	DNR	NA	NA	NA	NA	
850	120106	1	Flow Maintain (70)	4	Straight	2	Horizontal	NA	NA	0	45	PP	67.7	11.16	1.3827E+05	NA	NA	DNR	DNR	NA	NA	NA	NA	
851	120106	2	Flow Maintain (70)	4	Straight	2	Horizontal	NA	NA	0	45	PP	68.0	11.16	1.3827E+05	NA	NA	DNR	DNR	NA	NA	NA	NA	
852	120106	1	Flow Maintain (12)	1.5	Straight	0.75	Horizontal	NA	NA	0	0	PP	63.7	12.91	6.1608E+04	NA	NA	2	2.5	NA	NA	NA	NA	
853	120106	2	Flow Maintain (12)	1.5	Straight	0.75	Horizontal	NA	NA	0	0	PP	63.6	12.91	6.1608E+04	NA	NA	2	2.5	NA	NA	NA	NA	
854	120106	3	Flow Maintain (12)	1.5	Straight	0.75	Horizontal	NA	NA	0	0	PP	63.6	12.91	6.1608E+04	NA	NA	2	2.5	NA	NA	NA	NA	
855	120106	1	Flow Maintain (12)	1.5	Straight	0.75	Horizontal	NA	NA	0	45	PP	63.1	12.91	6.1608E+04	NA	NA	0.5	1	NA	NA	NA	NA	
856	120106	2	Flow Maintain (12)	1.5	Straight	0.75	Horizontal	NA	NA	0	45	PP	63.3	12.91	6.1608E+04	NA	NA	0.5	1	NA	NA	NA	NA	
857	120106	3	Flow Maintain (12)	1.5	Straight	0.75	Horizontal	NA	NA	0	45	PP	63.2	12.91	6.1608E+04	NA	NA	0.5	1	NA	NA	NA	NA	
858	120110	1	Flow Maintain (12)	1.5	Elbow	0.75	Vertical	Horizontal, Down	Perp to Flow	0	0	PP	66.4	12.96	6.1708E+04	NA	NA	Imm	1	NA	NA	NA	NA	
859	120110	2	Flow Maintain (12)	1.5	Elbow	0.75	Vertical	Horizontal, Down	Perp to Flow	0	0	PP	66.2	12.96	6.1708E+04	NA	NA	Imm	1	NA	NA	NA	NA	
860	120110	3	Flow Maintain (12)	1.5	Elbow	0.75	Vertical	Horizontal, Down	Perp to Flow	0	0	PP	65.4	12.96	6.1708E+04	NA	NA	Imm	1	NA	NA	NA	NA	
861	120110	1	Flow Maintain (10)	1.5	Elbow	0.75	Vertical	Horizontal, Down	Perp to Flow	0	0	PP	64.8	10.80	5.1424E+04	NA	NA	Imm	DNR	NA	NA	NA	NA	
862	120110	2	Flow Maintain (10)	1.5	Elbow	0.75	Vertical	Horizontal, Down	Perp to Flow	0	0	PP	64.7	10.80	5.1424E+04	NA	NA	Imm	DNR	NA	NA	NA	NA	
863	120110	3	Flow Maintain (10)	1.5	Elbow	0.75	Vertical	Horizontal, Down	Perp to Flow	0	0	PP	64.5	10.80	5.1424E+04	NA	NA	Imm	DNR	NA	NA	NA	NA	
864	120110	1	Flow Maintain (69)	4	Elbow	2	Vertical	Horizontal, Down	Perp to Flow	0	0	PP	66.9	11.69	1.4155E+05	NA	NA	DNR	DNR	NA	NA	NA	NA	
865	120110	2	Flow Maintain (69)	4	Elbow	2	Vertical	Horizontal, Down	Perp to Flow	0	0	PP	66.4	11.69	1.4155E+05	NA	NA	DNR	DNR	NA	NA	NA	NA	
866	120110	1	Flow Maintain (69), With Back Pressure (30 psi)	4	Elbow	2	Vertical	Horizontal, Down	Perp to Flow	0	0	PP	66.1	11.69	1.4155E+05	NA	NA	NA	NA	NA	NA	NA	DNR	DNR
867	120110	2	Flow Maintain (69), With Back Pressure (40 psi)	4	Elbow	2	Vertical	Horizontal, Down	Perp to Flow	0	0	PP	66.6	11.69	1.4155E+05	NA	NA	NA	NA	NA	NA	DNR	DNR	
868	120112	1	Flow Maintain (45)	4	Elbow	2	Horizontal	NA	Perp to Flow	0	0	PP	69.8	7.52	9.0994E+04	NA	NA	Imm	2	NA	NA	NA	NA	
869	120112	2	Flow Maintain (45)	4	Elbow	2	Horizontal	NA	Perp to Flow	0	0	PP	67.7	7.52	9.0994E+04	NA	NA	Imm	2.5	NA	NA	NA	NA	
870	120112	3	Flow Maintain (45)	4	Elbow	2	Horizontal	NA	Perp to Flow	0	0	PP	66.8	7.52	9.0994E+04	NA	NA	Imm	2	NA	NA	NA	NA	
871	120112	1	Flow Maintain (40)	4	Elbow	2	Horizontal	NA	Perp to Flow	0	0	PP	66.3	6.68	8.0884E+04	NA	NA	Imm	DNR	NA	NA	NA	NA	
872	120112	2	Flow Maintain (40)	4	Elbow	2	Horizontal	NA	Perp to Flow	0	0	PP	65.8	6.68	8.0884E+04	NA	NA	Imm	DNR	NA	NA	NA	NA	
873	120112	3	Flow Maintain (40)	4	Elbow	2	Horizontal	NA	Perp to Flow	0	0	PP	65.2	6.68	8.0884E+04	NA	NA	Imm	DNR	NA	NA	NA	NA	
874	120112	1	Flow Maintain (10)	1.5	Elbow	0.75	Horizontal	NA	Perp to Flow	0	0	PP	64.6	10.80	5.1424E+04	NA	NA	Imm	DNR	NA	NA	NA	NA	
875	120112	2	Flow Maintain (10)	1.5	Elbow	0.75	Horizontal	NA	Perp to Flow	0	0	PP	63.3	10.80	5.1424E+04	NA	NA	Imm	DNR	NA	NA	NA	NA	
876	120112	1	Flow Maintain (12)	1.5	Elbow	0.75	Horizontal	NA	Perp to Flow	0	0	PP	62.9	12.96	6.1708E+04	NA	NA	Imm	2	NA	NA	NA	NA	
877	120112	2	Flow Maintain (12)	1.5	Elbow	0.75	Horizontal	NA	Perp to Flow	0	0	PP	62.8	12.96	6.1708E+04	NA	NA	Imm	2	NA	NA	NA	NA	
878	120112	3	Flow Maintain (12)	1.5	Elbow	0.75	Horizontal	NA	Perp to Flow	0	0	PP	62.6	12.96	6.1708E+04	NA	NA	Imm	2	NA	NA	NA	NA	
879	120113	1	Flow Maintain (65)	3	Elbow	1.5	Vertical	Horizontal, Down	Perp to Flow	0	0	PP	66.9	16.83	1.6367E+05	NA	NA	1	5	NA	NA	NA	NA	Inconsistent fill times

Experiment	Date	Run	Description	Branch Size (in) (measured from outer wall of tube)	Piece	Spool Size (in)	Orientation	Flow Direction	Branch Leg Position	Slope (in)	Rotation (deg)	Material	Temperature (°C)	Velocity (ft/s)	Reynolds Number	BPI Visual Grade (FI)		BPI Visual Grade (FM)		BPI Visual Grade (PI)		BPI Visual Grade (PM)		Notes
																4	5	4	5	4	5	4	5	
																		(min)	(min)					
940	120118	2	Flow Maintain (8)	1.5	Straight	0.75	Vertical	Top-Bottom	NA	0	0	PP	68.7	8.61	4.1072E+04	NA	NA	Imm	DNR	NA	NA	NA	NA	
941	120119	1	Flow Maintain (55)	4	Straight	2	Vertical	Top-Bottom	NA	0	0	PP	73.3	8.77	1.0864E+05	NA	NA	Imm	DNR	NA	NA	NA	NA	
942	120119	2	Flow Maintain (55)	4	Straight	2	Vertical	Top-Bottom	NA	0	0	PP	72.6	8.77	1.0864E+05	NA	NA	Imm	DNR	NA	NA	NA	NA	
943	120119	1	Flow Maintain (60)	4	Straight	2	Vertical	Top-Bottom	NA	0	0	PP	70.5	9.56	1.1852E+05	NA	NA	Imm	DNR	NA	NA	NA	NA	
944	120119	2	Flow Maintain (60)	4	Straight	2	Vertical	Top-Bottom	NA	0	0	PP	61.9	9.56	1.1852E+05	NA	NA	Imm	DNR	NA	NA	NA	NA	
945	120119	1	Flow Maintain (65)	4	Straight	2	Vertical	Top-Bottom	NA	0	0	PP	74.2	10.36	1.2840E+04	NA	NA	Imm	1	NA	NA	NA	NA	
946	120119	2	Flow Maintain (65)	4	Straight	2	Vertical	Top-Bottom	NA	0	0	PP	73.3	10.36	1.2840E+04	NA	NA	Imm	1	NA	NA	NA	NA	
947	120119	3	Flow Maintain (65)	4	Straight	2	Vertical	Top-Bottom	NA	0	0	PP	73.0	10.36	1.2840E+04	NA	NA	Imm	1	NA	NA	NA	NA	
1041	120306	1	Flow Maintain (95)	4	Straight	2	Horizontal	NA	NA	0	90	PP	64.5	15.14	1.8766E+05	NA	NA	Imm	0.5	NA	NA	NA	NA	
1042	120306	2	Flow Maintain (95)	4	Straight	2	Horizontal	NA	NA	0	90	PP	64.3	15.14	1.8766E+05	NA	NA	Imm	0.5	NA	NA	NA	NA	
1043	120306	3	Flow Maintain (95)	4	Straight	2	Horizontal	NA	NA	0	90	PP	63.6	15.14	1.8766E+05	NA	NA	Imm	0.5	NA	NA	NA	NA	
1044	120306	1	Flow Maintain (45)	4	Straight	2	Horizontal	NA	NA	0	90	PP	63.6	7.17	8.8891E+04	NA	NA	3	DNR	NA	NA	NA	NA	
1045	120306	2	Flow Maintain (45)	4	Straight	2	Horizontal	NA	NA	0	90	PP	63.7	7.17	8.8891E+04	NA	NA	3	DNR	NA	NA	NA	NA	
1046	120306	1	Flow Maintain (50)	4	Straight	2	Horizontal	NA	NA	0	90	PP	63.4	7.97	9.8768E+04	NA	NA	1	DNR	NA	NA	NA	NA	
1047	120306	2	Flow Maintain (50)	4	Straight	2	Horizontal	NA	NA	0	90	PP	63.3	7.97	9.8768E+04	NA	NA	1	DNR	NA	NA	NA	NA	
1048	120306	1	Flow Maintain (95)	4	Straight	2	Horizontal	NA	NA	0	45	PP	64.9	15.14	1.8766E+05	NA	NA	Imm	1	NA	NA	NA	NA	
1049	120306	2	Flow Maintain (95)	4	Straight	2	Horizontal	NA	NA	0	45	PP	65.0	15.14	1.8766E+05	NA	NA	Imm	1	NA	NA	NA	NA	
1050	120306	3	Flow Maintain (95)	4	Straight	2	Horizontal	NA	NA	0	45	PP	65.0	15.14	1.8766E+05	NA	NA	Imm	1	NA	NA	NA	NA	
1051	120308	1	Flow Maintain (95)	4	Straight	2	Horizontal	NA	NA	0	0	PP	64.7	15.14	1.8766E+05	NA	NA	Imm	1	NA	NA	NA	NA	
1052	120308	2	Flow Maintain (95)	4	Straight	2	Horizontal	NA	NA	0	0	PP	64.4	15.14	1.8766E+05	NA	NA	Imm	1	NA	NA	NA	NA	
1053	120308	3	Flow Maintain (95)	4	Straight	2	Horizontal	NA	NA	0	0	PP	64.1	15.14	1.8766E+05	NA	NA	Imm	1	NA	NA	NA	NA	
1054	120308	1	Flow Maintain (14)	1.5	Straight	0.75	Horizontal	NA	NA	0	0	PP	64.7	15.07	7.1876E+04	NA	NA	0.5	1	NA	NA	NA	NA	
1055	120308	2	Flow Maintain (14)	1.5	Straight	0.75	Horizontal	NA	NA	0	0	PP	64.5	15.07	7.1876E+04	NA	NA	0.5	1	NA	NA	NA	NA	
1056	120308	3	Flow Maintain (14)	1.5	Straight	0.75	Horizontal	NA	NA	0	0	PP	64.2	15.07	7.1876E+04	NA	NA	0.5	1	NA	NA	NA	NA	
1057	120308	1	Flow Maintain (10)	1.5	Straight	0.75	Horizontal	NA	NA	0	0	PP	62.7	10.77	5.1340E+04	NA	NA	4	DNR	NA	NA	NA	NA	
1058	120308	2	Flow Maintain (10)	1.5	Straight	0.75	Horizontal	NA	NA	0	0	PP	62.6	10.77	5.1340E+04	NA	NA	4	DNR	NA	NA	NA	NA	
1059	120308	1	Flow Maintain (10)	1.5	Straight	0.75	Horizontal	NA	NA	0	45	PP	62.0	10.77	5.1340E+04	NA	NA	3	DNR	NA	NA	NA	NA	
1060	120308	2	Flow Maintain (10)	1.5	Straight	0.75	Horizontal	NA	NA	0	45	PP	61.8	10.77	5.1340E+04	NA	NA	3	DNR	NA	NA	NA	NA	
1061	120308	1	Flow Maintain (4)	1.5	Straight	0.75	Horizontal	NA	NA	0	90	PP	60.9	4.31	2.0536E+04	NA	NA	DNR	DNR	NA	NA	NA	NA	
1062	120308	2	Flow Maintain (4)	1.5	Straight	0.75	Horizontal	NA	NA	0	90	PP	60.8	4.31	2.0536E+04	NA	NA	DNR	DNR	NA	NA	NA	NA	

Experiment	Date	Run	Tee Plus Spool Tests					Tee Plus Spool Tests							Ambient Tests				Notes		
			Description	Branch Sizes (in) (measured from outer wall of tube)	Pieces	Spool and Tee Size (in)	Placement of Tee	Orientation	Flow Direction	Branch Leg Position	Slope (in)	Rotation (deg)	Material	Temperature (°C)	Velocity (ft/s)	Reynolds Number	BPI Visual Grade (Spool)			BPI Visual Grade (Tee)	
																	4 (min)	5 (min)		4 (min)	5 (min)
948	120119	1	Flow Maintain (75)	4	Straight + Tee	2	Before Spool	Horizontal	NA	NA	0	0	PP	63.2	12.30	1.5025E+05	Imm	DNR	Imm	3	
949	120119	2	Flow Maintain (75)	4	Straight + Tee	2	Before Spool	Horizontal	NA	NA	0	0	PP	63.9	12.30	1.5025E+05	Imm	DNR	Imm	3	
950	120119	3	Flow Maintain (75)	4	Straight + Tee	2	Before Spool	Horizontal	NA	NA	0	0	PP	64.4	12.30	1.5025E+05	Imm	DNR	Imm	3	
951	120119	1	Flow Maintain (80)	4	Straight + Tee	2	Before Spool	Horizontal	NA	NA	0	0	PP	65.2	13.11	1.6026E+05	Imm	3	Imm	2	
952	120119	2	Flow Maintain (80)	4	Straight + Tee	2	Before Spool	Horizontal	NA	NA	0	0	PP	65.8	13.11	1.6026E+05	Imm	4	Imm	2	
953	120119	3	Flow Maintain (80)	4	Straight + Tee	2	Before Spool	Horizontal	NA	NA	0	0	PP	66.2	13.11	1.6026E+05	Imm	3	Imm	2	
954	120119	1	Flow Maintain (70)	4	Straight + Tee	2	Before Spool	Horizontal	NA	NA	0	0	PP	67.5	11.48	1.4023E+05	Imm	DNR	Imm	4	
955	120119	2	Flow Maintain (70)	4	Straight + Tee	2	Before Spool	Horizontal	NA	NA	0	0	PP	67.9	11.48	1.4023E+05	Imm	DNR	Imm	4	
956	120119	3	Flow Maintain (70)	4	Straight + Tee	2	Before Spool	Horizontal	NA	NA	0	0	PP	68.4	11.48	1.4023E+05	Imm	DNR	Imm	5	
957	120119	1	Flow Maintain (65)	4	Straight + Tee	2	Before Spool	Horizontal	NA	NA	0	0	PP	69.0	10.66	1.3022E+05	DNR	DNR	Imm	DNR	
958	120119	2	Flow Maintain (65)	4	Straight + Tee	2	Before Spool	Horizontal	NA	NA	0	0	PP	69.3	10.66	1.3022E+05	DNR	DNR	Imm	DNR	
959	120119	3	Flow Maintain (65)	4	Straight + Tee	2	Before Spool	Horizontal	NA	NA	0	0	PP	70.0	10.66	1.3022E+05	DNR	DNR	1	DNR	
960	120120	1	Flow Maintain (75)	4	Straight + Tee	2	Before Spool	Horizontal	NA	NA	0	45	PP	35.7	12.30	1.5025E+05	Imm	DNR	Imm	4	
961	120120	2	Flow Maintain (75)	4	Straight + Tee	2	Before Spool	Horizontal	NA	NA	0	45	PP	37.4	12.30	1.5025E+05	Imm	DNR	Imm	3	
962	120120	3	Flow Maintain (75)	4	Straight + Tee	2	Before Spool	Horizontal	NA	NA	0	45	PP	38.4	12.30	1.5025E+05	Imm	DNR	Imm	3	
963	120120	1	Flow Maintain (80)	4	Straight + Tee	2	Before Spool	Horizontal	NA	NA	0	45	PP	40.6	13.11	1.6026E+05	Imm	4	Imm	3	
964	120120	2	Flow Maintain (80)	4	Straight + Tee	2	Before Spool	Horizontal	NA	NA	0	45	PP	44.6	13.11	1.6026E+05	Imm	3	Imm	2	
965	120120	3	Flow Maintain (80)	4	Straight + Tee	2	Before Spool	Horizontal	NA	NA	0	45	PP	45.3	13.11	1.6026E+05	Imm	3	Imm	2	
966	120120	1	Flow Maintain (70)	4	Straight + Tee	2	Before Spool	Horizontal	NA	NA	0	45	PP	46.6	11.48	1.4023E+05	Imm	DNR	Imm	DNR	
967	120120	2	Flow Maintain (70)	4	Straight + Tee	2	Before Spool	Horizontal	NA	NA	0	45	PP	47.7	11.48	1.4023E+05	Imm	DNR	Imm	DNR	
968	120120	3	Flow Maintain (70)	4	Straight + Tee	2	Before Spool	Horizontal	NA	NA	0	45	PP	48.8	11.48	1.4023E+05	Imm	DNR	Imm	DNR	
969	120124	1	Flow Maintain (55)	4	Straight + Tee	2	Before Spool	Horizontal	NA	NA	0	90	PP	14.8	9.02	1.1018E+05	5	DNR	DNR	DNR	
970	120124	2	Flow Maintain (55)	4	Straight + Tee	2	Before Spool	Horizontal	NA	NA	0	90	PP	16.6	9.02	1.1018E+05	4	DNR	DNR	DNR	
971	120124	1	Flow Maintain (60)	4	Straight + Tee	2	Before Spool	Horizontal	NA	NA	0	90	PP	17.9	9.84	1.2020E+05	3	DNR	DNR	DNR	
972	120124	2	Flow Maintain (60)	4	Straight + Tee	2	Before Spool	Horizontal	NA	NA	0	90	PP	19.8	9.84	1.2020E+05	3	DNR	DNR	DNR	
973	120124	1	Flow Maintain (65)	4	Straight + Tee	2	Before Spool	Horizontal	NA	NA	0	90	PP	22.6	10.66	1.3022E+05	1	DNR	3	DNR	
974	120124	2	Flow Maintain (65)	4	Straight + Tee	2	Before Spool	Horizontal	NA	NA	0	90	PP	24.6	10.66	1.3022E+05	1	5	3	DNR	
975	120124	1	Flow Maintain (70)	4	Straight + Tee	2	Before Spool	Horizontal	NA	NA	0	90	PP	25.5	11.48	1.4023E+05	Imm	2	1	2	Swirling Air, nearly imperceptible
976	120124	2	Flow Maintain (70)	4	Straight + Tee	2	Before Spool	Horizontal	NA	NA	0	90	PP	26.1	11.48	1.4023E+05	Imm	2	1	2	Swirling Air, nearly imperceptible
977	120124	3	Flow Maintain (70)	4	Straight + Tee	2	Before Spool	Horizontal	NA	NA	0	90	PP	26.9	11.48	1.4023E+05	Imm	2	Imm	2	Swirling Air, nearly imperceptible
978	120125	1	Flow Maintain (70)	4	Straight + Tee	2	After Spool	Horizontal	NA	NA	0	0	PP	21.9	11.48	1.4023E+05	Imm	DNR	4	DNR	
979	120125	2	Flow Maintain (70)	4	Straight + Tee	2	After Spool	Horizontal	NA	NA	0	0	PP	23.9	11.48	1.4023E+05	Imm	DNR	4	DNR	
980	120125	3	Flow Maintain (70)	4	Straight + Tee	2	After Spool	Horizontal	NA	NA	0	0	PP	25.3	11.48	1.4023E+05	Imm	DNR	4	DNR	
981	120125	1	Flow Maintain (75)	4	Straight + Tee	2	After Spool	Horizontal	NA	NA	0	0	PP	28.0	12.30	1.5025E+05	Imm	DNR	Imm	DNR	
982	120125	2	Flow Maintain (75)	4	Straight + Tee	2	After Spool	Horizontal	NA	NA	0	0	PP	29.2	12.30	1.5025E+05	Imm	DNR	Imm	DNR	
983	120125	3	Flow Maintain (75)	4	Straight + Tee	2	After Spool	Horizontal	NA	NA	0	0	PP	30.6	12.30	1.5025E+05	Imm	DNR	Imm	DNR	
984	120125	1	Flow Maintain (80)	4	Straight + Tee	2	After Spool	Horizontal	NA	NA	0	0	PP	32.8	13.11	1.6026E+05	Imm	3	Imm	4	
985	120125	2	Flow Maintain (80)	4	Straight + Tee	2	After Spool	Horizontal	NA	NA	0	0	PP	33.9	13.11	1.6026E+05	Imm	3	Imm	4	
986	120125	3	Flow Maintain (80)	4	Straight + Tee	2	After Spool	Horizontal	NA	NA	0	0	PP	35.2	13.11	1.6026E+05	Imm	3	Imm	4	
987	120126	1	Flow Maintain (80)	4	Straight + Tee	2	After Spool	Horizontal	NA	NA	0	45	PP	24.6	13.11	1.6026E+05	Imm	3	Imm	4.5	
988	120126	2	Flow Maintain (80)	4	Straight + Tee	2	After Spool	Horizontal	NA	NA	0	45	PP	26.0	13.11	1.6026E+05	Imm	3	Imm	4.5	
989	120126	3	Flow Maintain (80)	4	Straight + Tee	2	After Spool	Horizontal	NA	NA	0	45	PP	27.5	13.11	1.6026E+05	Imm	3	Imm	4.5	
990	120126	1	Flow Maintain (75)	4	Straight + Tee	2	After Spool	Horizontal	NA	NA	0	45	PP	27.1	12.30	1.5025E+05	Imm	4	Imm	DNR	
991	120126	2	Flow Maintain (75)	4	Straight + Tee	2	After Spool	Horizontal	NA	NA	0	45	PP	27.9	12.30	1.5025E+05	Imm	5	Imm	DNR	
992	120126	1	Flow Maintain (70)	4	Straight + Tee	2	After Spool	Horizontal	NA	NA	0	45	PP	29.9	11.48	1.4023E+05	DNR	DNR	4	DNR	
993	120126	2	Flow Maintain (70)	4	Straight + Tee	2	After Spool	Horizontal	NA	NA	0	45	PP	31.2	11.48	1.4023E+05	DNR	DNR	4	DNR	
994	120127	1	Flow Maintain (55)	4	Straight + Tee	2	After Spool	Horizontal	NA	NA	0	90	PP	25.7	9.02	1.1018E+05	Imm	5	Imm	DNR	

		Tee Plus Spool Tests														Ambient Tests																
Experiment	Date	Run	Description	Branch Sizes (in) (measured from outer wall of tube)	Pieces	Spool and Tee Size (in)	Placement of Tee	Orientation	Flow Direction	Tee Plus Spool Tests				Material	Temperature (°C)	Velocity (ft/s)	Reynolds Number	BPI Visual Grade (Spool)		BPI Visual Grade (Tee)		Notes										
										Branch Leg Position	Slope (in)	Rotation (deg)	Reynolds Number					Reynolds Number	Reynolds Number	Reynolds Number	Reynolds Number		Reynolds Number									
995	120127	2	Flow Maintain (55)	4	Straight + Tee	2	After Spool	Horizontal	NA	NA	0	90	PP	27.1	9.02	1.1018E+05	Imm	DNR	Imm	DNR												
996	120127	3	Flow Maintain (55)	4	Straight + Tee	2	After Spool	Horizontal	NA	NA	0	90	PP	28.7	9.02	1.1018E+05	Imm	5	Imm	DNR												
997	120127	1	Flow Maintain (60)	4	Straight + Tee	2	After Spool	Horizontal	NA	NA	0	90	PP	31.0	9.84	1.2020E+05	Imm	4	Imm	5												
998	120127	2	Flow Maintain (60)	4	Straight + Tee	2	After Spool	Horizontal	NA	NA	0	90	PP	32.1	9.84	1.2020E+05	Imm	4	Imm	DNR												
999	120127	3	Flow Maintain (60)	4	Straight + Tee	2	After Spool	Horizontal	NA	NA	0	90	PP	33.0	9.84	1.2020E+05	Imm	3	Imm	DNR												
1000	120127	1	Flow Maintain (65)	4	Straight + Tee	2	After Spool	Horizontal	NA	NA	0	90	PP	35.2	10.66	1.3022E+05	Imm	2	Imm	4	Swirling Air, nearly imperceptible											
1001	120127	2	Flow Maintain (65)	4	Straight + Tee	2	After Spool	Horizontal	NA	NA	0	90	PP	36.0	10.66	1.3022E+05	Imm	2	Imm	3	Swirling Air, nearly imperceptible											
1002	120127	3	Flow Maintain (65)	4	Straight + Tee	2	After Spool	Horizontal	NA	NA	0	90	PP	36.7	10.66	1.3022E+05	Imm	2	Imm	3	Swirling Air, nearly imperceptible											

Sorted Data BPI Visual Grade in (Flow Increase)													
Experiment	Date	Run	Description	Branch Size	Piece	Size (in)	Orientation	Slope (in)	Rotation (deg)	Material	Temperature (°C)	BPI Visual Grade 4	BPI Visual Grade 5
1	110718	1	Flow Increase (Initial)	L/D of 2	Straight	2	Horizontal	0	0	PP	33.5	55 gpm	60 gpm
2	110718	2	Flow Increase (Initial)	L/D of 2	Straight	2	Horizontal	0	0	PP	34.7	55 gpm	60 gpm
3	110718	3	Flow Increase (Initial)	L/D of 2	Straight	2	Horizontal	0	0	PP	35.8	55 gpm	60 gpm
4	110718	1	Flow Increase (Selected)	L/D of 2	Straight	2	Horizontal	0	0	PP	36.3	52 gpm	58 gpm
5	110718	2	Flow Increase (Selected)	L/D of 2	Straight	2	Horizontal	0	0	PP	36.9	52 gpm	58 gpm
6	110719	3	Flow Increase (Selected)	L/D of 2	Straight	2	Horizontal	0	0	PP	33.6	52 gpm	58 gpm
46	110721	1	Flow Increase (Initial)	L/D of 2	Straight	2	Horizontal	0	45	PP	34.4	55 gpm	65 gpm
47	110721	2	Flow Increase (Initial)	L/D of 2	Straight	2	Horizontal	0	45	PP	34.9	55 gpm	65 gpm
48	110721	3	Flow Increase (Initial)	L/D of 2	Straight	2	Horizontal	0	45	PP	35.3	55 gpm	65 gpm
49	110721	1	Flow Increase (Selected)	L/D of 2	Straight	2	Horizontal	0	45	PP	35.8	60 gpm	65 gpm
50	110721	2	Flow Increase (Selected)	L/D of 2	Straight	2	Horizontal	0	45	PP	36.3	60 gpm	65 gpm
51	110721	3	Flow Increase (Selected)	L/D of 2	Straight	2	Horizontal	0	45	PP	36.8	60 gpm	65 gpm
67	110725	1	Flow Increase	L/D of 2	Straight	2	Horizontal	0	90	PP	28.7	55 gpm	75 gpm
68	110725	2	Flow Increase	L/D of 2	Straight	2	Horizontal	0	90	PP	29.2	55 gpm	75 gpm
69	110725	3	Flow Increase	L/D of 2	Straight	2	Horizontal	0	90	PP	29.7	55 gpm	75 gpm
88	110726	1	Flow Increase (Initial)	L/D of 2	Straight	2	Horizontal	0.010416667	0	PP	28.8	60 gpm	75 gpm
89	110726	2	Flow Increase (Initial)	L/D of 2	Straight	2	Horizontal	0.010416667	0	PP	29.3	60 gpm	75 gpm
90	110726	3	Flow Increase (Initial)	L/D of 2	Straight	2	Horizontal	0.010416667	0	PP	29.7	60 gpm	75 gpm
91	110726	1	Flow Increase (Selected)	L/D of 2	Straight	2	Horizontal	0.010416667	0	PP	30.1	58 gpm	NA
92	110726	2	Flow Increase (Selected)	L/D of 2	Straight	2	Horizontal	0.010416667	0	PP	30.5	58 gpm	NA
93	110726	3	Flow Increase (Selected)	L/D of 2	Straight	2	Horizontal	0.010416667	0	PP	30.8	58 gpm	NA
106	110726	1	Flow Increase (Initial)	L/D of 2	Straight	2	Horizontal	0.010416667	45	PP	34.9	60 gpm	75 gpm
107	110726	2	Flow Increase (Initial)	L/D of 2	Straight	2	Horizontal	0.010416667	45	PP	34.4	60 gpm	75 gpm
108	110726	3	Flow Increase (Initial)	L/D of 2	Straight	2	Horizontal	0.010416667	45	PP	35.4	60 gpm	75 gpm
109	110726	1	Flow Increase (Selected)	L/D of 2	Straight	2	Horizontal	0.010416667	45	PP	35.8	58 gpm	NA
110	110726	2	Flow Increase (Selected)	L/D of 2	Straight	2	Horizontal	0.010416667	45	PP	36.1	58 gpm	NA
111	110726	3	Flow Increase (Selected)	L/D of 2	Straight	2	Horizontal	0.010416667	45	PP	36.5	58 gpm	NA
124	110727	1	Flow Increase (Initial)	L/D of 2	Straight	2	Horizontal	0.010416667	90	PP	35.3	60 gpm	75 gpm
125	110727	2	Flow Increase (Initial)	L/D of 2	Straight	2	Horizontal	0.010416667	90	PP	36.2	60 gpm	75 gpm
126	110727	3	Flow Increase (Initial)	L/D of 2	Straight	2	Horizontal	0.010416667	90	PP	36.5	60 gpm	75 gpm
127	110727	1	Flow Increase (Selected)	L/D of 2	Straight	2	Horizontal	0.010416667	90	PP	36.9	56 gpm	NA
128	110727	2	Flow Increase (Selected)	L/D of 2	Straight	2	Horizontal	0.010416667	90	PP	37.1	56 gpm	NA
129	110727	3	Flow Increase (Selected)	L/D of 2	Straight	2	Horizontal	0.010416667	90	PP	37.5	56 gpm	NA
142	110728	1	Flow Increase (Initial)	L/D of 2	Straight	2	Horizontal	-0.0104166	0	PP	34	60 gpm	75 gpm
143	110728	2	Flow Increase (Initial)	L/D of 2	Straight	2	Horizontal	-0.0104166	0	PP	34.3	60 gpm	75 gpm
144	110728	3	Flow Increase (Initial)	L/D of 2	Straight	2	Horizontal	-0.0104166	0	PP	34.6	60 gpm	75 gpm
145	110728	1	Flow Increase (Selected)	L/D of 2	Straight	2	Horizontal	-0.0104166	0	PP	35	58 gpm	NA
146	110728	2	Flow Increase (Selected)	L/D of 2	Straight	2	Horizontal	-0.0104166	0	PP	35.3	58 gpm	NA
147	110728	3	Flow Increase (Selected)	L/D of 2	Straight	2	Horizontal	-0.0104166	0	PP	35.5	58 gpm	NA
160	110728	1	Flow Increase (Initial)	L/D of 2	Straight	2	Horizontal	-0.0104166	45	PP	38.4	60 gpm	75 gpm
161	110728	2	Flow Increase (Initial)	L/D of 2	Straight	2	Horizontal	-0.0104166	45	PP	38.9	60 gpm	75 gpm
162	110729	3	Flow Increase (Initial)	L/D of 2	Straight	2	Horizontal	-0.0104166	45	PP	39.2	60 gpm	75 gpm
175	110729	1	Flow Increase	L/D of 2	Straight	2	Horizontal	-0.0104166	90	PP	37.2	50 gpm	75 gpm
176	110729	2	Flow Increase	L/D of 2	Straight	2	Horizontal	-0.0104166	90	PP	27.6	50 gpm	75 gpm
177	110801	3	Flow Increase	L/D of 2	Straight	2	Horizontal	-0.0104166	90	PP	28.1	50 gpm	75 gpm
205	110809	1	Flow Increase	L/D of 2	Straight	2	Vertical	0	0	PP	25.4	NA	45 gpm
206	110809	2	Flow Increase	L/D of 2	Straight	2	Vertical	0	0	PP	25.9	NA	45 gpm
207	110809	3	Flow Increase	L/D of 2	Straight	2	Vertical	0	0	PP	26.3	NA	45 gpm
217	110809	1	Flow Increase	L/D of 2	Straight	2	Vertical	-0.0104166	0	PP	28.1	NA	45 gpm
218	110809	2	Flow Increase	L/D of 2	Straight	2	Vertical	-0.0104166	0	PP	28.3	NA	45 gpm
219	110809	3	Flow Increase	L/D of 2	Straight	2	Vertical	-0.0104166	0	PP	28.6	NA	45 gpm
229	110809	1	Flow Increase	L/D of 2	Straight	2	Vertical	0.0104166	0	PP	29.6	NA	45 gpm
230	110809	2	Flow Increase	L/D of 2	Straight	2	Vertical	0.0104166	0	PP	30	NA	45 gpm
231	110809	3	Flow Increase	L/D of 2	Straight	2	Vertical	0.0104166	0	PP	30.2	NA	45 gpm
241	110812	1	Flow Increase	L/D of 2	Straight	2	Horizontal	0	45	PVC	31.8	NA	90 gpm
242	110812	2	Flow Increase	L/D of 2	Straight	2	Horizontal	0	45	PVC	32.2	NA	90 gpm
243	110812	3	Flow Increase	L/D of 2	Straight	2	Horizontal	0	45	PVC	32.4	NA	90 gpm
256	110819	1	Flow Increase	L/D of 2	Straight	2	Vertical	0	0	PP	25.2	45 gpm	60 gpm

257	110819	2	Flow Increase	L/D of 2	Straight	2	Vertical	0	0	PP	25.7	45 gpm	60 gpm
258	110819	3	Flow Increase	L/D of 2	Straight	2	Vertical	0	0	PP	26	45 gpm	60 gpm
265	110819	1	Flow Increase	L/D of 2	Straight	2	Vertical	0.0104166	0	PP	28.3	45 gpm	60 gpm
266	110819	2	Flow Increase	L/D of 2	Straight	2	Vertical	0.0104166	0	PP	28.7	45 gpm	60 gpm
267	110819	3	Flow Increase	L/D of 2	Straight	2	Vertical	0.0104166	0	PP	28.9	45 gpm	60 gpm
274	110822	1	Flow Increase	L/D of 2	Straight	2	Vertical	-0.0104166	0	PP	26.3	45 gpm	60 gpm
275	110822	2	Flow Increase	L/D of 2	Straight	2	Vertical	-0.0104166	0	PP	26.6	45 gpm	60 gpm
276	110822	3	Flow Increase	L/D of 2	Straight	2	Vertical	-0.0104166	0	PP	26.8	45 gpm	60 gpm
283	110823	1	Flow Increase	L/D of 2	Elbow	2	Vertical	0	0	PP	27.4	35 gpm	40 gpm
284	110823	2	Flow Increase	L/D of 2	Elbow	2	Vertical	0	0	PP	27.6	35 gpm	40 gpm
285	110823	3	Flow Increase	L/D of 2	Elbow	2	Vertical	0	0	PP	27.7	35 gpm	40 gpm
292	110823	1	Flow Increase	L/D of 2	Elbow	2	Vertical	0	0	PP	29.1	35 gpm	50 gpm
293	110823	2	Flow Increase	L/D of 2	Elbow	2	Vertical	0	0	PP	29.2	35 gpm	50 gpm
294	110823	3	Flow Increase	L/D of 2	Elbow	2	Vertical	0	0	PP	29.5	35 gpm	50 gpm
301	110824	1	Flow Increase	L/D of 2	Elbow	2	Vertical	0	0	PP	28.1	15 gpm	30 gpm
302	110824	2	Flow Increase	L/D of 2	Elbow	2	Vertical	0	0	PP	28.3	15 gpm	30 gpm
303	110824	3	Flow Increase	L/D of 2	Elbow	2	Vertical	0	0	PP	28.5	15 gpm	30 gpm
304	110824	1	Flow Increase	L/D of 2	Elbow	2	Vertical	0	0	PP	28.5	30 gpm	45 gpm
305	110824	2	Flow Increase	L/D of 2	Elbow	2	Vertical	0	0	PP	28.6	30 gpm	45 gpm
306	110824	3	Flow Increase	L/D of 2	Elbow	2	Vertical	0	0	PP	28.8	30 gpm	45 gpm
313	110825	1	Flow Increase	L/D of 2	Elbow	2	Vertical	0	0	PP	27.7	100 gpm	120 gpm
314	110825	2	Flow Increase	L/D of 2	Elbow	2	Vertical	0	0	PP	28.3	100 gpm	120 gpm
315	110825	3	Flow Increase	L/D of 2	Elbow	2	Vertical	0	0	PP	28.7	100 gpm	120 gpm
322	110825	1	Flow Increase	L/D of 2	Elbow	2	Horizontal	0	0	PP	31.1	20 gpm	45 gpm
323	110825	2	Flow Increase	L/D of 2	Elbow	2	Horizontal	0	0	PP	31.4	20 gpm	45 gpm
324	110825	3	Flow Increase	L/D of 2	Elbow	2	Horizontal	0	0	PP	31.8	20 gpm	45 gpm
331	110825	1	Flow Increase	L/D of 2	Elbow	2	Horizontal	0	0	PP	33.2	15 gpm	30 gpm
332	110825	2	Flow Increase	L/D of 2	Elbow	2	Horizontal	0	0	PP	33.3	15 gpm	30 gpm
333	110825	3	Flow Increase	L/D of 2	Elbow	2	Horizontal	0	0	PP	33.3	15 gpm	30 gpm
337	110830	1	Flow Increase	L/D of 2	Elbow	2	Horizontal	0.0104166	0	PP	23.6	15 gpm	30 gpm
338	110830	2	Flow Increase	L/D of 2	Elbow	2	Horizontal	0.0104166	0	PP	23.8	15 gpm	30 gpm
339	110830	3	Flow Increase	L/D of 2	Elbow	2	Horizontal	0.0104166	0	PP	24	15 gpm	30 gpm
343	110830	1	Flow Increase	L/D of 2	Elbow	2	Horizontal	-0.0104166	0	PP	24.5	15 gpm	30 gpm
344	110830	2	Flow Increase	L/D of 2	Elbow	2	Horizontal	-0.0104166	0	PP	24.9	15 gpm	30 gpm
345	110830	3	Flow Increase	L/D of 2	Elbow	2	Horizontal	-0.0104166	0	PP	24.9	15 gpm	30 gpm
349	110830	1	Flow Increase	L/D of 2	Elbow	2	Horizontal	-0.0104166	0	PP	25.5	45 gpm	50 gpm
350	110830	2	Flow Increase	L/D of 2	Elbow	2	Horizontal	-0.0104166	0	PP	25.8	45 gpm	50 gpm
351	110830	3	Flow Increase	L/D of 2	Elbow	2	Horizontal	-0.0104166	0	PP	26.2	45 gpm	50 gpm
358	110830	1	Flow Increase	L/D of 2	Elbow	2	Horizontal	0.0104166	0	PP	29	45 gpm	50 gpm
359	110830	2	Flow Increase	L/D of 2	Elbow	2	Horizontal	0.0104166	0	PP	29.3	45 gpm	50 gpm
360	110830	3	Flow Increase	L/D of 2	Elbow	2	Horizontal	0.0104166	0	PP	29.6	45 gpm	50 gpm
367	110831	1	Flow Increase	L/D of 2	Elbow	2	Vertical	0	0	PP	28.7	NA	30 gpm
368	110831	2	Flow Increase	L/D of 2	Elbow	2	Vertical	0	0	PP	29	NA	30 gpm
369	110831	3	Flow Increase	L/D of 2	Elbow	2	Vertical	0	0	PP	29.2	NA	30 gpm
373	110831	1	Flow Increase	L/D of 2	Elbow	2	Vertical	0	0	PP	29.3	NA	45 gpm
374	110831	2	Flow Increase	L/D of 2	Elbow	2	Vertical	0	0	PP	29.5	NA	45 gpm
375	110831	3	Flow Increase	L/D of 2	Elbow	2	Vertical	0	0	PP	29.7	NA	45 gpm
385	110913	1	Flow Increase	L/D of 2	Straight	0.75	Horizontal	0	0	PP	25.7	10 gpm	12 gpm
386	110913	2	Flow Increase	L/D of 2	Straight	0.75	Horizontal	0	0	PP	26	10 gpm	12 gpm
387	110913	3	Flow Increase	L/D of 2	Straight	0.75	Horizontal	0	0	PP	26.5	10 gpm	12 gpm
394	110917	1	Flow Increase	L/D of 2	Straight	0.75	Horizontal	0	45	PP	23.4	10 gpm	12 gpm
395	110917	2	Flow Increase	L/D of 2	Straight	0.75	Horizontal	0	45	PP	23.8	10 gpm	12 gpm
396	110917	3	Flow Increase	L/D of 2	Straight	0.75	Horizontal	0	45	PP	24.5	10 gpm	12 gpm
406	110922	1	Flow Increase	L/D of 2	Straight	0.75	Horizontal	0	90	PP	22.6	10 gpm	12 gpm
407	110922	2	Flow Increase	L/D of 2	Straight	0.75	Horizontal	0	90	PP	23	10 gpm	12 gpm
408	110922	3	Flow Increase	L/D of 2	Straight	0.75	Horizontal	0	90	PP	23.3	10 gpm	12 gpm
415	110923	1	Flow Increase	L/D of 2	Straight	0.75	Horizontal	0.0104166	0	PP	24.5	10 gpm	12 gpm
416	110923	2	Flow Increase	L/D of 2	Straight	0.75	Horizontal	0.0104166	0	PP	25.2	10 gpm	12 gpm
417	110923	3	Flow Increase	L/D of 2	Straight	0.75	Horizontal	0.0104166	0	PP	25.8	10 gpm	12 gpm
424	110926	1	Flow Increase	L/D of 2	Straight	0.75	Horizontal	0.0104166	45	PP	24.3	10 gpm	12 gpm
425	110926	2	Flow Increase	L/D of 2	Straight	0.75	Horizontal	0.0104166	45	PP	25	10 gpm	12 gpm
426	110926	3	Flow Increase	L/D of 2	Straight	0.75	Horizontal	0.0104166	45	PP	25.7	10 gpm	12 gpm

433	110927	1	Flow Increase	L/D of 2	Straight	0.75	Horizontal	0.0104166	90	PP	26.5	NA	10 gpm
434	110927	2	Flow Increase	L/D of 2	Straight	0.75	Horizontal	0.0104166	90	PP	26.9	NA	10 gpm
435	110927	3	Flow Increase	L/D of 2	Straight	0.75	Horizontal	0.0104166	90	PP	27.1	NA	10 gpm
442	110929	1	Flow Increase	L/D of 2	Straight	0.75	Horizontal	-0.0104166	0	PP	25	10 gpm	12 gpm
443	110929	2	Flow Increase	L/D of 2	Straight	0.75	Horizontal	-0.0104166	0	PP	25.3	10 gpm	12 gpm
444	110929	3	Flow Increase	L/D of 2	Straight	0.75	Horizontal	-0.0104166	0	PP	25.8	10 gpm	12 gpm
451	110929	1	Flow Increase	L/D of 2	Straight	0.75	Horizontal	-0.0104166	45	PP	27	10 gpm	12 gpm
452	110929	2	Flow Increase	L/D of 2	Straight	0.75	Horizontal	-0.0104166	45	PP	27.4	10 gpm	12 gpm
453	110929	3	Flow Increase	L/D of 2	Straight	0.75	Horizontal	-0.0104166	45	PP	27.7	10 gpm	12 gpm
460	110930	1	Flow Increase	L/D of 2	Straight	0.75	Horizontal	-0.0104166	90	PP	25.6	8 gpm	12 gpm
461	110930	2	Flow Increase	L/D of 2	Straight	0.75	Horizontal	-0.0104166	90	PP	26.3	8 gpm	12 gpm
462	110930	3	Flow Increase	L/D of 2	Straight	0.75	Horizontal	-0.0104166	90	PP	26.8	8 gpm	12 gpm
489	111003	1	Flow Increase	L/D of 2	Straight	1	Horizontal	0	0	PP	23.9	14 gpm	18 gpm
490	111003	2	Flow Increase	L/D of 2	Straight	1	Horizontal	0	0	PP	24.7	14 gpm	18 gpm
491	111003	3	Flow Increase	L/D of 2	Straight	1	Horizontal	0	0	PP	25.2	14 gpm	18 gpm
521	111006	1	Flow Increase	L/D of 2	Straight	0.75	Horizontal	0	0	PP	22.6	8 gpm	12 gpm
522	111006	2	Flow Increase	L/D of 2	Straight	0.75	Horizontal	0	0	PP	22.8	8 gpm	12 gpm
523	111006	3	Flow Increase	L/D of 2	Straight	0.75	Horizontal	0	0	PP	23	8 gpm	12 gpm
BPI Visual Grade 4 & 5 NA				BPI									
Experiment	Date	Run	Description	Branch Size	Piece	Size (in)	Orientation	Slope (in)	Rotation (deg)	Material	Temperature (°C)	BPI Visual Grade 4	BPI Visual Grade 5
7	110719	1	Flow Start-Up (30)	L/D of 2	Straight	2	Horizontal	0	0	PP	34.1	NA	NA
8	110719	2	Flow Start-Up (30)	L/D of 2	Straight	2	Horizontal	0	0	PP	34.2	NA	NA
9	110719	3	Flow Start-Up (30)	L/D of 2	Straight	2	Horizontal	0	0	PP	34.5	NA	NA
10	110719	1	Flow Start-Up (45)	L/D of 2	Straight	2	Horizontal	0	0	PP	34.4	NA	NA
11	110719	2	Flow Start-Up (45)	L/D of 2	Straight	2	Horizontal	0	0	PP	34.6	NA	NA
12	110719	3	Flow Start-Up (45)	L/D of 2	Straight	2	Horizontal	0	0	PP	34.6	NA	NA
13	110719	1	Flow Start-Up (50)	L/D of 2	Straight	2	Horizontal	0	0	PP	34.8	NA	NA
14	110719	2	Flow Start-Up (50)	L/D of 2	Straight	2	Horizontal	0	0	PP	35.3	NA	NA
15	110720	3	Flow Start-Up (50)	L/D of 2	Straight	2	Horizontal	0	0	PP	35.6	NA	NA
28	110720	1	Increase Back Pressure with Maintained Flow (30)	L/D of 2	Straight	2	Horizontal	0	0	PP	31.5	NA	NA
29	110720	2	Increase Back Pressure with Maintained Flow (30)	L/D of 2	Straight	2	Horizontal	0	0	PP	31.8	NA	NA
30	110720	3	Increase Back Pressure with Maintained Flow (30)	L/D of 2	Straight	2	Horizontal	0	0	PP	32.2	NA	NA
70	110725	1	Flow Start-Up (45)	L/D of 2	Straight	2	Horizontal	0	90	PP	30	NA	NA
71	110725	2	Flow Start-Up (45)	L/D of 2	Straight	2	Horizontal	0	90	PP	30.3	NA	NA
72	110725	3	Flow Start-Up (45)	L/D of 2	Straight	2	Horizontal	0	90	PP	30.5	NA	NA
73	110725	1	Flow Start-Up (50)	L/D of 2	Straight	2	Horizontal	0	90	PP	30.8	NA	NA
74	110725	2	Flow Start-Up (50)	L/D of 2	Straight	2	Horizontal	0	90	PP	31	NA	NA
75	110725	3	Flow Start-Up (50)	L/D of 2	Straight	2	Horizontal	0	90	PP	31.3	NA	NA
94	110726	1	Flow Start-Up (45)	L/D of 2	Straight	2	Horizontal	0.010416667	0	PP	31.1	NA	NA
95	110726	2	Flow Start-Up (45)	L/D of 2	Straight	2	Horizontal	0.010416667	0	PP	31.4	NA	NA
96	110726	3	Flow Start-Up (45)	L/D of 2	Straight	2	Horizontal	0.010416667	0	PP	31.7	NA	NA
97	110726	1	Flow Start-Up (50)	L/D of 2	Straight	2	Horizontal	0.010416667	0	PP	32	NA	NA
98	110726	2	Flow Start-Up (50)	L/D of 2	Straight	2	Horizontal	0.010416667	0	PP	32.4	NA	NA
99	110726	3	Flow Start-Up (50)	L/D of 2	Straight	2	Horizontal	0.010416667	0	PP	32.7	NA	NA
112	110726	1	Flow Start-Up (45)	L/D of 2	Straight	2	Horizontal	0.010416667	45	PP	37.1	NA	NA
113	110726	2	Flow Start-Up (45)	L/D of 2	Straight	2	Horizontal	0.010416667	45	PP	37.3	NA	NA
114	110726	3	Flow Start-Up (45)	L/D of 2	Straight	2	Horizontal	0.010416667	45	PP	37.6	NA	NA
115	110726	1	Flow Start-Up (50)	L/D of 2	Straight	2	Horizontal	0.010416667	45	PP	37.8	NA	NA
116	110726	2	Flow Start-Up (50)	L/D of 2	Straight	2	Horizontal	0.010416667	45	PP	38.2	NA	NA
117	110726	3	Flow Start-Up (50)	L/D of 2	Straight	2	Horizontal	0.010416667	45	PP	38.5	NA	NA
130	110727	1	Flow Start-Up (45)	L/D of 2	Straight	2	Horizontal	0.010416667	90	PP	37.7	NA	NA
131	110727	2	Flow Start-Up (45)	L/D of 2	Straight	2	Horizontal	0.010416667	90	PP	38	NA	NA
132	110727	3	Flow Start-Up (45)	L/D of 2	Straight	2	Horizontal	0.010416667	90	PP	38.2	NA	NA
133	110727	1	Flow Start-Up (50)	L/D of 2	Straight	2	Horizontal	0.010416667	90	PP	38	NA	NA
134	110727	2	Flow Start-Up (50)	L/D of 2	Straight	2	Horizontal	0.010416667	90	PP	38.3	NA	NA
135	110727	3	Flow Start-Up (50)	L/D of 2	Straight	2	Horizontal	0.010416667	90	PP	38.7	NA	NA
148	110728	1	Flow Start-Up (45)	L/D of 2	Straight	2	Horizontal	-0.0104166	0	PP	35.9	NA	NA
149	110728	2	Flow Start-Up (45)	L/D of 2	Straight	2	Horizontal	-0.0104166	0	PP	36	NA	NA
150	110728	3	Flow Start-Up (45)	L/D of 2	Straight	2	Horizontal	-0.0104166	0	PP	36.2	NA	NA

151	110728	1	Flow Start-Up (50)	L/D of 2	Straight	2	Horizontal	-0.0104166	0	PP	36.5	NA	NA
152	110728	2	Flow Start-Up (50)	L/D of 2	Straight	2	Horizontal	-0.0104166	0	PP	36.9	NA	NA
153	110728	3	Flow Start-Up (50)	L/D of 2	Straight	2	Horizontal	-0.0104166	0	PP	37.2	NA	NA
166	110729	1	Flow Start-Up (50)	L/D of 2	Straight	2	Horizontal	-0.0104166	45	PP	34.1	NA	NA
167	110729	2	Flow Start-Up (50)	L/D of 2	Straight	2	Horizontal	-0.0104166	45	PP	34.3	NA	NA
168	110729	3	Flow Start-Up (50)	L/D of 2	Straight	2	Horizontal	-0.0104166	45	PP	34.6	NA	NA
352	110830	1	Flow Start-Up (30)	L/D of 2	Elbow	2	Horizontal	-0.0104166	0	PP	26.6	NA	NA
353	110830	2	Flow Start-Up (30)	L/D of 2	Elbow	2	Horizontal	-0.0104166	0	PP	27.1	NA	NA
354	110830	3	Flow Start-Up (30)	L/D of 2	Elbow	2	Horizontal	-0.0104166	0	PP	27.4	NA	NA
361	110831	1	Flow Start-Up (30)	L/D of 2	Elbow	2	Horizontal	0.0104166	0	PP	27.2	NA	NA
362	110831	2	Flow Start-Up (30)	L/D of 2	Elbow	2	Horizontal	0.0104166	0	PP	27.6	NA	NA
363	110831	3	Flow Start-Up (30)	L/D of 2	Elbow	2	Horizontal	0.0104166	0	PP	27.9	NA	NA
376	110831	1	Flow Start-Up (30)	L/D of 2	Elbow	2	Vertical	0	0	PP	30	NA	NA
377	110831	2	Flow Start-Up (30)	L/D of 2	Elbow	2	Vertical	0	0	PP	30.2	NA	NA
378	110831	3	Flow Start-Up (30)	L/D of 2	Elbow	2	Vertical	0	0	PP	30.5	NA	NA
403	110917	1	Pressure Increase	L/D of 2	Straight	0.75	Horizontal	0	0	PP	26.1	NA	NA
404	110917	2	Pressure Increase	L/D of 2	Straight	0.75	Horizontal	0	0	PP	26.6	NA	NA
405	110917	3	Pressure Increase	L/D of 2	Straight	0.75	Horizontal	0	0	PP	27	NA	NA
541	111011	1	Flow Start-Up (15)	SO	Straight	1	Vertical	0	0	PP	23	NA	NA

Sorted Data BPI Visual Grade 4 Data in Min

Experiment	Date	Run	Description	Branch Size	Piece	Size (in)	Orientation	Slope (in)	Rotation (deg)	Material	Temperature (°C)	BPI Visual Grade 4	BPI Visual Grade 5
16	110720	1	Flow Start-Up (55)	L/D of 2	Straight	2	Horizontal	0	0	PP	36	5 min	NA
17	110720	2	Flow Start-Up (55)	L/D of 2	Straight	2	Horizontal	0	0	PP	36.3	5 min	NA
18	110720	3	Flow Start-Up (55)	L/D of 2	Straight	2	Horizontal	0	0	PP	36.1	5 min	NA
58	110721	1	Flow Start-Up (60)	L/D of 2	Straight	2	Horizontal	0	45	PP	39.2	5 min	NA
59	110721	2	Flow Start-Up (60)	L/D of 2	Straight	2	Horizontal	0	45	PP	39.6	5 min	NA
60	110721	3	Flow Start-Up (60)	L/D of 2	Straight	2	Horizontal	0	45	PP	39.9	5 min	NA
76	110725	1	Flow Start-Up (55)	L/D of 2	Straight	2	Horizontal	0	90	PP	31.6	3 min	NA
77	110725	2	Flow Start-Up (55)	L/D of 2	Straight	2	Horizontal	0	90	PP	32	3 min	NA
78	110725	3	Flow Start-Up (55)	L/D of 2	Straight	2	Horizontal	0	90	PP	32.3	3 min	NA
100	110726	1	Flow Start-Up (55)	L/D of 2	Straight	2	Horizontal	0.010416667	0	PP	33.2	6 min	NA
101	110726	2	Flow Start-Up (55)	L/D of 2	Straight	2	Horizontal	0.010416667	0	PP	33.6	6 min	NA
102	110726	3	Flow Start-Up (55)	L/D of 2	Straight	2	Horizontal	0.010416667	0	PP	34	6 min	NA
118	110727	1	Flow Start-Up (55)	L/D of 2	Straight	2	Horizontal	0.010416667	45	PP	32.4	6 min	NA
119	110727	2	Flow Start-Up (55)	L/D of 2	Straight	2	Horizontal	0.010416667	45	PP	32.8	6 min	NA
120	110727	3	Flow Start-Up (55)	L/D of 2	Straight	2	Horizontal	0.010416667	45	PP	33.3	6 min	NA
121	110727	1	Flow Start-Up (60)	L/D of 2	Straight	2	Horizontal	0.010416667	45	PP	33.7	3 min	NA
122	110727	2	Flow Start-Up (60)	L/D of 2	Straight	2	Horizontal	0.010416667	45	PP	34.2	3 min	NA
123	110727	3	Flow Start-Up (60)	L/D of 2	Straight	2	Horizontal	0.010416667	45	PP	34.6	3 min	NA
136	110727	1	Flow Start-Up (55)	L/D of 2	Straight	2	Horizontal	0.010416667	90	PP	39	2 min	NA
137	110727	2	Flow Start-Up (55)	L/D of 2	Straight	2	Horizontal	0.010416667	90	PP	39.3	2 min	NA
138	110727	3	Flow Start-Up (55)	L/D of 2	Straight	2	Horizontal	0.010416667	90	PP	39.5	2 min	NA
154	110728	1	Flow Start-Up (55)	L/D of 2	Straight	2	Horizontal	-0.0104166	0	PP	37.5	5 min	NA
155	110728	2	Flow Start-Up (55)	L/D of 2	Straight	2	Horizontal	-0.0104166	0	PP	37.5	5 min	NA
156	110728	3	Flow Start-Up (55)	L/D of 2	Straight	2	Horizontal	-0.0104166	0	PP	37.9	5 min	NA
169	110729	1	Flow Start-Up (55)	L/D of 2	Straight	2	Horizontal	-0.0104166	45	PP	34.9	6 min	NA
170	110729	2	Flow Start-Up (55)	L/D of 2	Straight	2	Horizontal	-0.0104166	45	PP	35.3	6 min	NA
171	110729	3	Flow Start-Up (55)	L/D of 2	Straight	2	Horizontal	-0.0104166	45	PP	35.8	6 min	NA
172	110729	1	Flow Start-Up (60)	L/D of 2	Straight	2	Horizontal	-0.0104166	45	PP	36.2	2 min	NA
173	110729	2	Flow Start-Up (60)	L/D of 2	Straight	2	Horizontal	-0.0104166	45	PP	36.3	2 min	NA
174	110729	3	Flow Start-Up (60)	L/D of 2	Straight	2	Horizontal	-0.0104166	45	PP	36.7	2 min	NA
178	110801	1	Flow Start-Up (50)	L/D of 2	Straight	2	Horizontal	-0.0104166	90	PP	28.5	2 min	NA
179	110801	2	Flow Start-Up (50)	L/D of 2	Straight	2	Horizontal	-0.0104166	90	PP	28.7	2 min	NA
180	110801	3	Flow Start-Up (50)	L/D of 2	Straight	2	Horizontal	-0.0104166	90	PP	29.1	2 min	NA
259	110819	1	Flow Start-Up (45)	L/D of 2	Straight	2	Vertical	0	0	PP	26.3	2 min	NA
260	110819	2	Flow Start-Up (45)	L/D of 2	Straight	2	Vertical	0	0	PP	26.9	2 min	NA
261	110819	3	Flow Start-Up (45)	L/D of 2	Straight	2	Vertical	0	0	PP	27.3	2 min	NA
268	110819	1	Flow Start-Up (45)	L/D of 2	Straight	2	Vertical	0.0104166	0	PP	29.3	1 min	NA
269	110819	2	Flow Start-Up (45)	L/D of 2	Straight	2	Vertical	0.0104166	0	PP	30	1 min	NA
270	110819	3	Flow Start-Up (45)	L/D of 2	Straight	2	Vertical	0.0104166	0	PP	30.5	1 min	NA

286	110823	1	Flow Start-Up (30)	L/D of 2	Elbow	2	Vertical	0	0	PP	28	5 min	NA
287	110823	2	Flow Start-Up (30)	L/D of 2	Elbow	2	Vertical	0	0	PP	28.3	5 min	NA
288	110823	3	Flow Start-Up (30)	L/D of 2	Elbow	2	Vertical	0	0	PP	28.5	5 min	NA
316	110825	1	Flow Start-Up (90)	L/D of 2	Elbow	2	Vertical	0	0	PP	29.2	4 min	NA
317	110825	2	Flow Start-Up (90)	L/D of 2	Elbow	2	Vertical	0	0	PP	29.6	4 min	NA
318	110825	3	Flow Start-Up (90)	L/D of 2	Elbow	2	Vertical	0	0	PP	30.1	4 min	NA
325	110825	1	Flow Start-Up (30)	L/D of 2	Elbow	2	Horizontal	0	0	PP	31.9	1 min	NA
326	110825	2	Flow Start-Up (30)	L/D of 2	Elbow	2	Horizontal	0	0	PP	32.2	1 min	NA
327	110825	3	Flow Start-Up (30)	L/D of 2	Elbow	2	Horizontal	0	0	PP	32.6	1 min	NA
463	110930	1	Flow Start-Up (8)	L/D of 2	Straight	0.75	Horizontal	-0.0104166	90	PP	27.5	1 min	NA
542	111011	1	Flow Start-Up (19)	SO	Straight	1	Vertical	0	0	PP	23.7	4 min	NA
548	111017	1	Flow Start-Up (8)	L/D of 2	Straight	1	Vertical	0	0	PP	24.2	1 min	NA
549	111017	2	Flow Start-Up (8)	L/D of 2	Straight	1	Vertical	0	0	PP	24.6	1 min	NA
553	111017	1	Flow Start-Up (6)	SO	Straight	1	Vertical	0	0	PP	25.3	1 min	NA
BPI Visual Grade 4 and 5 Data in Min													
Experiment	Date	Run	Description	Branch Size	Piece	Size (in)	Orientation	Slope (in)	Rotation (deg)	Material	Temperature (°C)	BPI Visual Grade 4	BPI Visual Grade 5
19	110720	1	Flow Start-Up (60)	L/D of 2	Straight	2	Horizontal	0	0	PP	36.3	1.5 min	2.5 min
20	110720	2	Flow Start-Up (60)	L/D of 2	Straight	2	Horizontal	0	0	PP	36.5	1.5 min	2.5 min
21	110720	3	Flow Start-Up (60)	L/D of 2	Straight	2	Horizontal	0	0	PP	36.7	1.5 min	2.5 min
22	110720	1	Flow Start-Up (75)	L/D of 2	Straight	2	Horizontal	0	0	PP	36.8	0.25 min	0.5 min
23	110720	2	Flow Start-Up (75)	L/D of 2	Straight	2	Horizontal	0	0	PP	36.9	0.25 min	0.5 min
24	110720	3	Flow Start-Up (75)	L/D of 2	Straight	2	Horizontal	0	0	PP	37	0.25 min	0.5 min
40	110720	1	Maintain Back Pressure with Maintained Flow (30, 60)	L/D of 2	Straight	2	Horizontal	0	0	PP	37.8	2 min	3 min
41	110720	2	Maintain Back Pressure with Maintained Flow (30, 60)	L/D of 2	Straight	2	Horizontal	0	0	PP	38	2 min	3 min
42	110720	3	Maintain Back Pressure with Maintained Flow (30, 60)	L/D of 2	Straight	2	Horizontal	0	0	PP	38.1	2 min	3 min
43	110720	1	Maintain Back Pressure with Maintained Flow (60, 60)	L/D of 2	Straight	2	Horizontal	0	0	PP	37.1	1.5 min	3 min
44	110720	2	Maintain Back Pressure with Maintained Flow (60, 60)	L/D of 2	Straight	2	Horizontal	0	0	PP	37.3	1.5 min	4 min
45	110720	3	Maintain Back Pressure with Maintained Flow (60, 60)	L/D of 2	Straight	2	Horizontal	0	0	PP	37.4	1.5 min	5 min
61	110721	1	Flow Start-Up (65)	L/D of 2	Straight	2	Horizontal	0	45	PP	40.3	1 min	5 min
62	110721	2	Flow Start-Up (65)	L/D of 2	Straight	2	Horizontal	0	45	PP	40.5	1 min	5 min
63	110721	3	Flow Start-Up (65)	L/D of 2	Straight	2	Horizontal	0	45	PP	40.7	1 min	5 min
64	110721	1	Flow Start-Up (75)	L/D of 2	Straight	2	Horizontal	0	45	PP	40.9	0.25 min	1.5 min
65	110721	2	Flow Start-Up (75)	L/D of 2	Straight	2	Horizontal	0	45	PP	41	0.25 min	1.5 min
66	110721	3	Flow Start-Up (75)	L/D of 2	Straight	2	Horizontal	0	45	PP	41.1	0.25 min	1.5 min
79	110725	1	Flow Start-Up (60)	L/D of 2	Straight	2	Horizontal	0	90	PP	32.6	1 min	4 min
80	110725	2	Flow Start-Up (60)	L/D of 2	Straight	2	Horizontal	0	90	PP	32.9	1 min	4 min
81	110725	3	Flow Start-Up (60)	L/D of 2	Straight	2	Horizontal	0	90	PP	33.1	1 min	4 min
103	110726	1	Flow Start-Up (60)	L/D of 2	Straight	2	Horizontal	0.010416667	0	PP	34.4	3 min	5 min
104	110726	2	Flow Start-Up (60)	L/D of 2	Straight	2	Horizontal	0.010416667	0	PP	34.7	3 min	5 min
105	110726	3	Flow Start-Up (60)	L/D of 2	Straight	2	Horizontal	0.010416667	0	PP	34.9	3 min	5 min
139	110727	1	Flow Start-Up (60)	L/D of 2	Straight	2	Horizontal	0.010416667	90	PP	39.8	1 min	3 min
140	110727	2	Flow Start-Up (60)	L/D of 2	Straight	2	Horizontal	0.010416667	90	PP	40	1 min	3 min
141	110727	3	Flow Start-Up (60)	L/D of 2	Straight	2	Horizontal	0.010416667	90	PP	40.1	1 min	3 min
157	110728	1	Flow Start-Up (60)	L/D of 2	Straight	2	Horizontal	-0.0104166	0	PP	38.3	3 min	4 min
158	110728	2	Flow Start-Up (60)	L/D of 2	Straight	2	Horizontal	-0.0104166	0	PP	38.5	3 min	4 min
159	110728	3	Flow Start-Up (60)	L/D of 2	Straight	2	Horizontal	-0.0104166	0	PP	38.3	3 min	4 min
181	110801	1	Flow Start-Up (60)	L/D of 2	Straight	2	Horizontal	-0.0104166	90	PP	28.5	1 min	3 min
182	110801	2	Flow Start-Up (60)	L/D of 2	Straight	2	Horizontal	-0.0104166	90	PP	28.7	1 min	3 min
183	110801	3	Flow Start-Up (60)	L/D of 2	Straight	2	Horizontal	-0.0104166	90	PP	29.1	1 min	3 min
184	110801	1	Flow Increase (verification, 60)	L/D of 2	Straight	2	Horizontal	0	0	PP	29.3	3 min	6 min
185	110801	2	Flow Increase (verification, 60)	L/D of 2	Straight	2	Horizontal	0	0	PP	29.5	3 min	6 min
186	110801	3	Flow Increase (verification, 60)	L/D of 2	Straight	2	Horizontal	0	0	PP	29.7	3 min	6 min
187	110801	1	Flow Increase (verification, 60)	L/D of 2	Straight	2	Horizontal	0	0	PP	30.1	3 min	6 min
188	110801	2	Flow Increase (verification, 60)	L/D of 2	Straight	2	Horizontal	0	0	PP	30.5	3 min	6 min
189	110801	3	Flow Increase (verification, 60)	L/D of 2	Straight	2	Horizontal	0	0	PP	30.8	3 min	6 min
190	110802	1	Flow Start-Up (30)	SO	Straight	2	Horizontal	0	0	PP	30.1	0.25 min	2 min
191	110802	2	Flow Start-Up (30)	SO	Straight	2	Horizontal	0	0	PP	30.2	0.25 min	2 min
192	110802	3	Flow Start-Up (30)	SO	Straight	2	Horizontal	0	0	PP	30.3	0.25 min	2 min
196	110802	1	Flow Start-Up (30)	SO	Straight	2	Horizontal	0	45	PP	30.8	2 min	5.5 min
197	110802	2	Flow Start-Up (30)	SO	Straight	2	Horizontal	0	45	PP	31.2	2 min	5.5 min

198	110802	3	Flow Start-Up (30)	SO	Straight	2	Horizontal	0	45	PP	31.5	2 min	5.5 min
238	110812	1	Flow Start-Up (150)	L/D of 2	Straight	2	Horizontal	0	0	PVC	29.4	1 min	3 min
239	110812	2	Flow Start-Up (150)	L/D of 2	Straight	2	Horizontal	0	0	PVC	30.5	1 min	3 min
240	110812	3	Flow Start-Up (150)	L/D of 2	Straight	2	Horizontal	0	0	PVC	31	1 min	3 min
247	110812	1	Flow Start-Up (60)	Standard	Straight	2	Horizontal	0	0	SS	26	2 min	4.5 min
248	110812	2	Flow Start-Up (60)	Standard	Straight	2	Horizontal	0	0	SS	26.5	2 min	4.5 min
249	110812	3	Flow Start-Up (60)	Standard	Straight	2	Horizontal	0	0	SS	26.8	2 min	4.5 min
262	110819	1	Flow Start-Up (60)	L/D of 2	Straight	2	Vertical	0	0	PP	27.7	1 min	1.5 min
263	110819	2	Flow Start-Up (60)	L/D of 2	Straight	2	Vertical	0	0	PP	27.8	1 min	1.5 min
264	110819	3	Flow Start-Up (60)	L/D of 2	Straight	2	Vertical	0	0	PP	28	1 min	1.5 min
271	110822	1	Flow Start-Up (60)	L/D of 2	Straight	2	Vertical	0.0104166	0	PP	25.7	1 min	1.5 min
272	110822	2	Flow Start-Up (60)	L/D of 2	Straight	2	Vertical	0.0104166	0	PP	26	1 min	1.5 min
273	110822	3	Flow Start-Up (60)	L/D of 2	Straight	2	Vertical	0.0104166	0	PP	26.1	1 min	1.5 min
277	110822	1	Flow Start-Up (45)	L/D of 2	Straight	2	Vertical	-0.0104166	0	PP	27.3	2 min	6 min
278	110822	2	Flow Start-Up (45)	L/D of 2	Straight	2	Vertical	-0.0104166	0	PP	27.7	2 min	6 min
279	110822	3	Flow Start-Up (45)	L/D of 2	Straight	2	Vertical	-0.0104166	0	PP	28.2	2 min	6 min
280	110822	1	Flow Start-Up (60)	L/D of 2	Straight	2	Vertical	-0.0104166	0	PP	28.7	1 min	1.5 min
281	110822	2	Flow Start-Up (60)	L/D of 2	Straight	2	Vertical	-0.0104166	0	PP	28.7	1 min	1.5 min
282	110822	3	Flow Start-Up (60)	L/D of 2	Straight	2	Vertical	-0.0104166	0	PP	28.9	1 min	1.5 min
307	110824	1	Flow Start-Up (30)	L/D of 2	Elbow	2	Vertical	0	0	PP	28.9	1 min	2 min
308	110824	2	Flow Start-Up (30)	L/D of 2	Elbow	2	Vertical	0	0	PP	29.1	1 min	2 min
309	110824	3	Flow Start-Up (30)	L/D of 2	Elbow	2	Vertical	0	0	PP	29.1	1 min	2 min
364	110831	1	Flow Start-Up (45)	L/D of 2	Elbow	2	Horizontal	0.0104166	0	PP	28.1	1 min	4 min
365	110831	2	Flow Start-Up (45)	L/D of 2	Elbow	2	Horizontal	0.0104166	0	PP	28.3	1 min	4 min
366	110831	3	Flow Start-Up (45)	L/D of 2	Elbow	2	Horizontal	0.0104166	0	PP	28.7	1 min	4 min
409	110922	1	Flow Start-Up (10)	L/D of 2	Straight	0.75	Horizontal	0	90	PP	23.4	0.5 min	1 min
410	110922	2	Flow Start-Up (10)	L/D of 2	Straight	0.75	Horizontal	0	90	PP	23.4	0.5 min	2 min
411	110922	3	Flow Start-Up (10)	L/D of 2	Straight	0.75	Horizontal	0	90	PP	23.5	0.5 min	3 min
436	110928	1	Flow Start-Up (8)	L/D of 2	Straight	0.75	Horizontal	0.0104166	90	PP	25.4	4 min	5 min
437	110928	2	Flow Start-Up (8)	L/D of 2	Straight	0.75	Horizontal	0.0104166	90	PP	25.7	4 min	5 min
438	110928	3	Flow Start-Up (8)	L/D of 2	Straight	0.75	Horizontal	0.0104166	90	PP	26	4 min	5 min
515	111004	1	Flow Start-Up (18)	SO	Straight	1	Horizontal	0	45	PP	26	3 min	5 min
516	111004	2	Flow Start-Up (18)	SO	Straight	1	Horizontal	0	45	PP	26.2	3 min	5 min
519	111004	1	Flow Start-Up (19)	SO	Straight	1	Horizontal	0	90	PP	27	1 min	5 min
520	111004	2	Flow Start-Up (19)	SO	Straight	1	Horizontal	0	90	PP	27.3	1 min	5 min
535	111011	1	Flow Start-Up (16)	L/D of 2	Straight	1	Vertical	0	0	PP	21.5	1 min	2 min
536	111011	2	Flow Start-Up (16)	L/D of 2	Straight	1	Vertical	0	0	PP	21.7	1 min	2 min
537	111011	3	Flow Start-Up (16)	L/D of 2	Straight	1	Vertical	0	0	PP	21.9	1 min	2 min
538	111011	1	Flow Start-Up (15)	L/D of 2	Straight	1	Vertical	0	0	PP	22.1	1 min	4 min
539	111011	2	Flow Start-Up (15)	L/D of 2	Straight	1	Vertical	0	0	PP	22.4	1 min	4 min
540	111011	3	Flow Start-Up (15)	L/D of 2	Straight	1	Vertical	0	0	PP	22.6	1 min	4 min
543	111011	1	Flow Start-Up (20)	SO	Straight	1	Vertical	0	0	PP	24	3 min	4 min
544	111011	2	Flow Start-Up (20)	SO	Straight	1	Vertical	0	0	PP	24.2	3 min	4 min
554	111017	2	Flow Start-Up (6)	SO	Straight	1	Vertical	0	0	PP	25.6	1 min	5 min
555	111017	3	Flow Start-Up (6)	SO	Straight	1	Vertical	0	0	PP	25.7	1 min	5 min

Sorted Data for BPI Visual Grade 4 as NA and BPI Visual Grade 5 1mm

Experiment	Date	Run	Description	Branch Size	Piece	Size (in)	Orientation	Slope (in)	Rotation (deg)	Material	Temperature (°C)	BPI Visual Grade 4	BPI Visual Grade 5
25	110720	1	Flow Start-Up (90)	L/D of 2	Straight	2	Horizontal	0	0	PP	37.2	NA	1mm
26	110720	2	Flow Start-Up (90)	L/D of 2	Straight	2	Horizontal	0	0	PP	37.2	NA	1mm
27	110720	3	Flow Start-Up (90)	L/D of 2	Straight	2	Horizontal	0	0	PP	37.2	NA	1mm
82	110725	1	Flow Start-Up (30)	L/D of 2	Straight	2	Horizontal	0	135	PP	32.6	NA	1mm
83	110725	2	Flow Start-Up (30)	L/D of 2	Straight	2	Horizontal	0	135	PP	32.5	NA	1mm
84	110725	3	Flow Start-Up (30)	L/D of 2	Straight	2	Horizontal	0	135	PP	32.5	NA	1mm
85	110725	1	Flow Start-Up (30)	L/D of 2	Straight	2	Horizontal	0	180	PP	32.2	NA	1mm
86	110725	2	Flow Start-Up (30)	L/D of 2	Straight	2	Horizontal	0	180	PP	32.2	NA	1mm
87	110725	3	Flow Start-Up (30)	L/D of 2	Straight	2	Horizontal	0	180	PP	32.2	NA	1mm
193	110802	1	Flow Start-Up (60)	SO	Straight	2	Horizontal	0	0	PP	30.3	NA	1mm
194	110802	2	Flow Start-Up (60)	SO	Straight	2	Horizontal	0	0	PP	30.5	NA	1mm
195	110802	3	Flow Start-Up (60)	SO	Straight	2	Horizontal	0	0	PP	30.5	NA	1mm
199	110802	1	Flow Start-Up (60)	SO	Straight	2	Horizontal	0	45	PP	31.2	NA	1mm

200	110802	2	Flow Start-Up (60)	SO	Straight	2	Horizontal	0	45	PP	31.6	NA	Imm
201	110802	3	Flow Start-Up (60)	SO	Straight	2	Horizontal	0	45	PP	31.6	NA	Imm
202	110802	1	Flow Start-Up (30)	SO	Straight	2	Horizontal	0	90	PP	31.6	NA	Imm
203	110802	2	Flow Start-Up (30)	SO	Straight	2	Horizontal	0	90	PP	31.9	NA	Imm
204	110802	3	Flow Start-Up (30)	SO	Straight	2	Horizontal	0	90	PP	31.8	NA	Imm
214	110809	1	Flow Start-Up (60)	L/D of 2	Straight	2	Vertical	0	0	PP	27.7	NA	Imm
215	110809	2	Flow Start-Up (60)	L/D of 2	Straight	2	Vertical	0	0	PP	27.8	NA	Imm
216	110809	3	Flow Start-Up (60)	L/D of 2	Straight	2	Vertical	0	0	PP	27.9	NA	Imm
226	110809	1	Flow Start-Up (60)	L/D of 2	Straight	2	Vertical	-0.0104166	0	PP	29.4	NA	Imm
227	110809	2	Flow Start-Up (60)	L/D of 2	Straight	2	Vertical	-0.0104166	0	PP	29.4	NA	Imm
228	110809	3	Flow Start-Up (60)	L/D of 2	Straight	2	Vertical	-0.0104166	0	PP	29.4	NA	Imm
244	110812	1	Flow Start-Up (45)	L/D of 2	Straight	2	Horizontal	0	90	PVC	32.7	NA	Imm
245	110812	2	Flow Start-Up (45)	L/D of 2	Straight	2	Horizontal	0	90	PVC	32.7	NA	Imm
246	110812	3	Flow Start-Up (45)	L/D of 2	Straight	2	Horizontal	0	90	PVC	32.7	NA	Imm
251	110818	2	Flow Start-Up (30)	L/D of 2	Straight	2	Vertical	0.0104166	0	PP	24.4	NA	Imm
252	110818	3	Flow Start-Up (30)	L/D of 2	Straight	2	Vertical	0.0104166	0	PP	24.4	NA	Imm
253	110818	1	Flow Start-Up (60)	L/D of 2	Straight	2	Vertical	0.0104166	0	PP	24.5	NA	Imm
254	110818	2	Flow Start-Up (60)	L/D of 2	Straight	2	Vertical	0.0104166	0	PP	24.6	NA	Imm
255	110818	3	Flow Start-Up (60)	L/D of 2	Straight	2	Vertical	0.0104166	0	PP	24.7	NA	Imm
310	110824	1	Flow Start-Up (45)	L/D of 2	Elbow	2	Vertical	0	0	PP	29.3	NA	Imm
311	110824	2	Flow Start-Up (45)	L/D of 2	Elbow	2	Vertical	0	0	PP	29.3	NA	Imm
312	110824	3	Flow Start-Up (45)	L/D of 2	Elbow	2	Vertical	0	0	PP	29.3	NA	Imm
334	110825	1	Flow Start-Up (30)	L/D of 2	Elbow	2	Horizontal	0	0	PP	33.1	NA	Imm
335	110825	2	Flow Start-Up (30)	L/D of 2	Elbow	2	Horizontal	0	0	PP	33.3	NA	Imm
336	110825	3	Flow Start-Up (30)	L/D of 2	Elbow	2	Horizontal	0	0	PP	33.3	NA	Imm
340	110830	1	Flow Start-Up (30)	L/D of 2	Elbow	2	Horizontal	0.0104166	0	PP	24.3	NA	Imm
341	110830	2	Flow Start-Up (30)	L/D of 2	Elbow	2	Horizontal	0.0104166	0	PP	24.3	NA	Imm
342	110830	3	Flow Start-Up (30)	L/D of 2	Elbow	2	Horizontal	0.0104166	0	PP	24.4	NA	Imm
346	110830	1	Flow Start-Up (30)	L/D of 2	Elbow	2	Horizontal	-0.0104166	0	PP	25.1	NA	Imm
347	110830	2	Flow Start-Up (30)	L/D of 2	Elbow	2	Horizontal	-0.0104166	0	PP	25.1	NA	Imm
348	110830	3	Flow Start-Up (30)	L/D of 2	Elbow	2	Horizontal	-0.0104166	0	PP	25.2	NA	Imm
370	110831	1	Flow Start-Up (30)	L/D of 2	Elbow	2	Vertical	0	0	PP	29.2	NA	Imm
371	110831	2	Flow Start-Up (30)	L/D of 2	Elbow	2	Vertical	0	0	PP	29.2	NA	Imm
372	110831	3	Flow Start-Up (30)	L/D of 2	Elbow	2	Vertical	0	0	PP	29.2	NA	Imm
379	110831	1	Flow Start-Up (45)	L/D of 2	Elbow	2	Vertical	0	0	PP	30.6	NA	Imm
380	110831	2	Flow Start-Up (45)	L/D of 2	Elbow	2	Vertical	0	0	PP	30.6	NA	Imm
381	110831	3	Flow Start-Up (45)	L/D of 2	Elbow	2	Vertical	0	0	PP	30.6	NA	Imm
382	110831	1	Flow Start-Up (30)	SO	Elbow	2	Vertical	0	0	PP	30.9	NA	Imm
383	110831	2	Flow Start-Up (30)	SO	Elbow	2	Vertical	0	0	PP	30.9	NA	Imm
384	110831	3	Flow Start-Up (30)	SO	Elbow	2	Vertical	0	0	PP	30.9	NA	Imm
412	110922	1	Flow Start-Up (12)	L/D of 2	Straight	0.75	Horizontal	0	90	PP	23.5	NA	Imm
413	110922	2	Flow Start-Up (12)	L/D of 2	Straight	0.75	Horizontal	0	90	PP	23.6	NA	Imm
414	110922	3	Flow Start-Up (12)	L/D of 2	Straight	0.75	Horizontal	0	90	PP	23.7	NA	Imm
439	110928	1	Flow Start-Up (10)	L/D of 2	Straight	0.75	Horizontal	0.0104166	90	PP	24.5	NA	Imm
440	110928	2	Flow Start-Up (10)	L/D of 2	Straight	0.75	Horizontal	0.0104166	90	PP	25	NA	Imm
441	110928	3	Flow Start-Up (10)	L/D of 2	Straight	0.75	Horizontal	0.0104166	90	PP	25	NA	Imm

Sorted Data for BPI Visual Grade 4 in psig and BPI Visual Grade 5 NA

Experiment	Date	Run	Description	Branch Size	Piece	Size (in)	Orientation	Slope (in)	Rotation (deg)	Material	Temperature (°C)	BPI Visual Grade 4	BPI Visual Grade 5
31	110720	1	Increase Back Pressure with Maintained Flow (45)	L/D of 2	Straight	2	Horizontal	0	0	PP	32.4	45 psig	NA
32	110720	2	Increase Back Pressure with Maintained Flow (45)	L/D of 2	Straight	2	Horizontal	0	0	PP	32.7	45 psig	NA
33	110720	3	Increase Back Pressure with Maintained Flow (45)	L/D of 2	Straight	2	Horizontal	0	0	PP	33.2	45 psig	NA
34	110720	1	Increase Back Pressure with Maintained Flow (50)	L/D of 2	Straight	2	Horizontal	0	0	PP	33.5	30 psig	NA
35	110720	2	Increase Back Pressure with Maintained Flow (50)	L/D of 2	Straight	2	Horizontal	0	0	PP	33.9	30 psig	NA
36	110720	3	Increase Back Pressure with Maintained Flow (50)	L/D of 2	Straight	2	Horizontal	0	0	PP	34.2	30 psig	NA

Sorted Data for BPI Visual Grade 4 in psig and BPI Visual Grade 5 in psig

Experiment	Date	Run	Description	Branch Size	Piece	Size (in)	Orientation	Slope (in)	Rotation (deg)	Material	Temperature (°C)	BPI Visual Grade 4	BPI Visual Grade 5
37	110720	1	Increase Back Pressure with Maintained Flow (60)	L/D of 2	Straight	2	Horizontal	0	0	PP	34.6	2 psig	30 psig
38	110720	2	Increase Back Pressure with Maintained Flow (60)	L/D of 2	Straight	2	Horizontal	0	0	PP	34.9	2 psig	30 psig

39	110720	3	Increase Back Pressure with Maintained Flow (60)	L/D of 2	Straight	2	Horizontal	0	0	PP	35.3	2 psig	30 psig
Sorted Data for BPI Visual Grade 4 in mm and BPI Visual Grade 5 in min and NA													
Experiment	Date	Run	Description	Branch Size	Piece	Size (in)	Orientation	Slope (in)	Rotation (deg)	Material	Temperature (°C)	BPI Visual Grade 4	BPI Visual Grade 5
289	110823	1	Flow Start-Up (40)	L/D of 2	Elbow	2	Vertical	0	0	PP	28.7	Imm	0.75 min
290	110823	2	Flow Start-Up (40)	L/D of 2	Elbow	2	Vertical	0	0	PP	28.8	Imm	0.75 min
291	110823	3	Flow Start-Up (40)	L/D of 2	Elbow	2	Vertical	0	0	PP	28.9	Imm	0.75 min
296	110823	2	Flow Start-Up (40)	L/D of 2	Elbow	2	Vertical	0	0	PP	30.1	Imm	NA
297	110823	3	Flow Start-Up (40)	L/D of 2	Elbow	2	Vertical	0	0	PP	30.4	Imm	NA
298	110823	1	Flow Start-Up (50)	L/D of 2	Elbow	2	Vertical	0	0	PP	30.8	Imm	4.5 min
299	110823	2	Flow Start-Up (50)	L/D of 2	Elbow	2	Vertical	0	0	PP	31.1	Imm	4.5 min
300	110823	3	Flow Start-Up (50)	L/D of 2	Elbow	2	Vertical	0	0	PP	31.3	Imm	4.5 min
319	110825	1	Flow Start-Up (110)	L/D of 2	Elbow	2	Vertical	0	0	PP	30.5	Imm	2 min
320	110825	2	Flow Start-Up (110)	L/D of 2	Elbow	2	Vertical	0	0	PP	30.7	Imm	2 min
321	110825	3	Flow Start-Up (110)	L/D of 2	Elbow	2	Vertical	0	0	PP	31	Imm	2 min
328	110825	1	Flow Start-Up (45)	L/D of 2	Elbow	2	Horizontal	0	0	PP	32.7	Imm	1 min
329	110825	2	Flow Start-Up (45)	L/D of 2	Elbow	2	Horizontal	0	0	PP	32.8	Imm	1 min
330	110825	3	Flow Start-Up (45)	L/D of 2	Elbow	2	Horizontal	0	0	PP	32.9	Imm	1 min
355	110830	1	Flow Start-Up (45)	L/D of 2	Elbow	2	Horizontal	-0.0104166	0	PP	27.7	Imm	4 min
356	110830	2	Flow Start-Up (45)	L/D of 2	Elbow	2	Horizontal	-0.0104166	0	PP	28.4	Imm	4 min
357	110830	3	Flow Start-Up (45)	L/D of 2	Elbow	2	Horizontal	-0.0104166	0	PP	28.6	Imm	4 min
388	110913	1	Flow Start-Up (10)	L/D of 2	Straight	0.75	Horizontal	0	0	PP	26.5	Imm	NA
389	110913	2	Flow Start-Up (10)	L/D of 2	Straight	0.75	Horizontal	0	0	PP	26.7	Imm	NA
390	110913	3	Flow Start-Up (10)	L/D of 2	Straight	0.75	Horizontal	0	0	PP	27	Imm	NA
391	110913	1	Flow Start-Up (12)	L/D of 2	Straight	0.75	Horizontal	0	0	PP	27.1	Imm	1 min
392	110913	2	Flow Start-Up (12)	L/D of 2	Straight	0.75	Horizontal	0	0	PP	27.2	Imm	1 min
393	110913	3	Flow Start-Up (12)	L/D of 2	Straight	0.75	Horizontal	0	0	PP	27.2	Imm	1 min
397	110917	1	Flow Start-Up (10)	L/D of 2	Straight	0.75	Horizontal	0	45	PP	24.9	Imm	4.5 min
398	110917	2	Flow Start-Up (10)	L/D of 2	Straight	0.75	Horizontal	0	45	PP	25.1	Imm	4.5 min
399	110917	3	Flow Start-Up (10)	L/D of 2	Straight	0.75	Horizontal	0	45	PP	25.3	Imm	4.5 min
400	110917	1	Flow Start-Up (12)	L/D of 2	Straight	0.75	Horizontal	0	45	PP	25.3	Imm	1 min
401	110917	2	Flow Start-Up (12)	L/D of 2	Straight	0.75	Horizontal	0	45	PP	25.4	Imm	1 min
402	110917	3	Flow Start-Up (12)	L/D of 2	Straight	0.75	Horizontal	0	45	PP	25.5	Imm	1 min
418	110923	1	Flow Start-Up (10)	L/D of 2	Straight	0.75	Horizontal	0.0104166	0	PP	26.1	Imm	4 min
419	110923	2	Flow Start-Up (10)	L/D of 2	Straight	0.75	Horizontal	0.0104166	0	PP	26.4	Imm	4 min
420	110923	3	Flow Start-Up (10)	L/D of 2	Straight	0.75	Horizontal	0.0104166	0	PP	26.6	Imm	4 min
421	110923	1	Flow Start-Up (12)	L/D of 2	Straight	0.75	Horizontal	0.0104166	0	PP	26.7	Imm	0.75 min
422	110923	2	Flow Start-Up (12)	L/D of 2	Straight	0.75	Horizontal	0.0104166	0	PP	26.7	Imm	0.75 min
423	110923	3	Flow Start-Up (12)	L/D of 2	Straight	0.75	Horizontal	0.0104166	0	PP	26.7	Imm	0.75 min
427	110926	1	Flow Start-Up (10)	L/D of 2	Straight	0.75	Horizontal	0.0104166	45	PP	26.4	Imm	4 min
428	110926	2	Flow Start-Up (10)	L/D of 2	Straight	0.75	Horizontal	0.0104166	45	PP	26.6	Imm	4 min
429	110926	3	Flow Start-Up (10)	L/D of 2	Straight	0.75	Horizontal	0.0104166	45	PP	26.8	Imm	4 min
430	110926	1	Flow Start-Up (12)	L/D of 2	Straight	0.75	Horizontal	0.0104166	45	PP	27	Imm	0.75 min
431	110926	2	Flow Start-Up (12)	L/D of 2	Straight	0.75	Horizontal	0.0104166	45	PP	27	Imm	0.75 min
432	110926	3	Flow Start-Up (12)	L/D of 2	Straight	0.75	Horizontal	0.0104166	45	PP	27	Imm	0.75 min
445	110929	1	Flow Start-Up (10)	L/D of 2	Straight	0.75	Horizontal	-0.0104166	0	PP	25.8	Imm	5 min
446	110929	2	Flow Start-Up (10)	L/D of 2	Straight	0.75	Horizontal	-0.0104166	0	PP	26	Imm	5 min
447	110929	3	Flow Start-Up (10)	L/D of 2	Straight	0.75	Horizontal	-0.0104166	0	PP	26.2	Imm	5 min
448	110929	1	Flow Start-Up (12)	L/D of 2	Straight	0.75	Horizontal	-0.0104166	0	PP	26.4	Imm	1 min
449	110929	2	Flow Start-Up (12)	L/D of 2	Straight	0.75	Horizontal	-0.0104166	0	PP	26.5	Imm	1 min
450	110929	3	Flow Start-Up (12)	L/D of 2	Straight	0.75	Horizontal	-0.0104166	0	PP	26.5	Imm	1 min
454	110930	1	Flow Start-Up (10)	L/D of 2	Straight	0.75	Horizontal	-0.0104166	45	PP	24.5	Imm	4 min
455	110930	2	Flow Start-Up (10)	L/D of 2	Straight	0.75	Horizontal	-0.0104166	45	PP	24.7	Imm	4 min
456	110930	3	Flow Start-Up (10)	L/D of 2	Straight	0.75	Horizontal	-0.0104166	45	PP	24.9	Imm	4 min
457	110930	1	Flow Start-Up (12)	L/D of 2	Straight	0.75	Horizontal	-0.0104166	45	PP	25	Imm	1 min
458	110930	2	Flow Start-Up (12)	L/D of 2	Straight	0.75	Horizontal	-0.0104166	45	PP	25.1	Imm	1 min
459	110930	3	Flow Start-Up (12)	L/D of 2	Straight	0.75	Horizontal	-0.0104166	45	PP	25.1	Imm	1 min
464	110930	2	Flow Start-Up (8)	L/D of 2	Straight	0.75	Horizontal	-0.0104166	90	PP	27.5	Imm	1.5 min
465	110930	3	Flow Start-Up (8)	L/D of 2	Straight	0.75	Horizontal	-0.0104166	90	PP	27.7	Imm	1.5 min
466	110930	1	Flow Start-Up (10)	L/D of 2	Straight	0.75	Horizontal	-0.0104166	90	PP	26.9	Imm	1 min
467	110930	2	Flow Start-Up (10)	L/D of 2	Straight	0.75	Horizontal	-0.0104166	90	PP	27	Imm	1 min

468	110930	3	Flow Start-Up (10)	L/D of 2	Straight	0.75	Horizontal	-0.0104166	90	PP	27.1	Imm	1 min
469	111001	1	Flow Start-Up (8)	SO	Straight	0.75	Horizontal	0	0	PP	25.3	Imm	NA
470	111001	2	Flow Start-Up (8)	SO	Straight	0.75	Horizontal	0	0	PP	25.8	Imm	NA
471	111001	1	Flow Start-Up (10)	SO	Straight	0.75	Horizontal	0	0	PP	26	Imm	NA
472	111001	2	Flow Start-Up (10)	SO	Straight	0.75	Horizontal	0	0	PP	26.2	Imm	NA
473	111001	1	Flow Start-Up (12)	SO	Straight	0.75	Horizontal	0	0	PP	26.5	Imm	NA
474	111001	2	Flow Start-Up (12)	SO	Straight	0.75	Horizontal	0	0	PP	26.8	Imm	NA
475	111001	1	Flow Start-Up (15)	SO	Straight	0.75	Horizontal	0	0	PP	27.3	Imm	2 min
476	111001	2	Flow Start-Up (15)	SO	Straight	0.75	Horizontal	0	0	PP	27.4	Imm	2 min
477	111001	3	Flow Start-Up (15)	SO	Straight	0.75	Horizontal	0	0	PP	27.5	Imm	2 min
478	111001	1	Flow Start-Up (15)	SO	Straight	0.75	Horizontal	0	45	PP	28.6	Imm	1 min
479	111001	2	Flow Start-Up (15)	SO	Straight	0.75	Horizontal	0	45	PP	28.6	Imm	1 min
480	111001	3	Flow Start-Up (15)	SO	Straight	0.75	Horizontal	0	45	PP	28.7	Imm	1 min
481	111001	1	Flow Start-Up (12)	SO	Straight	0.75	Horizontal	0	45	PP	27.9	Imm	NA
482	111001	2	Flow Start-Up (12)	SO	Straight	0.75	Horizontal	0	45	PP	28.1	Imm	NA
483	111001	3	Flow Start-Up (12)	SO	Straight	0.75	Horizontal	0	45	PP	28.4	Imm	NA
484	111001	1	Flow Start-Up (12)	SO	Straight	0.75	Horizontal	0	90	PP	29	Imm	2 min
485	111001	2	Flow Start-Up (12)	SO	Straight	0.75	Horizontal	0	90	PP	29.1	Imm	2 min
486	111001	3	Flow Start-Up (12)	SO	Straight	0.75	Horizontal	0	90	PP	29.3	Imm	2 min
487	111001	1	Flow Start-Up (10)	SO	Straight	0.75	Horizontal	0	90	PP	289.5	Imm	NA
488	111001	2	Flow Start-Up (10)	SO	Straight	0.75	Horizontal	0	90	PP	29.7	Imm	NA
492	111003	1	Flow Start-Up (16)	L/D of 2	Straight	1	Horizontal	0	0	PP	25.5	Imm	2 min
493	111003	2	Flow Start-Up (16)	L/D of 2	Straight	1	Horizontal	0	0	PP	25.6	Imm	2 min
494	111003	3	Flow Start-Up (16)	L/D of 2	Straight	1	Horizontal	0	0	PP	25.8	Imm	2 min
495	111003	1	Flow Start-Up (14)	L/D of 2	Straight	1	Horizontal	0	0	PP	26.3	Imm	NA
496	111003	2	Flow Start-Up (14)	L/D of 2	Straight	1	Horizontal	0	0	PP	26.5	Imm	NA
497	111003	1	Flow Start-Up (16)	L/D of 2	Straight	1	Horizontal	0	45	PP	26.6	Imm	3 min
498	111003	2	Flow Start-Up (16)	L/D of 2	Straight	1	Horizontal	0	45	PP	26.7	Imm	3 min
499	111003	3	Flow Start-Up (16)	L/D of 2	Straight	1	Horizontal	0	45	PP	26.9	Imm	3 min
500	111003	1	Flow Start-Up (14)	L/D of 2	Straight	1	Horizontal	0	45	PP	27.2	Imm	NA
501	111003	2	Flow Start-Up (14)	L/D of 2	Straight	1	Horizontal	0	45	PP	27.5	Imm	NA
502	111003	1	Flow Start-Up (16)	L/D of 2	Straight	1	Horizontal	0	90	PP	27.6	Imm	1 min
503	111003	2	Flow Start-Up (16)	L/D of 2	Straight	1	Horizontal	0	90	PP	27.6	Imm	1 min
504	111003	3	Flow Start-Up (16)	L/D of 2	Straight	1	Horizontal	0	90	PP	27.6	Imm	1 min
505	111003	1	Flow Start-Up (14)	L/D of 2	Straight	1	Horizontal	0	90	PP	27.8	Imm	2 min
506	111003	2	Flow Start-Up (14)	L/D of 2	Straight	1	Horizontal	0	90	PP	27.9	Imm	2 min
507	111003	3	Flow Start-Up (14)	L/D of 2	Straight	1	Horizontal	0	90	PP	28	Imm	2 min
508	111003	1	Flow Start-Up (12)	L/D of 2	Straight	1	Horizontal	0	90	PP	28.2	Imm	3 min
509	111003	2	Flow Start-Up (12)	L/D of 2	Straight	1	Horizontal	0	90	PP	28.3	Imm	3 min
510	111003	3	Flow Start-Up (12)	L/D of 2	Straight	1	Horizontal	0	90	PP	28.4	Imm	3 min
511	111004	1	Flow Start-Up (16)	SO	Straight	1	Horizontal	0	0	PP	25	Imm	NA
512	111004	1	Flow Start-Up (18)	SO	Straight	1	Horizontal	0	0	PP	25.3	Imm	5 min
513	111004	2	Flow Start-Up (18)	SO	Straight	1	Horizontal	0	0	PP	25.6	Imm	5 min
514	111004	3	Flow Start-Up (18)	SO	Straight	1	Horizontal	0	0	PP	25.8	Imm	5 min
524	111007	1	Flow Start-Up (12)	L/D of 2	Straight	0.75	Vertical	0	0	PP	20.7	Imm	1 min
525	111007	2	Flow Start-Up (12)	L/D of 2	Straight	0.75	Vertical	0	0	PP	21	Imm	1 min
526	111007	3	Flow Start-Up (12)	L/D of 2	Straight	0.75	Vertical	0	0	PP	21.1	Imm	1 min
527	111007	1	Flow Start-Up (10)	L/D of 2	Straight	0.75	Vertical	0	0	PP	21.5	Imm	4 min
528	111007	2	Flow Start-Up (10)	L/D of 2	Straight	0.75	Vertical	0	0	PP	21.7	Imm	4 min
529	111007	3	Flow Start-Up (10)	L/D of 2	Straight	0.75	Vertical	0	0	PP	21.9	Imm	4 min
530	111007	1	Flow Start-Up (10)	SO	Straight	0.75	Vertical	0	0	PP	22.2	Imm	NA
531	111007	2	Flow Start-Up (10)	SO	Straight	0.75	Vertical	0	0	PP	22.4	Imm	NA
532	111007	1	Flow Start-Up (12)	SO	Straight	0.75	Vertical	0	0	PP	22.6	Imm	4 min
533	111007	2	Flow Start-Up (12)	SO	Straight	0.75	Vertical	0	0	PP	22.9	Imm	6 min
534	111007	3	Flow Start-Up (12)	SO	Straight	0.75	Vertical	0	0	PP	23.1	Imm	5 min
545	111014	1	Flow Start-Up (10)	L/D of 2	Straight	1	Vertical	0	0	PP	21.5	Imm	1 min
546	111014	2	Flow Start-Up (10)	L/D of 2	Straight	1	Vertical	0	0	PP	21.6	Imm	1 min
547	111014	3	Flow Start-Up (10)	L/D of 2	Straight	1	Vertical	0	0	PP	21.8	Imm	1 min
550	111017	1	Flow Start-Up (8)	SO	Straight	1	Vertical	0	0	PP	24.8	Imm	1 min
551	111017	2	Flow Start-Up (8)	SO	Straight	1	Vertical	0	0	PP	24.7	Imm	1 min
552	111017	3	Flow Start-Up (8)	SO	Straight	1	Vertical	0	0	PP	24.7	Imm	1 min

Spool Component	Nominal Size		Outside Diameter		Inside Diameter		Wall Thickness	
	(inch)	(mm)	(inch)	(mm)	(inch)	(mm)	(inch)	(mm)
Polypropylene Straight Tee (2" L/D of 2)	1.97	50	1.982	50.343	1.601	40.672	0.190	4.836
Polypropylene Elbow (2" L/D of 2)	1.97	50	1.978	50.248	1.564	39.719	0.207	5.264
Polypropylene Straight Tee (2" SO)	1.97	50	1.979	50.260	1.577	40.056	0.201	5.102
Polypropylene Elbow (2" SO)	1.97	50	1.978	50.229	1.561	39.637	0.209	5.296
Polypropylene Straight Tee (0.75" L/D of 2)	0.79	20	0.788	20.003	0.616	15.640	0.086	2.181
Polypropylene Elbow (0.75" L/D of 2)	0.79	20	0.795	20.187	0.615	15.608	0.090	2.289
Polypropylene Straight Tee (0.75" SO)	0.79	20	0.790	20.060	0.618	15.697	0.086	2.181
Polypropylene Elbow (0.75" SO)	0.79	20	0.794	20.174	0.618	15.685	0.088	2.245
Polypropylene Straight Tee (1" L/D of 2)	0.98	25	0.990	25.146	0.783	19.895	0.103	2.626
Polypropylene Elbow (1" L/D of 2)	0.98	25	0.990	25.152	0.786	19.964	0.102	2.594
Polypropylene Straight Tee (1" SO)	0.98	25	0.990	25.152	0.786	19.958	0.102	2.597
Polypropylene Elbow (1" SO)	0.98	25	0.990	25.146	0.785	19.945	0.102	2.600
Polypropylene Straight Tee (1.5" L/D of 2)	1.57	40	1.574	39.980	1.256	31.890	0.159	4.045
Polypropylene Elbow (1.5" L/D of 2)	1.57	40	1.582	40.183	1.259	31.979	0.162	4.102
Polypropylene Straight Tee (1.5" SO)	1.57	40	1.571	39.897	1.248	31.687	0.162	4.105
Polypropylene Elbow (1.5" SO)	1.57	40	1.582	40.176	1.264	32.099	0.159	4.039
Polypropylene Tee (2")	1.97	50	1.952	49.572	1.557	39.535	0.198	5.019
PVC Straight Tube	1.5	38.1	1.900	48.266	1.573	39.948	0.164	4.159
PVC Tee	1.5	38.1	2.236	56.782	1.831	46.507	0.202	5.137
Stainless Steel Pipe	2	50.8	2.004	50.889	1.863	47.320	0.070	1.784
Stainless Steel Tee (Standard)	2	50.8	1.998	50.743	1.872	47.536	0.063	1.603

APPENDIX G: REPRESENTATIVE TEST GRAPHS

The following graphs are the committee's test results:

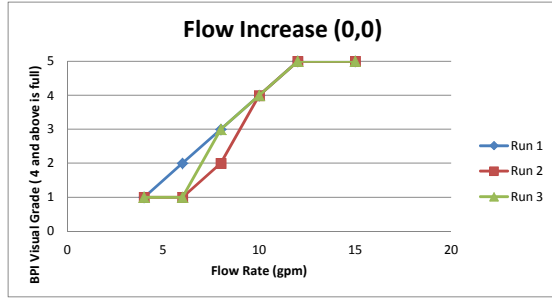
- 3/4 inch graphs
- 1 inch graphs
- 1.5 inch graphs
- 2 inch graphs

- 2 inch Horizontal Air Scale Test graphs
- Hot Test graphs
- Tee-Plus graphs
- Time to Clear

3/4 in 2D Horizontal Flow Increase

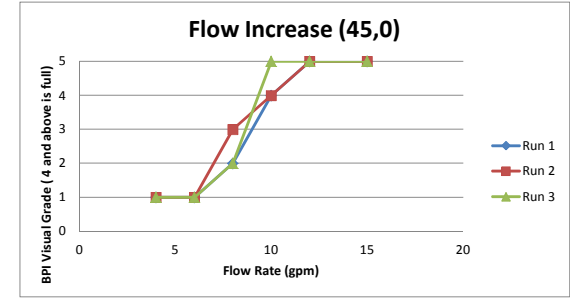
Experiment 385-387

Flow Rate	Run 1	Run 2	Run 3
4	1	1	1
6	2	1	1
8	3	2	3
10	4	4	4
12	5	5	5
15	5	5	5



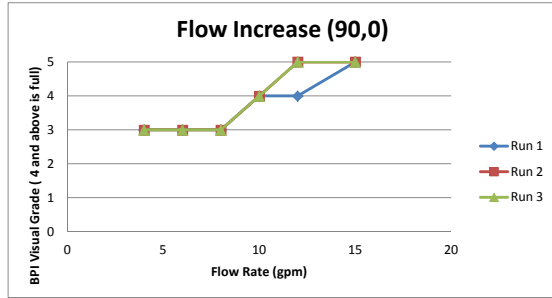
Experiment 394-396

Flow Rate	Run 1	Run 2	Run 3
4	1	1	1
6	1	1	1
8	2	3	2
10	4	4	5
12	5	5	5
15	5	5	5



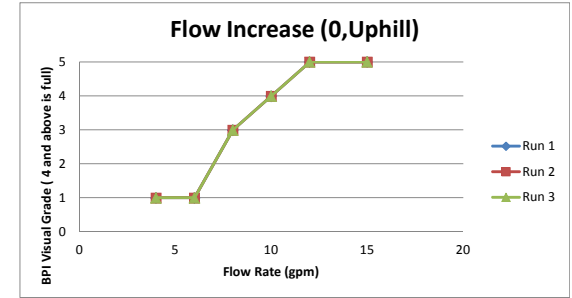
Experiment 406-408

Flow Rate	Run 1	Run 2	Run 3
4	3	3	3
6	3	3	3
8	3	3	3
10	4	4	4
12	4	5	5
15	5	5	5



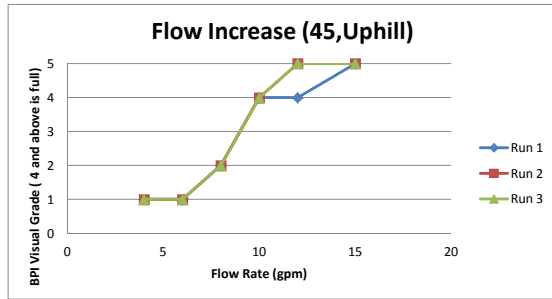
Experiment 415-417

Flow Rate	Run 1	Run 2	Run 3
4	1	1	1
6	1	1	1
8	3	3	3
10	4	4	4
12	5	5	5
15	5	5	5



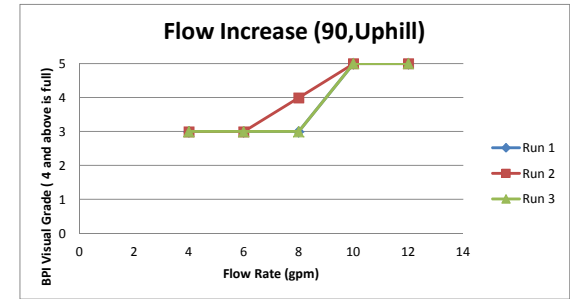
Experiment 424-426

Flow Rate	Run 1	Run 2	Run 3
4	1	1	1
6	1	1	1
8	2	2	2
10	4	4	4
12	4	5	5
15	5	5	5



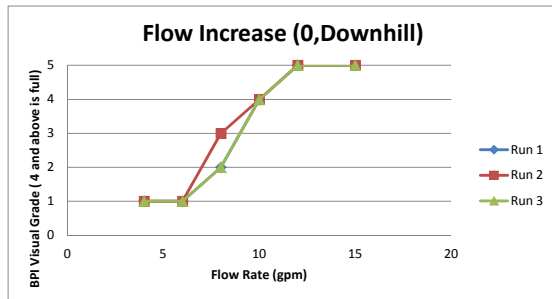
Experiment 433-435

Flow Rate	Run 1	Run 2	Run 3
4	3	3	3
6	3	3	3
8	3	4	3
10	5	5	5
12	5	5	5



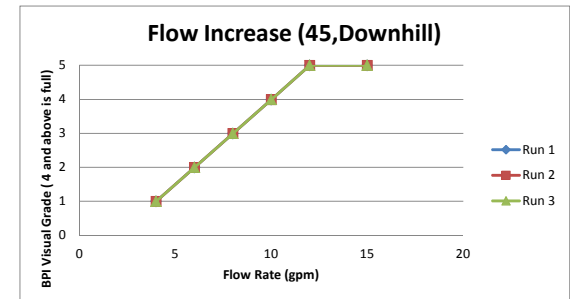
Experiment 442-444

Flow Rate	Run 1	Run 2	Run 3
4	1	1	1
6	1	1	1
8	2	3	2
10	4	4	4
12	5	5	5
15	5	5	5



Experiment 451-453

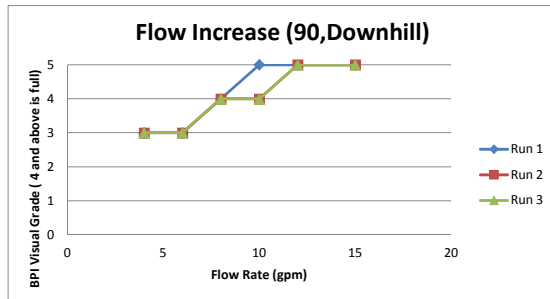
Flow Rate	Run 1	Run 2	Run 3
4	1	1	1
6	2	2	2
8	3	3	3
10	4	4	4
12	5	5	5
15	5	5	5



3/4 in 2D Horizontal Flow Increase

Experiment 460-462

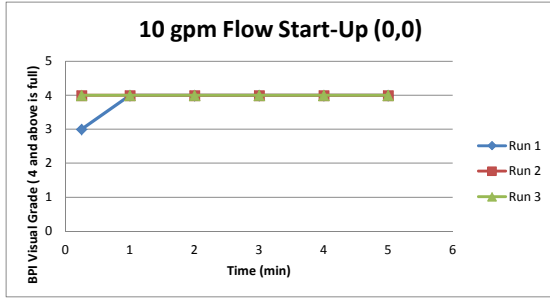
Flow Rate	Run 1	Run 2	Run 3
4	3	3	3
6	3	3	3
8	4	4	4
10	5	4	4
12	5	5	5
15	5	5	5



3/4 inch 2D Horizontal Flow Maintain

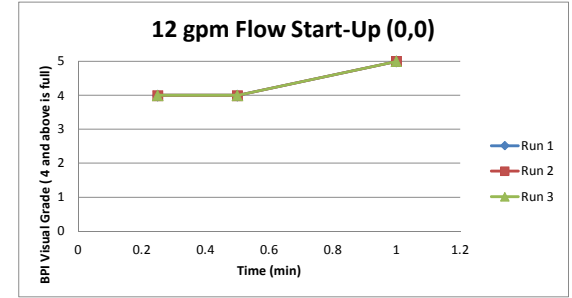
Experiment 388-390

Time	Run 1	Run 2	Run 3
0.25	3	4	4
1	4	4	4
2	4	4	4
3	4	4	4
4	4	4	4
5	4	4	4



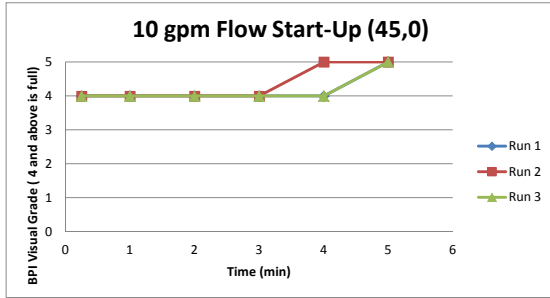
Experiment 391-393

Time	Run 1	Run 2	Run 3
0.25	4	4	4
0.5	4	4	4
1	5	5	5



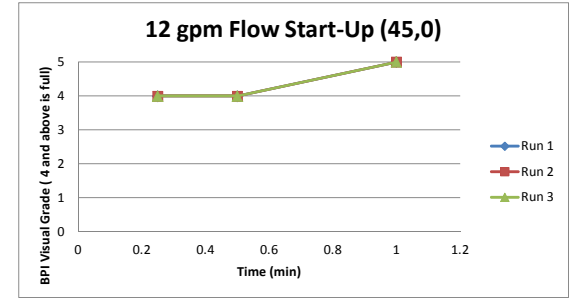
Experiment 397-399

Time	Run 1	Run 2	Run 3
0.25	4	4	4
1	4	4	4
2	4	4	4
3	4	4	4
4	4	5	4
5	5	5	5



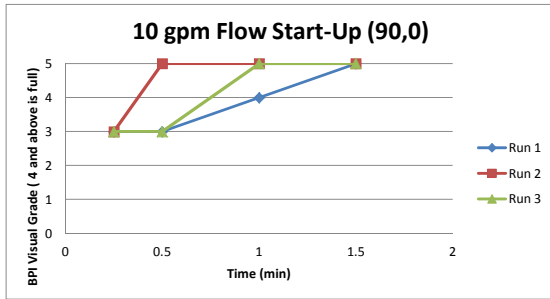
Experiment 400-402

Time	Run 1	Run 2	Run 3
0.25	4	4	4
0.5	4	4	4
1	5	5	5



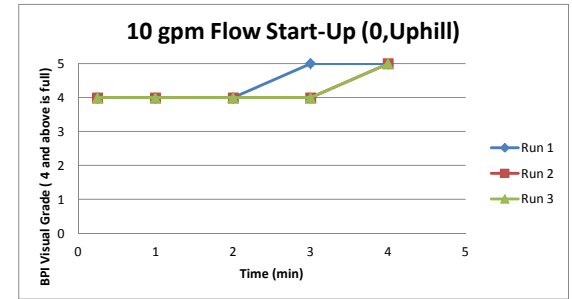
Experiment 409-411

Time	Run 1	Run 2	Run 3
0.25	3	3	3
0.5	3	5	3
1	4	5	5
1.5	5	5	5



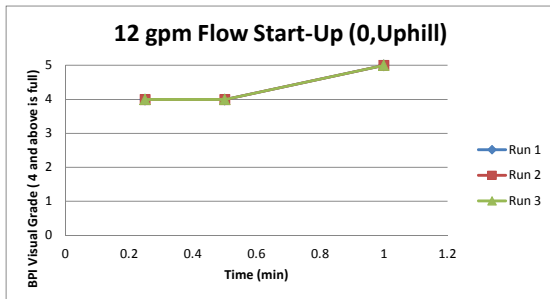
Experiment 418-420

Time	Run 1	Run 2	Run 3
0.25	4	4	4
1	4	4	4
2	4	4	4
3	5	4	4
4	5	5	5



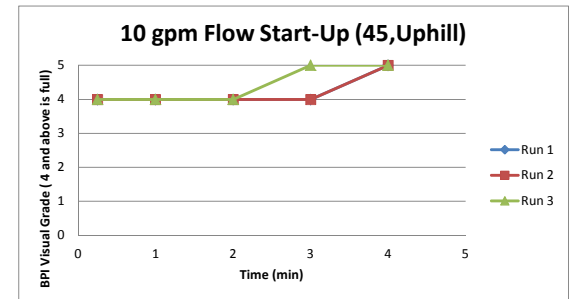
Experiment 421-423

Time	Run 1	Run 2	Run 3
0.25	4	4	4
0.5	4	4	4
1	5	5	5



Experiment 427-429

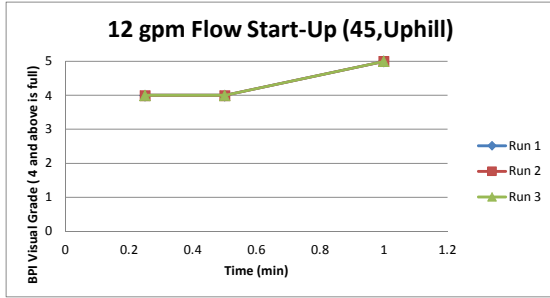
Time	Run 1	Run 2	Run 3
0.25	4	4	4
1	4	4	4
2	4	4	4
3	4	4	5
4	5	5	5



3/4 inch 2D Horizontal Flow Maintain

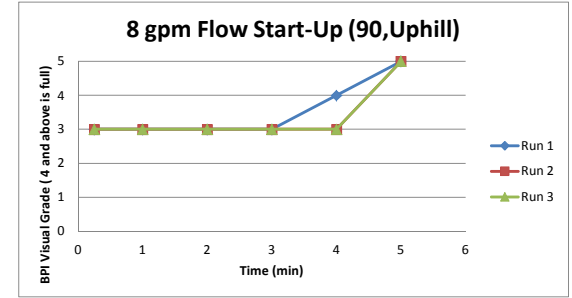
Experiment 430-432

Time	Run 1	Run 2	Run 3
0.25	4	4	4
0.5	4	4	4
1	5	5	5



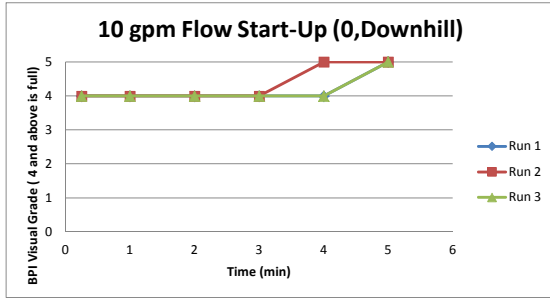
Experiment 436-438

Time	Run 1	Run 2	Run 3
0.25	3	3	3
1	3	3	3
2	3	3	3
3	3	3	3
4	4	4	3
5	5	5	5



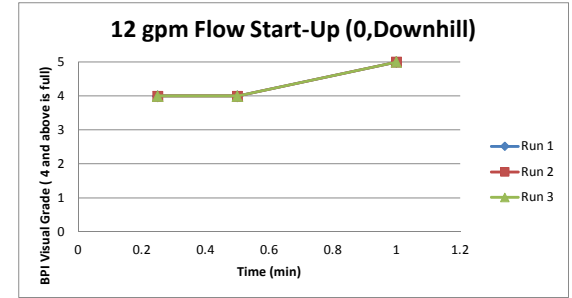
Experiment 445-447

Time	Run 1	Run 2	Run 3
0.25	4	4	4
1	4	4	4
2	4	4	4
3	4	4	4
4	4	5	4
5	5	5	5



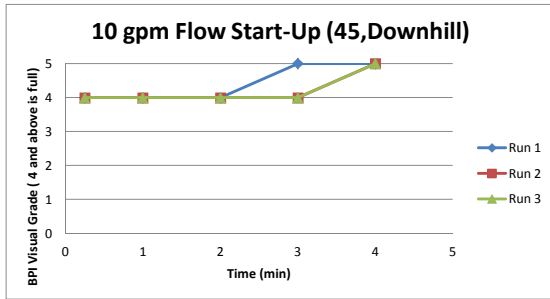
Experiment 448-450

Time	Run 1	Run 2	Run 3
0.25	4	4	4
0.5	4	4	4
1	5	5	5



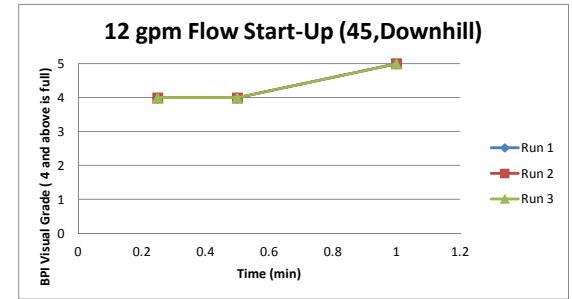
Experiment 454-456

Time	Run 1	Run 2	Run 3
0.25	4	4	4
1	4	4	4
2	4	4	4
3	5	4	4
4	5	5	5



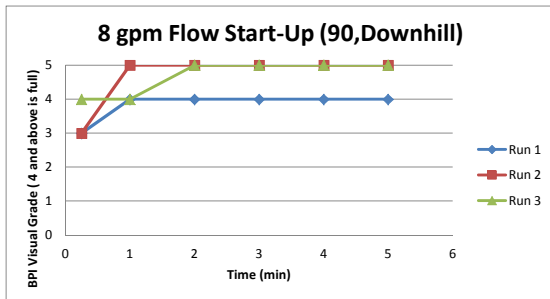
Experiment 457-459

Time	Run 1	Run 2	Run 3
0.25	4	4	4
0.5	4	4	4
1	5	5	5



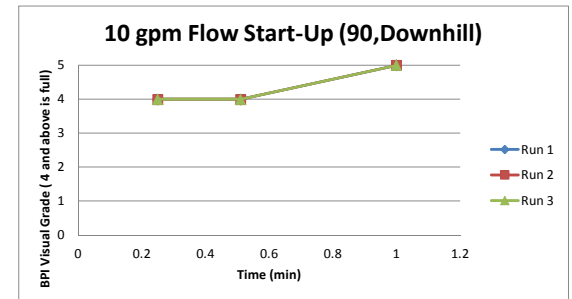
Experiment 463-465

Time	Run 1	Run 2	Run 3
0.25	3	3	4
1	4	5	4
2	4	5	5
3	4	5	5
4	4	5	5
5	4	5	5



Experiment 466-468

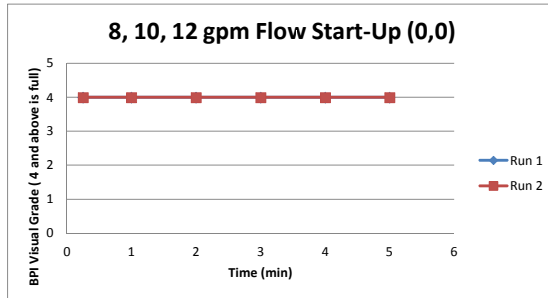
Time	Run 1	Run 2	Run 3
0.25	4	4	4
0.51	4	4	4
1	5	5	5



3/4 inch SO Horizontal Tests

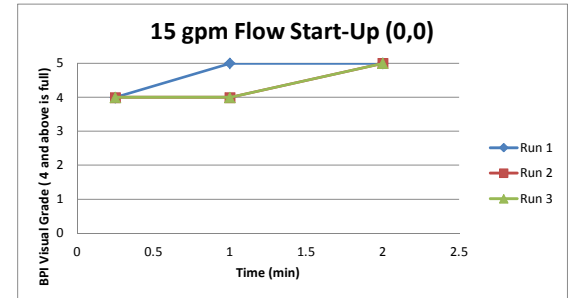
Experiment 469-474

Time	Run 1	Run 2
0.25	4	4
1	4	4
2	4	4
3	4	4
4	4	4
5	4	4



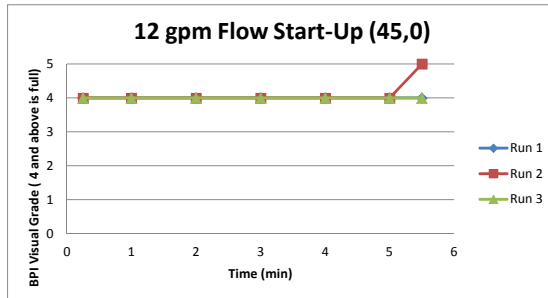
Experiment 475-477

Time	Run 1	Run 2	Run 3
0.25	4	4	4
1	5	4	4
2	5	5	5



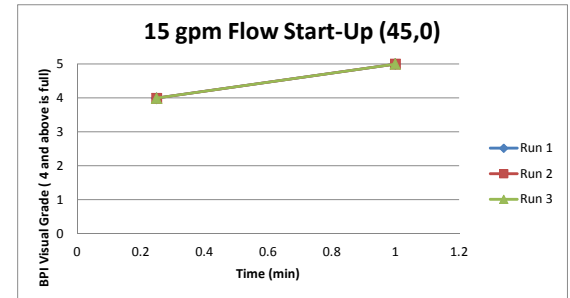
Experiment 478-480

Time	Run 1	Run 2	Run 3
0.25	4	4	4
1	4	4	4
2	4	4	4
3	4	4	4
4	4	4	4
5	4	4	4
5.5	4	5	4



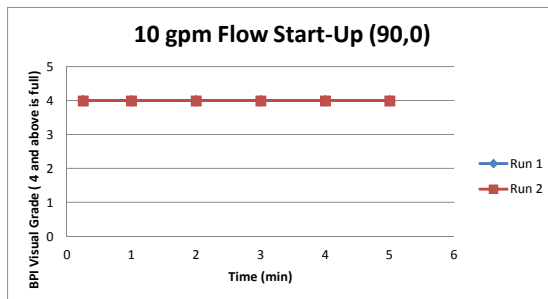
Experiment 481-483

Time	Run 1	Run 2	Run 3
0.25	4	4	4
1	5	5	5



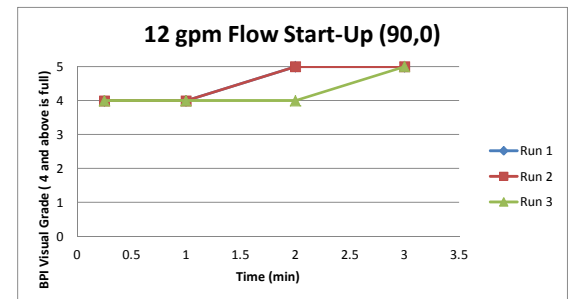
Experiment 487-488

Time	Run 1	Run 2
0.25	4	4
1	4	4
2	4	4
3	4	4
4	4	4
5	4	4



Experiment 484-486

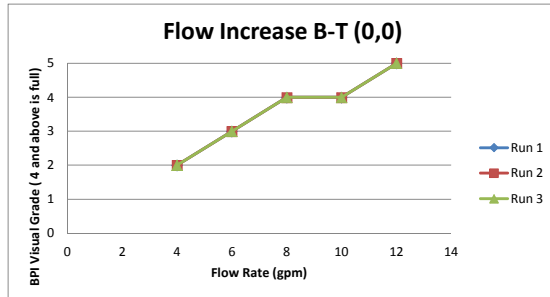
Time	Run 1	Run 2	Run 3
0.25	4	4	4
1	4	4	4
2	5	5	4
3	5	5	5



3/4 inch 2D Vertical Flow Increase

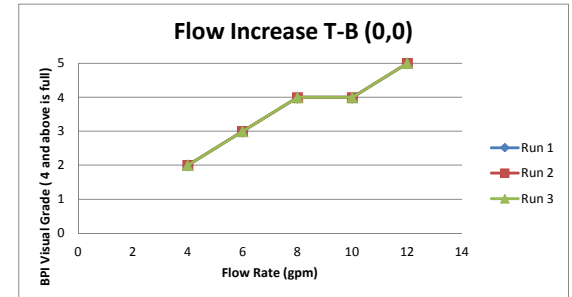
Experiment 521-523

Flow Rate	Run 1	Run 2	Run 3
4	2	2	2
6	3	3	3
8	4	4	4
10	4	4	4
12	5	5	5



Experiment 561-563

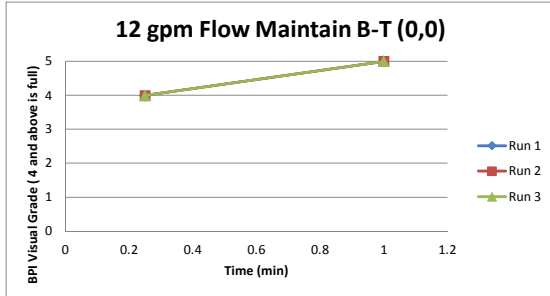
Flow Rate	Run 1	Run 2	Run 3
4	4	4	4
6	4	4	4
8	4	4	4
10	5	5	5



3/4 inch 2D Vertical Flow Maintain

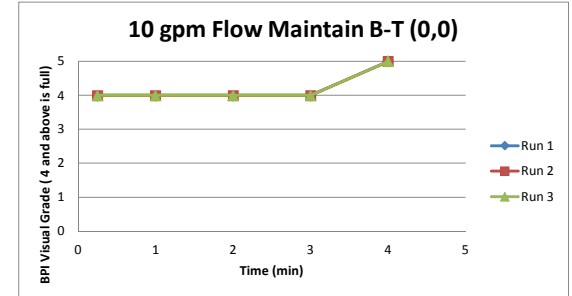
Experiement 524-526

Time	Run 1	Run 2	Run 3
0.25	4	4	4
1	5	5	5



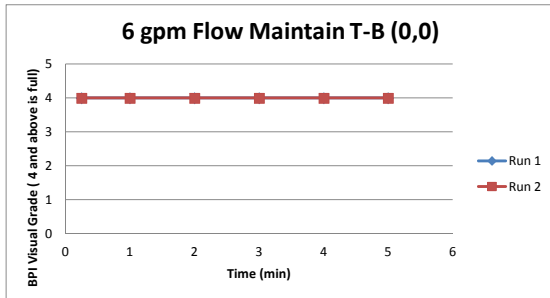
Experiement 527-529

Time	Run 1	Run 2	Run 3
0.25	4	4	4
1	4	4	4
2	4	4	4
3	4	4	4
4	5	5	5



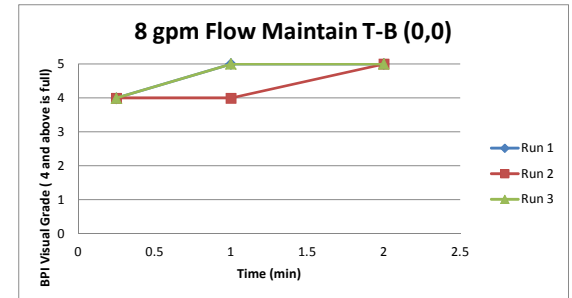
Experiement 556-557

Time	Run 1	Run 2
0.25	4	4
1	4	4
2	4	4
3	4	4
4	4	4
5	4	4



Experiement 558-560

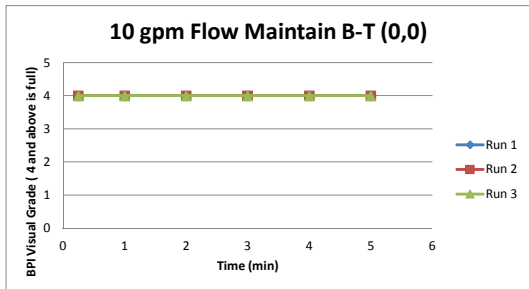
Time	Run 1	Run 2	Run 3
0.25	4	4	4
1	5	4	5
2	5	5	5



3/4 inch SO Vertical Tests

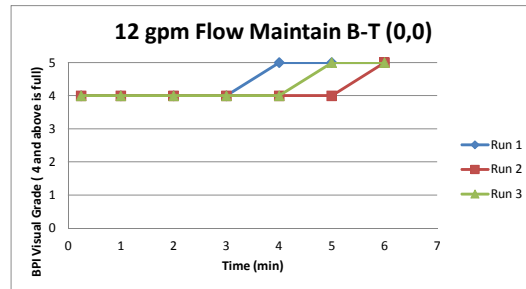
Experiement 530-531

Time	Run 1	Run 2	Run 3
0.25	4	4	4
1	4	4	4
2	4	4	4
3	4	4	4
4	4	4	4
5	4	4	4



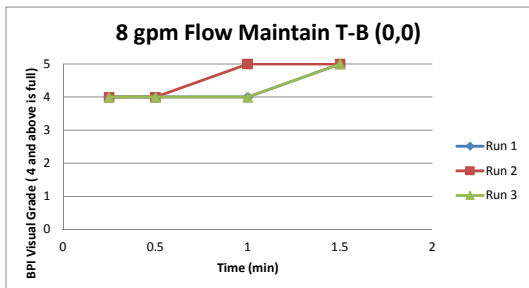
Experiement 532-534

Time	Run 1	Run 2	Run 3
0.25	4	4	4
1	4	4	4
2	4	4	4
3	4	4	4
4	5	4	4
5	5	4	5
6	5	5	5



Experiement 565-567

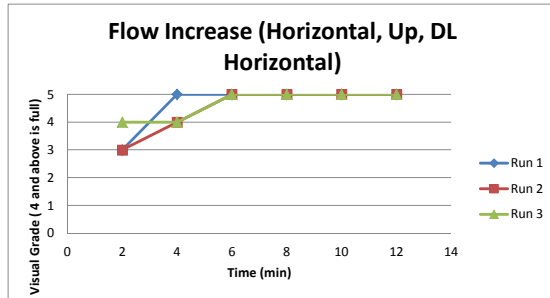
Time	Run 1	Run 2	Run 3
0.25	4	4	4
0.5	4	4	4
1	4	5	4
1.5	5	5	5



3/4 inch 2D Elbow Flow Increase

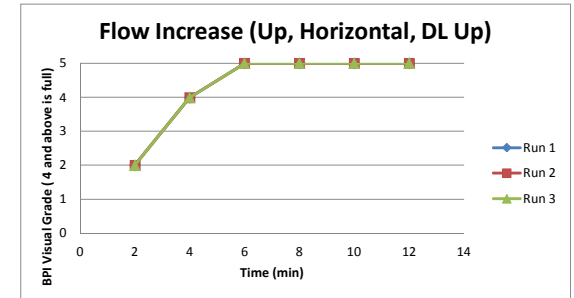
Experiement 618-620

Flow	Run 1	Run 2	Run 3
2	3	3	4
4	5	4	4
6	5	5	5
8	5	5	5
10	5	5	5
12	5	5	5



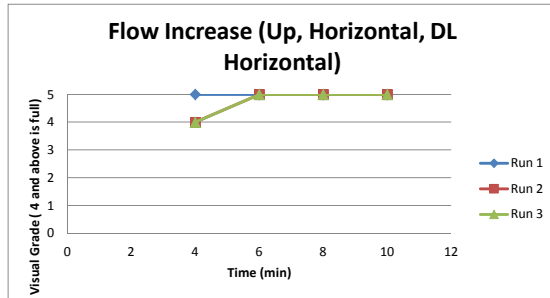
Experiement 655-657

Flow	Run 1	Run 2	Run 3
2	2	2	2
4	4	4	4
6	5	5	5
8	5	5	5
10	5	5	5
12	5	5	5



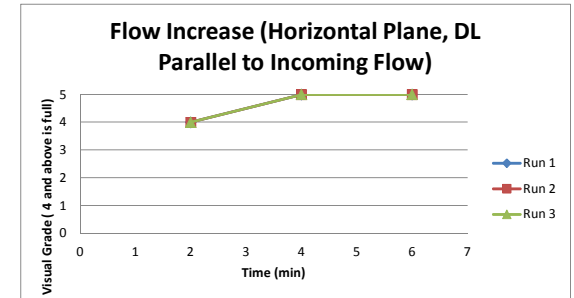
Experiement 626-628

Flow	Run 1	Run 2	Run 3
4	5	4	4
6	5	5	5
8	5	5	5
10	5	5	5



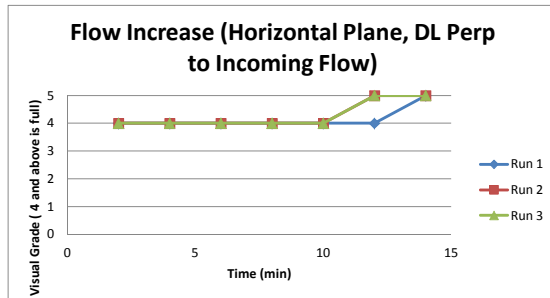
Experiement 666-668

Flow	Run 1	Run 2	Run 3
2	4	4	4
4	5	5	5
6	5	5	5



Experiement 683-685

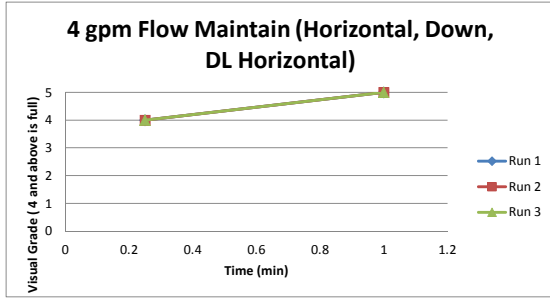
Flow	Run 1	Run 2	Run 3
2	4	4	4
4	4	4	4
6	4	4	4
8	4	4	4
10	4	4	4
12	4	5	5
14	5	5	5



3/4 inch 2D Elbow Flow Maintain

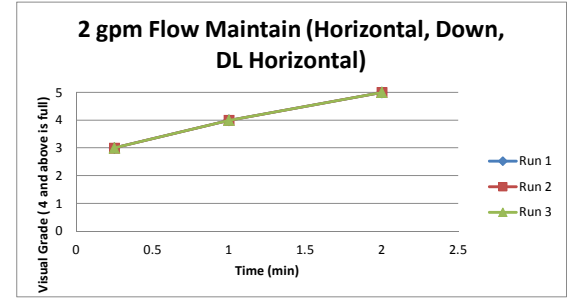
Experiement 568-570

Time	Run 1	Run 2	Run 3
0.25	4	4	4
1	5	5	5



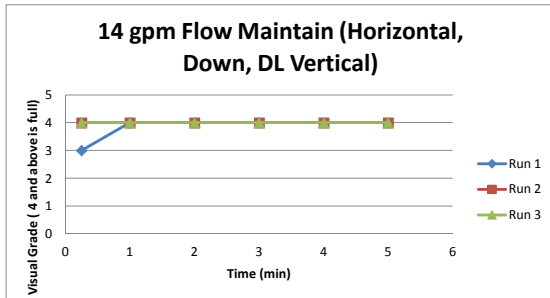
Experiement 571-572

Time	Run 1	Run 2	Run 3
0.25	3	3	3
1	4	4	4
2	5	5	5



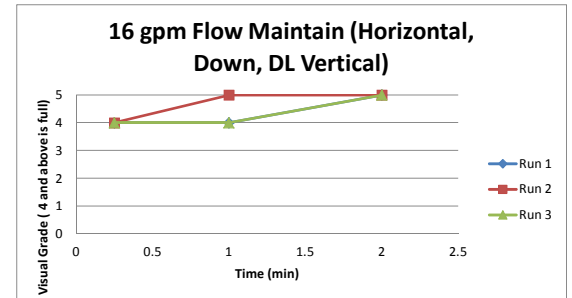
Experiement 573-575

Time	Run 1	Run 2	Run 3
0.25	3	4	4
1	4	4	4
2	4	4	4
3	4	4	4
4	4	4	4
5	4	4	4



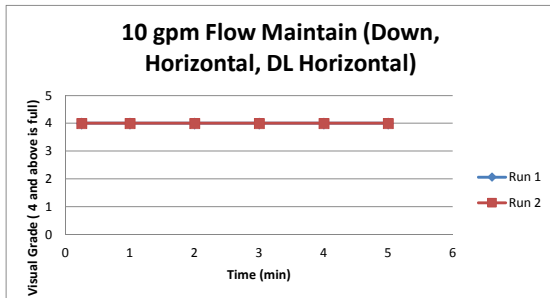
Experiement 576-578

Time	Run 1	Run 2	Run 3
0.25	4	4	4
1	4	5	4
2	5	5	5



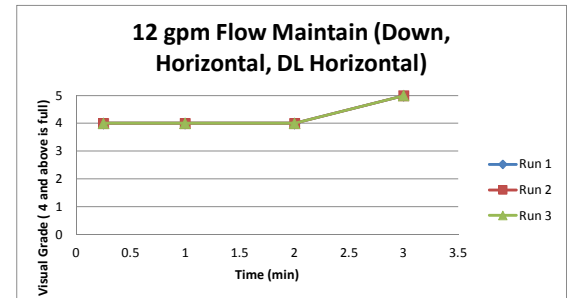
Experiement 609-610

Time	Run 1	Run 2
0.25	4	4
1	4	4
2	4	4
3	4	4
4	4	4
5	4	4



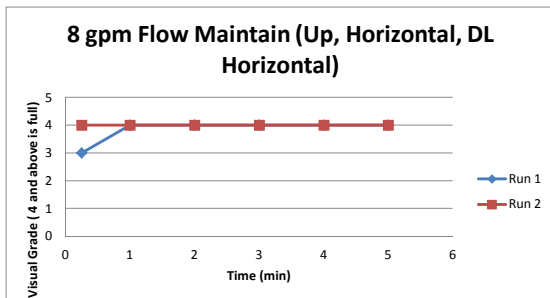
Experiement 611-613

Time	Run 1	Run 2	Run 3
0.25	4	4	4
1	4	4	4
2	4	4	4
3	5	5	5



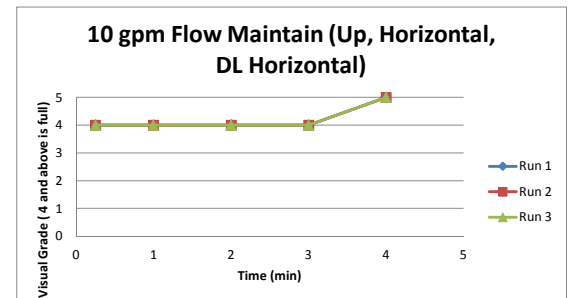
Experiement 629-630

Time	Run 1	Run 2
0.25	3	4
1	4	4
2	4	4
3	4	4
4	4	4
5	4	4



Experiement 631-633

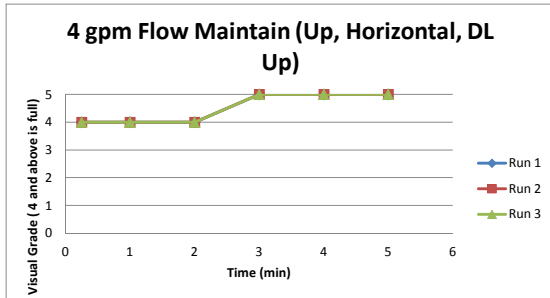
Time	Run 1	Run 2	Run 3
0.25	4	4	4
1	4	4	4
2	4	4	4
3	4	4	4
4	5	5	5



3/4 inch 2D Elbow Flow Maintain

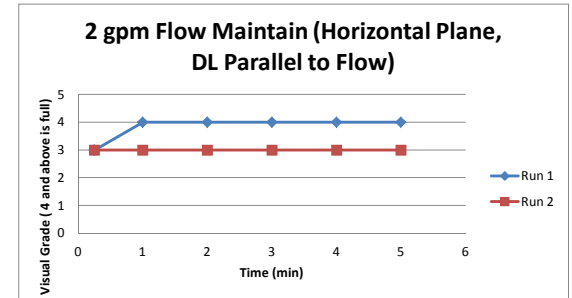
Experiement 658-660

Time	Run 1	Run 2	Run 3
0.25	4	4	4
1	4	4	4
2	4	4	4
3	5	5	5
4	5	5	5
5	5	5	5



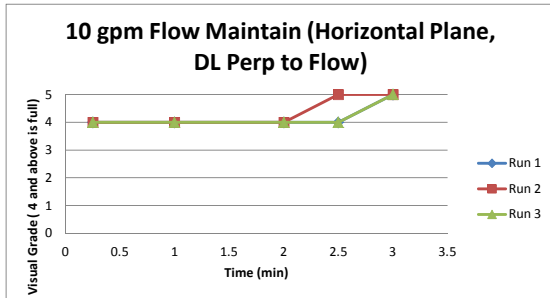
Experiement 669-670

Time	Run 1	Run 2
0.25	3	3
1	4	3
2	4	3
3	4	3
4	4	3
5	4	3



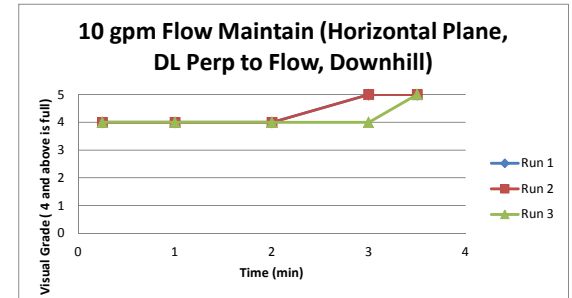
Experiement 686-688

Time	Run 1	Run 2	Run 3
0.25	4	4	4
1	4	4	4
2	4	4	4
2.5	4	5	4
3	5	5	5



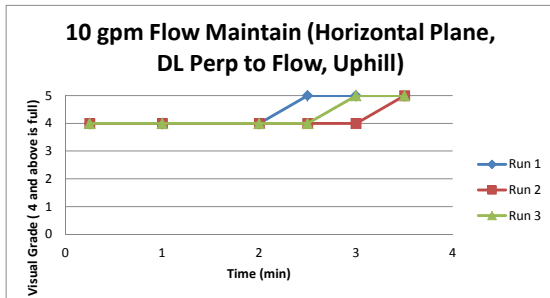
Experiement 689-691

Time	Run 1	Run 2	Run 3
0.25	4	4	4
1	4	4	4
2	4	4	4
3	5	5	4
3.5	5	5	5



Experiement 692-694

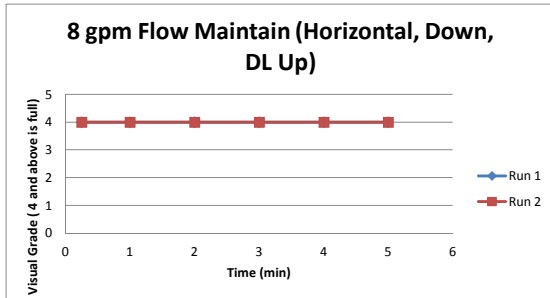
Time	Run 1	Run 2	Run 3
0.25	4	4	4
1	4	4	4
2	4	4	4
2.5	5	4	4
3	5	4	5
3.5	5	5	5



3/4 inch SO Elbow Tests

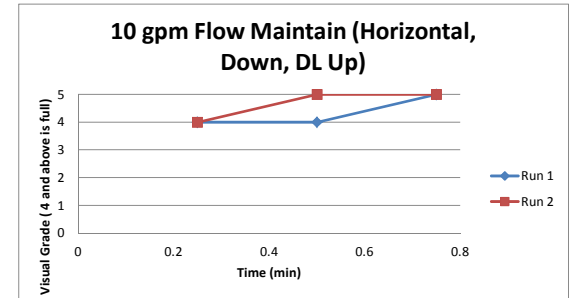
Experiement 581-582

Time	Run 1	Run 2
0.25	4	4
1	4	4
2	4	4
3	4	4
4	4	4
5	4	4



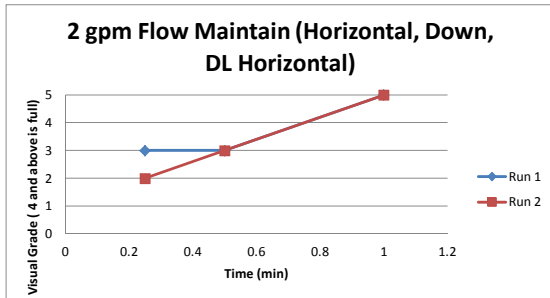
Experiement 583-584

Time	Run 1	Run 2
0.25	4	4
0.5	4	5
0.75	5	5



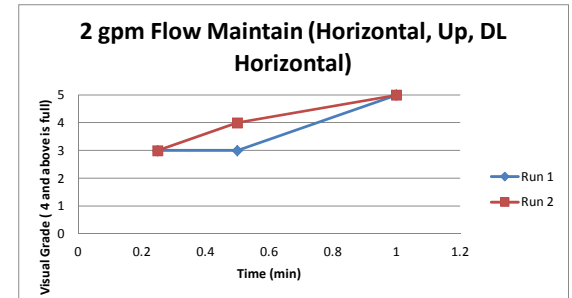
Experiement 585-586

Time	Run 1	Run 2
0.25	3	2
0.5	3	3
1	5	5



Experiement 624-625

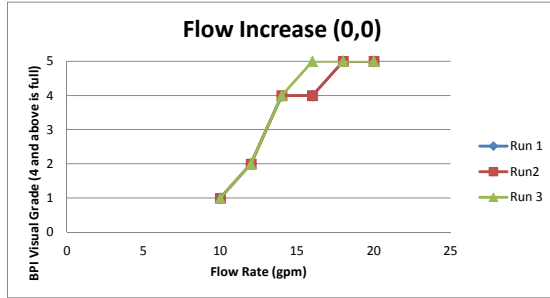
Time	Run 1	Run 2
0.25	3	3
0.5	3	4
1	5	5



1 inch 2D Horizontal Tests

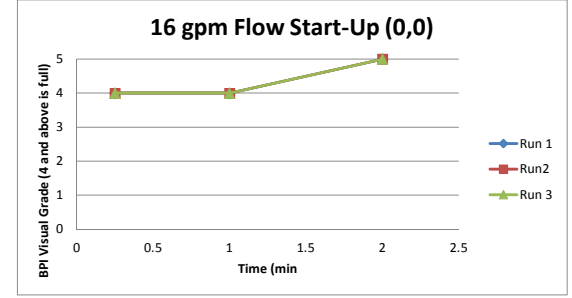
Experiment 489-491

Flow Rate	Run 1	Run2	Run 3
10	1	1	1
12	2	2	2
14	4	4	4
16	4	4	5
18	5	5	5
20	5	5	5



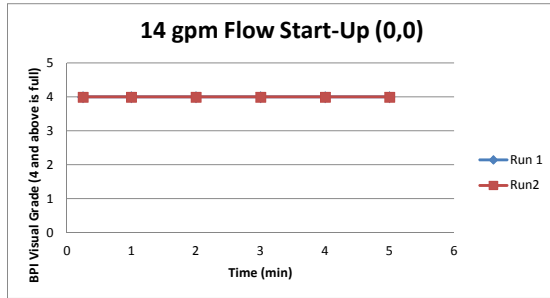
Experiment 492-494

Time	Run 1	Run2	Run 3
0.25	4	4	4
1	4	4	4
2	5	5	5



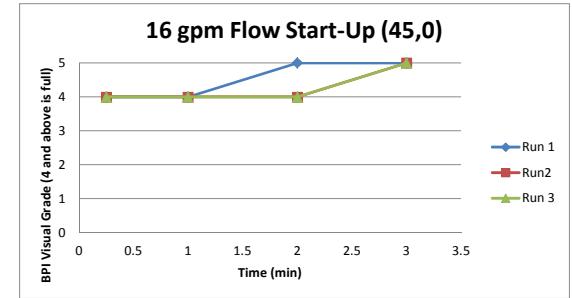
Experiment 495-496

Time	Run 1	Run2
0.25	4	4
1	4	4
2	4	4
3	4	4
4	4	4
5	4	4



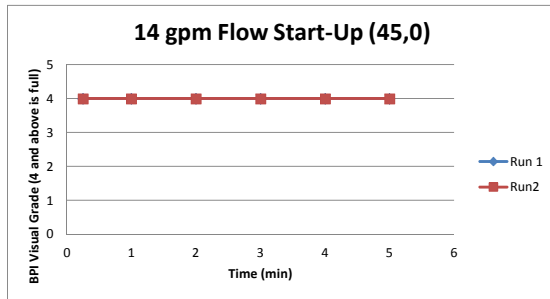
Experiment 497-499

Time	Run 1	Run2	Run 3
0.25	4	4	4
1	4	4	4
2	5	4	4
3	5	5	5



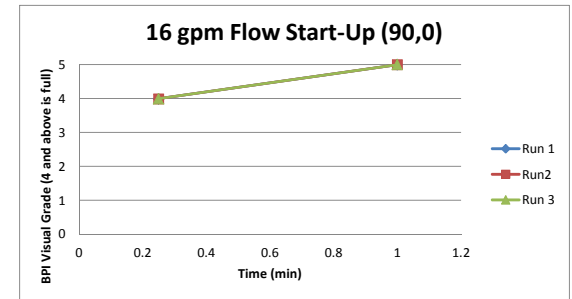
Experiment 500-501

Time	Run 1	Run2
0.25	4	4
1	4	4
2	4	4
3	4	4
4	4	4
5	4	4



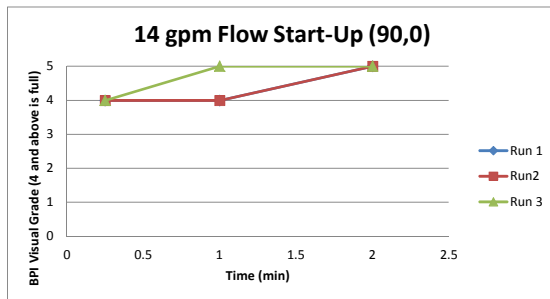
Experiment 502-504

Time	Run 1	Run2	Run 3
0.25	4	4	4
1	5	5	5



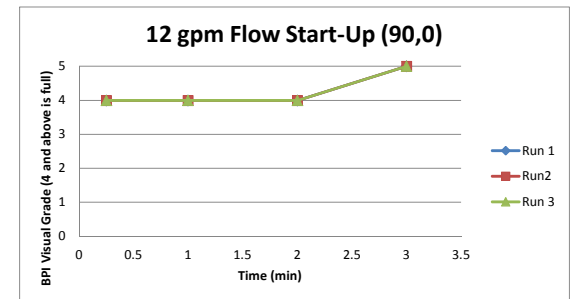
Experiment 505-507

Time	Run 1	Run2	Run 3
0.25	4	4	4
1	4	4	5
2	5	5	5



Experiment 508-510

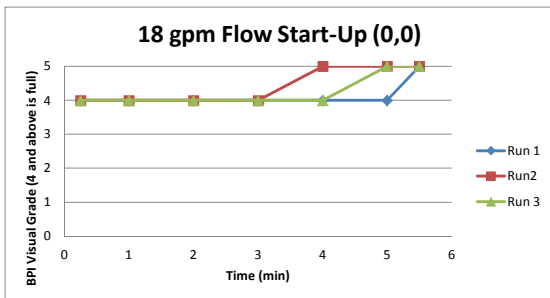
Time	Run 1	Run2	Run 3
0.25	4	4	4
1	4	4	4
2	4	4	4
3	5	5	5



1 inch SO Horizontal Tests

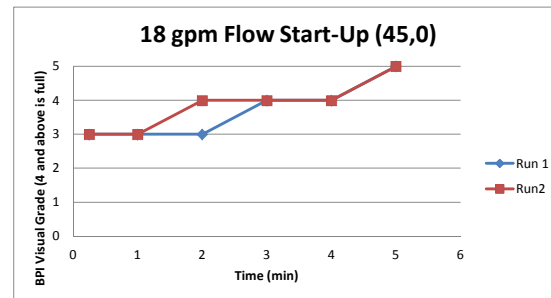
Experiment 512-514

Time	Run 1	Run2	Run 3
0.25	4	4	4
1	4	4	4
2	4	4	4
3	4	4	4
4	4	5	4
5	4	5	5
5.5	5	5	5



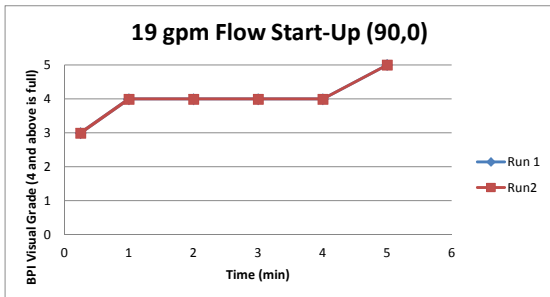
Experiment 515-516

Time	Run 1	Run2
0.25	3	3
1	3	3
2	3	4
3	4	4
4	4	4
5	5	5



Experiment 519-520

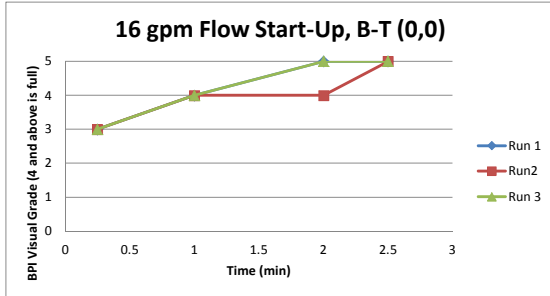
Time	Run 1	Run2
0.25	3	3
1	4	4
2	4	4
3	4	4
4	4	4
5	5	5



1 inch 2D Vertical Tests

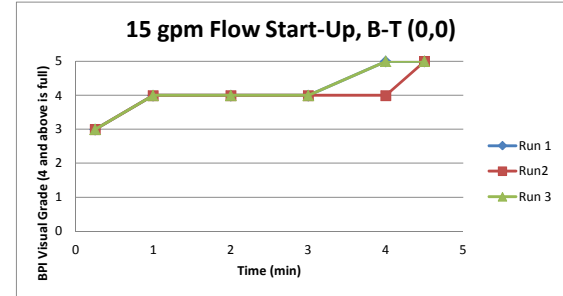
Experiment 535-537

Time	Run 1	Run2	Run 3
0.25	3	3	3
1	4	4	4
2	5	4	5
2.5	5	5	5



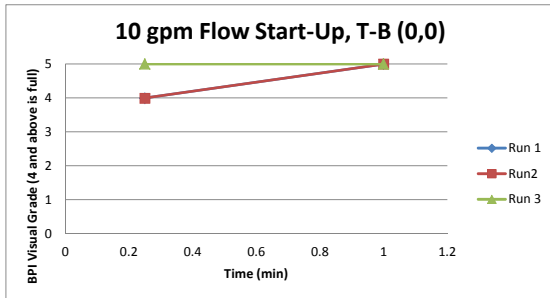
Experiment 538-540

Time	Run 1	Run2	Run 3
0.25	3	3	3
1	4	4	4
2	4	4	4
3	4	4	4
4	5	4	5
4.5	5	5	5



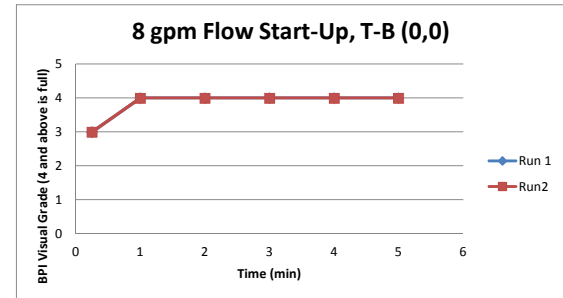
Experiment 545-547

Time	Run 1	Run2	Run 3
0.25	4	4	5
1	5	5	5



Experiment 548-549

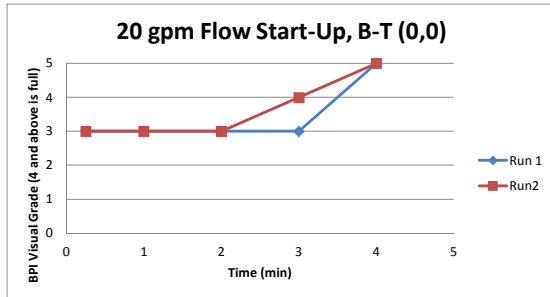
Time	Run 1	Run2
0.25	3	3
1	4	4
2	4	4
3	4	4
4	4	4
5	4	4



1 inch SO Vertical Tests

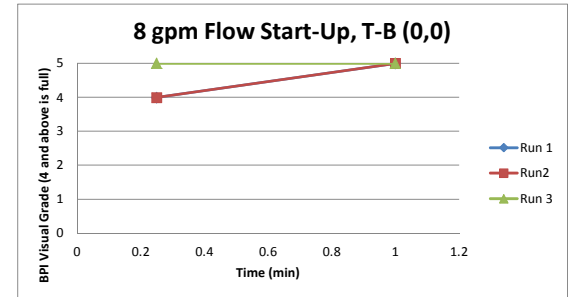
Experiment 543-544

Time	Run 1	Run2
0.25	3	3
1	3	3
2	3	3
3	3	4
4	5	5



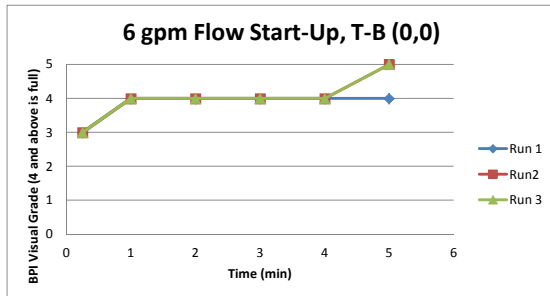
Experiment 550-552

Time	Run 1	Run2	Run 3
0.25	4	4	5
1	5	5	5



Experiment 553-555

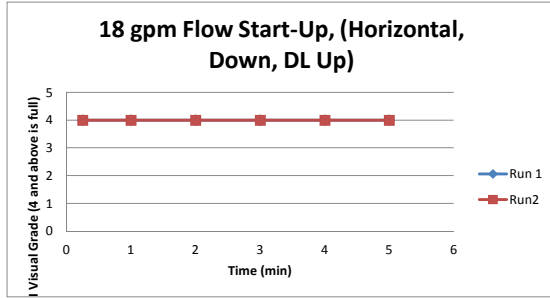
Time	Run 1	Run2	Run 3
0.25	3	3	3
1	4	4	4
2	4	4	4
3	4	4	4
4	4	4	4
5	4	5	5



1 inch 2D Elbow Tests

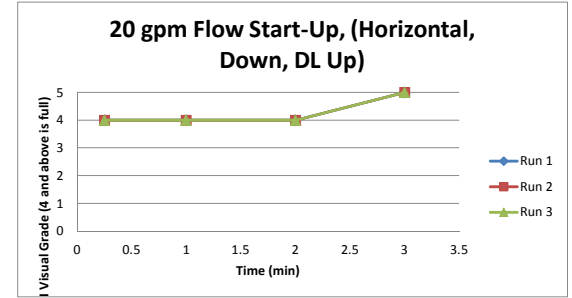
Experiment 587-588

Time	Run 1	Run 2
0.25	4	4
1	4	4
2	4	4
3	4	4
4	4	4
5	4	4



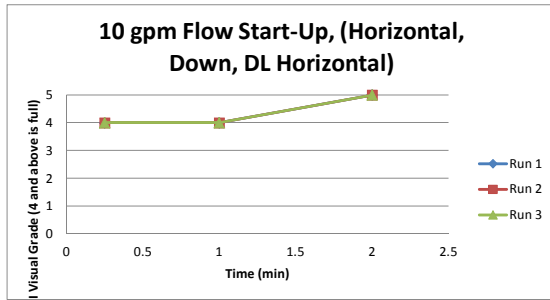
Experiment 589-591

Time	Run 1	Run 2	Run 3
0.25	4	4	4
1	4	4	4
2	4	4	4
3	5	5	5



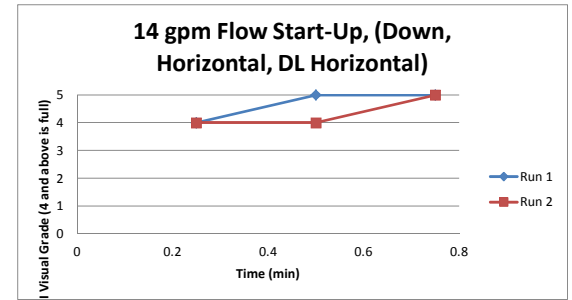
Experiment 592-594

Time	Run 1	Run 2	Run 3
0.25	4	4	4
1	4	4	4
2	5	5	5



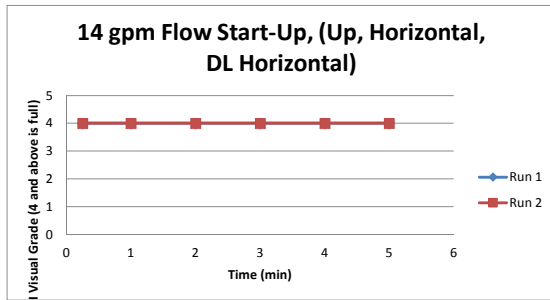
Experiment 614-615

Time	Run 1	Run 2
0.25	4	4
0.5	5	4
0.75	5	5



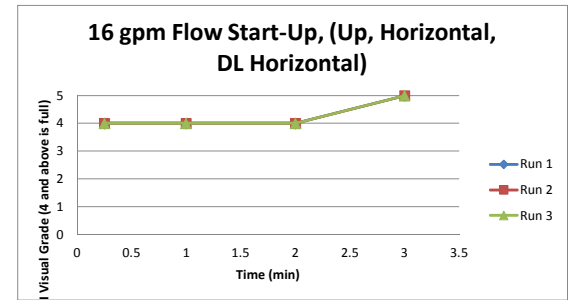
Experiment 641-642

Time	Run 1	Run 2
0.25	4	4
1	4	4
2	4	4
3	4	4
4	4	4
5	4	4



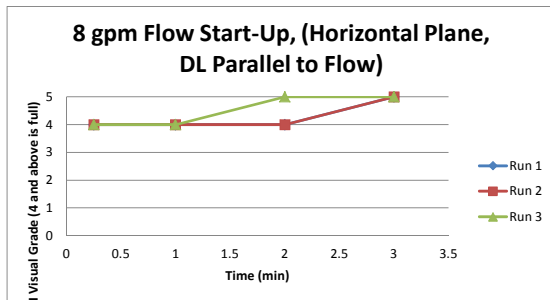
Experiment 643-645

Time	Run 1	Run 2	Run 3
0.25	4	4	4
1	4	4	4
2	4	4	4
3	5	5	5



Experiment 703-705

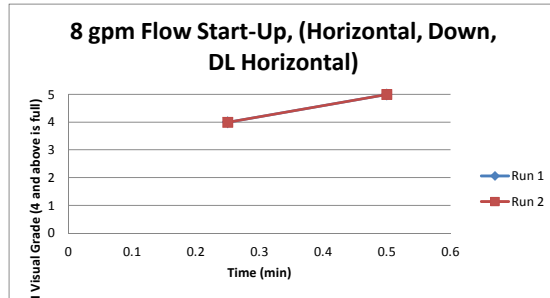
Time	Run 1	Run 2	Run 3
0.25	4	4	4
1	4	4	4
2	4	4	5
3	5	5	5



1 inch SO Elbow Tests

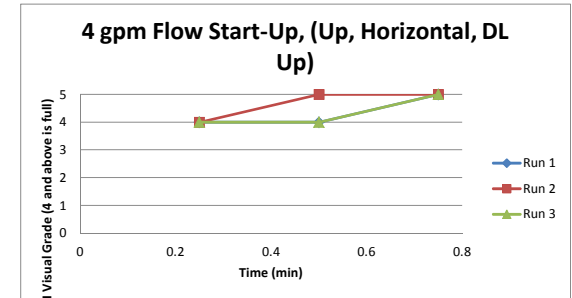
Experiment 595-596

Time	Run 1	Run 2
0.25	4	4
0.5	5	5



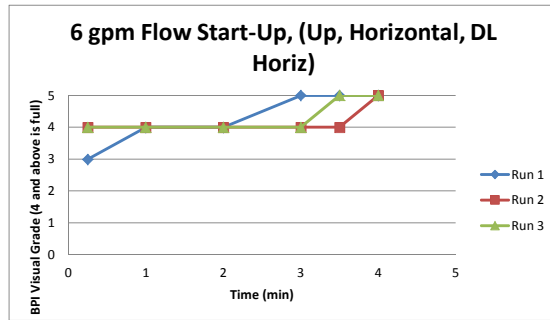
Experiment 649-651

Time	Run 1	Run 2	Run 3
0.25	4	4	4
0.5	4	5	4
0.75	5	5	5



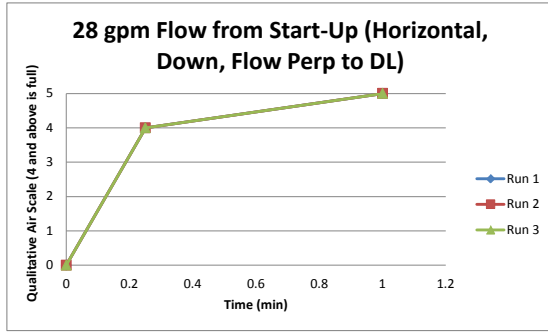
Experiment 652-654

Time	Run 1	Run 2	Run 3
0.25	3	4	4
1	4	4	4
2	4	4	4
3	5	4	4
3.5	5	4	5
4	5	5	5



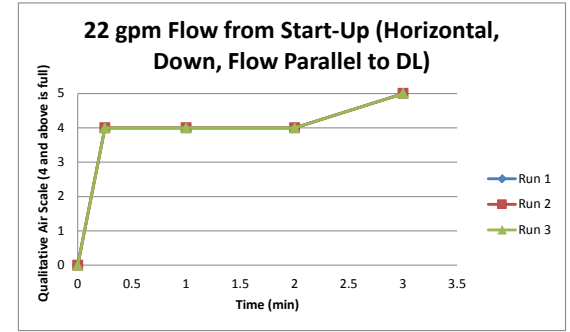
Experiment 760-762

Time	Run 1	Run 2	Run 3
0	0	0	0
0.25	4	4	4
1	5	5	5



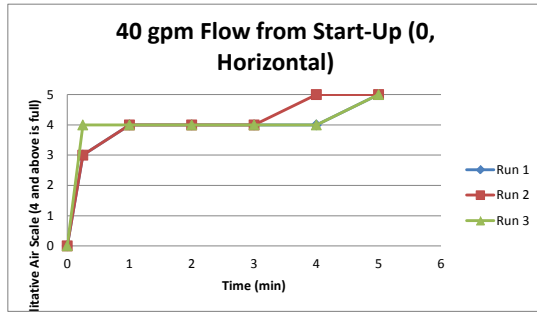
Experiment 763-765

Time	Run 1	Run 2	Run 3
0	0	0	0
0.25	4	4	4
1	4	4	4
2	4	4	4
3	5	5	5



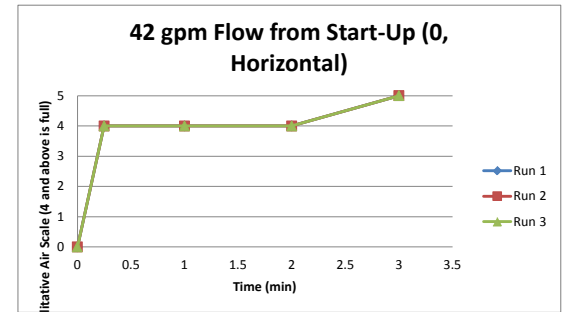
Experiment 725-727

Time	Run 1	Run 2	Run 3
0	0	0	0
0.25	3	3	4
1	4	4	4
2	4	4	4
3	4	4	4
4	4	5	4
5	5	5	5



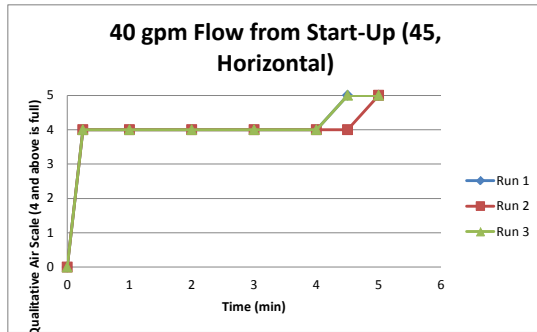
Experiment 728-730

Time	Run 1	Run 2	Run 3
0	0	0	0
0.25	4	4	4
1	4	4	4
2	4	4	4
3	5	5	5



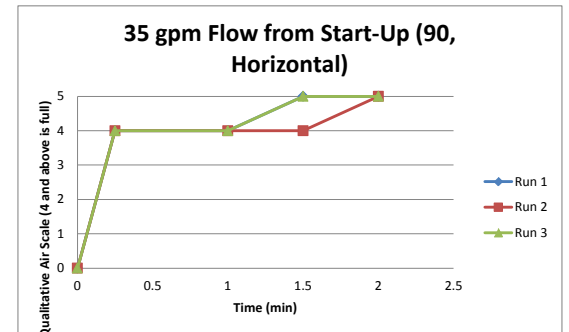
Experiment 733-735

Time	Run 1	Run 2	Run 3
0	0	0	0
0.25	4	4	4
1	4	4	4
2	4	4	4
3	4	4	4
4	4	4	4
4.5	5	4	5
5	5	5	5



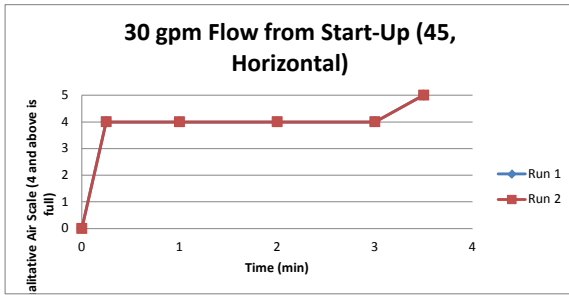
Experiment 736-738

Time	Run 1	Run 2	Run 3
0	0	0	0
0.25	4	4	4
1	4	4	4
1.5	5	4	5
2	5	5	5



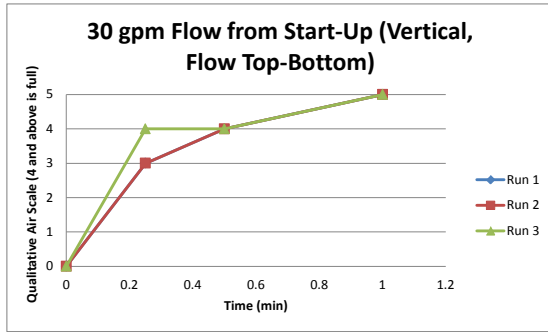
Experiment 739-740

Time	Run 1	Run 2
0	0	0
0.25	4	4
1	4	4
2	4	4
3	4	4
3.5	5	5



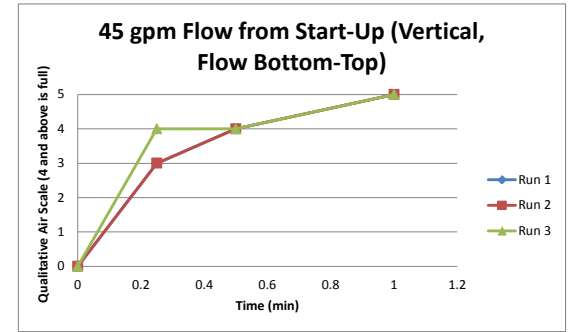
Experiment 786-788

Time	Run 1	Run 2	Run 3
0	0	0	0
0.25	3	3	4
0.5	4	4	4
1	5	5	5



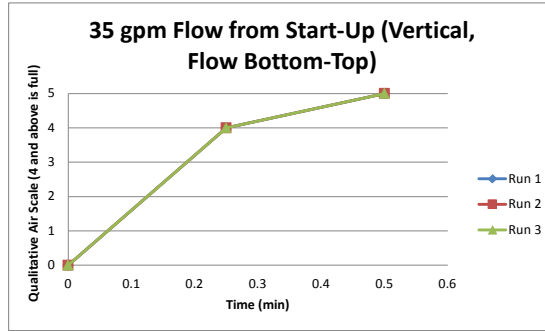
Experiment 792-794

Time	Run 1	Run 2	Run 3
0	0	0	0
0.25	4	4	4
1	4	4	4
2	4	4	4
3	4	4	4
3.5	5	4	5
4	5	5	5



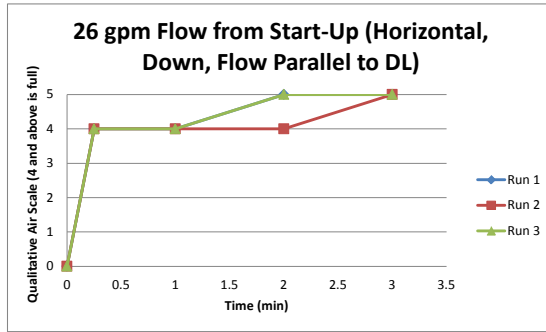
Experiment 789-791

Time	Run 1	Run 2	Run 3
0	0	0	0
0.25	4	4	4
0.5	5	5	5



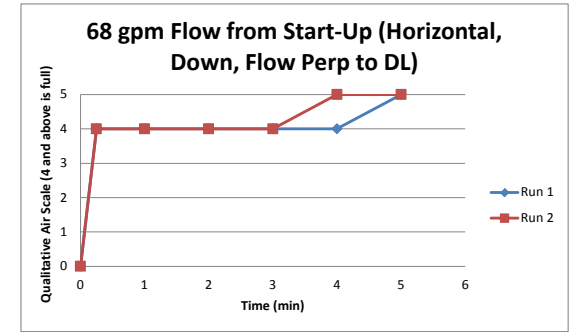
Experiment 743-745

Time	Run 1	Run 2	Run 3
0	0	0	0
0.25	4	4	4
1	4	4	4
2	5	4	5
3	5	5	5



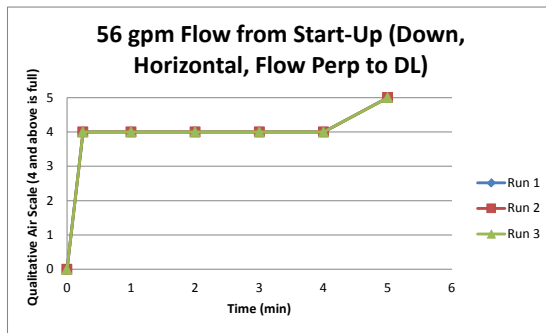
Experiment 746-747

Time	Run 1	Run 2
0	0	0
0.25	4	4
1	4	4
2	4	4
3	4	4
4	4	5
5	5	5



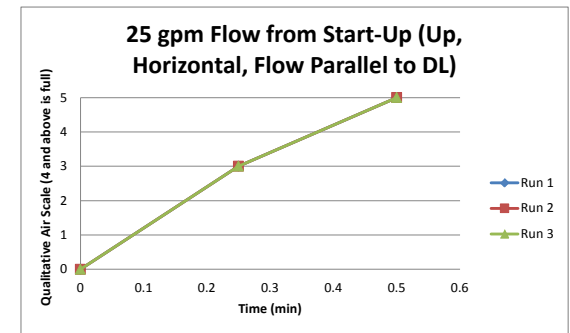
Experiment 776-778

Time	Run 1	Run 2	Run 3
0	0	0	0
0.25	4	4	4
1	4	4	4
2	4	4	4
3	4	4	4
4	4	4	4
5	5	5	5



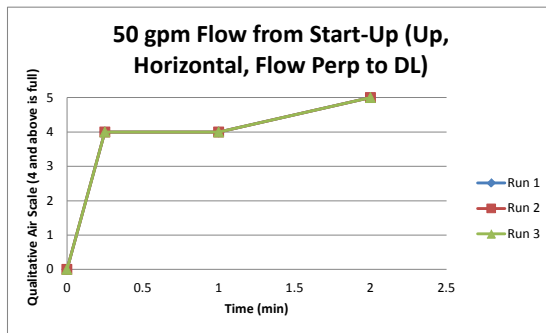
Experiment 798-800

Time	Run 1	Run 2	Run 3
0	0	0	0
0.25	3	3	3
0.5	5	5	5



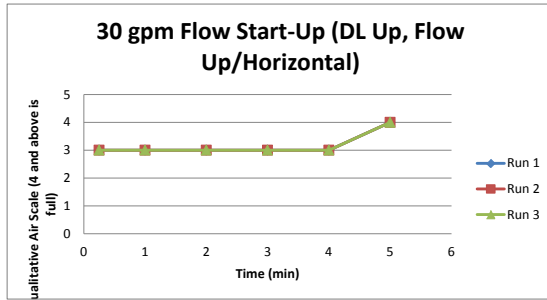
Experiment 801-803

Time	Run 1	Run 2	Run 3
0	0	0	0
0.25	4	4	4
1	4	4	4
2	5	5	5



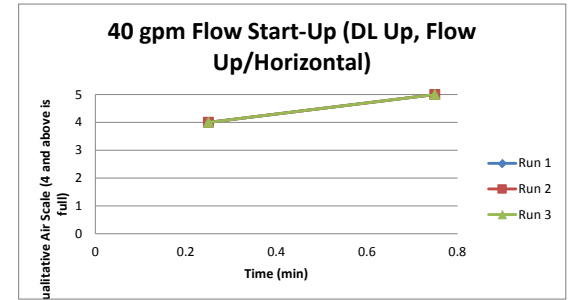
Experiment 286-288

Time	Run 1	Run 2	Run 3
0.25	3	3	3
1	3	3	3
2	3	3	3
3	3	3	3
4	3	3	3
5	4	4	4



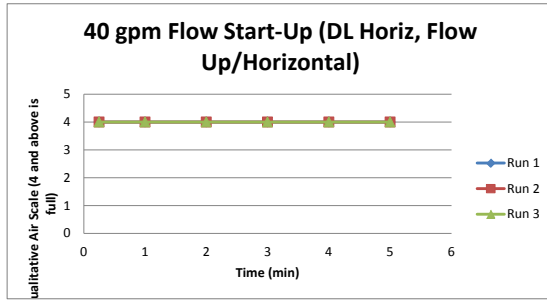
Experiment 289-291

Time	Run 1	Run 2	Run 3
0.25	4	4	4
0.75	5	5	5



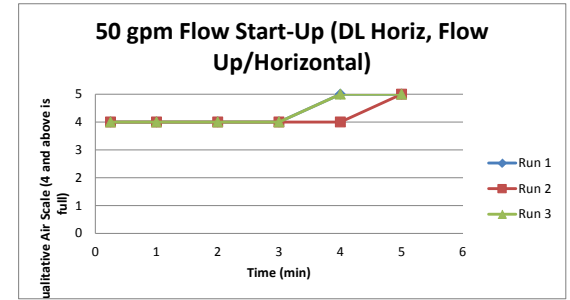
Experiment 295-297

Time	Run 1	Run 2	Run 3
0.25	4	4	4
1	4	4	4
2	4	4	4
3	4	4	4
4	4	4	4
5	4	4	4



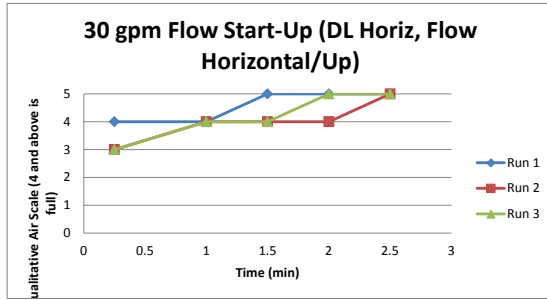
Experiment 298-300

Time	Run 1	Run 2	Run 3
0.25	4	4	4
1	4	4	4
2	4	4	4
3	4	4	4
4	5	4	5
5	5	5	5



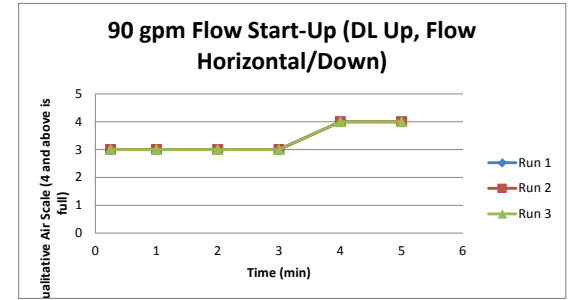
Experiment 307-309

Time	Run 1	Run 2	Run 3
0.25	4	3	3
1	4	4	4
1.5	5	4	4
2	5	4	5
2.5	5	5	5



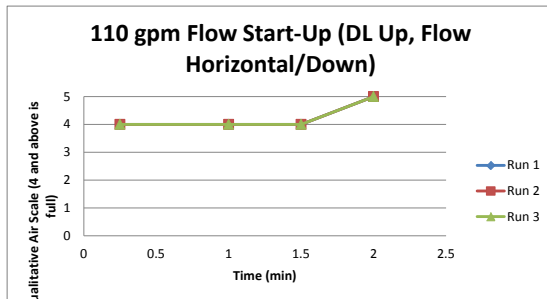
Experiment 316-318

Time	Run 1	Run 2	Run 3
0.25	3	3	3
1	3	3	3
2	3	3	3
3	3	3	3
4	4	4	4
5	4	4	4



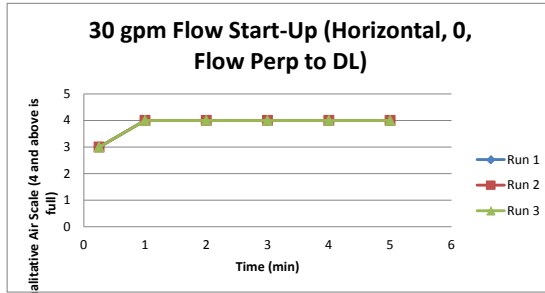
Experiment 319-321

Time	Run 1	Run 2	Run 3
0.25	4	4	4
1	4	4	4
1.5	4	4	4
2	5	5	5



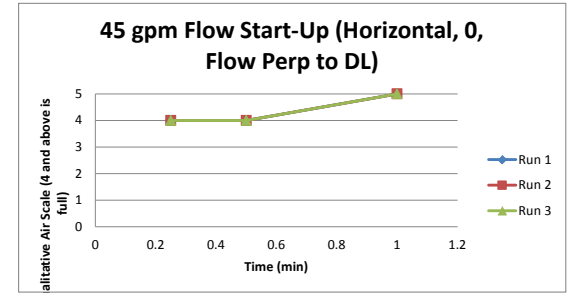
Experiment 325-327

Time	Run 1	Run 2	Run 3
0.25	3	3	3
1	4	4	4
2	4	4	4
3	4	4	4
4	4	4	4
5	4	4	4



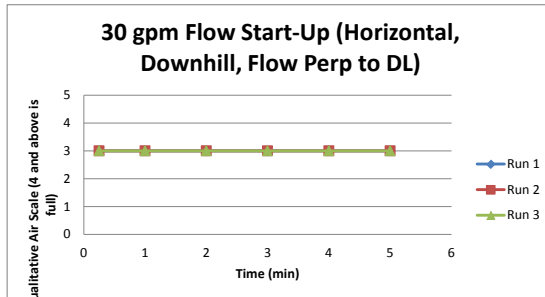
Experiment 328-330

Time	Run 1	Run 2	Run 3
0.25	4	4	4
0.5	4	4	4
1	5	5	5



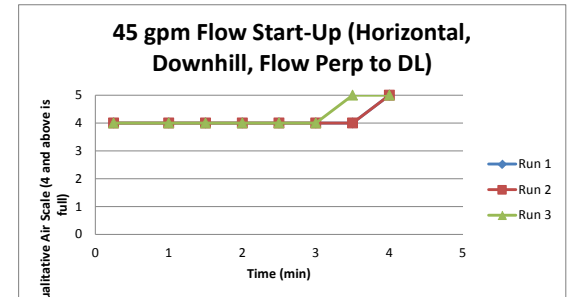
Experiment 352-354

Time	Run 1	Run 2	Run 3
0.25	3	3	3
1	3	3	3
2	3	3	3
3	3	3	3
4	3	3	3
5	3	3	3



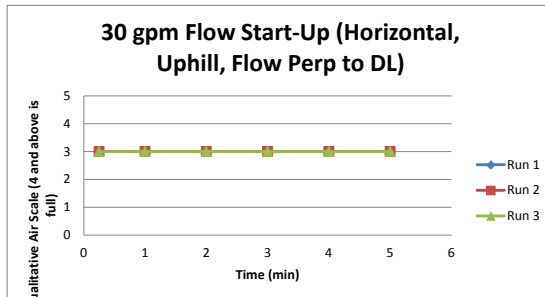
Experiment 355-357

Time	Run 1	Run 2	Run 3
0.25	4	4	4
1	4	4	4
1.5	4	4	4
2	4	4	4
2.5	4	4	4
3	4	4	4
3.5	4	4	5
4	5	5	5



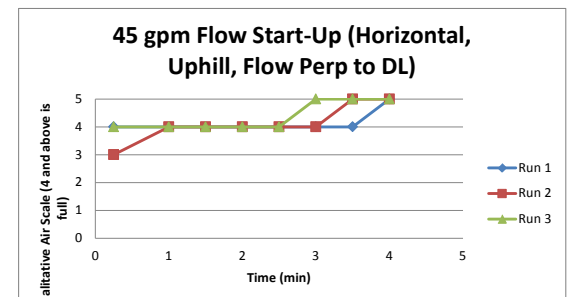
Experiment 361-363

Time	Run 1	Run 2	Run 3
0.25	3	3	3
1	3	3	3
2	3	3	3
3	3	3	3
4	3	3	3
5	3	3	3



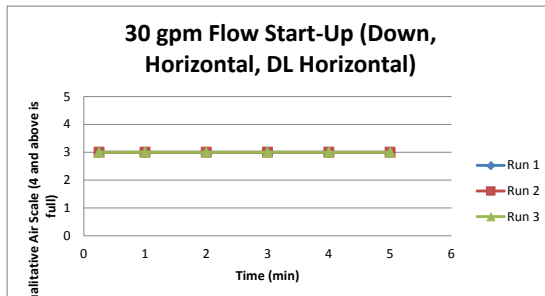
Experiment 364-366

Time	Run 1	Run 2	Run 3
0.25	4	3	4
1	4	4	4
1.5	4	4	4
2	4	4	4
2.5	4	4	4
3	4	4	5
3.5	4	5	5
4	5	5	5



Experiment 376-378

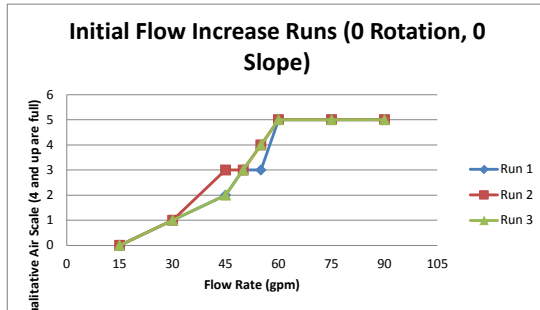
Time	Run 1	Run 2	Run 3
0.25	3	3	3
1	3	3	3
2	3	3	3
3	3	3	3
4	3	3	3
5	3	3	3



Experiment 1-3

Initial Runs

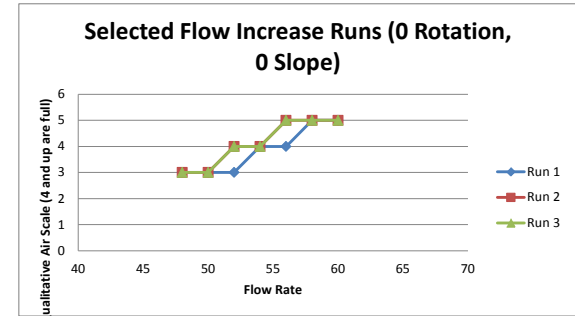
Flow Rate	Run 1	Run 2	Run 3
15	0	0	0
30	1	1	1
45	2	3	2
50	3	3	3
55	3	4	4
60	5	5	5
75	5	5	5
90	5	5	5



Experiment 4-6

Selected Runs

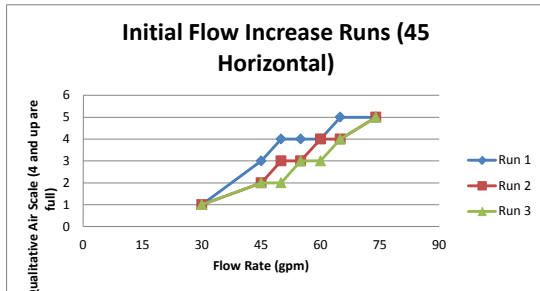
Flow Rate	Run 1	Run 2	Run 3
48	3	3	3
50	3	3	3
52	3	4	4
54	4	4	4
56	4	5	5
58	5	5	5
60	5	5	5



Experiment 46-48

Initial Runs

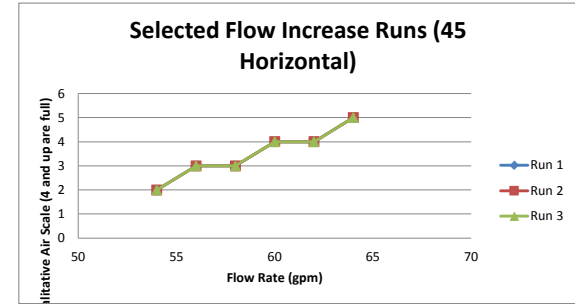
Flow Rate	Run 1	Run 2	Run 3
30	1	1	1
45	3	2	2
50	4	3	2
55	4	3	3
60	4	4	3
65	5	4	4
74	5	5	5



Experiment 49-51

Selected Runs

Flow Rate	Run 1	Run 2	Run 3
54	2	2	2
56	3	3	3
58	3	3	3
60	4	4	4
62	4	4	4
64	5	5	5



Experiment 67-69

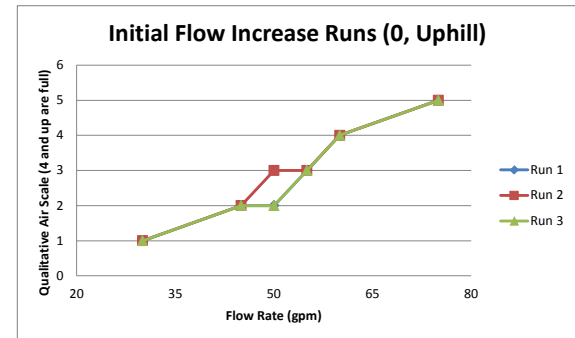
Flow Rate	Run 1	Run 2	Run 3
30	3	3	3
45	3	3	3
50	3	4	3
55	4	4	4
60	4	4	4
75	5	5	5



Experiment 88-90

Initial Runs

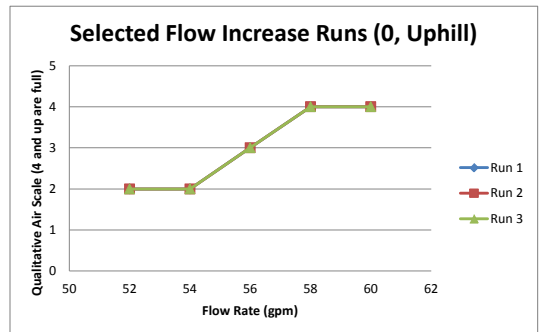
Flow Rate	Run 1	Run 2	Run 3
30	1	1	1
45	2	2	2
50	2	3	2
55	3	3	3
60	4	4	4
75	5	5	5



Experiment 91-93

Selected Runs

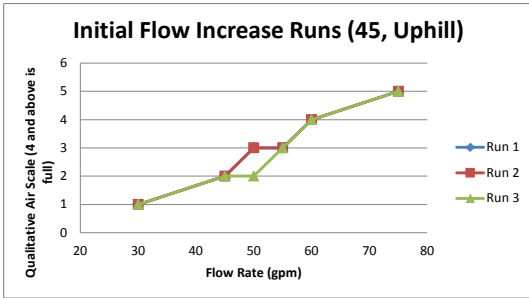
Flow Rate	Run 1	Run 2	Run 3
52	2	2	2
54	2	2	2
56	3	3	3
58	4	4	4
60	4	4	4



Experiment 106-108

Initial Runs

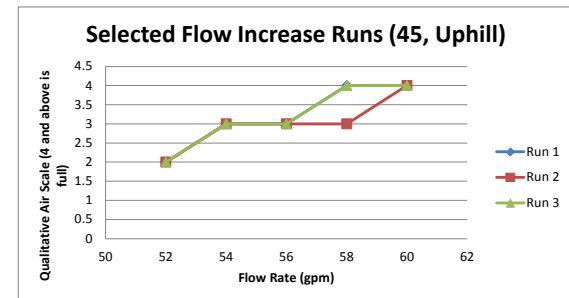
Flow Rate	Run 1	Run 2	Run 3
30	1	1	1
45	2	2	2
50	3	3	2
55	3	3	3
60	4	4	4
75	5	5	5



Experiment 109-111

Selected Runs

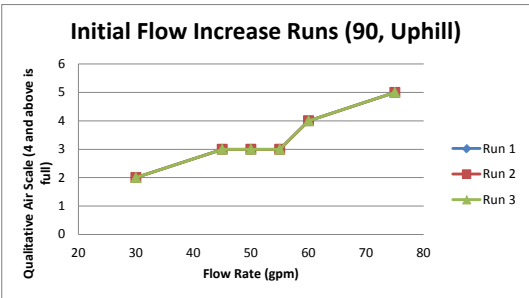
Flow Rate	Run 1	Run 2	Run 3
52	2	2	2
54	3	3	3
56	3	3	3
58	4	3	4
60	4	4	4



Experiment 124-126

Initial Runs

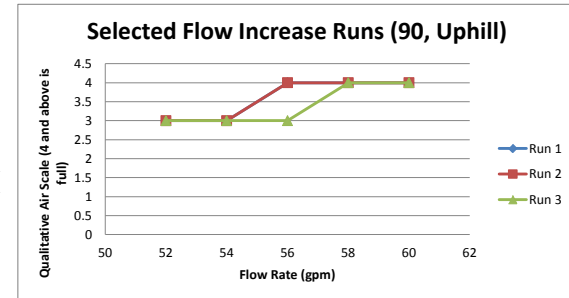
Flow Rate	Run 1	Run 2	Run 3
30	2	2	2
45	3	3	3
50	3	3	3
55	3	3	3
60	4	4	4
75	5	5	5



Experiment 127-129

Selected Runs

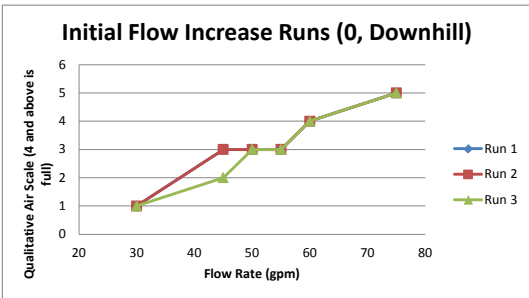
Flow Rate	Run 1	Run 2	Run 3
52	3	3	3
54	3	3	3
56	4	4	3
58	4	4	4
60	4	4	4



Experiment 142-144

Initial Runs

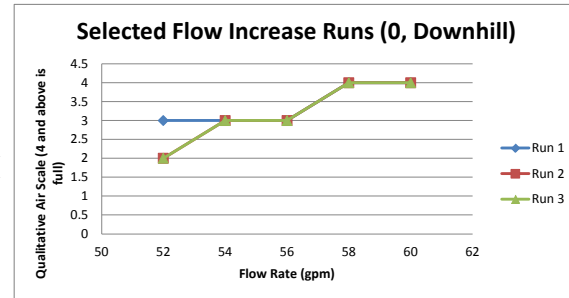
Flow Rate	Run 1	Run 2	Run 3
30	1	1	1
45	3	3	2
50	3	3	3
55	3	3	3
60	4	4	4
75	5	5	5



Experiment 145-147

Selected Runs

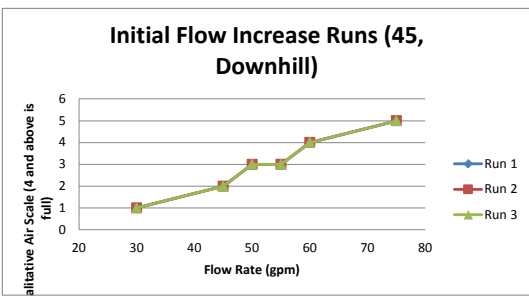
Flow Rate	Run 1	Run 2	Run 3
52	3	2	2
54	3	3	3
56	3	3	3
58	4	4	4
60	4	4	4



Experiment 160-162

Initial Runs

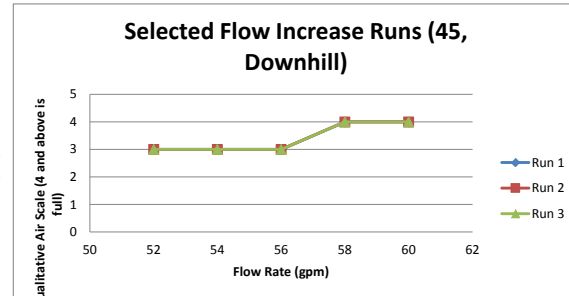
Flow Rate	Run 1	Run 2	Run 3
30	1	1	1
45	2	2	2
50	3	3	3
55	3	3	3
60	4	4	4
75	5	5	5



Experiment 163-165

Selected Runs

Flow Rate	Run 1	Run 2	Run 3
52	3	3	3
54	3	3	3
56	3	3	3
58	4	4	4
60	4	4	4



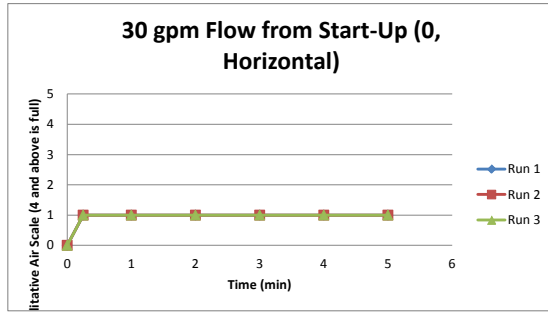
Experiment 176-178

Flow Rate	Run 1	Run 2	Run 3
30	3	3	3
45	3	3	3
50	4	4	4
55	4	4	4
60	4	4	4
75	5	5	5



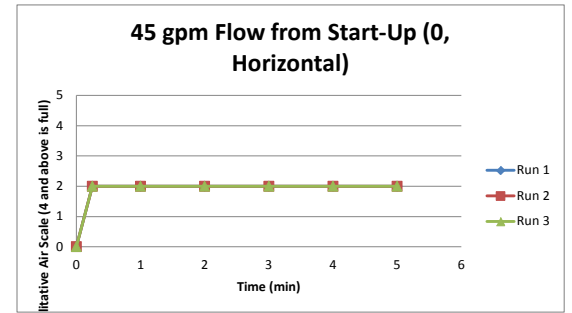
Experiment 7-9

Time	Run 1	Run 2	Run 3
0	0	0	0
0.25	1	1	1
1	1	1	1
2	1	1	1
3	1	1	1
4	1	1	1
5	1	1	1



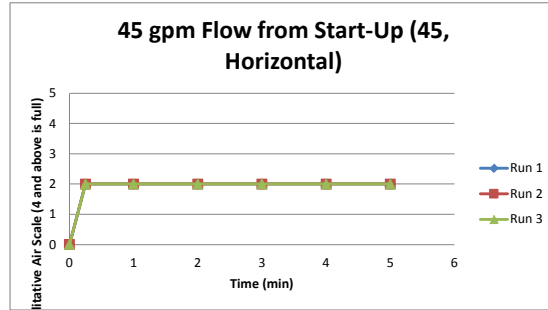
Experiment 10-12

Time	Run 1	Run 2	Run 3
0	0	0	0
0.25	2	2	2
1	2	2	2
2	2	2	2
3	2	2	2
4	2	2	2
5	2	2	2



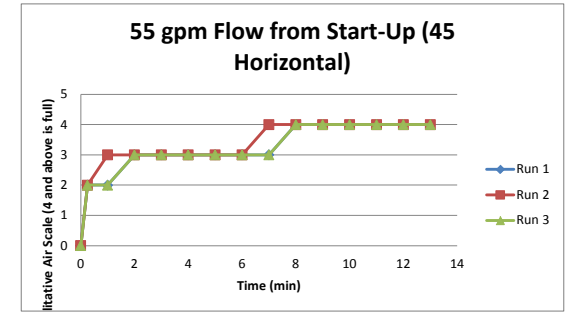
Experiment 52-54

Time	Run 1	Run 2	Run 3
0	0	0	0
0.25	2	2	2
1	2	2	2
2	2	2	2
3	2	2	2
4	2	2	2
5	2	2	2



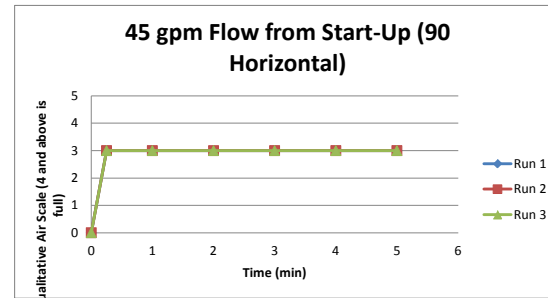
Experiment 55-57

Time	Run 1	Run 2	Run 3
0	0	0	0
0.25	2	2	2
1	2	3	2
2	3	3	3
3	3	3	3
4	3	3	3
5	3	3	3
6	3	3	3
7	3	4	3
8	4	4	4
9	4	4	4
10	4	4	4
11	4	4	4
12	4	4	4
13	4	4	4



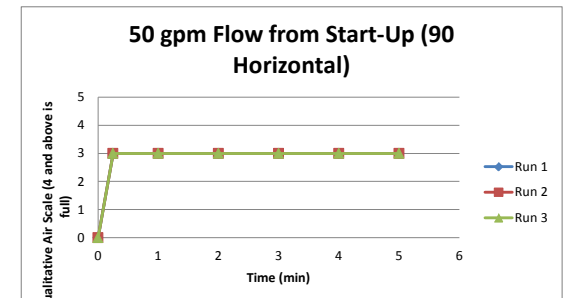
Experiment 70-72

Time	Run 1	Run 2	Run 3
0	0	0	0
0.25	3	3	3
1	3	3	3
2	3	3	3
3	3	3	3
4	3	3	3
5	3	3	3



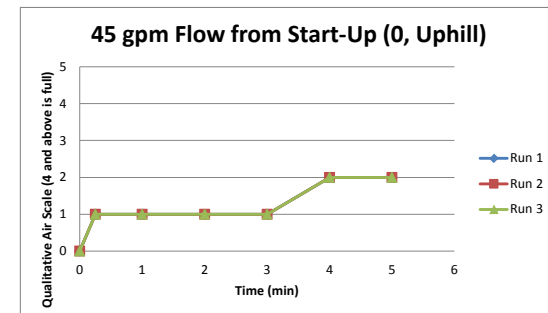
Experiment 73-75

Time	Run 1	Run 2	Run 3
0	0	0	0
0.25	3	3	3
1	3	3	3
2	3	3	3
3	3	3	3
4	3	3	3
5	3	3	3



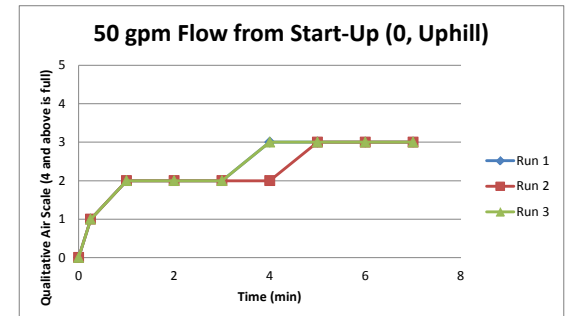
Experiment 94-96

Time	Run 1	Run 2	Run 3
0	0	0	0
0.25	1	1	1
1	1	1	1
2	1	1	1
3	1	1	1
4	2	2	2
5	2	2	2



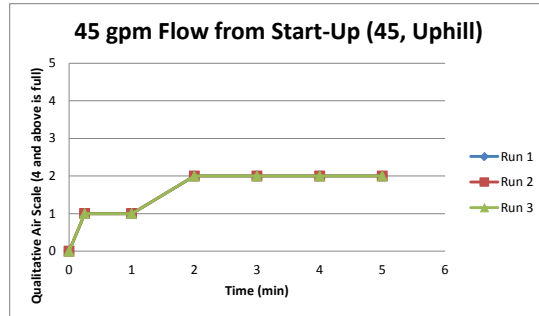
Experiment 97-99

Time	Run 1	Run 2	Run 3
0	0	0	0
0.25	1	1	1
1	2	2	2
2	2	2	2
3	2	2	2
4	3	2	3
5	3	3	3
6	3	3	3
7	3	3	3



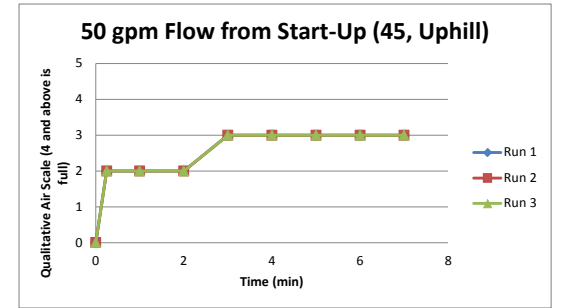
Experiment 112-114

Time	Run 1	Run 2	Run 3
0	0	0	0
0.25	1	1	1
1	1	1	1
2	2	2	2
3	2	2	2
4	2	2	2
5	2	2	2



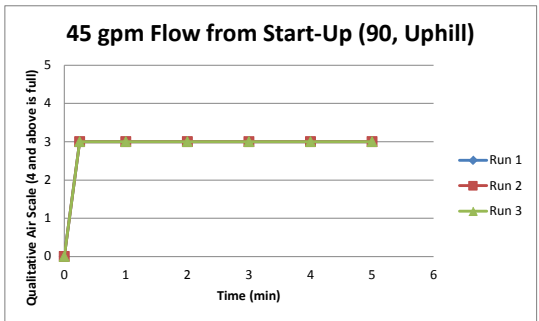
Experiment 115-117

Time	Run 1	Run 2	Run 3
0	0	0	0
0.25	2	2	2
1	2	2	2
2	2	2	2
3	3	3	3
4	3	3	3
5	3	3	3
6	3	3	3
7	3	3	3



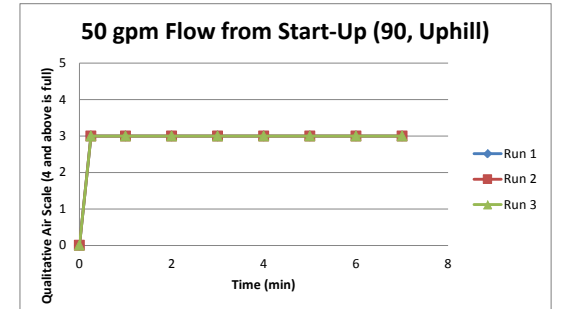
Experiment 130-132

Time	Run 1	Run 2	Run 3
0	0	0	0
0.25	3	3	3
1	3	3	3
2	3	3	3
3	3	3	3
4	3	3	3
5	3	3	3



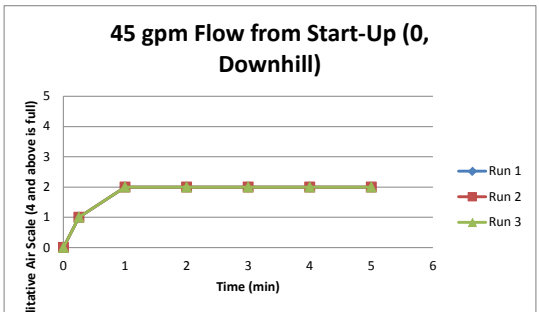
Experiment 133-135

Time	Run 1	Run 2	Run 3
0	0	0	0
0.25	3	3	3
1	3	3	3
2	3	3	3
3	3	3	3
4	3	3	3
5	3	3	3
6	3	3	3
7	3	3	3



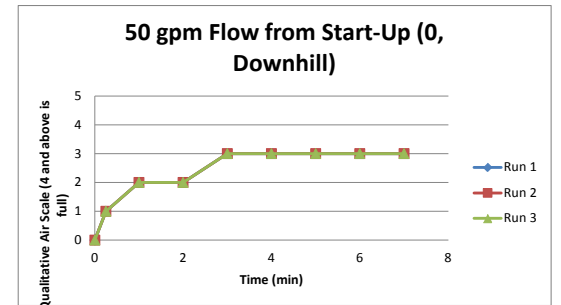
Experiment 148-150

Time	Run 1	Run 2	Run 3
0	0	0	0
0.25	1	1	1
1	2	2	2
2	2	2	2
3	2	2	2
4	2	2	2
5	2	2	2



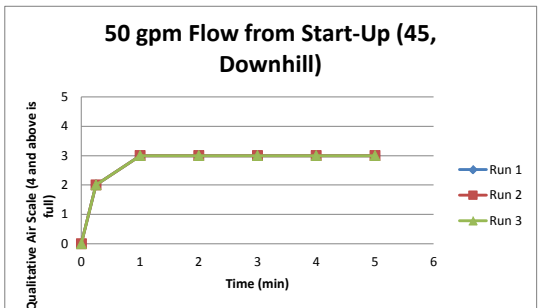
Experiment 151-153

Time	Run 1	Run 2	Run 3
0	0	0	0
0.25	1	1	1
1	2	2	2
2	2	2	2
3	3	3	3
4	3	3	3
5	3	3	3
6	3	3	3
7	3	3	3



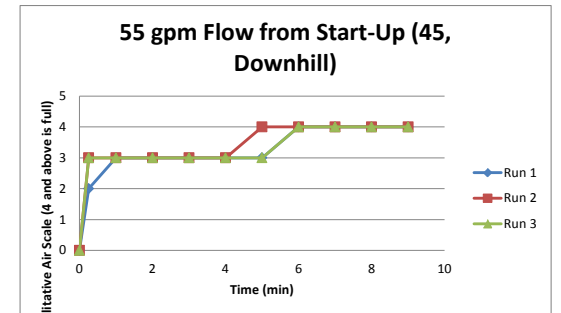
Experiment 166-168

Time	Run 1	Run 2	Run 3
0	0	0	0
0.25	2	2	2
1	3	3	3
2	3	3	3
3	3	3	3
4	3	3	3
5	3	3	3



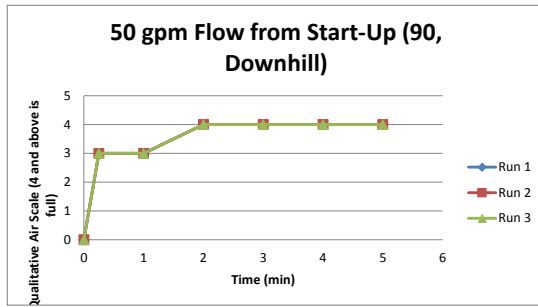
Experiment 169-171

Time	Run 1	Run 2	Run 3
0	0	0	0
0.25	2	3	3
1	3	3	3
2	3	3	3
3	3	3	3
4	3	3	3
5	3	4	3
6	4	4	4
7	4	4	4
8	4	4	4
9	4	4	4



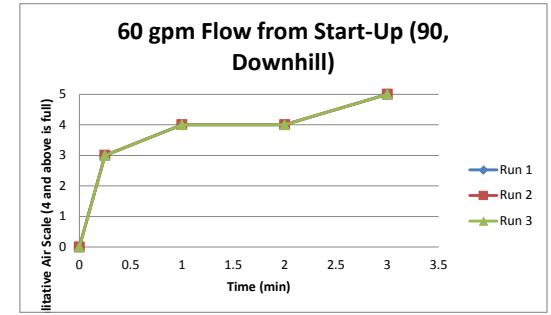
Experiment 166-168

Time	Run 1	Run 2	Run 3
0	0	0	0
0.25	3	3	3
1	3	3	3
2	4	4	4
3	4	4	4
4	4	4	4
5	4	4	4



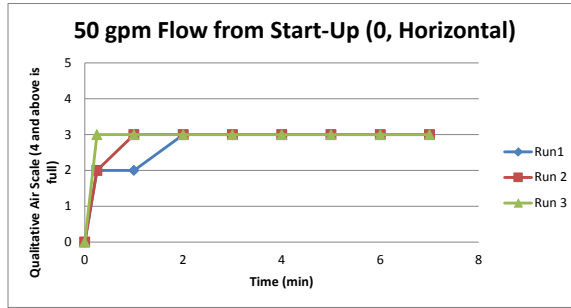
Experiment 166-168

Time	Run 1	Run 2	Run 3
0	0	0	0
0.25	3	3	3
1	4	4	4
2	4	4	4
3	5	5	5



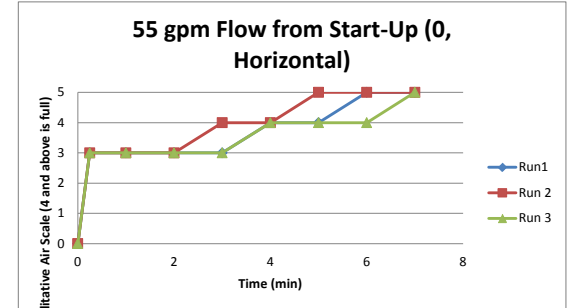
Experiment 13-15

Time	Run1	Run 2	Run 3
0	0	0	0
0.25	2	2	3
1	2	3	3
2	3	3	3
3	3	3	3
4	3	3	3
5	3	3	3
6	3	3	3
7	3	3	3



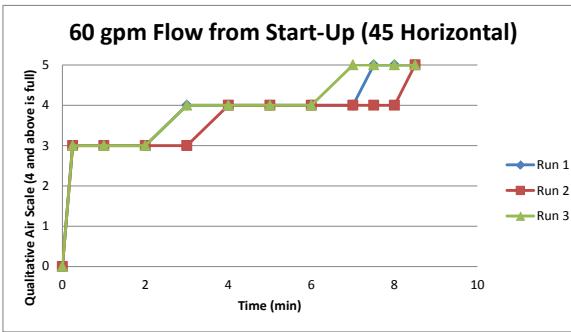
Experiment 16-18

Time	Run1	Run 2	Run 3
0	0	0	0
0.25	3	3	3
1	3	3	3
2	3	3	3
3	3	4	3
4	4	4	4
5	4	5	4
6	5	5	4
7	5	5	5



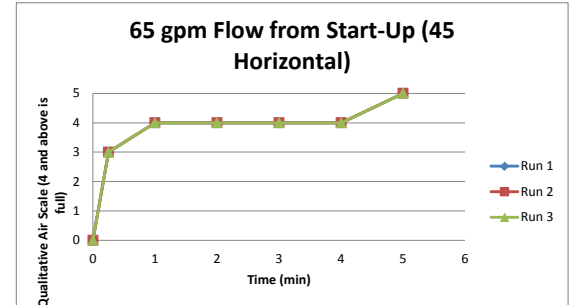
Experiment 58-60

Time	Run 1	Run 2	Run 3
0	0	0	0
0.25	3	3	3
1	3	3	3
2	3	3	3
3	4	3	4
4	4	4	4
5	4	4	4
6	4	4	4
7	4	4	5
7.5	5	4	5
8	5	4	5
8.5	5	5	5



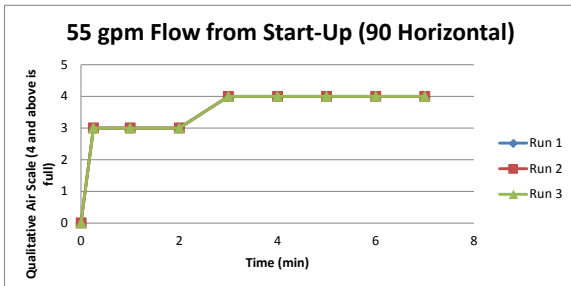
Experiment 61-63

Time	Run 1	Run 2	Run 3
0	0	0	0
0.25	3	3	3
1	4	4	4
2	4	4	4
3	4	4	4
4	4	4	4
5	5	5	5



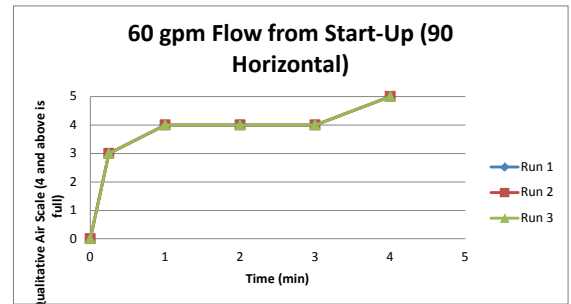
Experiment 76-78

Time	Run 1	Run 2	Run 3
0	0	0	0
0.25	3	3	3
1	3	3	3
2	3	3	3
3	4	4	4
4	4	4	4
5	4	4	4
6	4	4	4
7	4	4	4



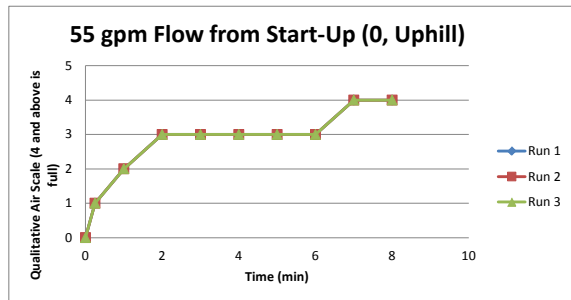
Experiment 79-81

Time	Run 1	Run 2	Run 3
0	0	0	0
0.25	3	3	3
1	4	4	4
2	4	4	4
3	4	4	4
4	5	5	5



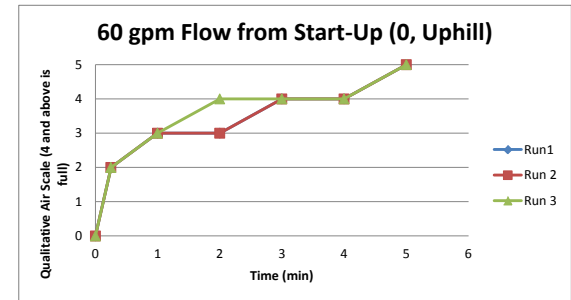
Experiment 100-102

Time	Run 1	Run 2	Run 3
0	0	0	0
0.25	1	1	1
1	2	2	2
2	3	3	3
3	3	3	3
4	3	3	3
5	3	3	3
6	3	3	3
7	4	4	4
8	4	4	4



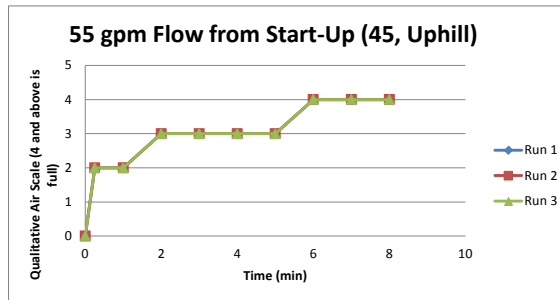
Experiment 103-105

Time	Run1	Run 2	Run 3
0	0	0	0
0.25	2	2	2
1	3	3	3
2	3	3	4
3	4	4	4
4	4	4	4
5	5	5	5



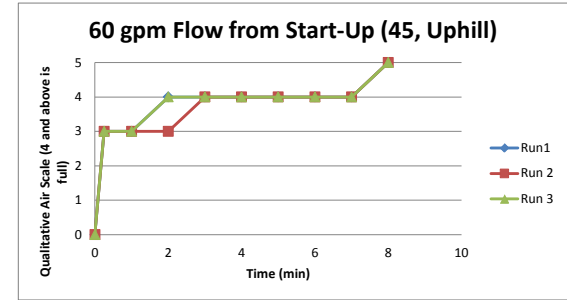
Experiment 118-120

Time	Run 1	Run 2	Run 3
0	0	0	0
0.25	2	2	2
1	2	2	2
2	3	3	3
3	3	3	3
4	3	3	3
5	3	3	3
6	4	4	4
7	4	4	4
8	4	4	4



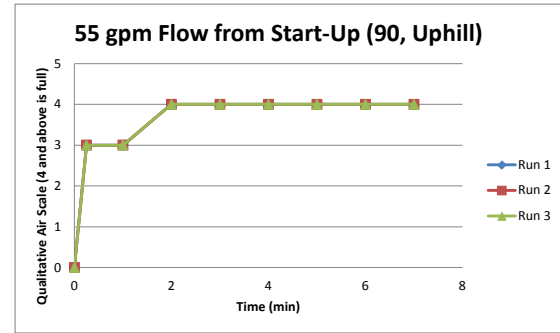
Experiment 121-123

Time	Run1	Run 2	Run 3
0	0	0	0
0.25	3	3	3
1	3	3	3
2	4	3	4
3	4	4	4
4	4	4	4
5	4	4	4
6	4	4	4
7	4	4	4
8	5	5	5



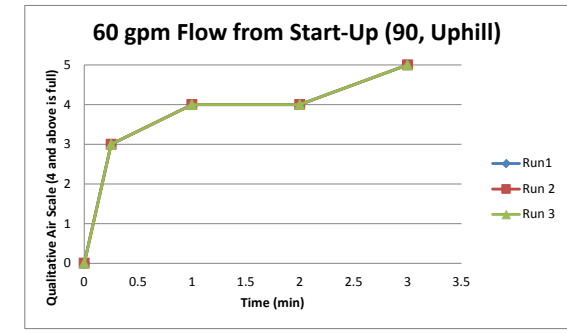
Experiment 136-138

Time	Run 1	Run 2	Run 3
0	0	0	0
0.25	3	3	3
1	3	3	3
2	4	4	4
3	4	4	4
4	4	4	4
5	4	4	4
6	4	4	4
7	4	4	4



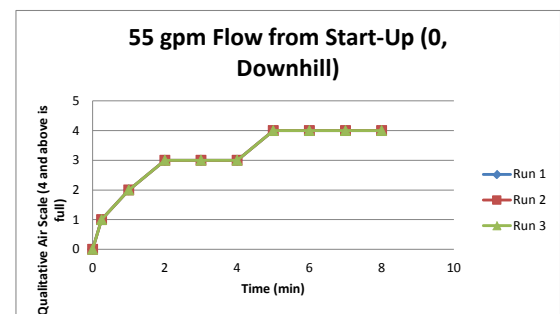
Experiment 139-141

Time	Run1	Run 2	Run 3
0	0	0	0
0.25	3	3	3
1	4	4	4
2	4	4	4
3	5	5	5



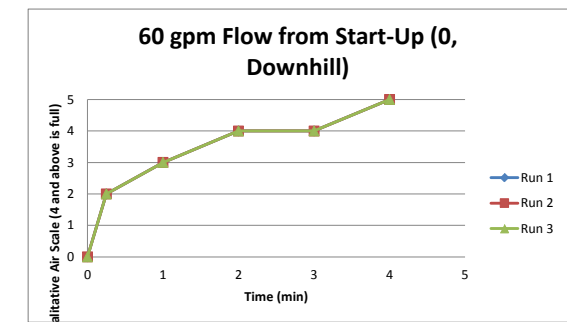
Experiment 154-156

Time	Run 1	Run 2	Run 3
0	0	0	0
0.25	1	1	1
1	2	2	2
2	3	3	3
3	3	3	3
4	3	3	3
5	4	4	4
6	4	4	4
7	4	4	4
8	4	4	4



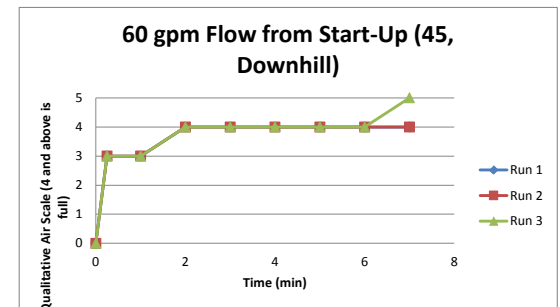
Experiment 157-159

Time	Run 1	Run 2	Run 3
0	0	0	0
0.25	2	2	2
1	3	3	3
2	4	4	4
3	4	4	4
4	5	5	5



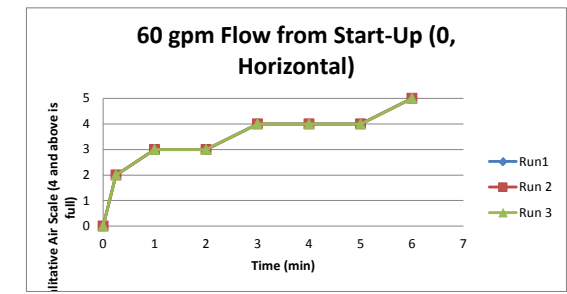
Experiment 172-174

Time	Run 1	Run 2	Run 3
0	0	0	0
0.25	3	3	3
1	3	3	3
2	4	4	4
3	4	4	4
4	4	4	4
5	4	4	4
6	4	4	4
7	4	4	5



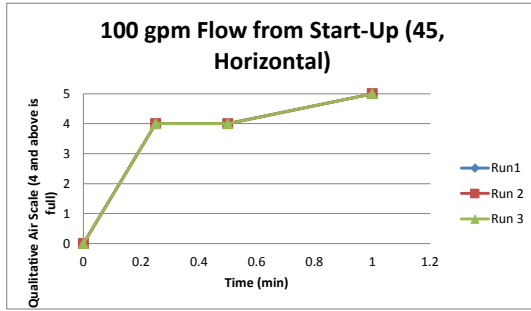
Experiment 187-189

Time	Run1	Run 2	Run 3
0	0	0	0
0.25	2	2	2
1	3	3	3
2	3	3	3
3	4	4	4
4	4	4	4
5	4	4	4
6	5	5	5



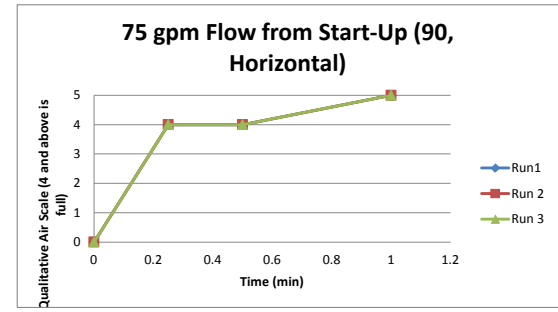
Experiment 1035-1037

Time	Run1	Run 2	Run 3
0	0	0	0
0.25	4	4	4
0.5	4	4	4
1	5	5	5



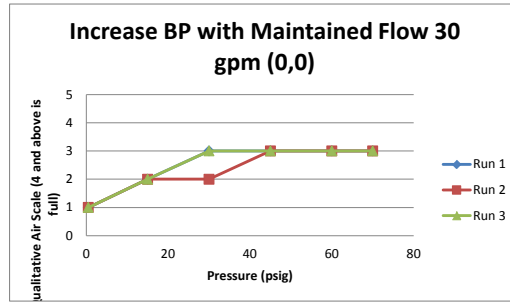
Experiment 1038-1040

Time	Run1	Run 2	Run 3
0	0	0	0
0.25	4	4	4
0.5	4	4	4
1	5	5	5



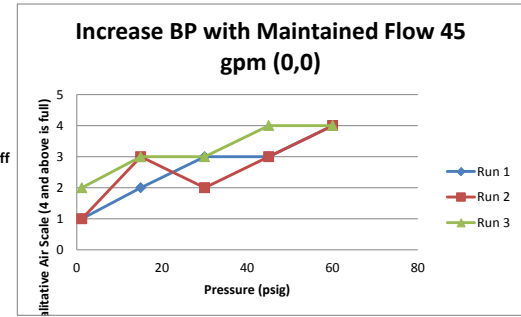
Experiment 28-30

Pressure	Run 1	Run 2	Run 3
0.5	1	1	1
15	2	2	2
30	3	2	3
45	3	3	3
60	3	3	3
70	3	3	3
0	2	1	1 Pump Off



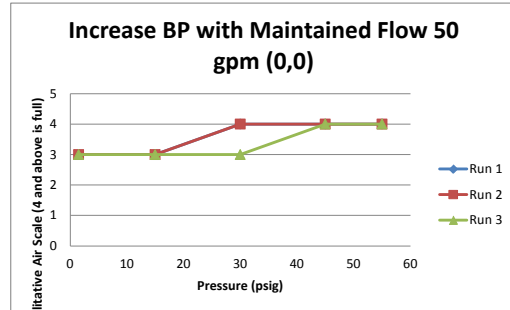
Experiment 31-33

Pressure	Run 1	Run 2	Run 3
1.2	1	1	2
15	2	3	3
30	3	2	3
45	3	3	4
60	4	4	4
0	3	3	3 Pump Off



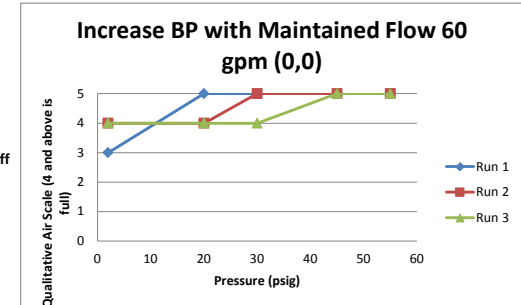
Experiment 34-36

Pressure	Run 1	Run 2	Run 3
1.5	3	3	3
15	3	3	3
30	4	4	3
45	4	4	4
55	4	4	4
0	4	4	3 Pump Off



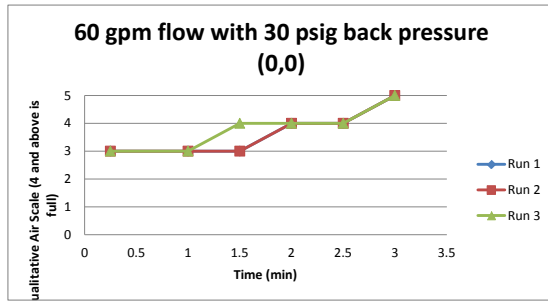
Experiment 37-39

Pressure	Run 1	Run 2	Run 3
2	3	4	4
20	5	4	4
30	5	5	4
45	5	5	5
55	5	5	5
0	5	5	5 Pump Off



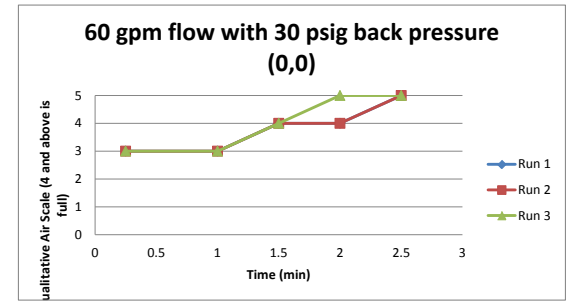
Experiment 40-42

Time	Run 1	Run 2	Run 3
0.25	3	3	3
1	3	3	3
1.5	3	3	4
2	4	4	4
2.5	4	4	4
3	5	5	5



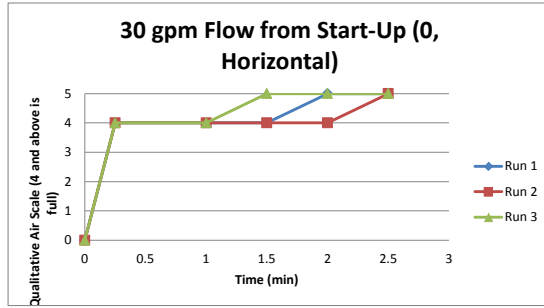
Experiment 43-45

Time	Run 1	Run 2	Run 3
0.25	3	3	3
1	3	3	3
1.5	4	4	4
2	4	4	5
2.5	5	5	5



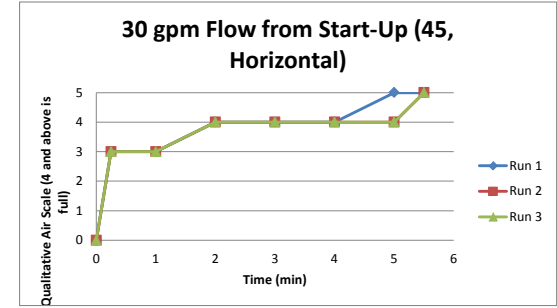
Experiment 190-192

Time	Run 1	Run 2	Run 3
0	0	0	0
0.25	4	4	4
1	4	4	4
1.5	4	4	5
2	5	4	5
2.5	5	5	5



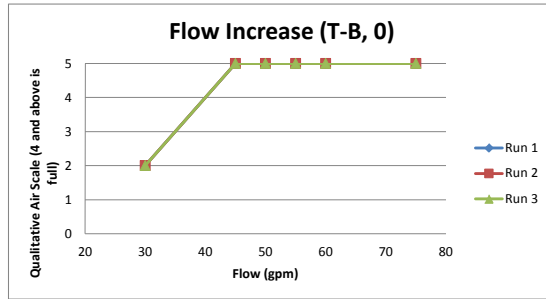
Experiment 196-198

Time	Run 1	Run 2	Run 3
0	0	0	0
0.25	3	3	3
1	3	3	3
2	4	4	4
3	4	4	4
4	4	4	4
5	5	4	4
5.5	5	5	5



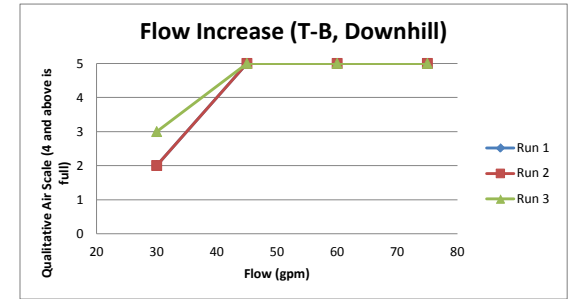
Experiment 205-207

Flow	Run 1	Run 2	Run 3
30	2	2	2
45	5	5	5
50	5	5	5
55	5	5	5
60	5	5	5
75	5	5	5



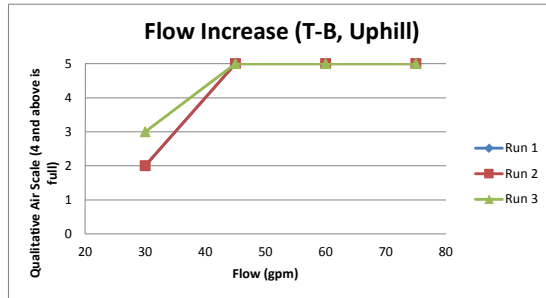
Experiment 217-219

Flow	Run 1	Run 2	Run 3
30	2	2	3
45	5	5	5
60	5	5	5
75	5	5	5



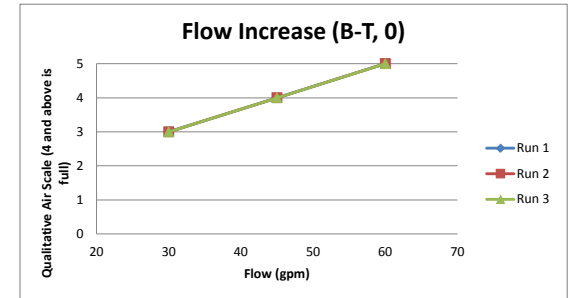
Experiment 229-231

Flow	Run 1	Run 2	Run 3
30	2	2	3
45	5	5	5
60	5	5	5
75	5	5	5



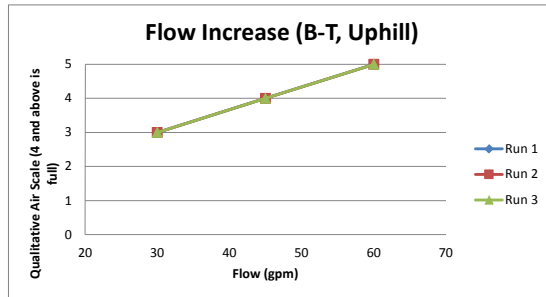
Experiment 256-258

Flow	Run 1	Run 2	Run 3
30	3	3	3
45	4	4	4
60	5	5	5



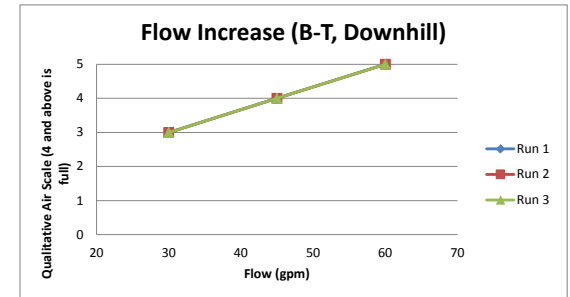
Experiment 265-267

Flow	Run 1	Run 2	Run 3
30	3	3	3
45	4	4	4
60	5	5	5



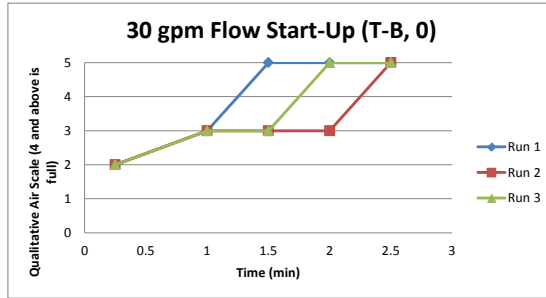
Experiment 2674-276

Flow	Run 1	Run 2	Run 3
30	3	3	3
45	4	4	4
60	5	5	5



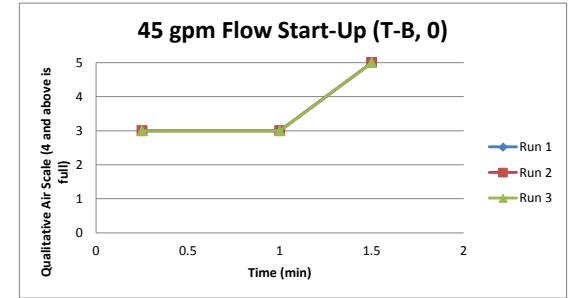
Experiment 208-210

Time	Run 1	Run 2	Run 3
0.25	2	2	2
1	3	3	3
1.5	5	3	3
2	5	3	5
2.5	5	5	5



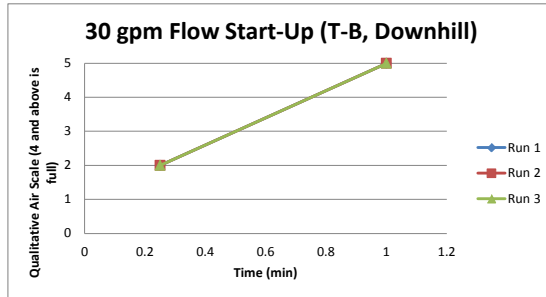
Experiment 211-213

Time	Run 1	Run 2	Run 3
0.25	3	3	3
1	3	3	3
1.5	5	5	5



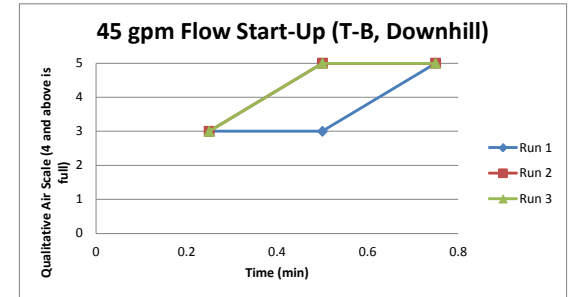
Experiment 220-222

Time	Run 1	Run 2	Run 3
0.25	2	2	2
1	5	5	5



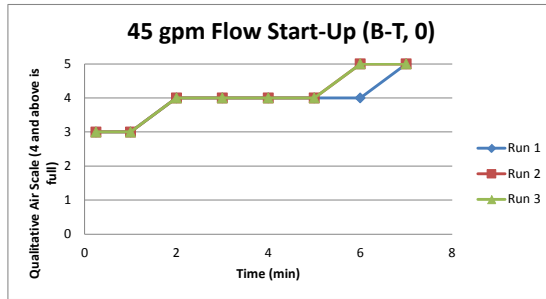
Experiment 223-225

Time	Run 1	Run 2	Run 3
0.25	3	3	3
0.5	3	5	5
0.75	5	5	5



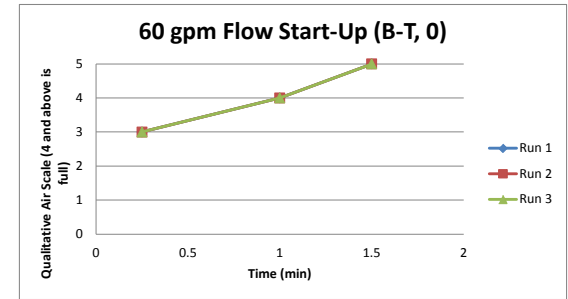
Experiment 259-261

Time	Run 1	Run 2	Run 3
0.25	3	3	3
1	3	3	3
2	4	4	4
3	4	4	4
4	4	4	4
5	4	4	4
6	4	5	5
7	5	5	5



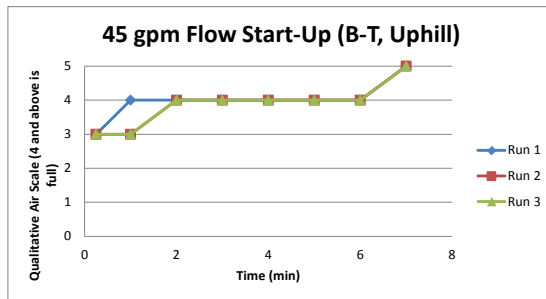
Experiment 262-264

Time	Run 1	Run 2	Run 3
0.25	3	3	3
1	4	4	4
1.5	5	5	5



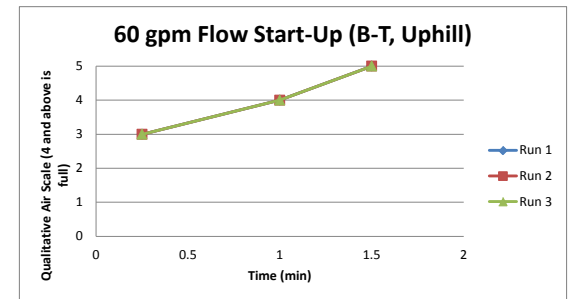
Experiment 268-270

Time	Run 1	Run 2	Run 3
0.25	3	3	3
1	4	3	3
2	4	4	4
3	4	4	4
4	4	4	4
5	4	4	4
6	4	4	4
7	5	5	5



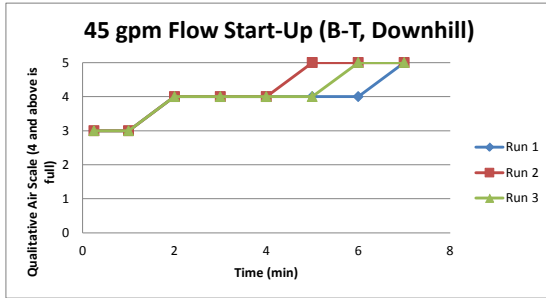
Experiment 271-273

Time	Run 1	Run 2	Run 3
0.25	3	3	3
1	4	4	4
1.5	5	5	5



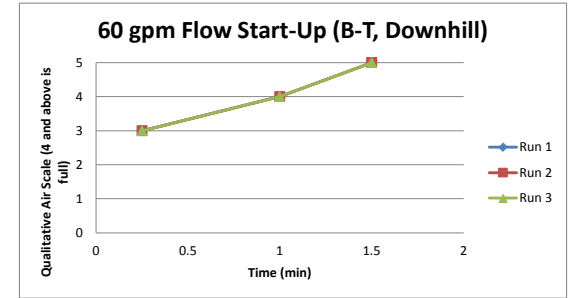
Experiment 277-279

Time	Run 1	Run 2	Run 3
0.25	3	3	3
1	3	3	3
2	4	4	4
3	4	4	4
4	4	4	4
5	4	5	4
6	4	5	5
7	5	5	5



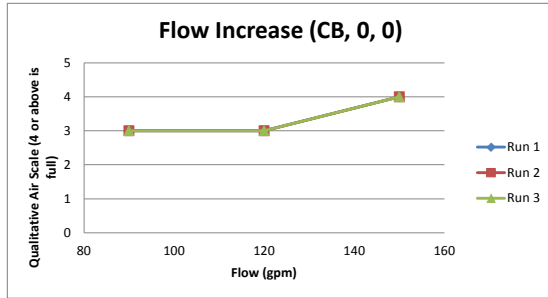
Experiment 280-282

Time	Run 1	Run 2	Run 3
0.25	3	3	3
1	4	4	4
1.5	5	5	5



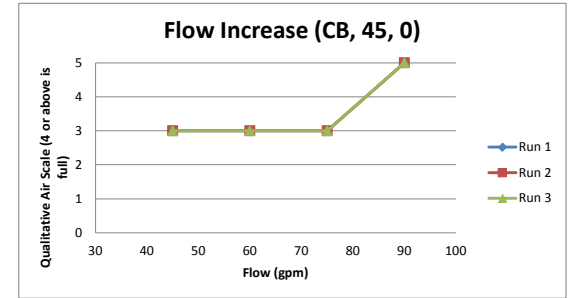
Experiment 235-237

Flow	Run 1	Run 2	Run 3
90	3	3	3
120	3	3	3
150	4	4	4



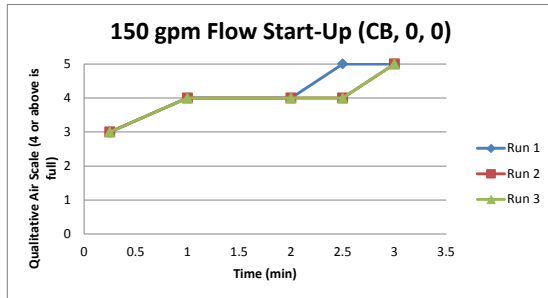
Experiment 241-243

Flow	Run 1	Run 2	Run 3
45	3	3	3
60	3	3	3
75	3	3	3
90	5	5	5



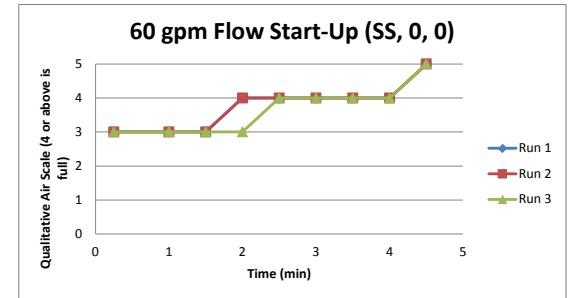
Experiment 238-240

Time	Run 1	Run 2	Run 3
0.25	3	3	3
1	4	4	4
2	4	4	4
2.5	5	4	4
3	5	5	5



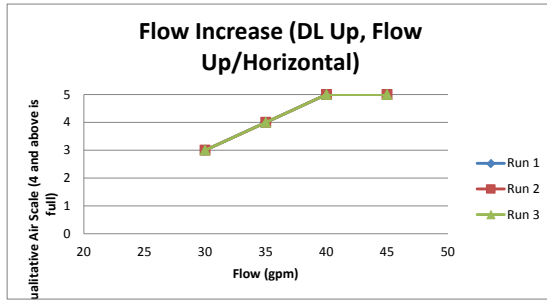
Experiment 247-249

Time	Run 1	Run 2	Run 3
0.25	3	3	3
1	3	3	3
1.5	3	3	3
2	4	4	3
2.5	4	4	4
3	4	4	4
3.5	4	4	4
4	4	4	4
4.5	5	5	5



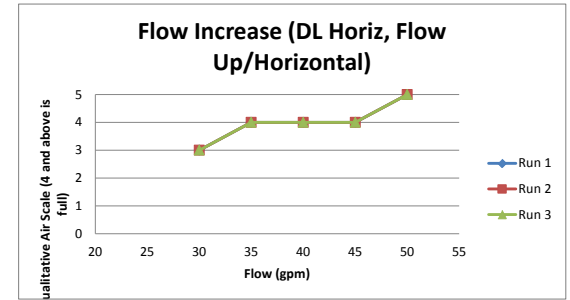
Experiment 283-285

Flow	Run 1	Run 2	Run 3
30	3	3	3
35	4	4	4
40	5	5	5
45	5	5	5



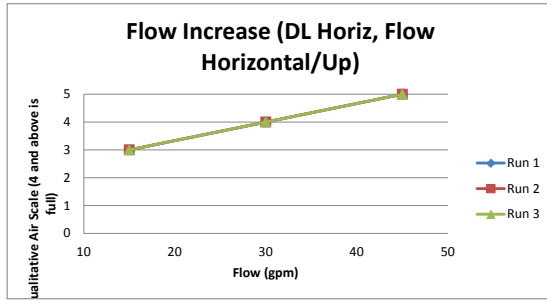
Experiment 292-294

Flow	Run 1	Run 2	Run 3
30	3	3	3
35	4	4	4
40	4	4	4
45	4	4	4
50	5	5	5



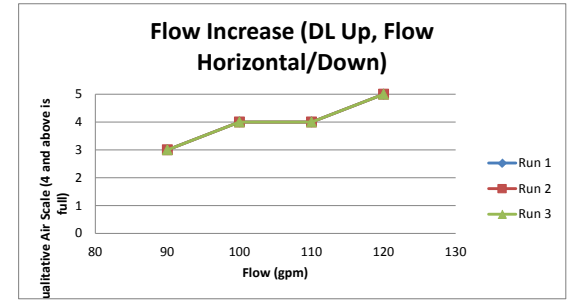
Experiment 301-303

Flow	Run 1	Run 2	Run 3
15	3	3	3
30	4	4	4
45	5	5	5



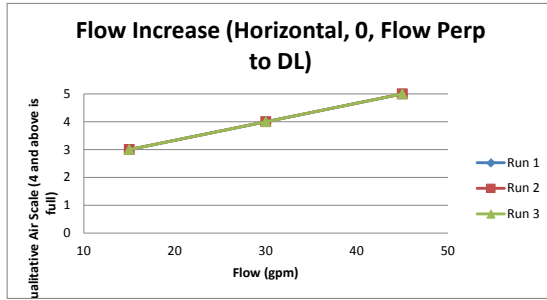
Experiment 313-315

Flow	Run 1	Run 2	Run 3
90	3	3	3
100	4	4	4
110	4	4	4
120	5	5	5



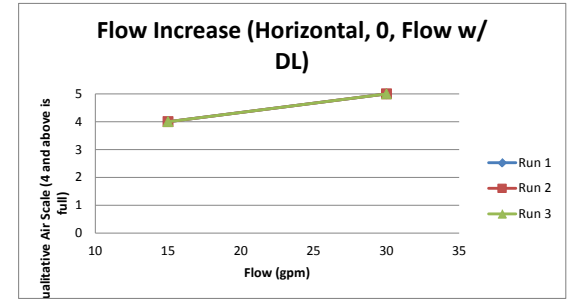
Experiment 322-324

Flow	Run 1	Run 2	Run 3
15	3	3	3
30	4	4	4
45	5	5	5



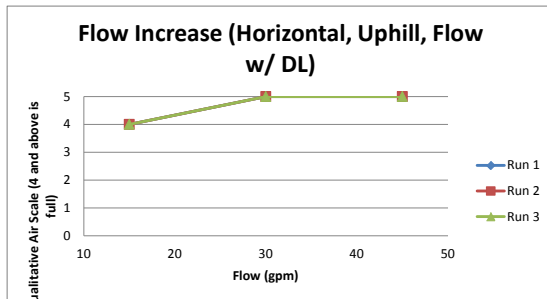
Experiment 331-333

Flow	Run 1	Run 2	Run 3
15	4	4	4
30	5	5	5



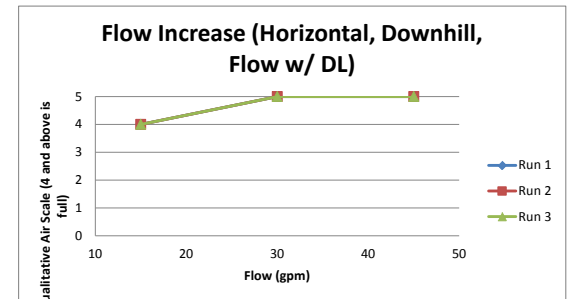
Experiment 337-339

Flow	Run 1	Run 2	Run 3
15	4	4	4
30	5	5	5
45	5	5	5



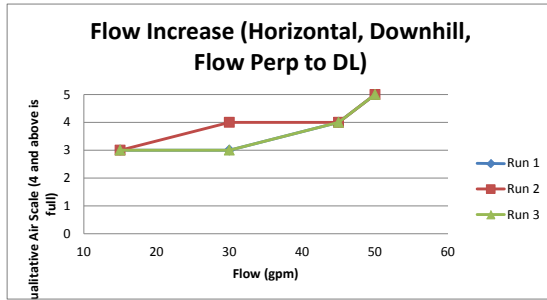
Experiment 343-345

Flow	Run 1	Run 2	Run 3
15	4	4	4
30	5	5	5
45	5	5	5



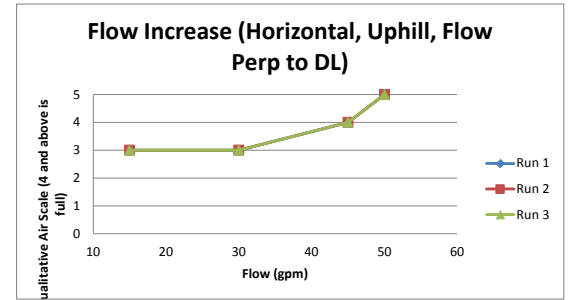
Experiment 349-351

Flow	Run 1	Run 2	Run 3
15	3	3	3
30	3	4	3
45	4	4	4
50	5	5	5



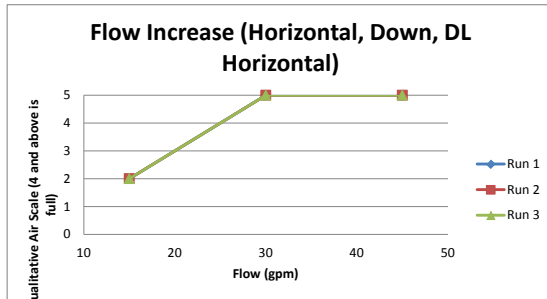
Experiment 358-360

Flow	Run 1	Run 2	Run 3
15	3	3	3
30	3	3	3
45	4	4	4
50	5	5	5



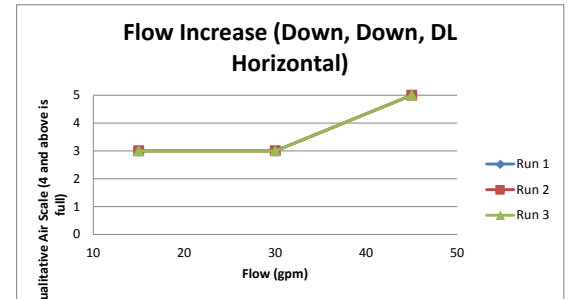
Experiment 367-369

Flow	Run 1	Run 2	Run 3
15	2	2	2
30	5	5	5
45	5	5	5

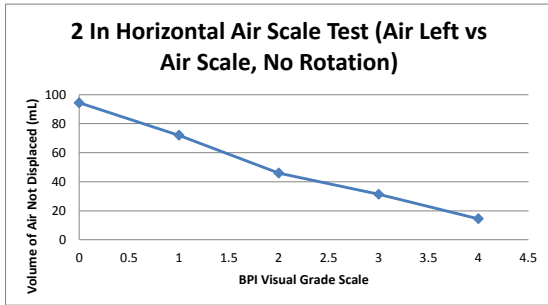


Experiment 373-375

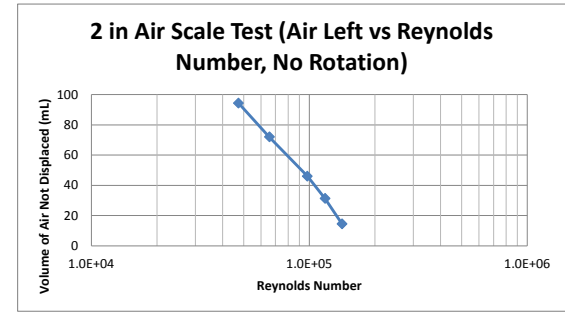
Flow	Run 1	Run 2	Run 3
15	3	3	3
30	3	3	3
45	5	5	5



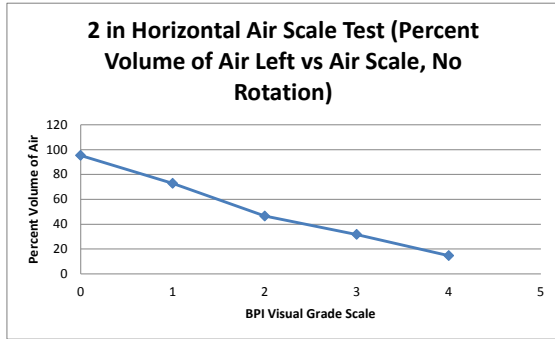
Air Scale	Volume of Air Left (mL)
0	94.33 ± 1.53
1	72.00 ± 2.65
2	46.00 ± 2.00
3	31.33 ± 2.31
4	14.50 ± 4.80



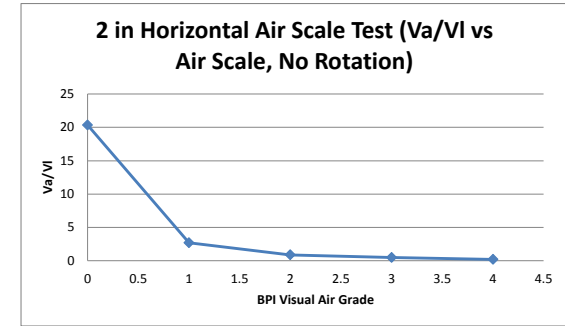
Reynolds Number	Volume of Air Left (mL)
4.7310E+04	94.33 ± 1.53
6.5628E+04	72.00 ± 2.65
9.7905E+04	46.00 ± 2.00
1.1818E+05	31.33 ± 2.31
1.4141E+05	14.50 ± 4.80



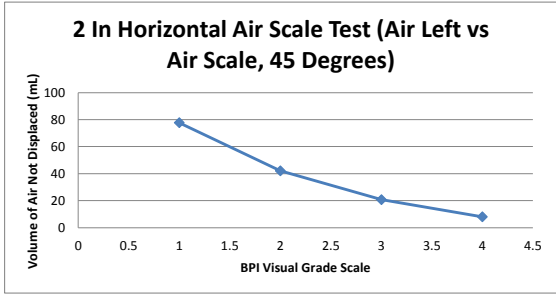
Air Scale	Percent Volume of Air
0	95.32
1	72.75
2	46.48
3	31.66
4	14.65



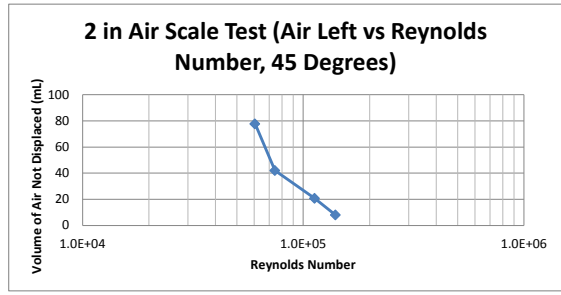
Air Scale	Va/VI
0	20.35
1	2.67
2	0.87
3	0.46
4	0.17



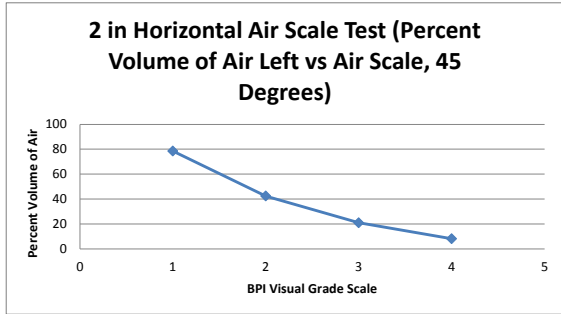
Air Scale	Volume of Air Left (mL)
1	77.67 ± 2.52
2	42.00 ± 3.61
3	20.67 ± 1.53
4	8.00 ± 3.00



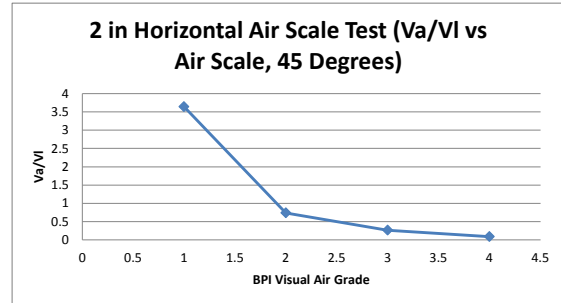
Reynolds Number	Volume of Air Left (mL)
6.0420E+04	77.67 ± 2.52
7.4425E+04	42.00 ± 3.61
1.1250E+05	20.67 ± 1.53
1.3996E+05	8.00 ± 3.00



Air Scale	Percent Volume of Air
1	78.47
2	42.44
3	20.88
4	8.08

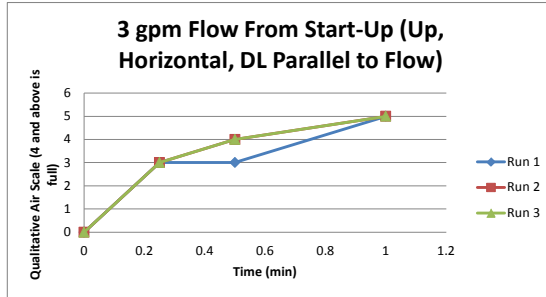


Air Scale	Va/VI
1	3.65
2	0.74
3	0.26
4	0.09



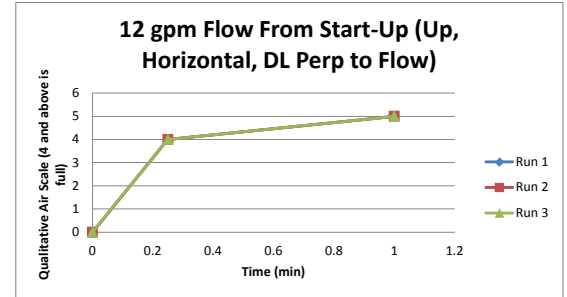
Experiment 832-834

Time	Run 1	Run 2	Run 3
0	0	0	0
0.25	3	3	3
0.5	3	4	4
1	5	5	5



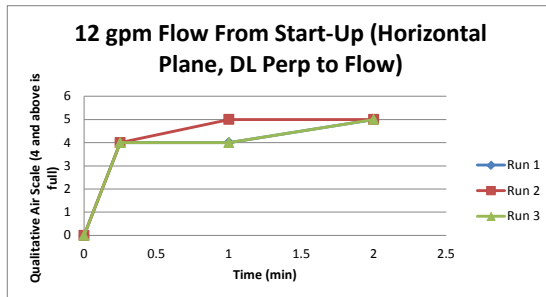
Experiment 836-838

Time	Run 1	Run 2	Run 3
0	0	0	0
0.25	4	4	4
1	5	5	5



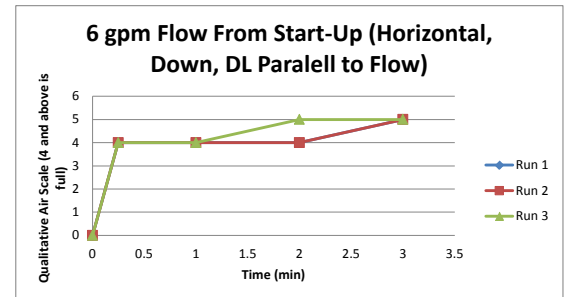
Experiment 876-878

Time	Run 1	Run 2	Run 3
0	0	0	0
0.25	4	4	4
1	4	5	4
2	5	5	5



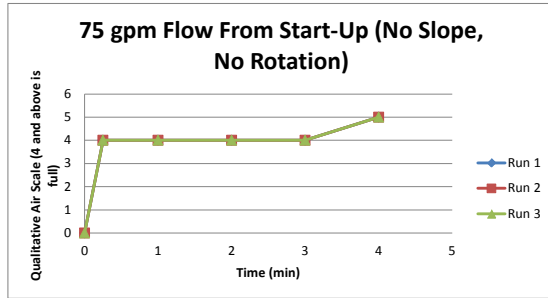
Experiment 931-933

Time	Run 1	Run 2	Run 3
0	0	0	0
0.25	4	4	4
1	4	4	4
2	4	4	5
3	5	5	5



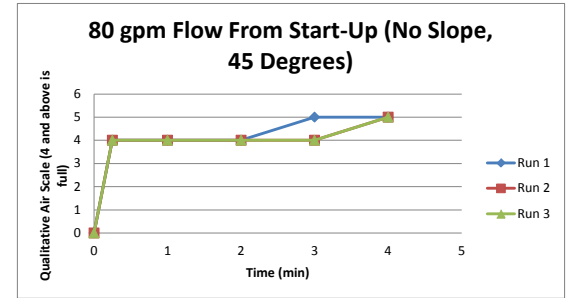
Experiment 901-903

Time	Run 1	Run 2	Run 3
0	0	0	0
0.25	4	4	4
1	4	4	4
2	4	4	4
3	4	4	4
4	5	5	5



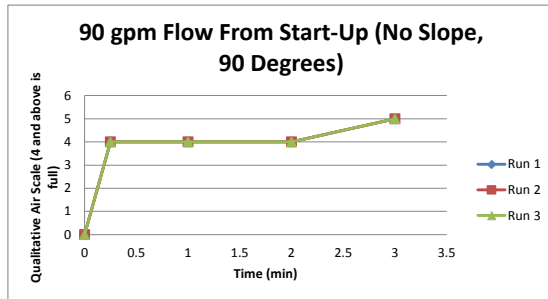
Experiment 908-910

Time	Run 1	Run 2	Run 3
0	0	0	0
0.25	4	4	4
1	4	4	4
2	4	4	4
3	5	4	4
4	5	5	5



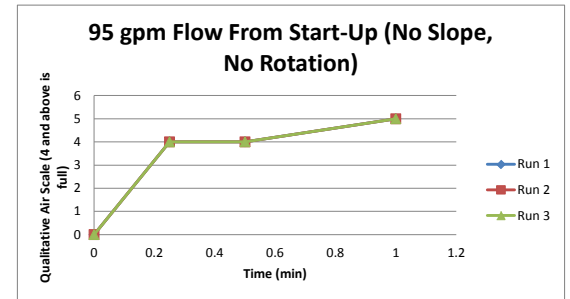
Experiment 915-917

Time	Run 1	Run 2	Run 3
0	0	0	0
0.25	4	4	4
1	4	4	4
2	4	4	4
3	5	5	5



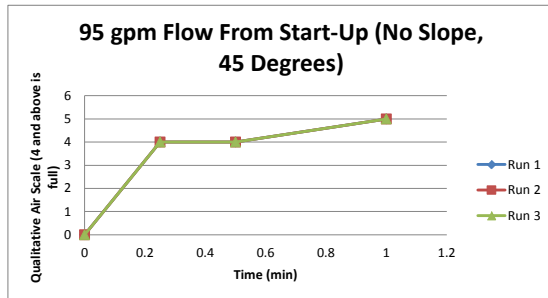
Experiment 1051-1053

Time	Run 1	Run 2	Run 3
0	0	0	0
0.25	4	4	4
0.5	4	4	4
1	5	5	5



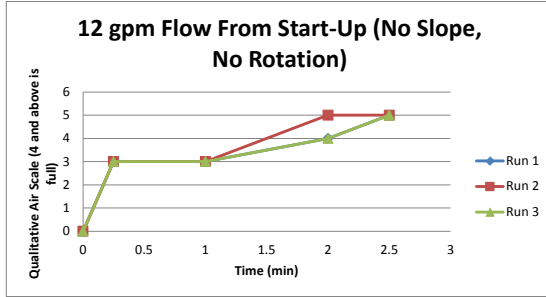
Experiment 1048-1050

Time	Run 1	Run 2	Run 3
0	0	0	0
0.25	4	4	4
0.5	4	4	4
1	5	5	5



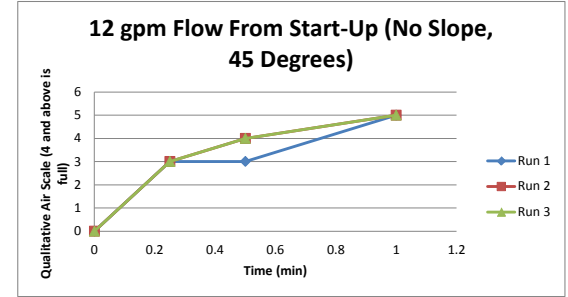
Experiment 852-854

Time	Run 1	Run 2	Run 3
0	0	0	0
0.25	3	3	3
1	3	3	3
2	4	5	4
2.5	5	5	5



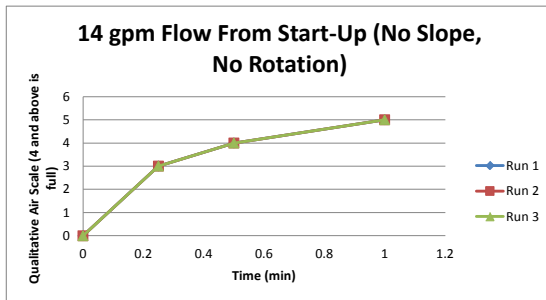
Experiment 855-857

Time	Run 1	Run 2	Run 3
0	0	0	0
0.25	3	3	3
0.5	3	4	4
1	5	5	5



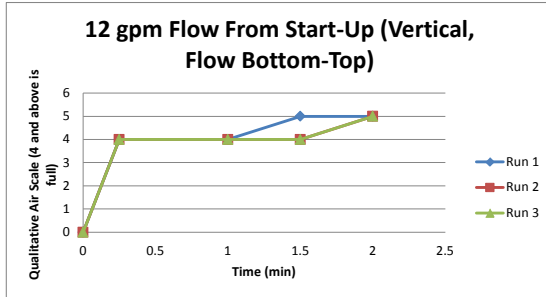
Experiment 1054-1056

Time	Run 1	Run 2	Run 3
0	0	0	0
0.25	3	3	3
0.5	4	4	4
1	5	5	5



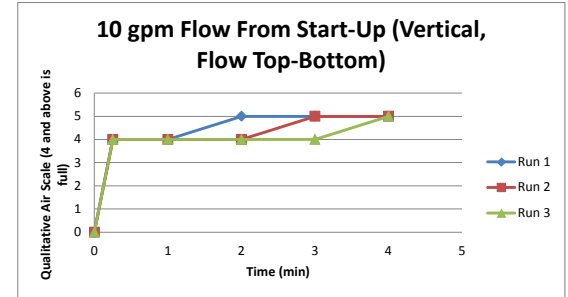
Experiment 840-842

Time	Run 1	Run 2	Run 3
0	0	0	0
0.25	4	4	4
1	4	4	4
1.5	5	4	4
2	5	5	5



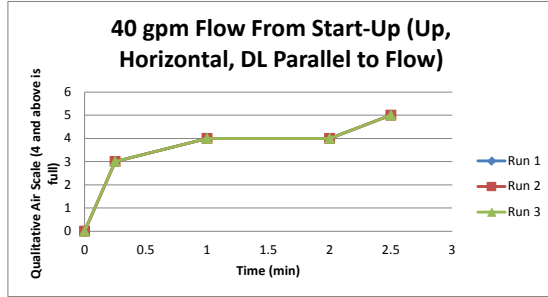
Experiment 936-938

Time	Run 1	Run 2	Run 3
0	0	0	0
0.25	4	4	4
1	4	4	4
2	5	4	4
3	5	5	4
4	5	5	5



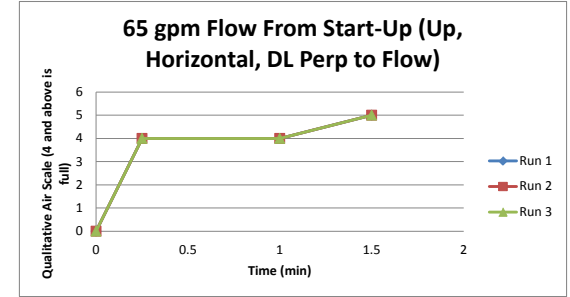
Experiment 820-822

Time	Run 1	Run 2	Run 3
0	0	0	0
0.25	3	3	3
1	4	4	4
2	4	4	4
2.5	5	5	5



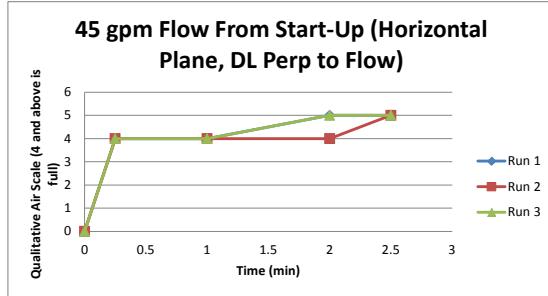
Experiment 829-831

Time	Run 1	Run 2	Run 3
0	0	0	0
0.25	4	4	4
1	4	4	4
1.5	5	5	5



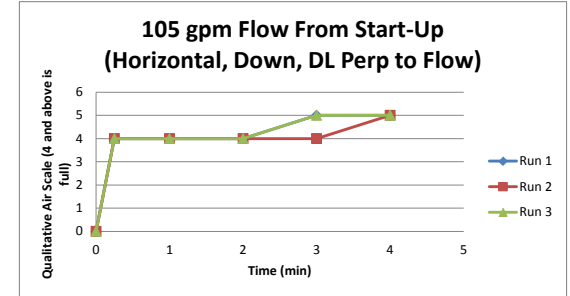
Experiment 868-870

Time	Run 1	Run 2	Run 3
0	0	0	0
0.25	4	4	4
1	4	4	4
2	5	4	5
2.5	5	5	5



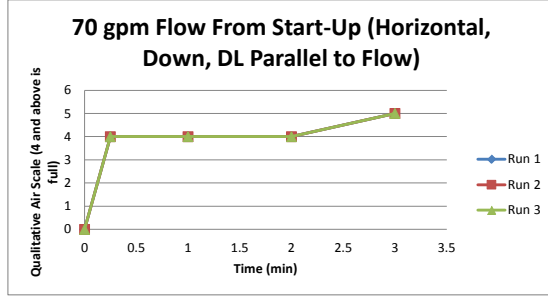
Experiment 921-923

Time	Run 1	Run 2	Run 3
0	0	0	0
0.25	4	4	4
1	4	4	4
2	4	4	4
3	5	4	5
4	5	5	5



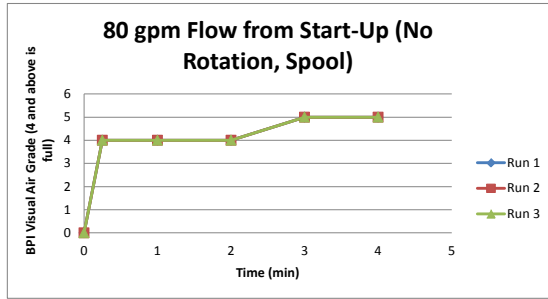
Experiment 928-930

Time	Run 1	Run 2	Run 3
0	0	0	0
0.25	4	4	4
1	4	4	4
2	4	4	4
3	5	5	5



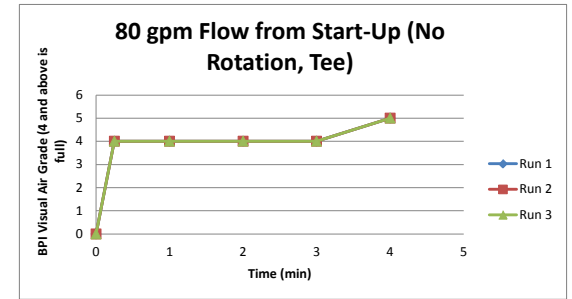
Experiment 984-986

Time	Spool		
	Run 1	Run 2	Run 3
0	0	0	0
0.25	4	4	4
1	4	4	4
2	4	4	4
3	5	5	5
4	5	5	5



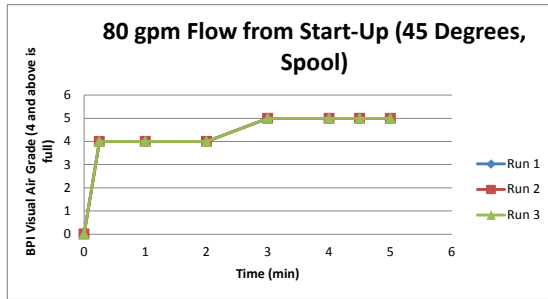
Experiment 984-986

Time	Tee		
	Run 1	Run 2	Run 3
0	0	0	0
0.25	4	4	4
1	4	4	4
2	4	4	4
3	4	4	4
4	5	5	5



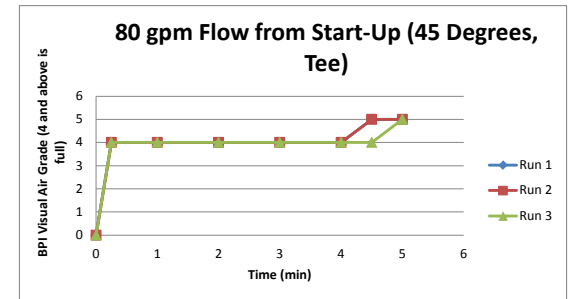
Experiment 987-989

Time	Spool		
	Run 1	Run 2	Run 3
0	0	0	0
0.25	4	4	4
1	4	4	4
2	4	4	4
3	5	5	5
4	5	5	5
4.5	5	5	5
5	5	5	5



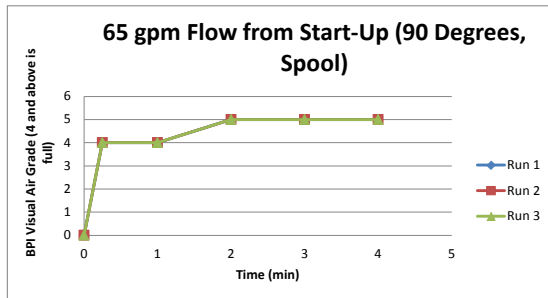
Experiment 987-989

Time	Tee		
	Run 1	Run 2	Run 3
0	0	0	0
0.25	4	4	4
1	4	4	4
2	4	4	4
3	4	4	4
4	4	4	4
4.5	5	5	4
5	5	5	5



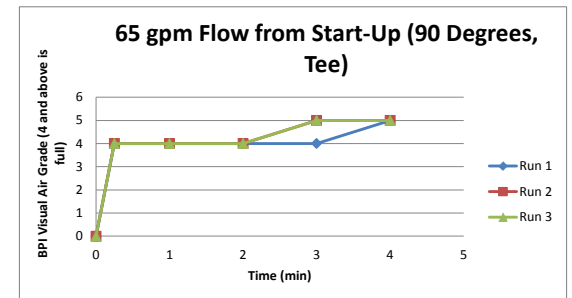
Experiment 1000-1002

Time	Spool		
	Run 1	Run 2	Run 3
0	0	0	0
0.25	4	4	4
1	4	4	4
2	5	5	5
3	5	5	5
4	5	5	5



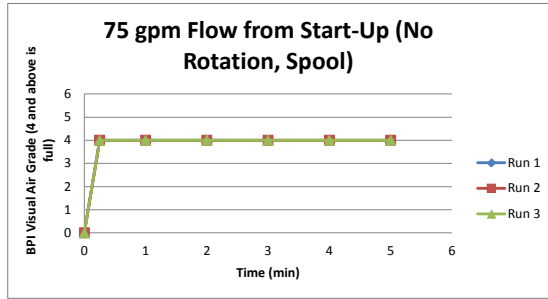
Experiment 1000-1002

Time	Tee		
	Run 1	Run 2	Run 3
0	0	0	0
0.25	4	4	4
1	4	4	4
2	4	4	4
3	4	5	5
4	5	5	5



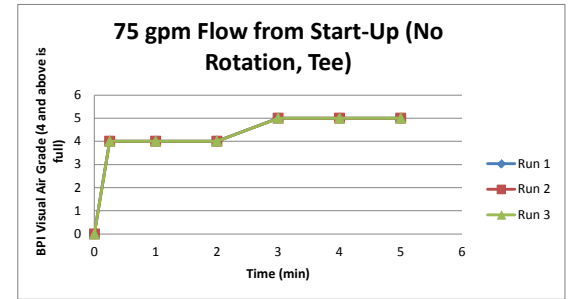
Experiment 948-950

Time	Spool		
	Run 1	Run 2	Run 3
0	0	0	0
0.25	4	4	4
1	4	4	4
2	4	4	4
3	4	4	4
4	4	4	4
5	4	4	4



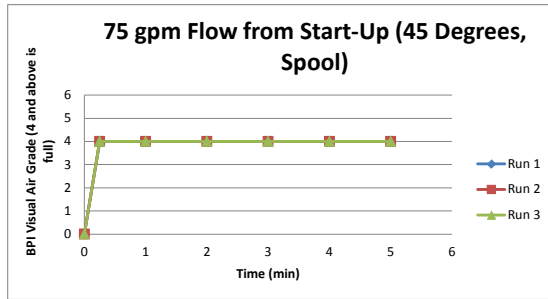
Experiment 948-950

Time	Tee		
	Run 1	Run 2	Run 3
0	0	0	0
0.25	4	4	4
1	4	4	4
2	4	4	4
3	5	5	5
4	5	5	5
5	5	5	5



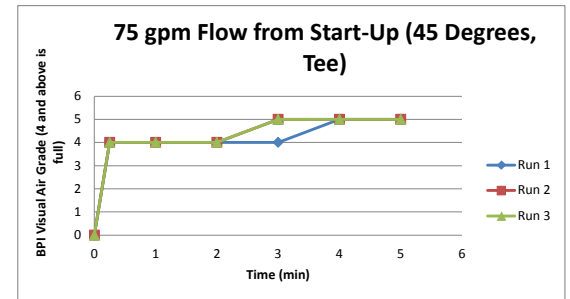
Experiment 960-962

Time	Spool		
	Run 1	Run 2	Run 3
0	0	0	0
0.25	4	4	4
1	4	4	4
2	4	4	4
3	4	4	4
4	4	4	4
5	4	4	4



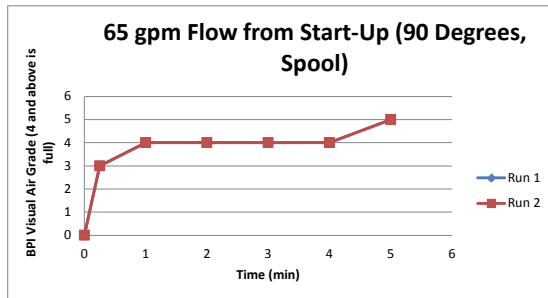
Experiment 960-962

Time	Tee		
	Run 1	Run 2	Run 3
0	0	0	0
0.25	4	4	4
1	4	4	4
2	4	4	4
3	4	5	5
4	5	5	5
5	5	5	5



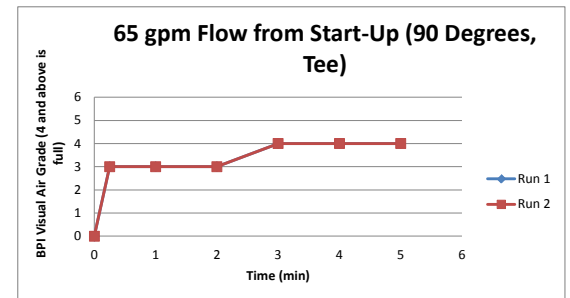
Experiment 973-974

Time	Spool	
	Run 1	Run 2
0	0	0
0.25	3	3
1	4	4
2	4	4
3	4	4
4	4	4
5	5	5



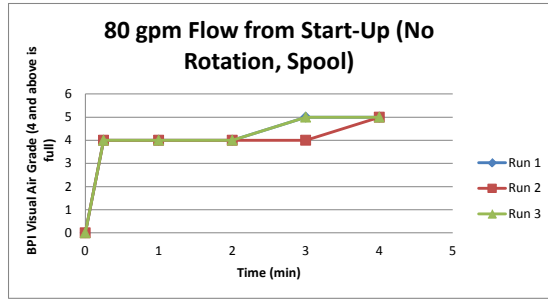
Experiment 973-974

Time	Tee	
	Run 1	Run 2
0	0	0
0.25	3	3
1	3	3
2	3	3
3	4	4
4	4	4
5	4	4



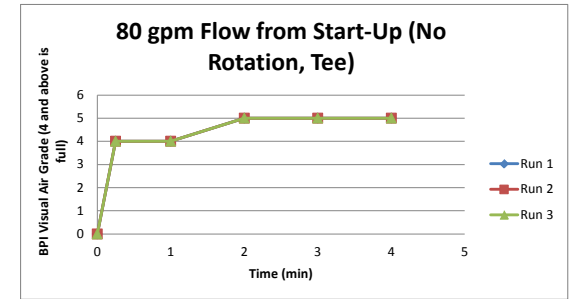
Experiment 951-953

Time	Spool		
	Run 1	Run 2	Run 3
0	0	0	0
0.25	4	4	4
1	4	4	4
2	4	4	4
3	5	4	5
4	5	5	5



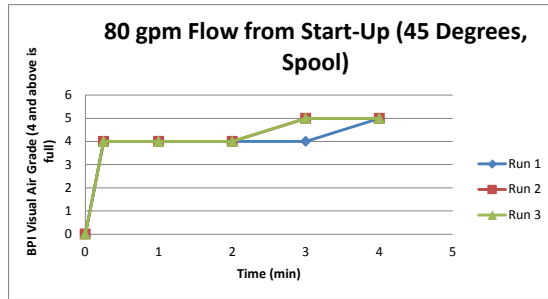
Experiment 951-953

Time	Tee		
	Run 1	Run 2	Run 3
0	0	0	0
0.25	4	4	4
1	4	4	4
2	5	5	5
3	5	5	5
4	5	5	5



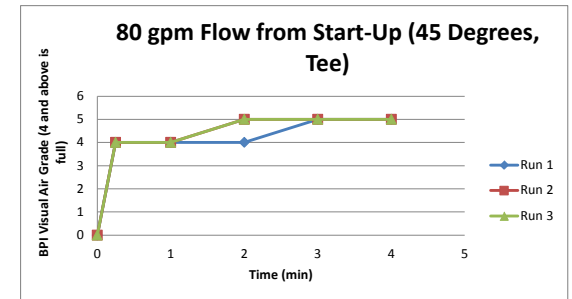
Experiment 963-965

Time	Spool		
	Run 1	Run 2	Run 3
0	0	0	0
0.25	4	4	4
1	4	4	4
2	4	4	4
3	4	5	5
4	5	5	5



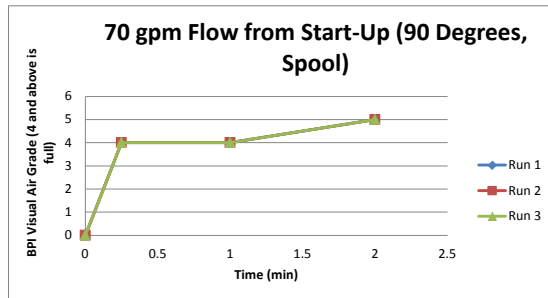
Experiment 963-965

Time	Tee		
	Run 1	Run 2	Run 3
0	0	0	0
0.25	4	4	4
1	4	4	4
2	4	5	5
3	5	5	5
4	5	5	5



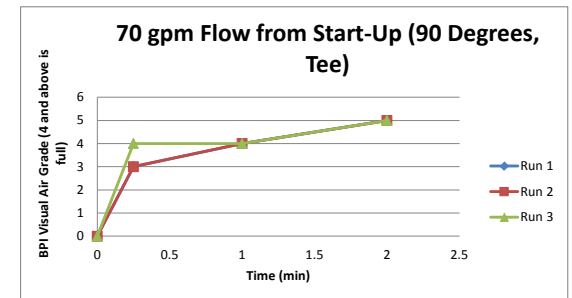
Experiment 975-977

Time	Spool		
	Run 1	Run 2	Run 3
0	0	0	0
0.25	4	4	4
1	4	4	4
2	5	5	5



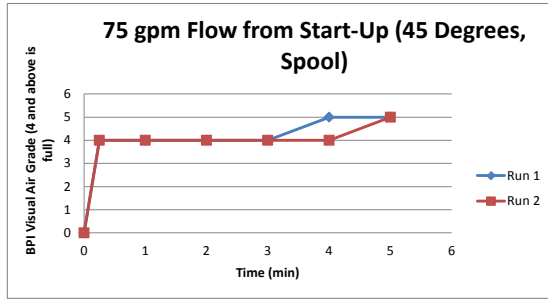
Experiment 975-977

Time	Tee		
	Run 1	Run 2	Run 3
0	0	0	0
0.25	3	3	4
1	4	4	4
2	5	5	5



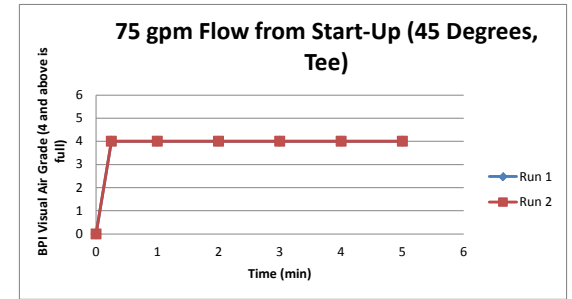
Experiment 990-991

Time	Spool	
	Run 1	Run 2
0	0	0
0.25	4	4
1	4	4
2	4	4
3	4	4
4	5	4
5	5	5



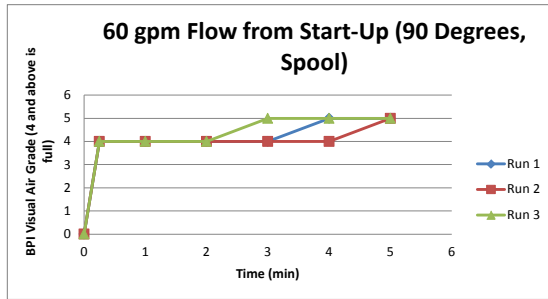
Experiment 990-991

Time	Tee	
	Run 1	Run 2
0	0	0
0.25	4	4
1	4	4
2	4	4
3	4	4
4	4	4
5	4	4



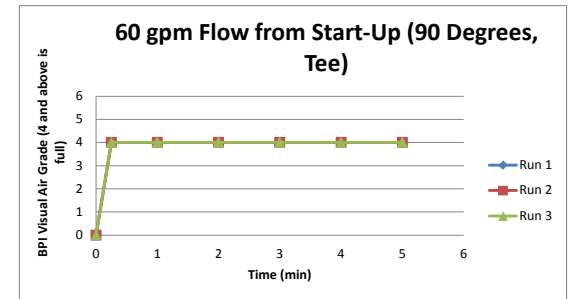
Experiment 997-999

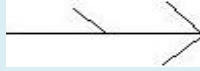
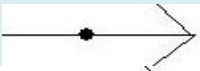
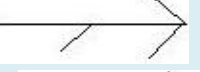
Time	Spool		
	Run 1	Run 2	Run 3
0	0	0	0
0.25	4	4	4
1	4	4	4
2	4	4	4
3	4	4	5
4	5	4	5
5	5	5	5



Experiment 997-999

Time	Tee		
	Run 1	Run 2	Run 3
0	0	0	0
0.25	4	4	4
1	4	4	4
2	4	4	4
3	4	4	4
4	4	4	4
5	4	4	4



Flow Rate (gpm)		Velocity (ft/s)				
60		9.8805				
Tube	Rotation (degrees)	Slope (1/8" by 12")	Orientation	Time to Clear (s)	Reynolds Number	
2" T Horizontal	0	0		360		
2" T Horizontal	45	0		460		
2" T Horizontal	90	0		240		
2" T Horizontal	135	0		1		
2" T Horizontal	180	0		1		
2" T Horizontal	0	Uphill		300		
2" T Horizontal	45	Uphill		480		
2" T Horizontal	90	Uphill		180		
2" T Horizontal	0	Downhill		240		
2" T Horizontal	45	Downhill		420		
2" T Horizontal	90	Downhill		180		

APPENDIX H: LITERATURE

The following literatures are supplements in the development of this document:

- Dead-end Considerations based on Literature and own work, *Bo Boye Busk Jensen*
- Testing to Determine Flow rates Required to Flood Piping, *Jeff J. Gaerke P.E*
- Characteristics of flow field and water concentration in a horizontal Deadleg, *M.A. Habib*
- On the Development of Deadleg Criterion, *M.A. Habib*

Dead-end considerations based on literature and own work.

Bo Boye Busk Jensen, 2010

On the topic of understanding the hygienically design issues around the so-called “dead-end” geometry, that can appear in any process line or piece of equipment, some work has already been done. This document tries to collect the most important results from these.

- Grasshoff work
- EHEDG movies
- CFD work by Jensen
- Experimental work by Jensen

The general rules on L/d found in different guidelines and standards are:

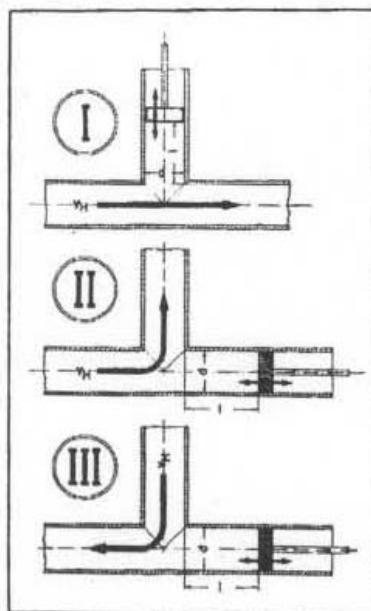
- ASME BPE: $L/d < 2:1$
- 3-A: $L/d < 2:1$ (T-613-00 – not yet published)
- EHEDG: $L/d < 1:1$ (Guideline no.: 10)
- Japan: $L/D < 1.5:1$ (Sei presentation at ASME BPE 2011 – Philly)

Grasshoff

Has published a number of papers that uses data from experimental work that he did – but the one where the data was established is this one:

- 1980: Untersuchungen zum Strömungsverhalten von Flüssigkeiten in zylindrischen Toträumen von Rohrleitungssystemen, in Kieler Milchwirtschaftliche forschungsbereich

The three different configurations Grasshoff deals with – in German: “Strömungsaufall”



The piping in the test section was made from $\varnothing 50$ plexiglass to allow flow visualisation. Upstream the test section a 2 m straight pipe was present to allow a fully developed flow before the test section. The length of the dead-end was adjusted by a moveable plunger. L is the distance from where the dead-end pipe is attached to the main pipe (see figure above) and d is the diameter of the dead-end pipe.

The flow inside the pipe varied between 1 and 5 m/s giving Reynolds numbers between 45,000-224,000 at 16C and 90,000-452,000 at 50C

The tests that Grasshoff performed on these configurations was:

- Flow visualization using VESTYPOR $\varnothing 0.5$ mm particles with a density of 1000 kg/m^3
- Flow quantification using flow visualization
- Fluid exchange investigating the replacement of a conducting liquid with a non-conducting liquid.

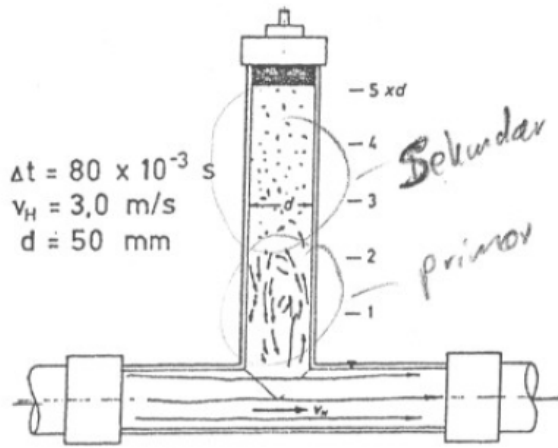
Flow Visualization:

Flow was visualized inside the three different configurations by a camera with a long exposure.

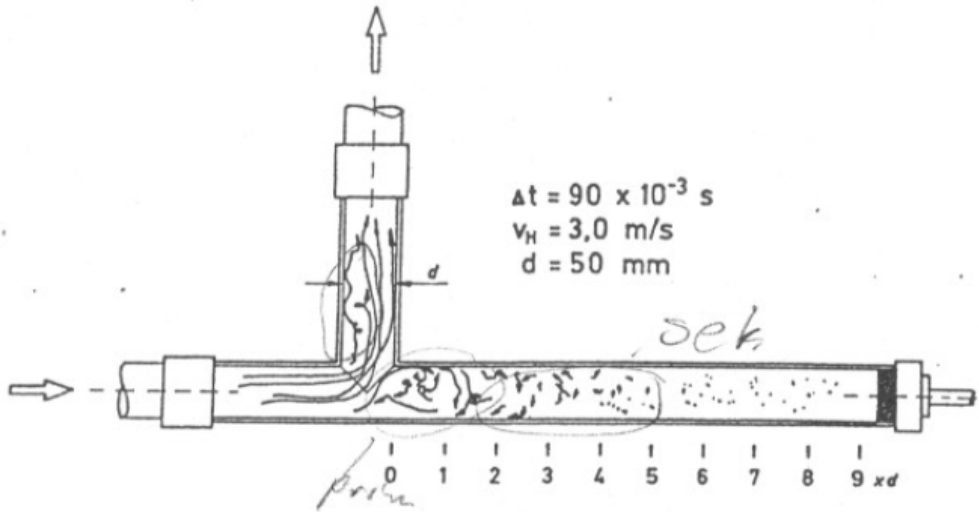
The pictures show that for all three configurations there is a primary and a secondary recirculation zone in the dead-end. The locations of these two zones are approximately:

- Case 1: $L/D = 2$ (little or no action in secondary)
- Case 2: $L/D = 2-3$ (more intense secondary up to 5)
- Case 3: $L/D = 2$ (little or no action in secondary)

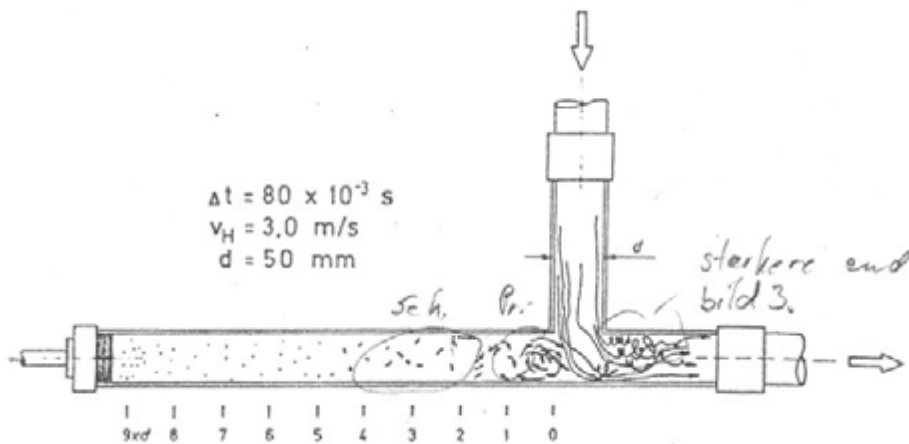
The visualization shown here from Grasshoff is done at a high Reynolds number. So one would ask what would happen if the velocity was reduced or increased. As the Reynolds number from 1 m/s up to 5 m/s in all cases are above 30,000 then the theory tells that the flow pattern will be the same regardless of Reynolds number and thereby velocity. Of course the intensity (velocity of the primary and secondary recirculations zones) depends on the velocity in the main flow, but the positions and sizes of the recirculations zones does not change. The higher the velocity the more exchange between main flow and primary and secondary recirculation will take place is shown later.



Case 1



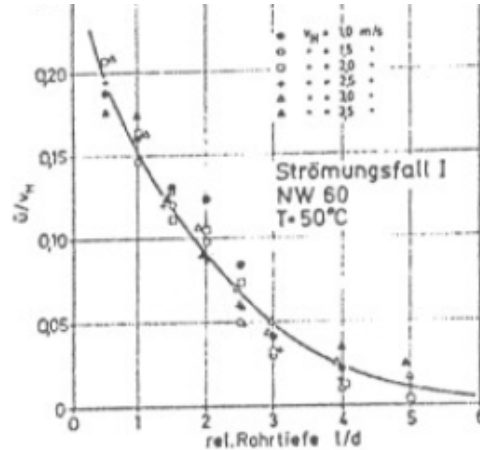
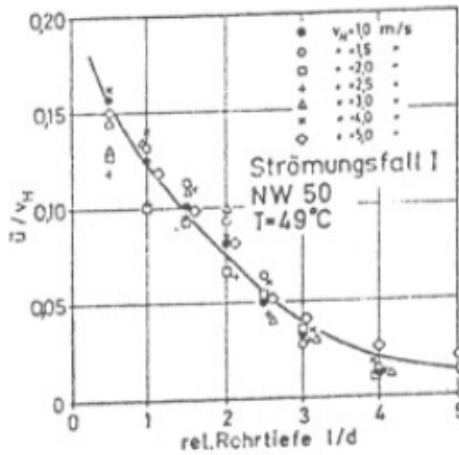
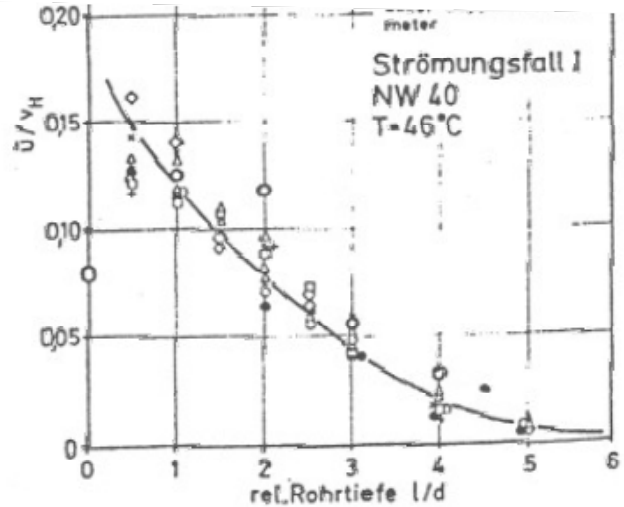
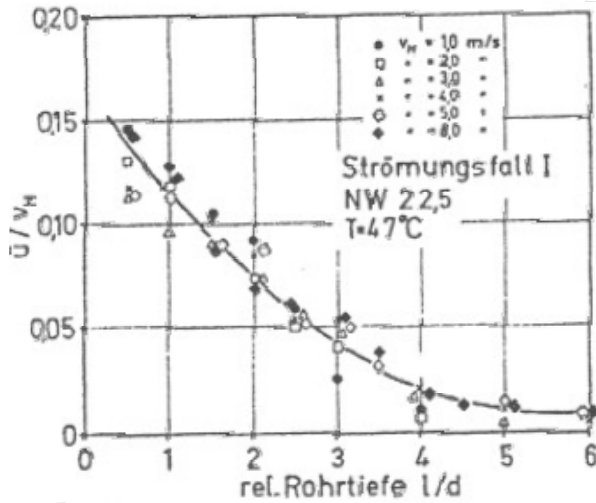
Case 2



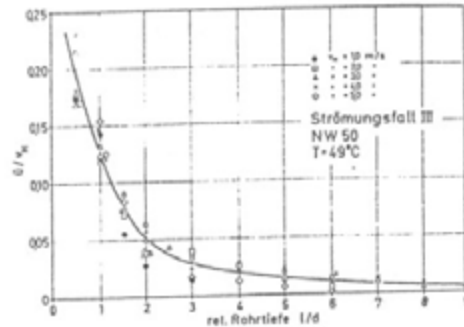
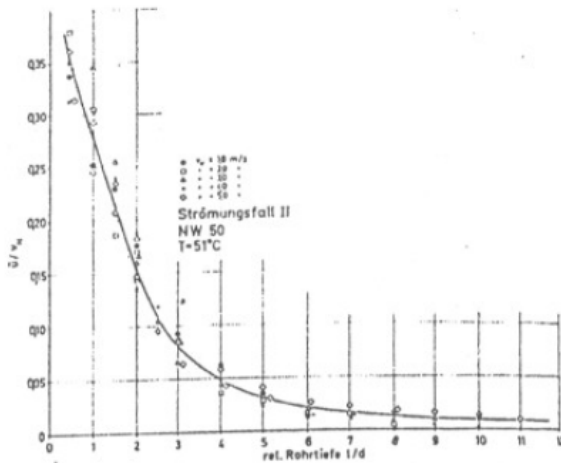
Case 3

Velocity in dead-end

The flow velocity in the dead-end as a function of velocity was also provided by Grasshoff. For Case 1 the measurements were done for $\varnothing 22.5$, $\varnothing 40$, $\varnothing 50$ and $\varnothing 60$. The graphs below show that the pipe diameter has no influence on the velocity in the dead-end. For all 4 pipe sizes the velocity at $L/d = 1$ is below 0.125 (1/8) of that in the main pipe. This means that the wall shear stress in this area is a MAXIMUM of 0.025 of the wall shear stress found in the main pipe. In many areas this is probably much lower due to local variations in flow velocity in the primary recirculation zone. Going further into the dead-end only makes this worse. This is the same for Case 3 configuration.



For Case 2 configuration of dead-end the average velocity in the dead-end is below 0.275 of that in the main pipe at $l/d > 1$.



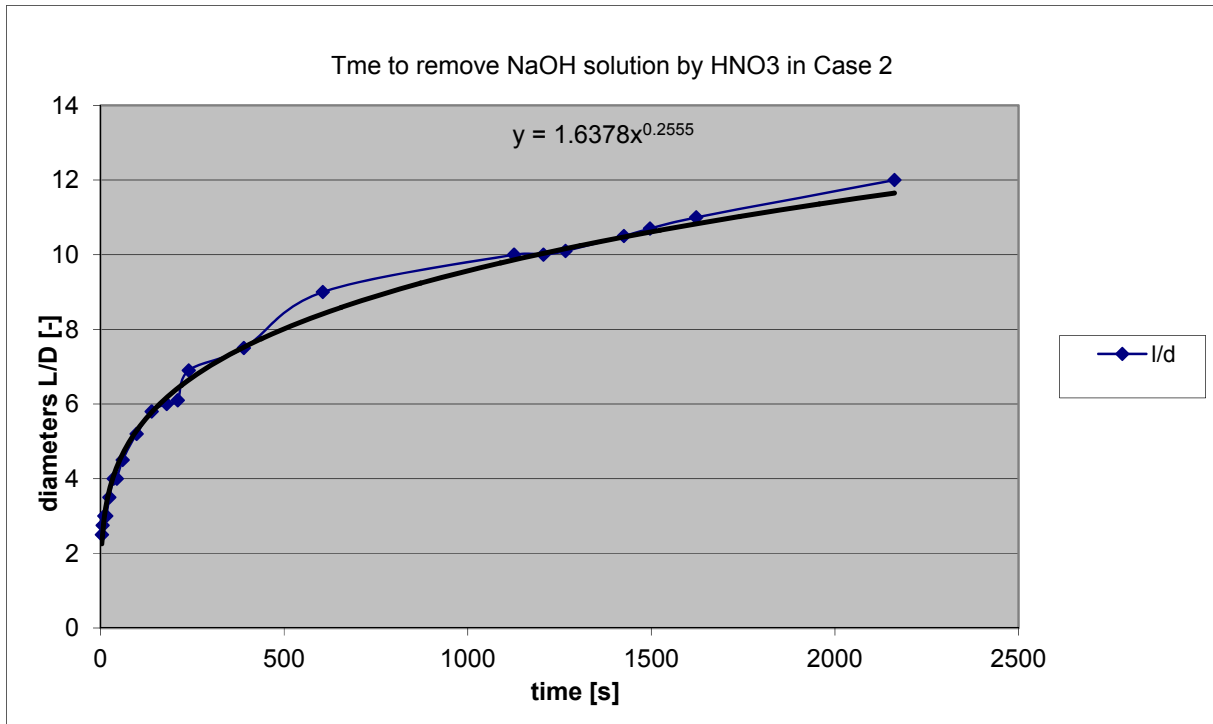
This means that the mechanical (wall shear stress) cleaning effect of the flow is very low in the primary recirculation that stretches up to L/d of approx. 2 for all 3 cases. This, in combination with the lower mass and heat transfer in the recirculation zones, decreases the cleaning rate.

Fluid exchange in dead-end

Grasshoff uses a 0.1-n-NaOH solution with added Phenolphthalein. The Phenolphthalein is added to colour the fluid. The pipe system is filled with this liquid. Then the pipe system is cleaned pumping through a HNO_3 solution. This both flush out the NaOH solution and neutralizes the NaOH solution so that the Phenolphthalein changes colour from a red to a colourless solution. The exchange of fluid is measured by conductive changes in the system.

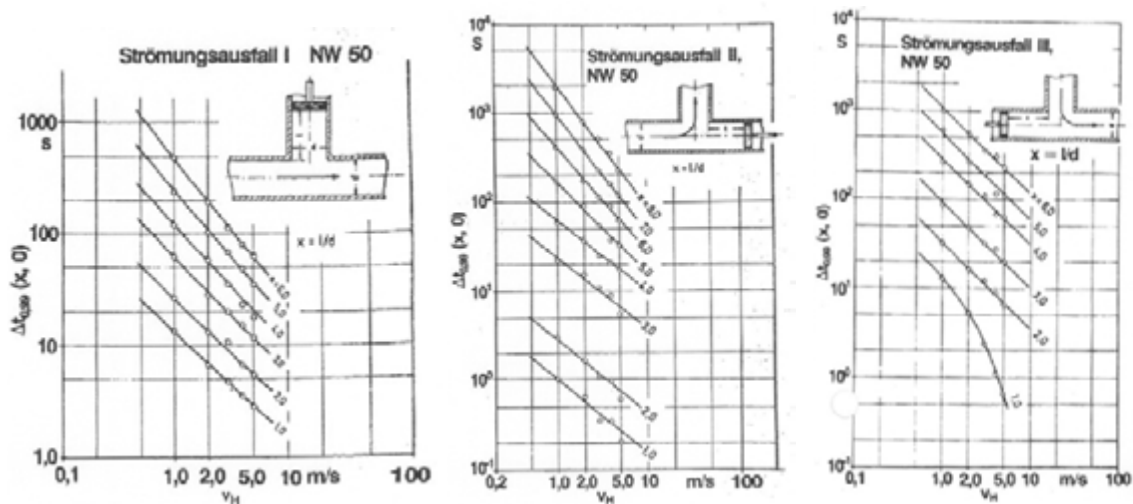
In the papers there are pictures taken of the colour shift length (L/d) as a function of time. Plotting these as a function of time it can be seen how the time for fluid exchange increases slowly from L/d 2.5 to around 6, from where any further exchanges takes longer time.

- Fluid exchange in a NW50 V_pipe = 2,6 – case II



The data for the conductivity measurement for showing the time it takes to changes the conductivity to 99% of the original shows:

- Case 1: worse than flow against. No jump in the time for fluid exchange between L/d's.
- Case 2: Up to L/d < 2 gives the fastest exchange of the tree. But going to L/d = 3 makes a large difference in fluid exchange time (at 1.5 m/s going from l/d = 2 to l/d = 3 the fluid exchange time increases with a factor of 10). Above 2 it actually becomes just as bad as Case 1.
- Case 3: This only works well at high velocity (approx. 5 m/s) at L/d = 1. Below that the fluid exchange is very poor.



The fluid exchange or the velocity (wall shear stress) cannot be looked upon solely to evaluate the cleaning effect. This is a combination of fluid exchange and wall shear stress.

The primary recirculation zone in the dead-ends extents around $1\frac{1}{2}$ - $2\cdot D$ into the dead-end for the best configuration (Case 2).

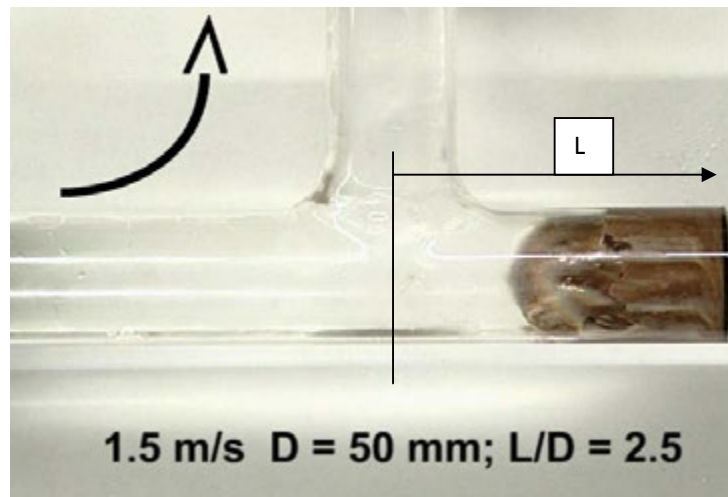
Case II could have L/d one larger than that of Case I and III as cleaning is better in case II

EHEDG movies

As part of EHEDG educational toolbox for teaching courses in hygienic design the EHEDG has produced a DVD that contains movies that shows:

- How chocolate is removed from a dead-end at different velocities and dead-end length. The diameter is $\varnothing 50$ and $\varnothing 75$ and the geometry is made from glass.
- How spherical balls are flushed out of the dead-end at different velocities and dead-end length.

L/D is measured from the center line of the main pipe to the end of the dead-end. This means that the L/D used in this section is 0.5 larger compared to the L/D used in the previous section (and the one normally used by ASME BPE, 3-A and EHEDG).



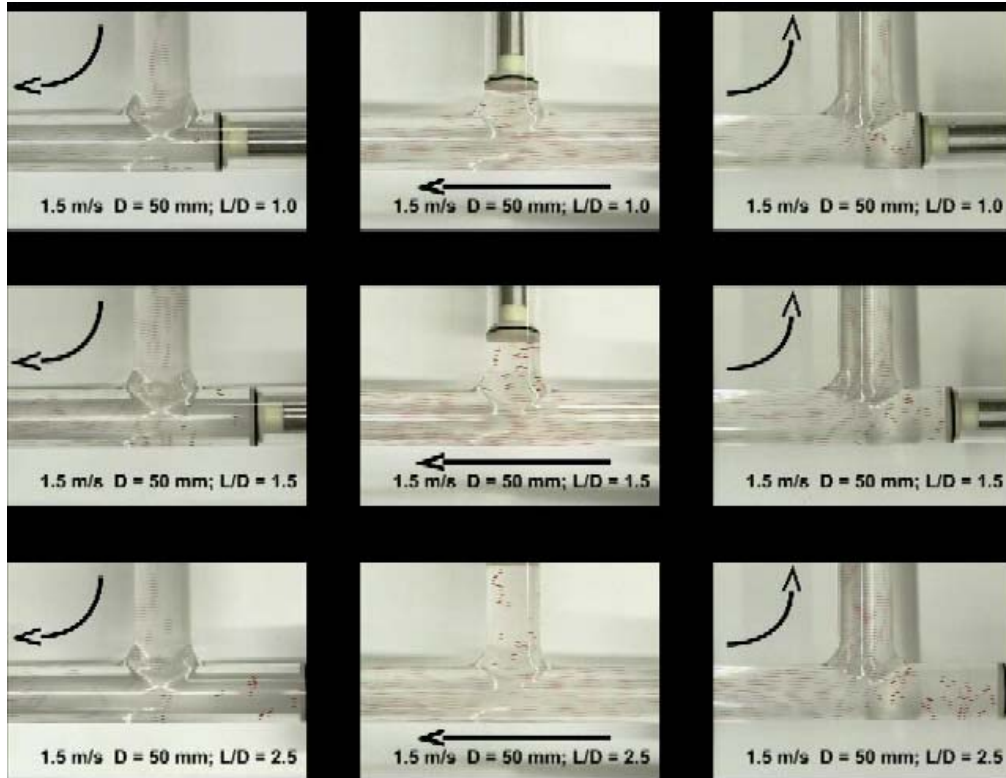
From EHEDG training video (Courtesy of EHEDG) – for INTERNAL ASME BPE USE ONLY.

Overview of configurations investigated with chocolate cleaning:

L/D	velocity	Diameter	Case	Removed	Cleaning time [s]	Comment
1	1.5	50	2	Chocolate (Nutella)	8	
1.5	1.5	50	2	Chocolate (Nutella)	49	Takes long time to remove the soil in the corner at the end of the dead-end. Most is cleaned out in

						30 s
2.5	1.5	50	2	Chocolate (Nutella)	>300	Last 0.5D is not cleaned after 300s.

For the experiments with small spheres (red) a number of combinations of experiments has been performed. The velocity range tested is 0.3 m/s to 1.5 m/s and the dead-end length is between 0.5 and 2.5 L/D at two different pipe diameters.



From EHEDG training video (Courtesy of EHEDG) – for INTERNAL ASME BPE USE ONLY.

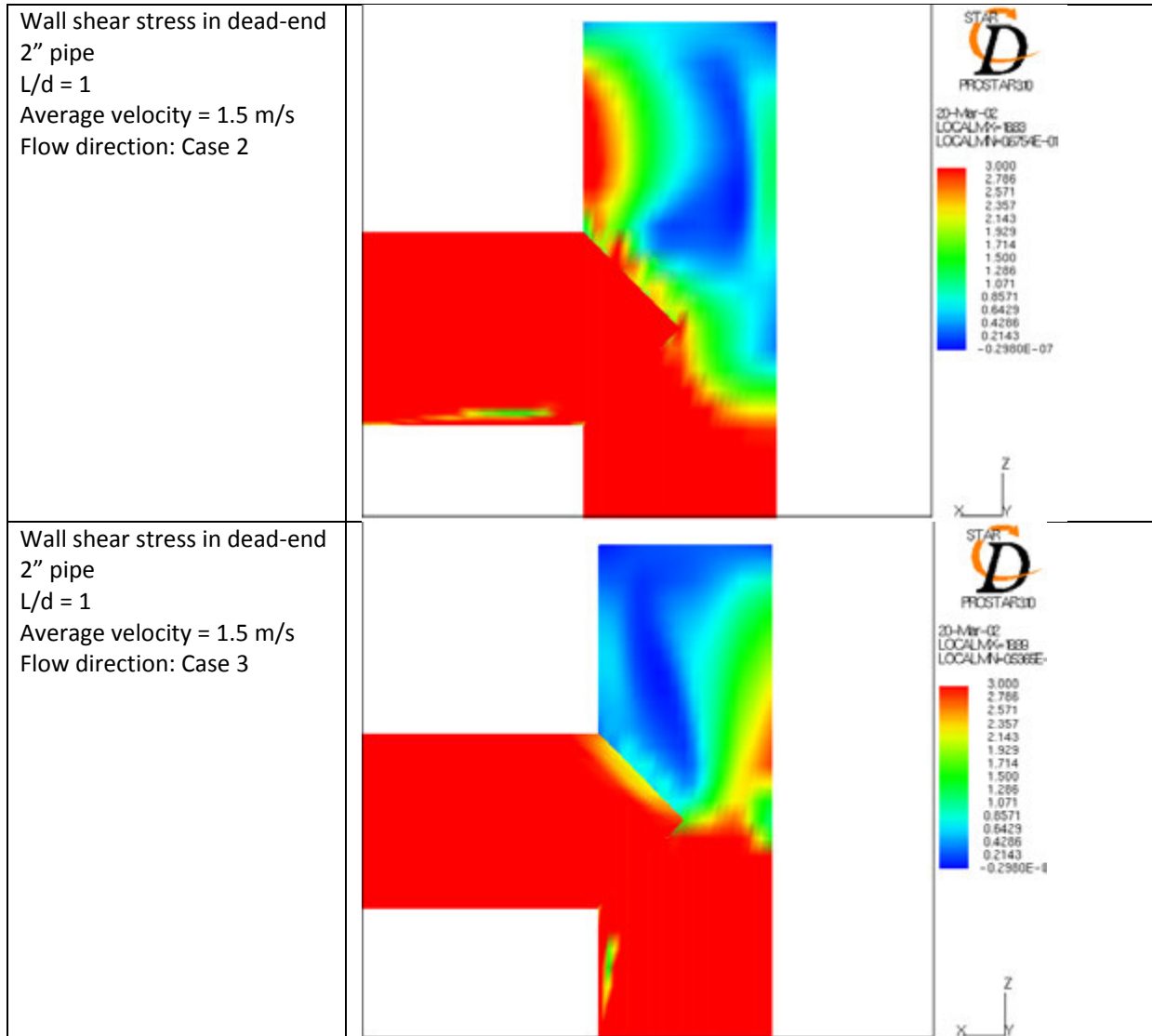
Observations:

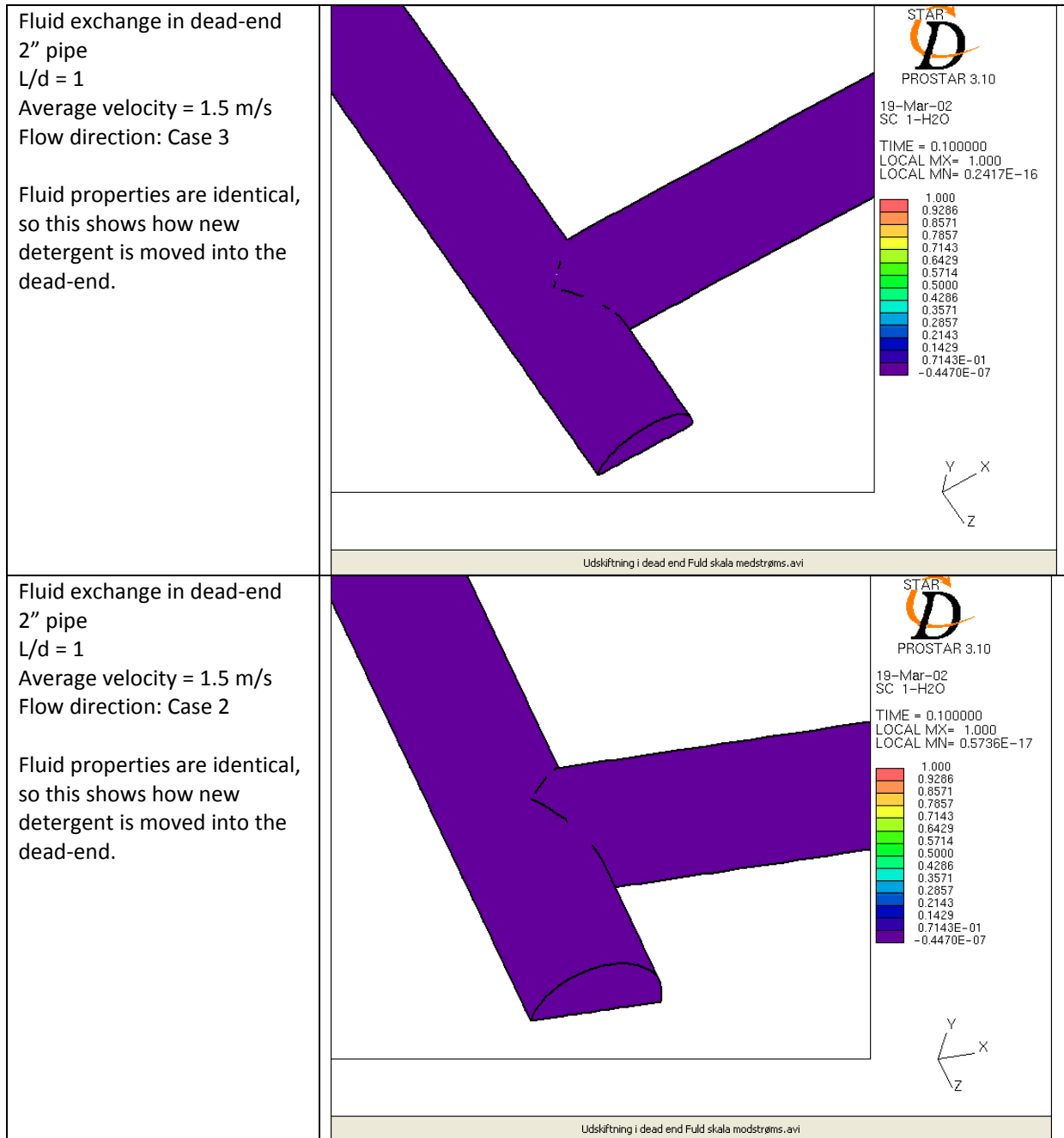
- For Case 1 and 3 there is a primary and a secondary recirculation zone when L/D is 2.5. This is not the case for Case 2.
- For L/D = 1.5 there is only a primary recirculation zone in all cases.
- Difficult to see if there is a difference between $\varnothing 50$ and $\varnothing 75$

Similar movies have been made på by APV. I think it is called “Clean around the bend”. I have a copy of this on VHS tape.

CFD work by Jensen

As part of my work at the Univeristy I did some numerical work on different dead-ends design and configurations. Below is show some of the results achieved in these CFD studies





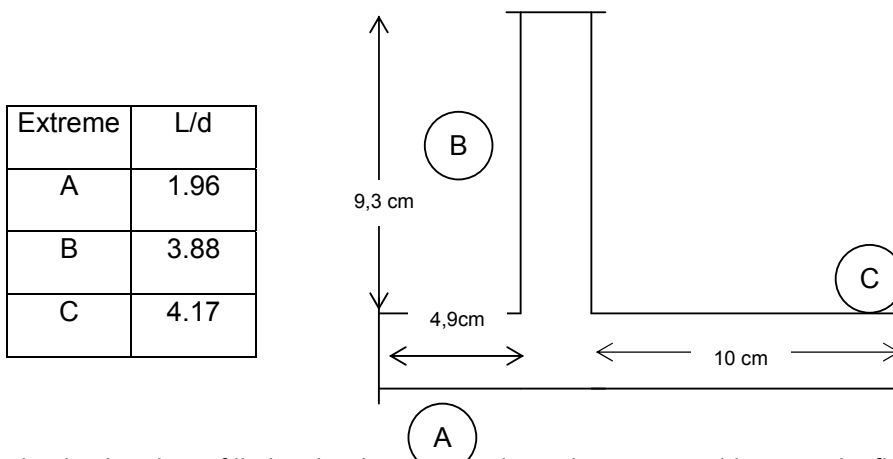
Also we did some work looking at what happens to the flow field and wall shear stress inside an dead-end when pulsating the inlet flow. The work was done on a $\varnothing 50$ mm pipe dead-end case 1 system with L/d of 1. Experimental work was done by smearing mustard onto the surfaces in the dead-end and the cleaning was monitored visually as a function of time. This shows that cleaning in the dead-end takes longest time in the corner where the dead-end wall and end cap meets and also in an area on both sides of the dead-end wall. This area can be predicted slow to clean from the CFD predictions of the wall shear stress distribution on the dead-end walls (see movies in PPT file – “flow in dead-end.ppt”).

Experiemental work by Jensen

As part of my work at the University I did some experimental work on flows in dead-ends. Below is show some of the results.

As student of mine did a lot of experiements, but I must admit that the work was never finally concluded upon. The most interesting test performed compared to that of Grasshoff, was the insertion of a flow diverter to force flow into dead-end.

Plexiglas dead-end, and depending on the pipe connections, different dead-end lengths can be obtained (see table).



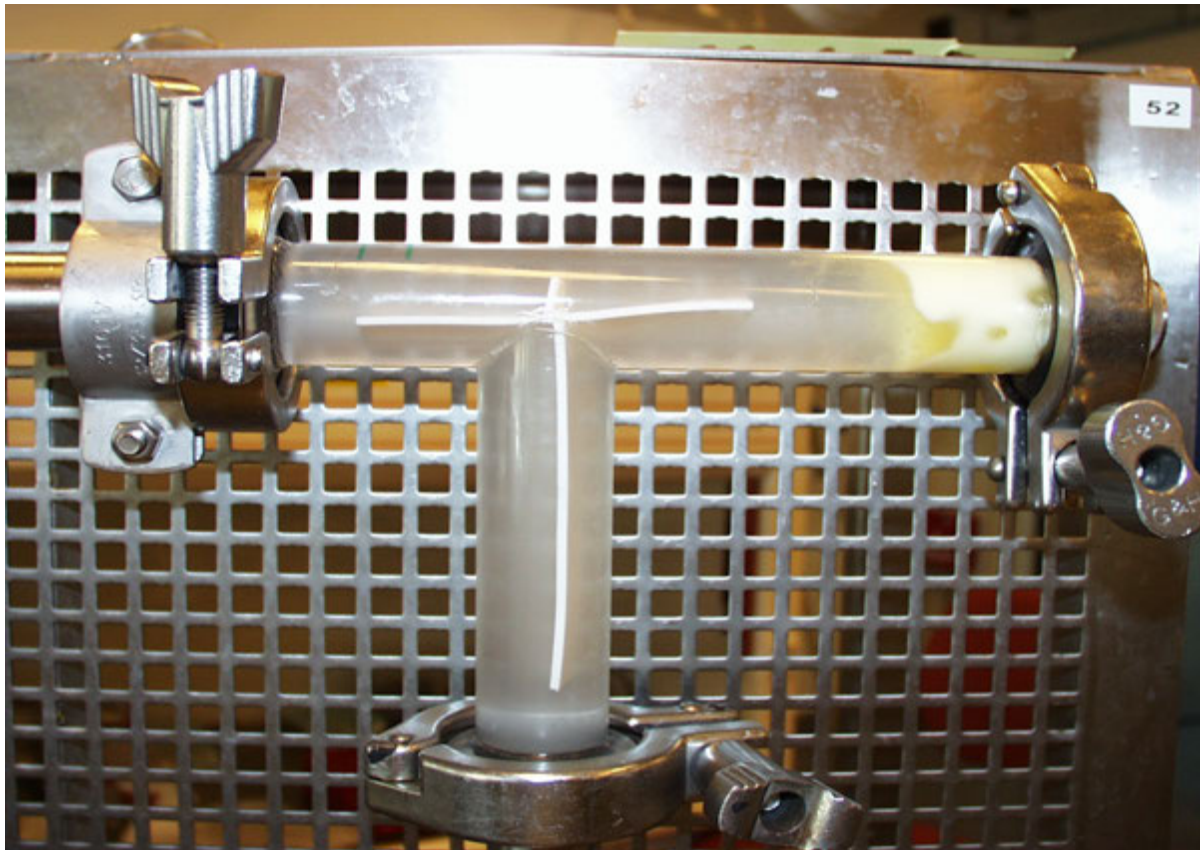
The dead-end was filled with salt and then cleaned out using cold water. The flow rate of 1500 l/h corresponds to 1 m/s.

Results for a dead-end system without flow diverter:

Date	Product	Flow (l/h)	Flow diverter	Flow case	Dead end	Removal time (min)	Observations
24/04/01	Salt	1500	N	2	A	1:31	Salt forming aggregates
24/04/01	Salt	1500	N	2	A	1:25	Salt in powder
24/04/01	Salt	1500	N	2	A		Not recorded
24/04/01	Salt	1500	N	3	A	10	Still something left
24/04/01	Salt	1500	N	3	A	-	
24/04/01	Salt	1500	N	2	C	7:45	Still something left

03/05/01	Salt	1500	N	2	C	18	Still something left
03/05/01	Salt	1500	N	3	C	30	Still something left
31/05/01	Salt	1500	Y	3	A	-	Dead end not completely filled. Not useful.
31/05/01	Salt	1500	Y	3	A	3 sec.	Instantaneously removed
31/05/01	Salt	1500	Y	3	C	32 sec	(see (1))

This shows a large difference in the cleaning time for an $L/d = 2$ if the flow is case 2 or case 3. Also a large increase in removal time is seen going to the large $L/d = 4.2$. Also it shows that there is a potential of inserting a flow diverter into the flow. This is only possibility if this flow diverter can be mounted and constructed in a hygienically designed way.



Except for the salt removal trails there were several other experiments comparing with and without flow diverter using other products as well. The results of these are collected in the table below.

Date	Product	Flow (l/h)	Flow diverter	Flow direction	Dead end	Removal time (min)	Temp (°C)		Observations
							Init	final	
19/06/01	butter	1500	N	L	Long (C)	10	58	69	Air-oil bubble
19/06/01	butter	1500	Y	L	Long (C)	1	71	70	Air-oil bubble
19/06/01	butter	1500	Y	R	Long (C)	1:10	54	56	
19/06/01	butter	1500	N	R	Long (C)	3	56,6		Air-oil bubble

Date	Product	Flow (l/h)	Flow diverter	Flow direction	Dead end	Removal time	Temp (°C)		Observations
							Init	final	
20/06/01	mustard	1500	N	R	Long (C)	3 min 6 min empty Q = 2200	59,5	70	Stop removing Still the same No effect Some more cleaning
20/06/01	mustard	1500	Y	R	Long (C)	16 sec	53	70	Completely cleaned
20/06/01	mustard	1500	Y	L	Long (C)	1:30 min 2:30 min (Q = 2200)	54	56	Almost all out More removed Something left
20/06/01	mustard	1500	N	L	Long (C)	5 min 7 min (Q=2200) 12 min	55,1		Only L/2 removed More removal No more removal

Testing to Determine Flowrates Required to Flood Piping

06 June 2011

Jeff J. Gaerke P.E.

Abstract

This report documents the results of a study to determine the flowrates required to flood¹ piping ranging from 0.5 to 4 inches in diameter with water. Flooding flowrates were determined for piping installed in both a horizontal and vertical orientation. The impact that outlet type, pipe slope, pump type, water temperature, and back pressure had on the flooding flowrate was evaluated. Data was also collected on liquid heights in horizontal piping at different points along the length of the piping for flowrates less than the flooding flowrate. Empirical equations, based on the inside diameter of the piping, were generated from the test results and can be used to determine the flooding flowrate of piping under a variety of installation conditions and outlet types.

Keywords

Flooding flowrate, liquid height, CIP

¹ Note: the definition of “flood” is dependent upon the pipe orientation. This is defined later in this document.

Table of Contents

1. INTRODUCTION	4
2. THE TEST SETUP.....	4
2.1. DESCRIPTION OF CIRCULATING PUMPING SKID AND COMPONENTS USED FOR TESTING	4
2.1.1. <i>General flow path</i>	5
2.1.2. <i>Listing of major components used in testing skid</i>	5
2.1.3. <i>Selection of piping components used for testing</i>	6
2.1.4. <i>Data collected</i>	7
2.1.5. <i>Variables evaluated</i>	7
2.2. TEST PLAN.....	8
2.2.1. <i>Testing performed on all pipe sizes evaluated</i>	9
2.2.2. <i>Additional testing performed only on 2" piping</i>	13
3. RESULTS AND DISCUSSION OF TESTING.....	14
3.1. RESULTS OF DETERMINATION OF LIQUID HEIGHT VERSUS DISTANCE FROM PIPE OUTLET.....	14
3.2. DISCUSSION OF DETERMINATION OF LIQUID HEIGHT VERSUS DISTANCE FROM PIPE OUTLET	19
3.2.1. <i>Discussion of liquid height versus flowrate</i>	19
3.2.2. <i>Discussion of liquid height versus distance from the pipe outlet</i>	19
3.3. RESULTS OF DETERMINATION OF FLOWRATE REQUIRED TO FLOOD A 6 FOOT HORIZONTAL PIPE OPEN ON END	19
3.4. DISCUSSION OF DETERMINATION OF FLOWRATE REQUIRED TO FLOOD A 6 FOOT HORIZONTAL PIPE OPEN ON END	21
3.5. RESULTS OF DETERMINATION OF FLOWRATE REQUIRED TO FLOOD A 6 FOOT HORIZONTAL PIPE WITH A ONE FOOT OPEN ENDED VERTICAL PIPE DIRECTED DOWNWARD	23
3.6. DISCUSSION OF DETERMINATION OF FLOWRATE REQUIRED TO FLOOD A 6 FOOT HORIZONTAL PIPE WITH A ONE FOOT OPEN ENDED VERTICAL PIPE DIRECTED DOWNWARD	25
3.7. RESULTS OF DETERMINATION OF FLOWRATE REQUIRED TO FLOOD A 6 FOOT HORIZONTAL PIPE WITH A TWO FOOT VERTICAL PIPE DIRECTED DOWNWARD THAT IS SEALED ON THE END.....	26
3.8. DISCUSSION OF DETERMINATION OF FLOWRATE REQUIRED TO FLOOD A 6 FOOT HORIZONTAL PIPE WITH A TWO FOOT VERTICAL PIPE DIRECTED DOWNWARD THAT IS SEALED ON THE END.....	28
3.9. RESULTS AND DISCUSSION OF OVERALL IMPACT OF OUTLET CONDITION ON FLOODING FLOWRATE:	29
3.10. RESULTS AND DISCUSSION OF IMPACT OF INCREASED 60°C TEMPERATURE ON LIQUID HEIGHTS AND FLOODING FLOWRATES ON 2" PIPING.	31
3.10.1. <i>Impact of increased 60°C temperature on liquid height of 2" piping.</i>	31
3.11. RESULTS AND DISCUSSION OF IMPACT OF INCREASED 70°C TEMPERATURE ON FLOODING FLOWRATES ON PIPING.	34
3.12. RESULTS AND DISCUSSION OF IMPACT OF PIPE SLOPE ON FLOODING FLOWRATES.	39
3.12.1. <i>Pipe slope</i>	39
3.13. RESULTS AND DISCUSSION OF IMPACT OF PUMP TYPE ON FLOODING FLOWRATES.	42
3.14. RESULTS AND DISCUSSION OF IMPACT OF BACKPRESSURE ON FLOODING FLOWRATES.....	43
4. CONCLUSIONS.....	44
5. REFERENCES	46

1. INTRODUCTION

A study was performed to determine the flowrates required to flood piping ranging from 0.5 to 4 inches in diameter with water. Flooding flowrates were determined for piping installed in a horizontal, downward sloped, and vertical orientation. The impact that water temperature, pipe slope, pump type, and back pressure had on the flooding flowrate was evaluated. Data was also collected on liquid heights in horizontal piping at different points along the length of the piping for flowrates less than the flooding flowrate.

2. THE TEST SETUP

This section contains a description of the pumping skid and piping configuration used to perform the testing.

2.1. DESCRIPTION OF CIRCULATING PUMPING SKID AND COMPONENTS USED FOR TESTING

A schematic of the testing arrangement follows as Figure 1 and a picture of the test arrangement follows as Figure 2:

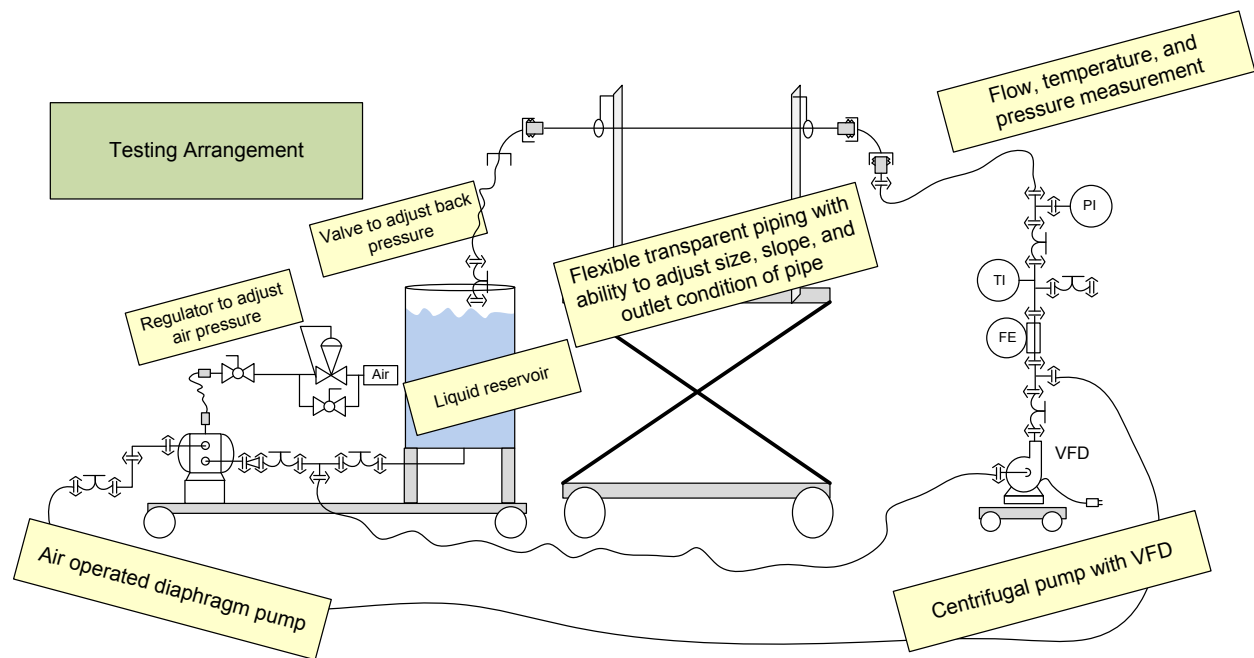


Figure 1 - Schematic of testing arrangement

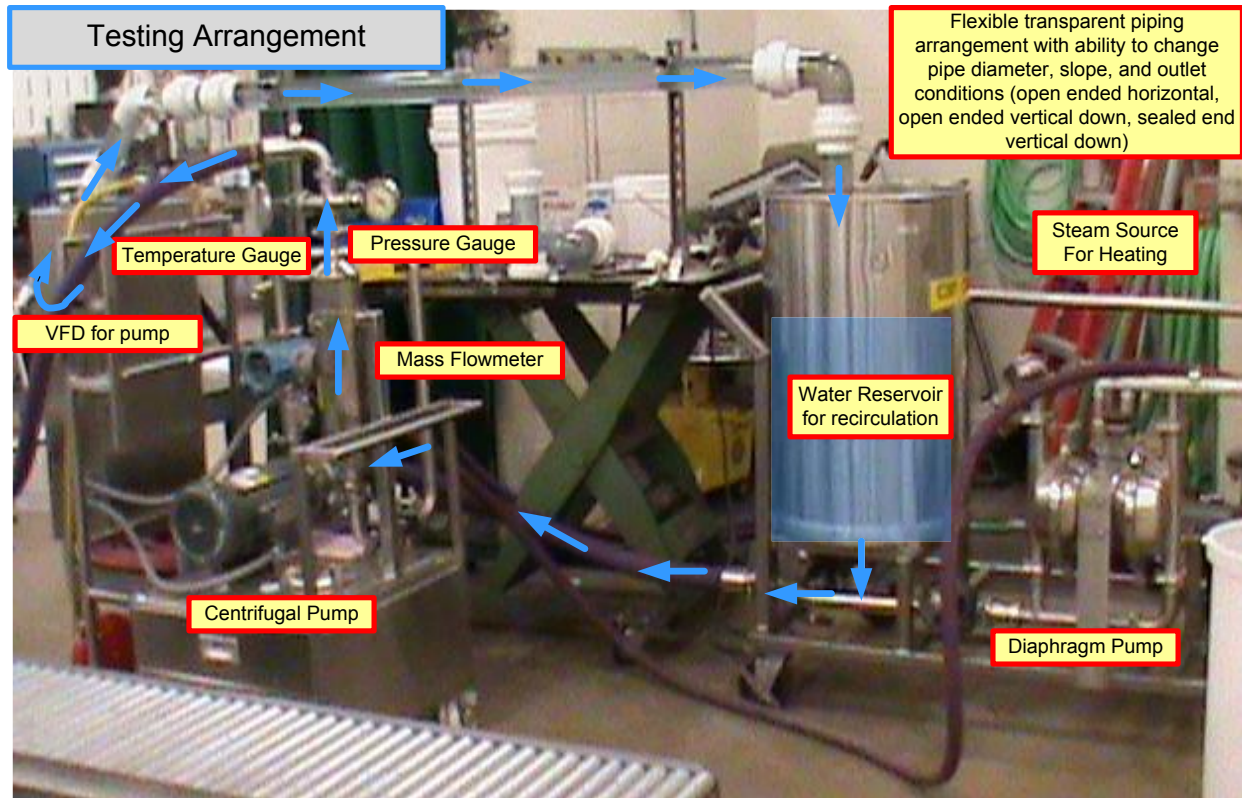


Figure 2 - Picture of test setup

2.1.1. General flow path

A quantity of water added to a 200 L drum serves as the liquid reservoir. Water that flows out of the bottom of this drum is directed to a pump which provides the driving force to move the liquid at the desired flowrate through a mass flowmeter, a temperature gauge, and a pressure gauge. Flexhoses are used to direct the fluid to the inlet of the transparent pipe being evaluated. Water flows through the transparent piping and is directed back to the liquid reservoir where it is recirculated.

2.1.2. Listing of major components used in testing skid

- Waukesha Cherry Burrell centrifugal pump, model 220 66LV – serial #3185020
 - Note: this centrifugal pump is equipped with a variable frequency drive (VFD) used to control the speed of the motor. The VFD is programmed with a “soft start” feature to ramp up the speed from being off to the desired speed setpoint over approximately 5 seconds.
- Murzan air operated diaphragm pump –model # P150SL, serial #9401 1865.
- Micromotion mass flowmeter – model # T100T6738CAUEZZZZ, serial #907723, calibration date = 9/13/10.
- Ashcroft pressure gauge, 0-160 psig, calibration date = 9/13/10.
- Ashcroft temperature gauge, 0-200° C, calibration date = 9/13/10.

2.1.3. Selection of piping components used for testing

Hygienic pharmaceutical process piping is typically fabricated from stainless steel tubing rather than piping. One difference between tubing and piping is the inside diameter (ID) dimension. The nominal size for tubing refers to the outside diameter (OD) dimension. As an example, 2" 16 gauge tubing has an outside diameter of 2" and a wall thickness of 0.065", which results in an inside diameter of 1.87". The transparent PVC piping and components used for testing were available as schedule 40 or schedule 80 piping (not available in tubing ID dimensions). The schedule of the piping refers to the wall thickness (schedule 80 piping and components have a greater wall thickness than schedule 40 components). The outside diameter of schedule 40 and 80 piping is the same, but it is not the same as the nominal pipe size. As an example, 2" piping has an OD of 2.375" and the ID is dependent upon the schedule of the piping purchased. For nominal 2" piping, the ID is 2.07" for schedule 40 components and 1.94" for schedule 80 components. When selecting the clear PVC piping for this testing, the piping schedule that resulted in an ID as close as possible to that of commonly used tubing sizes was chosen. The piping and unions used in the testing were available in both schedule 40 and schedule 80, but the 90° elbows were only available as schedule 40. In some cases this resulted in schedule 40 clear PVC 90° elbows being connected to schedule 80 clear PVC pipe. In this document, when an inside diameter is listed, it refers to the ID of the *piping* used in the testing unless otherwise noted. Table 1 lists the pipe schedule and dimensions of the PVC piping components purchased for the testing.

Component	Nominal Size		Piping Schedule	Wall Thickness		Outside Diameter		Inside Diameter	
	(Inch)	(mm)		(Inch)	(mm)	(Inch)	(mm)	(Inch)	(mm)
Elbow 90 deg	4	101.6	40	0.24	6.02	4.50	114.30	4.03	102.26
Pipe	4	101.6	40	0.24	6.02	4.50	114.30	4.03	102.26
Union	4	101.6	40	0.24	6.02	4.50	114.30	4.03	102.26
Elbow 90 deg	3	76.2	40	0.22	5.49	3.50	88.90	3.07	77.93
Pipe	3	76.2	40	0.22	5.49	3.50	88.90	3.07	77.93
Union	3	76.2	40	0.22	5.49	3.50	88.90	3.07	77.93
Elbow 90 deg	2	50.8	40	0.15	3.91	2.38	60.33	2.07	52.50
Pipe	2	50.8	80	0.22	5.54	2.38	60.33	1.94	49.25
Union	2	50.8	80	0.22	5.54	2.38	60.33	1.94	49.25
Elbow 90 deg	1.5	38.1	40	0.15	3.68	1.90	48.26	1.61	40.89
Pipe	1.5	38.1	80	0.20	5.08	1.90	48.26	1.50	38.10
Union	1.5	38.1	80	0.20	5.08	1.90	48.26	1.50	38.10
Elbow 90 deg	1	25.4	40	0.13	3.38	1.32	33.40	1.05	26.64
Pipe	1	25.4	80	0.18	4.55	1.32	33.40	0.96	24.31
Union	1	25.4	80	0.18	4.55	1.32	33.40	0.96	24.31
Elbow 90 deg	0.75	19.1	40	0.11	2.87	1.05	26.67	0.82	20.93
Pipe	0.75	19.1	80	0.15	3.91	1.05	26.67	0.74	18.85
Union	0.75	19.1	80	0.15	3.91	1.05	26.67	0.74	18.85
Elbow 90 deg	0.375	9.5	40	0.09	2.31	0.68	17.15	0.49	12.52
Pipe	0.375	9.5	80	0.13	3.20	0.68	17.15	0.42	10.74
Union	0.375	9.5	80	0.13	3.20	0.68	17.15	0.42	10.74

Table 1 – Pipe schedule and dimensions of components tested.

2.1.4. Data collected

Visual observations, and where applicable liquid heights, were recorded on the water passing through the transparent piping. Flowrate, temperature, and pressure data were recorded where applicable. All observations, measurement data collected, and calibration information on the instruments used are documented in Laboratory Notebook number 18960 pages 1-78. “Unique test numbers” listed throughout this document refer to individual tests documented in the laboratory notebook.

2.1.5. Variables evaluated

The flexible test setup allowed for the evaluation of the following variables associated with pipe flooding flowrates.

Pipe diameter

Several pipe sizes were evaluated. Nominal pipe diameters ranged from 3/8" to 4".

Distance from outlet of the 6 foot horizontal spool piece

Liquid heights within the piping were taken at different distances from the outlet of the 6 foot horizontal spool piece.

Pipe outlet condition

Three different pipe outlet conditions were tested as follows:

- “Open end horizontal outlet” – is defined as nothing added to outlet of horizontal 6 foot spool piece of piping. Water freefalls from outlet of horizontal piping.
- “Open end vertical outlet” – is defined as a 90° elbow is connected to the outlet of the horizontal 6 foot spool piece, and a 12 inch spool piece is connected to the 90° elbow directed downward. A 6 inch air gap is maintained between the outlet of the vertical spool piece and the liquid level in the drum.
- “Sealed end vertical outlet” – is defined as a 90° elbow is connected to the outlet of the horizontal 6 foot spool piece, and a 24 inch spool piece is connected to the 90° elbow directed downward. The end of the 24 inch spool piece is submersed 6 inches in the water in the drum, sealing the outlet.

Pipe slope

0% (no slope or horizontal), 5% upward, and 5% downward slope were evaluated on a 6 foot spool piece of transparent piping mounted horizontally. The piping was also evaluated in the vertical orientation. The outlet piping was evaluated when installed vertically straight up and down, and at angles of 30°, 45°, and 60° as measured from the horizontal (0° being horizontal).

Water temperature

Several temperatures were evaluated: ambient temperature (approximately 20°C) and hotter temperatures at 60-70°C.

Pump type

Two different pumps were evaluated: a centrifugal pump which provides a consistent flow (without pulsations) and an air operated diaphragm pump which delivers pulsating flow.

Backpressure

The impact that increasing the backpressure has on the flooding flowrate was evaluated. Testing was performed with essentially zero backpressure and with 30 psig backpressure.

2.2. TEST PLAN

Due to the large number of variables to be tested, a small number of tests were performed on each pipe size, and then more extensive testing was performed on the 2" piping. It is assumed that the observations from the additional testing using the 2" piping also apply to the other piping sizes.

2.2.1. Testing performed on all pipe sizes evaluated

This section contains descriptions of the tests performed on each pipe size tested.

Determination of liquid height versus distance from pipe outlet

Liquid was supplied from the pumping skid to the transparent PVC pipe via flexhose. In connecting to the PVC pipe, the flexhose always came from a lower elevation, and the pipe size always transitioned gradually via reducers from the flexhose to the PVC pipe. The PVC piping was configured to include a 6 foot horizontal spool piece of transparent piping installed flat (0% slope – determined by a calibrated digital level) with an open end horizontal outlet (see Figure 3).

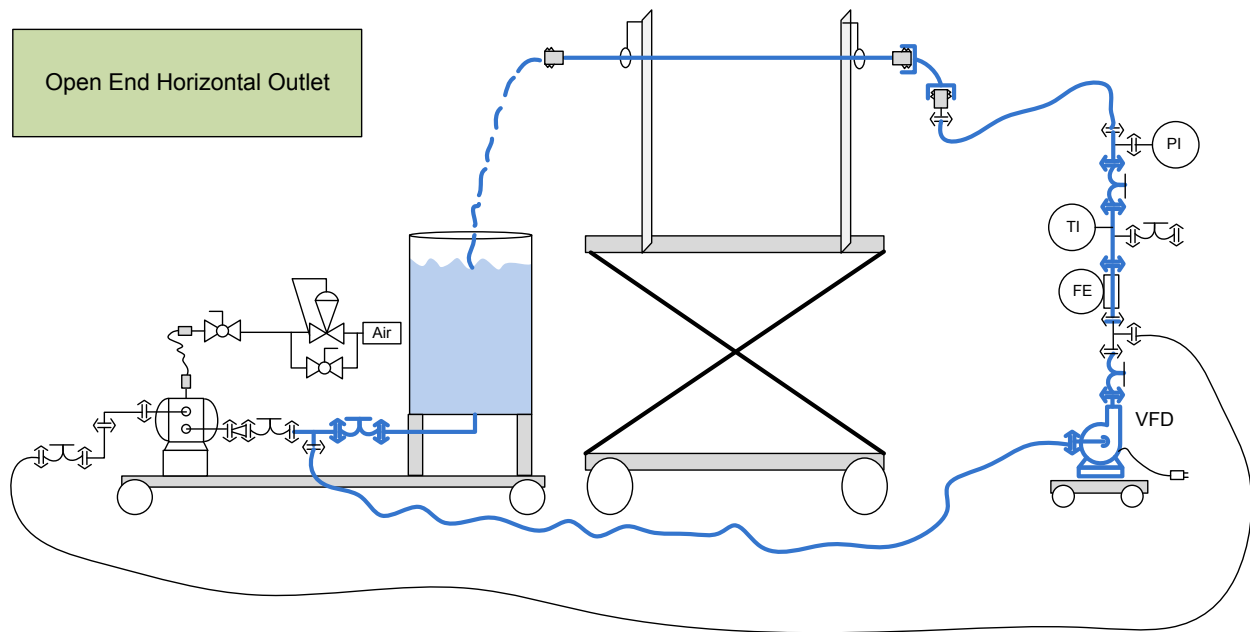


Figure 3 – Schematic of open end horizontal outlet

This testing was performed using the centrifugal pump. The flowrate of the water supplied to the PVC pipe was controlled by adjusting the speed of the pump via the VFD. This testing was performed using ambient temperature water. Liquid heights within the piping were measured at three distances from the outlet of the horizontal spool piece: 6 inches from the outlet, 36 inches from the outlet, and 66 inches from the outlet (see Figure 4).

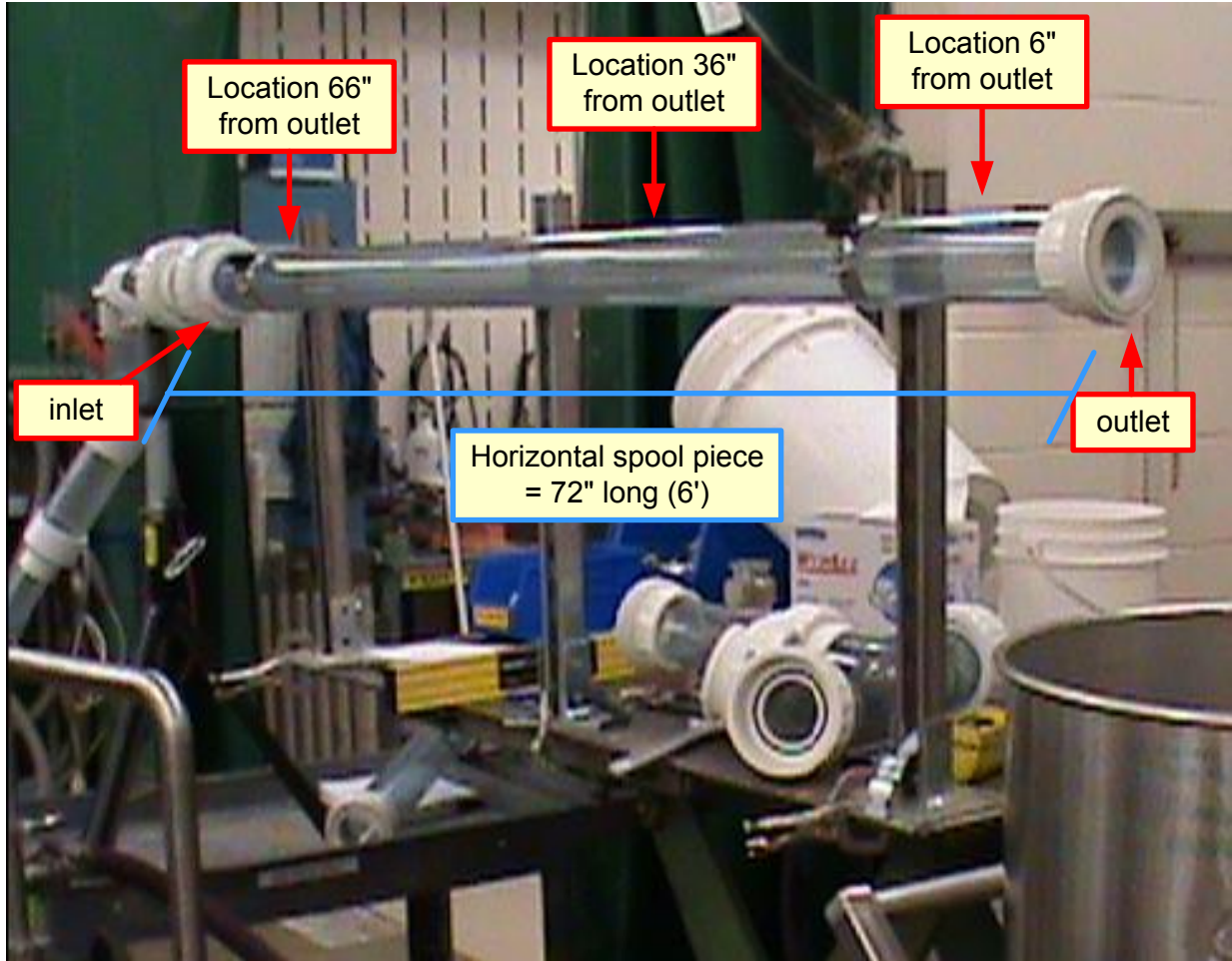


Figure 4 – Picture showing three locations where liquid height measurements were taken

Liquid height measurements were measured using a modified small square fitted with a bubble level and a ruler that measured in millimeters (see Figure 5).



Figure 5 – Picture of modified level used to measure liquid heights

To take height measurements, the square was placed at the required distance from the pipe outlet on the outside bottom of the transparent pipe, the square was leveled, and the liquid height measurement was recorded. The actual liquid height was later determined by subtracting the

wall thickness of the piping from the recorded liquid height. In some cases ripples were observed in the piping (see Figure 6).



Figure 6 – Picture of ripple

If a ripple occurred at the measurement location, the height of the liquid formed by the ripple was recorded (in some cases a peak and in other cases a valley).

Determination of flooding flowrate of 6 foot horizontal pipe open on end

Using the same setup described for determining the liquid heights at various distances from the pipe outlet, the flowrate required to flood a 6 foot open ended horizontal pipe was determined. The horizontal pipe was defined as “flooded” when all of the air was displaced from the pipe to a point no more than 6 inches from the outlet of the horizontal pipe within 60 seconds of starting the pump.

Note: the starting point was always a completely empty pipe with the pump off. Several different flowrates were quickly tested to determine the flowrate that would first flood the piping within the 60 second time period. Testing was then generally performed in triplicate, and results were recorded at this pump speed/flowrate.

Determination of flooding flowrate of 6 foot horizontal pipe with 12 inch vertical pipe open on end

The setup for this testing was similar to that described in determining the flooding flowrate of a 6 foot open ended horizontal pipe. The only differences are that a 90° clear PVC elbow was added to the horizontal 6 foot spool piece and a 12 inch spool piece was connected to the 90° elbow directed straight downward. A 6 inch air gap was maintained between the outlet of the vertical spool piece and the liquid level in the drum (see Figure 7).

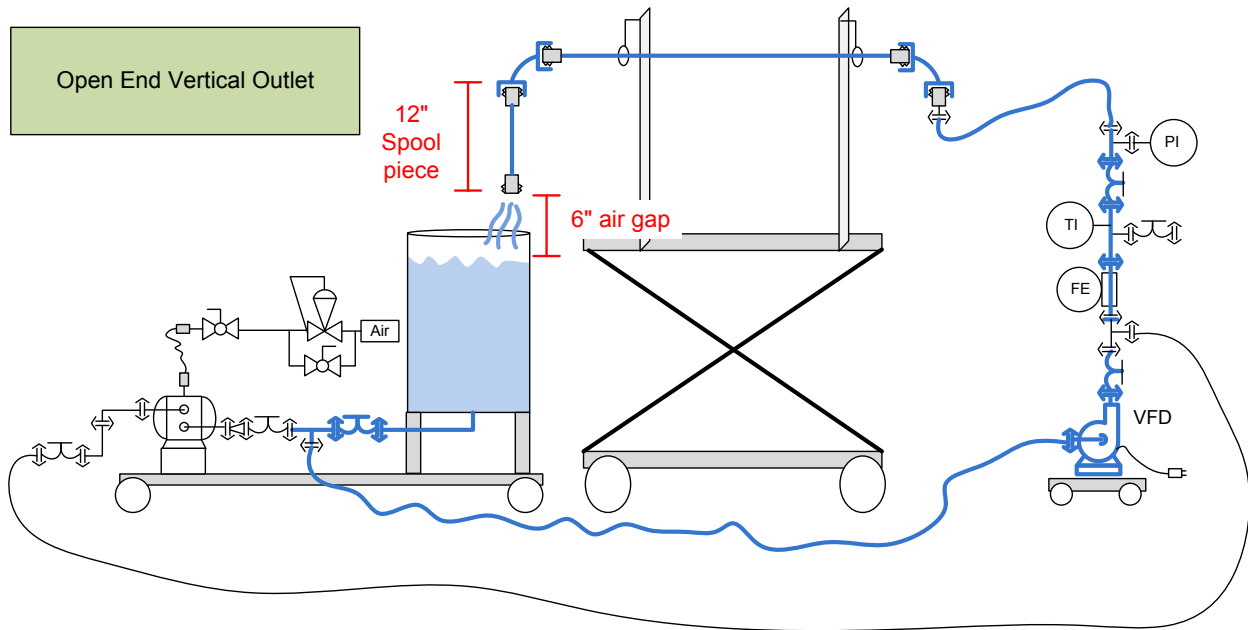


Figure 7 - Schematic of open end vertical outlet

The vertical pipe was defined as “flooded” when all of the air was displaced from the horizontal pipe, the 90° clear PVC elbow, and the vertical pipe (no air remained in the piping system).

Note: the starting point was always a completely empty pipe with the pump off. Several different flowrates were quickly tested to determine the flowrate that would first flood the piping within the 60 second time period. Testing was then generally performed in triplicate, and results were recorded at this pump speed/flowrate.

Determination of flooding flowrate of 6 foot horizontal pipe with 24 inch vertical pipe sealed on end

The setup for this testing was similar to that described in determining the flooding flowrate of a 12 inch open end vertical pipe. The only differences are that instead of using a 12 inch spool piece with a 6 inch air gap, a 24 inch spool piece was used and the end of the spool piece was submersed 6 inches in the water, sealing the end of the spool piece (see Figure 8).

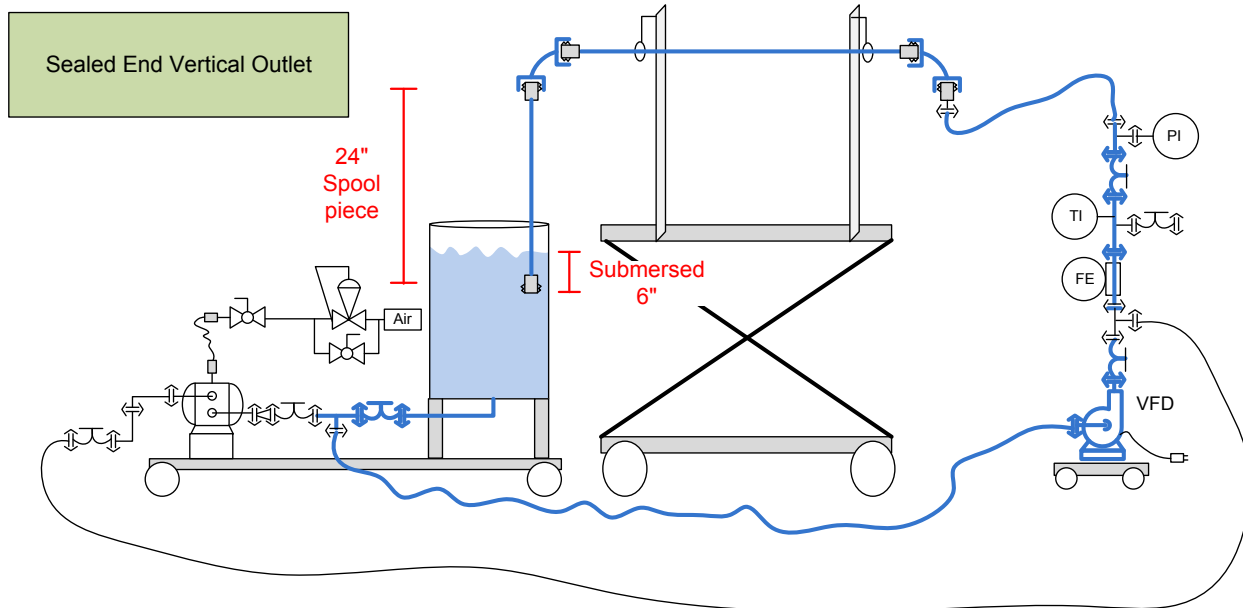


Figure 8 - Schematic of vertical pipe with sealed outlet

The vertical pipe was defined as “flooded” when all of the air was displaced from the horizontal pipe, the 90° clear PVC elbow, and the vertical pipe (no air remaining in the piping system).

Note: the starting point was always a completely empty pipe with the pump off. Several different flowrates were quickly tested to determine the flowrate that would first flood the piping within the 60 second time period. Testing was then generally performed in triplicate, and results were recorded at this pump speed/flowrate.

2.2.2. Additional testing performed only on 2" piping

Additional testing was performed on the 2" transparent piping as follows:

Pipe slope

In addition to testing with the 6 foot horizontal spool piece being installed completely horizontal (0% slope), testing was performed with all three pipe outlet conditions previously described with both a 5% upward and 5% downward slope on the 6 foot spool piece of transparent piping mounted in a horizontal plane.

The vertical piping was evaluated when installed straight up and down and at angles of 30°, 45°, and 60° as measured from the horizontal (0° being horizontal).

Water temperature

In addition to testing with ambient temperature water, testing was also performed with 60° C and 70° C water with all three outlet types previously described. The reservoir of water was heated by direct injecting steam into the drum of water while circulating.

Note: although this testing was only initially planned to be performed at 60° C with 2" piping, additional testing was performed on piping ranging in diameter from 3/8" to 4" at an elevated temperature of approximately 70° C. 70° C is a common temperature used in clean-in-place

(CIP) applications for cleaning piping, and this additional testing was performed to better understand the flowrates required to flood piping under typical CIP conditions.

Pump type

In addition to testing with a centrifugal pump, additional testing was performed using an air operated diaphragm pump. The purpose of this test was to determine the impact that the pulsating flow delivered by the diaphragm pump had on both the height of liquid in the pipe and the flooding flowrate as compared to that obtained from the consistent flow supplied by the centrifugal pump.

Backpressure

The impact that increasing the backpressure had on the flooding flowrate was also evaluated. Testing was performed with essentially zero backpressure and with 30 psig backpressure.

3. RESULTS AND DISCUSSION OF TESTING

3.1. RESULTS OF DETERMINATION OF LIQUID HEIGHT VERSUS DISTANCE FROM PIPE OUTLET

Table 2 lists the liquid height measurement within the pipe taken at three different distances from the outlet of the 6 foot horizontal pipe for different pipe sizes at various flowrates. The liquid height was measured from the outside bottom of the transparent pipe. The wall thickness of the piping was then subtracted from the measured values to determine the actual height of liquid inside the piping. These values were used in the liquid height graphs.

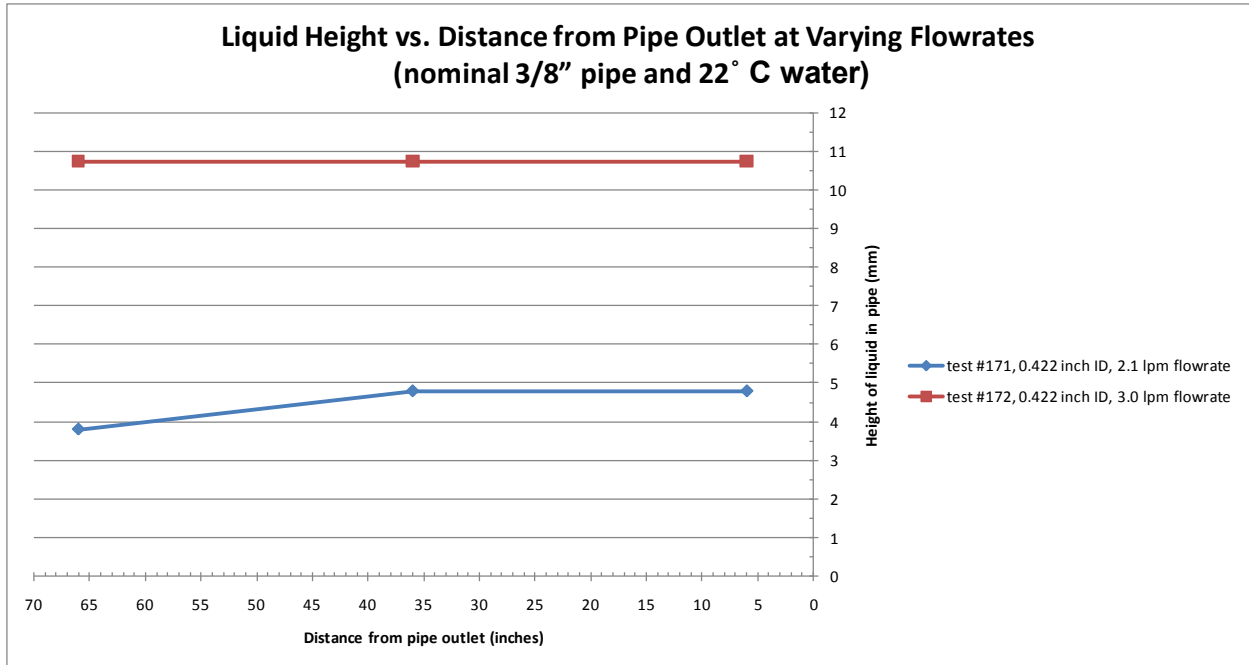
Graphs 1-6 indicate the liquid height versus location from the pipe outlet at different flowrates. These graphs were completed for nominal pipe diameters of 3/8", 3/4", 1", 1.5", 2" and 3". The values plotted are the liquid heights from the inside bottom of the pipe.

Data was also collected on 4" piping, but towards the end of testing, it was determined that the horizontal piping support had slipped and was no longer completely flat. Instead of a 0% slope, the piping was sloped 0.3% downward towards the outlet. Because of this the 4" liquid height data is not presented in this report.

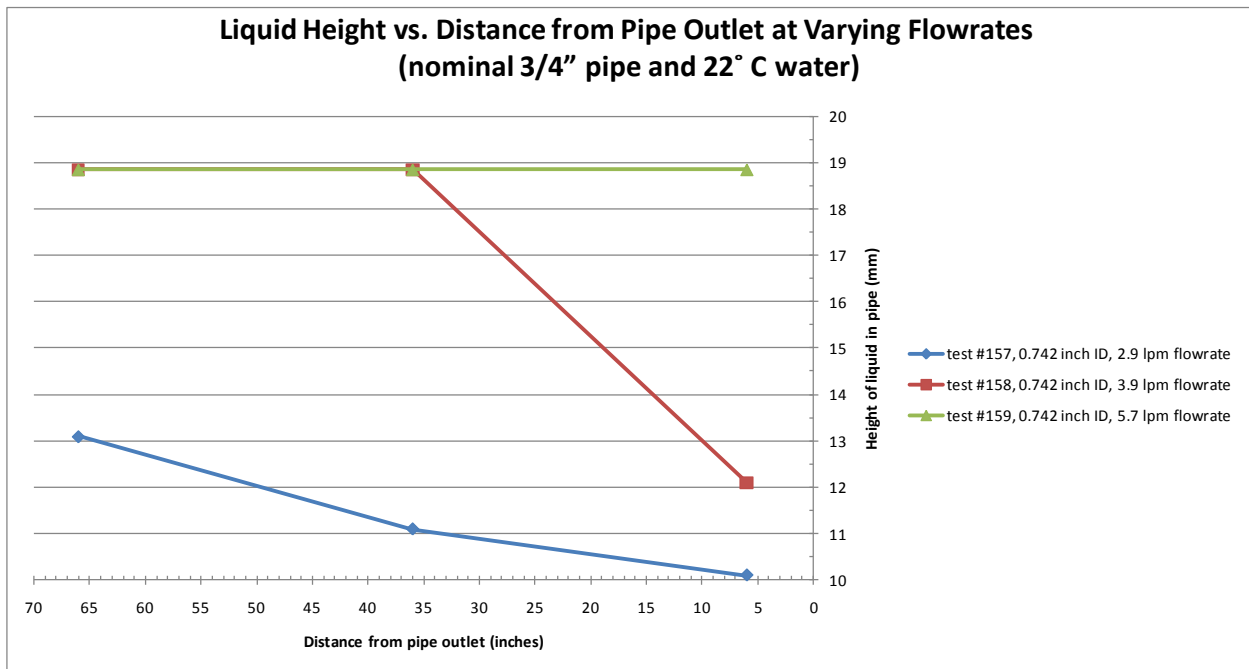
It should also be noted that the 3/8" and 3/4" transparent piping was not as rigid as the larger sizes tested. Because of this, it was difficult to install the 6 foot spool piece of piping completely flat. Additional supports were added, but it was still difficult to install the 6 foot length of piping without any bows/local low points in it. The presence of slight bows in the piping may have impacted the liquid heights measured in the 3/8" and 3/4" piping.

Unique # for Test Result	Nominal Pipe Size (in)	Pipe Schedule	Pipe ID (mm)	Pipe Wall Thickness (mm)	Water Temp (°C)	Flowrate (lpm)	Height from Outside Bottom of Pipe (mm)			Height from Inside Bottom of Pipe (mm)			Height from Outside Bottom of Pipe when Flooded (mm)
							66" from Outlet	36" from Outlet	6" from Outlet	66" from Outlet	36" from Outlet	6" from Outlet	
171	0.38	80	10.74	3.20	22	2.1	7	8	8	4	5	5	14
172	0.38	80	10.74	3.20	22	3.0	14	14	14	11	11	11	14
157	0.75	80	18.85	3.91	22	2.9	17	15	14	13	11	10	23
158	0.75	80	18.85	3.91	22	3.9	23	23	16	19	19	12	23
159	0.75	80	18.85	3.91	22	5.7	23	23	23	19	19	19	23
107	1.00	80	26.64	3.38	23	2.9	25	23	18	22	20	15	30
108	1.00	80	26.64	3.38	23	4.1	29	27	21	26	24	18	30
109	1.00	80	26.64	3.38	23	4.6	30	30	23	27	27	20	30
110	1.00	80	26.64	3.38	23	5.3	30	30	30	27	27	27	30
77	1.50	80	38.10	5.08	22	8.4	34	29	24	29	24	19	43
78	1.50	80	38.10	5.08	22	13.2	40	35	29	35	30	24	43
79	1.50	80	38.10	5.08	22	15.2	43	38	31	38	33	26	43
80	1.50	80	38.10	5.08	22	19.6	43	43	34	38	38	29	43
81	1.50	80	38.10	5.08	22	24.2	43	43	43	38	38	38	43
20	2.00	80	49.25	5.54	26	16.2	38	35	30	32	29	24	55
21	2.00	80	49.25	5.54	26	22.8	43	40	33	37	34	27	55
22	2.00	80	49.25	5.54	26	28.7	49	44	38	43	38	32	55
23	2.00	80	49.25	5.54	26	32.2	53	47	39	47	41	33	55
24	2.00	80	49.25	5.54	26	36.6	55	52	42	49	46	36	55
25	2.00	80	49.25	5.54	26	40.4	55	55	43	49	49	37	55
26	2.00	80	49.25	5.54	26	43.9	55	55	55	49	49	49	55
54	3.00	40	77.93	5.49	24	10.6	28	26	22	23	21	17	83
55	3.00	40	77.93	5.49	24	21.4	38	35	30	33	30	25	83
56	3.00	40	77.93	5.49	24	35.6	46	42	36	41	37	31	83
57	3.00	40	77.93	5.49	24	48.6	53	49	42	48	44	37	83
58	3.00	40	77.93	5.49	24	67.6	62	58	49	57	53	44	83
59	3.00	40	77.93	5.49	24	79.1	66	62	52	61	57	47	83
60	3.00	40	77.93	5.49	24	92.3	70	66	55	65	61	50	83
61	3.00	40	77.93	5.49	24	107.1	76	72	59	71	67	54	83
62	3.00	40	77.93	5.49	24	116.2	79	74	62	74	69	57	83
63	3.00	40	77.93	5.49	24	123.6	81	77	64	76	72	59	83
64	3.00	40	77.93	5.49	24	128.4	83	79	65	78	74	60	83
65	3.00	40	77.93	5.49	24	140.6	83	83	70	78	78	65	83
67	3.00	40	77.93	5.49	24	151.2	83	83	83	78	78	78	83

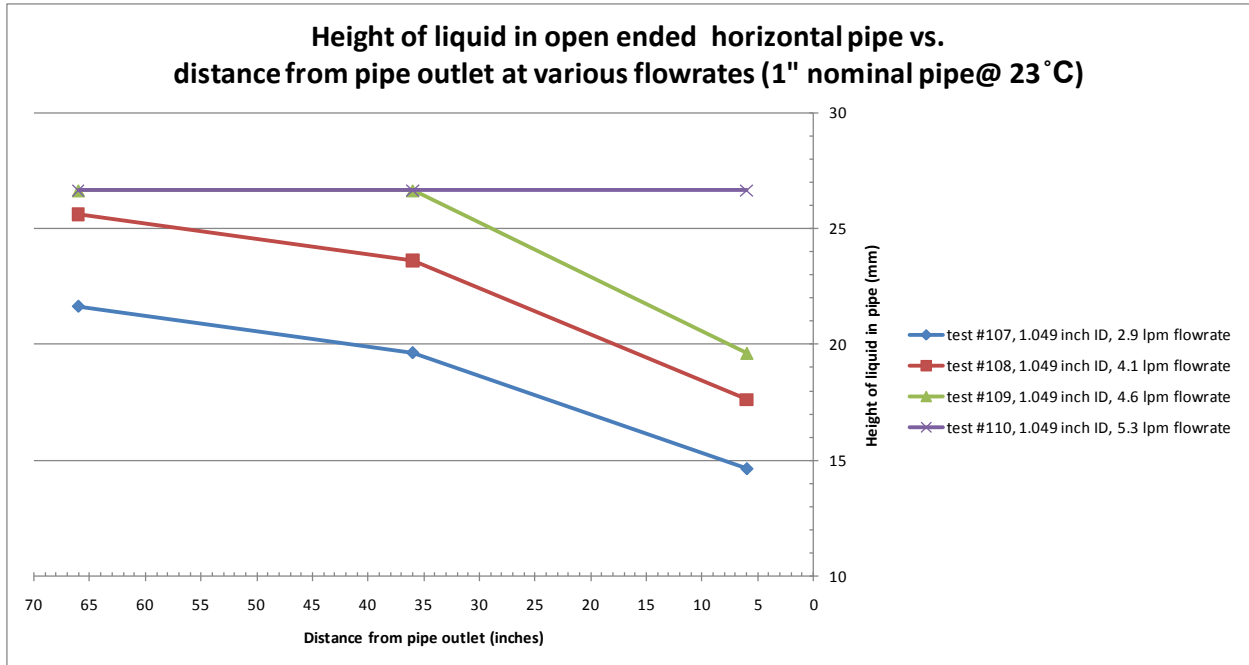
Table 2 – Liquid height test results at different locations from pipe outlet for various pipe diameters



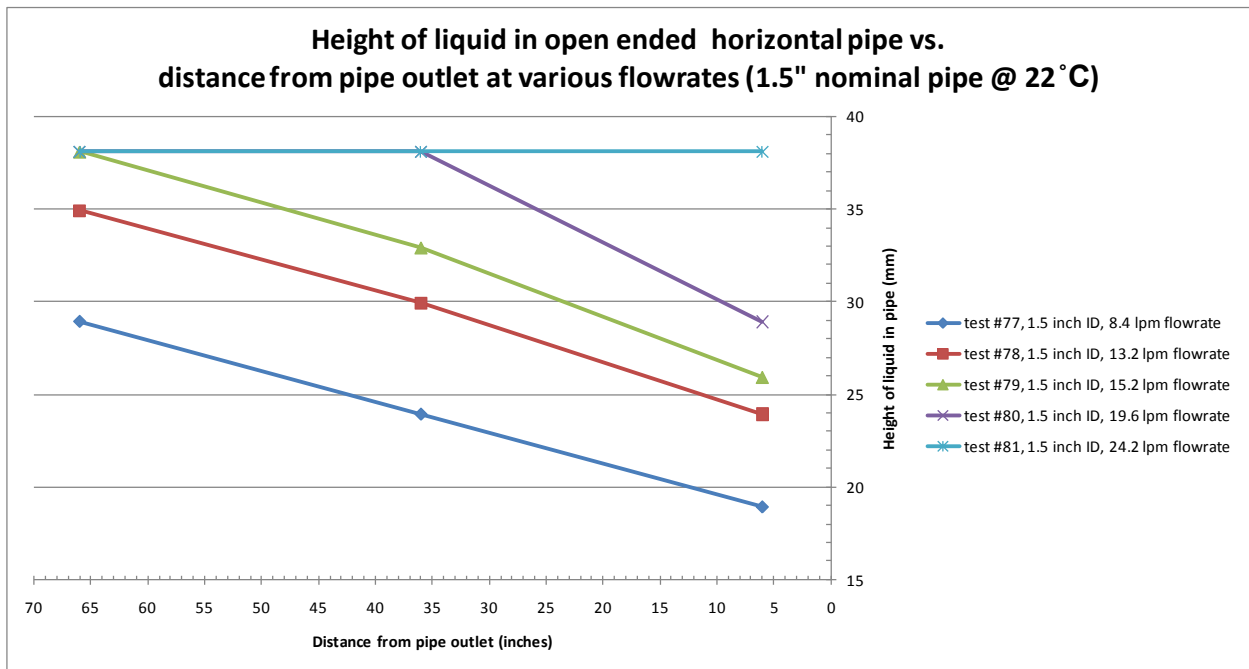
Graph 1 - Liquid height at different distances from pipe outlet for nominal 3/8" piping at various flowrates.



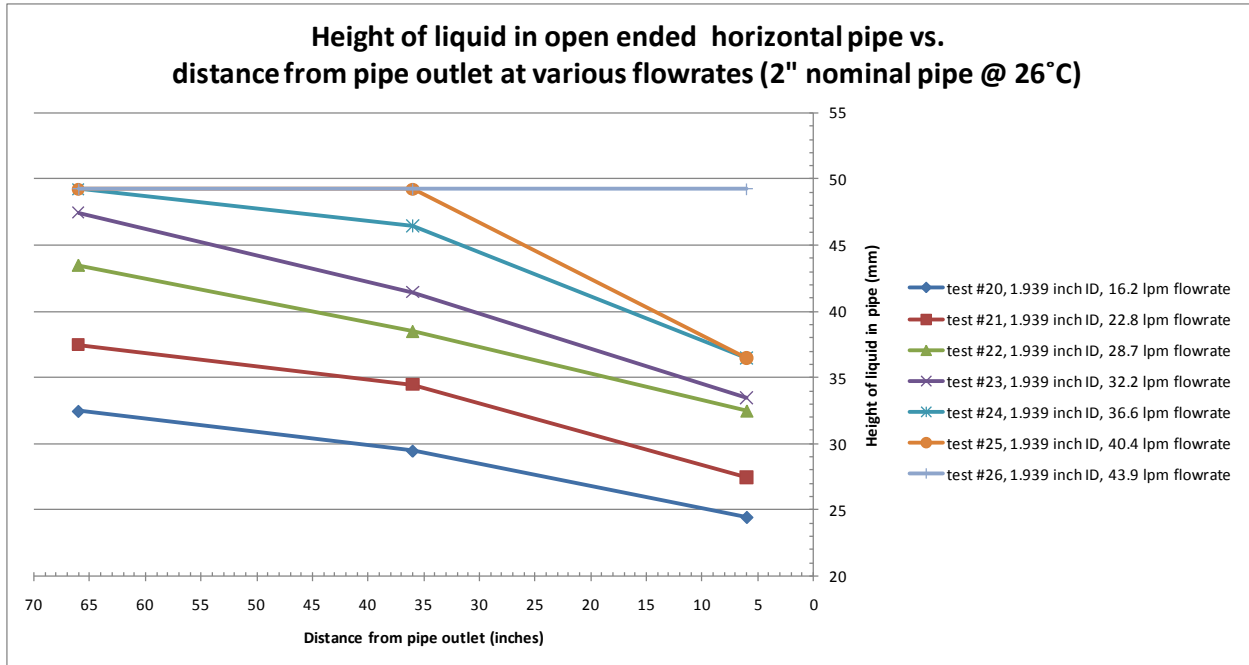
Graph 2 - Liquid height at different distances from pipe outlet for nominal 3/4" piping at various flowrates.



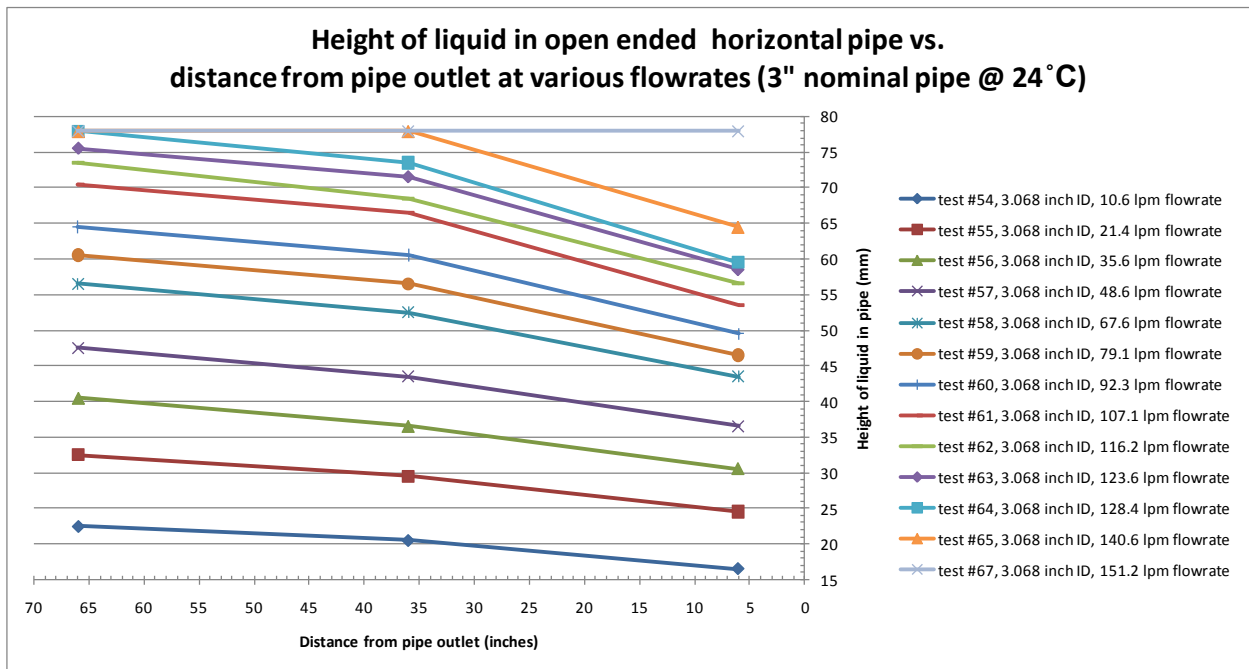
Graph 3 - Liquid height at different distances from pipe outlet for nominal 1" piping at various flowrates.



Graph 4 - Liquid height at different distances from pipe outlet for nominal 1.5" piping at various flowrates



Graph 5 - Liquid height at different distances from pipe outlet for nominal 2" piping at various flowrates.



Graph 6 - Liquid height at different distances from pipe outlet for nominal 3" piping at various flowrates.

3.2. DISCUSSION OF DETERMINATION OF LIQUID HEIGHT VERSUS DISTANCE FROM PIPE OUTLET

3.2.1. Discussion of liquid height versus flowrate

As the flowrate of liquid through the pipe increased, the height of liquid at the three locations measured also increased.

3.2.2. Discussion of liquid height versus distance from the pipe outlet

The height of the liquid at a given flowrate generally decreased as the distance from the pipe outlet decreased.

Note: this was not observed on the 3/8" testing. It is expected that this is due to the presence of a local low spot in the piping which impacted the liquid heights.

Within the 6 foot horizontal spool piece, the liquid height was generally lowest at the pipe outlet and highest at the location furthest from the outlet. Although measurements were only taken at 3 locations, a general trend observed from the liquid height versus distance from the pipe outlet graphs is that the slope of the line flattens as the distance from the pipe outlet increases.

3.3. RESULTS OF DETERMINATION OF FLOWRATE REQUIRED TO FLOOD A 6 FOOT HORIZONTAL PIPE OPEN ON END

Testing was performed with piping that ranged from 3/8" – 4" nominal pipe diameter. Data from this testing is included in Table 3.

Unique #ers for Test Result	Nominal Pipe Size (inch)	Pipe Schedule	Pipe ID (inch)	Pipe ID (mm)	Water Temp (°C)	Flowrate Required to Flood Horizontal Piping (lpm)	Comment
172-174	0.38	80	0.42	10.74	22	3.0	Flowrate required to flood pipe may have been impacted by local low points due to sagging of the horizontal pipe.
159-161	0.75	80	0.74	18.85	22	5.7	
112-114	1.00	80	0.96	24.31	23	6.0	
81-83	1.50	80	1.50	38.10	22	24.2	
26	2.00	80	1.94	49.25	26	43.9	
187-189	3.00	40	3.07	77.93	23	158.0	
143-145	4.00	40	4.03	102.26	28	370.0	

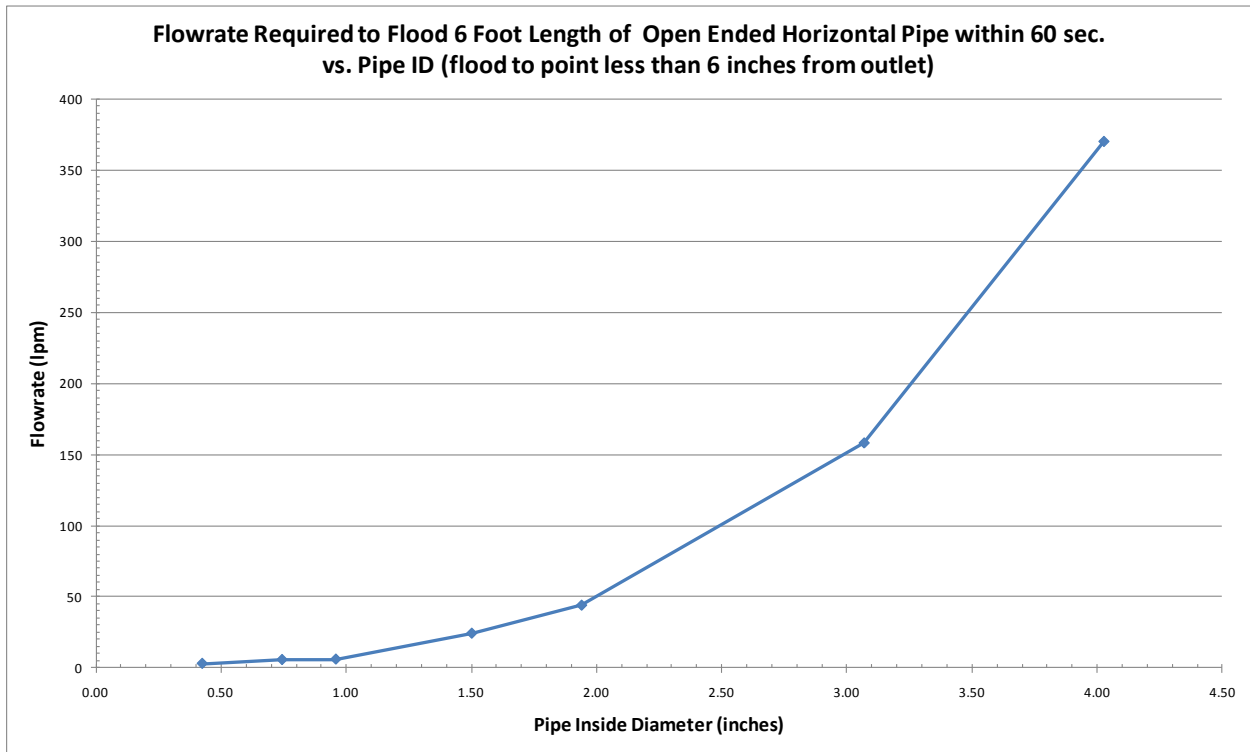
Table 3 - Test results of flowrate required to flood horizontal piping open on end

It was difficult to maintain 3/8" and 3/4" transparent piping completely horizontal due to the flexibility of this piping. Minor sagging in the piping between supports may have impacted the flowrates required to flood the piping.

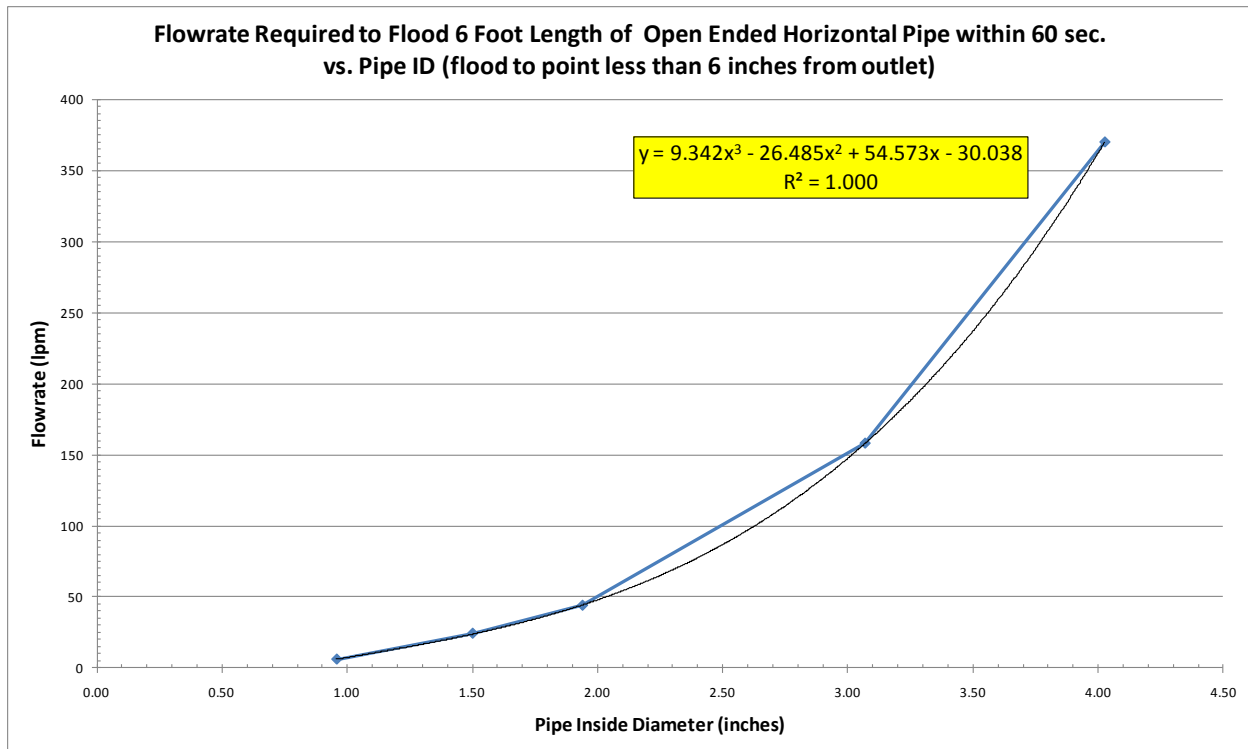
Graph 7 is a plot of the flowrate required to flood the piping with diameters ranging from a nominal 3/8" to 4".

Graph 8 is a similar plot, but the 3/8" and 3/4" data has been excluded (due to the challenges with maintaining the smaller diameter pipe completely horizontal without local low spots). A third order polynomial trend line has been added to this plot (third order polynomial chosen because

third order provided the best fit for the data). The listed R^2 value for the trendline indicates that the trendline is a good fit of the data.



Graph 7 – Flowrate required to flood horizontal piping open on end versus pipe ID



Graph 8 - Flowrate required to flood horizontal piping open on end versus pipe ID with trendline

3.4. DISCUSSION OF DETERMINATION OF FLOWRATE REQUIRED TO FLOOD A 6 FOOT HORIZONTAL PIPE OPEN ON END

Generally the horizontal piping would first flood at the point furthest from the outlet. Once the piping became flooded (liquid sealed) at a point in the piping, the portion of the piping that was liquid sealed would then slowly move towards the outlet - length of horizontal pipe is becoming more and more flooded over time - up to a point. If the flowrate wasn't high enough, only a portion of the pipe would be flooded (eg. first 36 inches). The variable frequency drive on the centrifugal pump allowed for fine adjustment of the water flowrate. In adjusting the water flowrate up and down, one could control the amount of the horizontal pipe that was flooded. As stated previously, the horizontal pipe was defined as "flooded" when all of the air was displaced from the pipe to a point no more than 6 inches from the outlet of the horizontal pipe within 60 seconds of starting the pump. As indicated in Figure 9, the height of liquid in the horizontal pipe drops off just prior to the outlet. This was particularly noticeable in the larger piping sizes tested (eg. nominal 3 and 4" piping). To completely flood the entire length of the piping (100% liquid filled at the point where the water was discharged from the pipe) required much higher flowrates and determining the flowrate at which the outlet was flooded was very subjective/difficult. Defining "flooding" as the point where all of the air was displaced from the pipe to a point no more than 6 inches from the outlet of the horizontal pipe removed this subjectivity.



Figure 9 – Picture indicating how liquid height drops off close to outlet of horizontal pipe

The equation of the trendline from Graph 8 can be used to estimate the flowrate required to flood a horizontal pipe within the range of inside diameters of approximately 1-4 inches. This is listed as Equation 1.

Equation 1

Legend

- Horizontal Pipe Flooding Flowrate = flowrate required to flood a horizontal pipe (lpm)
- x = pipe inside diameter (inches)

The graphs of liquid height versus distance from the pipe outlet indicate that the liquid height increases as the distance from the pipe outlet increases. The data suggests that the liquid height would be greater at locations further from the outlet in the longer pipe which would cause the pipe to become liquid sealed at somewhat reduced flowrates compared to the flowrate determined from the testing performed on the 6 foot spool piece. Once the pipe becomes sealed, the sealed flow then travels towards the pipe outlet. The speed at which the sealed flow travels towards the pipe outlet is dependent upon the flowrate. In defining the “flooding flowrate” as the flowrate required to completely flood 5.5 foot of horizontal piping within 60 seconds, the minimum velocity at which the sealed flow travels is at least 5.5 ft/min. The time required to move the sealed flow down the line to the outlet should be considered when determining the time required to completely flood a horizontal line. Based on the data, one would expect that a horizontal pipe longer than the 6 foot spool piece evaluated in this testing would also flood at the listed flooding flowrate but it might take longer than 60 seconds for the pipe to be flooded to a point 6 inches from the outlet.

3.5. RESULTS OF DETERMINATION OF FLOWRATE REQUIRED TO FLOOD A 6 FOOT HORIZONTAL PIPE WITH A ONE FOOT OPEN ENDED VERTICAL PIPE DIRECTED DOWNWARD

Testing was performed with piping that ranged from 3/8" – 4" nominal pipe diameter. The test skid was unable to deliver a flowrate high enough to flood the 4" pipe directed downward (the highest flowrate tested was 405 lpm). Data from the testing performed is included in Table 4.

Unique #ers for Test Result	Nominal Pipe Size (inch)	Piping			90° Elbow			Water Temp (°C)	Flowrate Required to Flood 1 Foot Vertical Pipe Directed Downward Open on End (lpm)	Comment
		Pipe Schedule	ID (inch)	ID (mm)	Pipe Schedule	ID (inch)	ID (mm)			
178-180	0.38	80	0.42	10.74	40	0.49	12.52	22	4.5	Exact flooding flowrate was a somewhat difficult to determine due to use of centrifugal pump and hydraulics of the system.
165-167	0.75	80	0.74	18.85	40	0.82	20.93	22	9.3	
119-121	1.00	80	0.96	24.31	40	1.05	26.64	23	12.3	
93-95	1.50	80	1.50	38.10	40	1.61	40.89	22	39.5	
32-34	2.00	80	1.94	49.25	40	2.07	52.50	25	102.7	
194-198	3.00	40	3.07	77.93	40	3.07	77.93	24	378.0	

Table 4 - Test results of flowrate required to flood vertical pipe directed downward open on end

A common observation with all pipe sizes tested was that the measured flowrate immediately increased to a new value when the open ended vertical pipe became completely liquid filled/flooded. This occurs with the test configuration due to the fact that the hydraulics of the system change when the vertical pipe becomes liquid filled. It was common to observe two flowrates during the testing, the initial lower flowrate was typically present for just under 60 seconds (before the vertical pipe became liquid filled), and then a higher flowrate was present after the vertical pipe became liquid filled. As an example, when testing the 2" schedule 80 pipe, the initial flowrate was 102.7 lpm until the vertical pipe became liquid filled; when the pipe was liquid filled the flowrate immediately jumped to 105.6 lpm.

At the flooding flowrate, the horizontal pipe would flood first, then the air would be displaced from the 90° elbow, and then the vertical pipe directed downward would become liquid filled.

Because the air was already displaced from the 90° elbow prior to the vertical pipe flooding, the flowrates recorded in the Table 4 and represented in Graph 9 as the flowrate required to flood the vertical pipe were the first lower values (this is the flowrate where the pipe flooded). When the vertical pipe becomes liquid filled, the liquid head/backpressure that the centrifugal pump is pumping against decreases which in turn causes an increase in the flowrate.

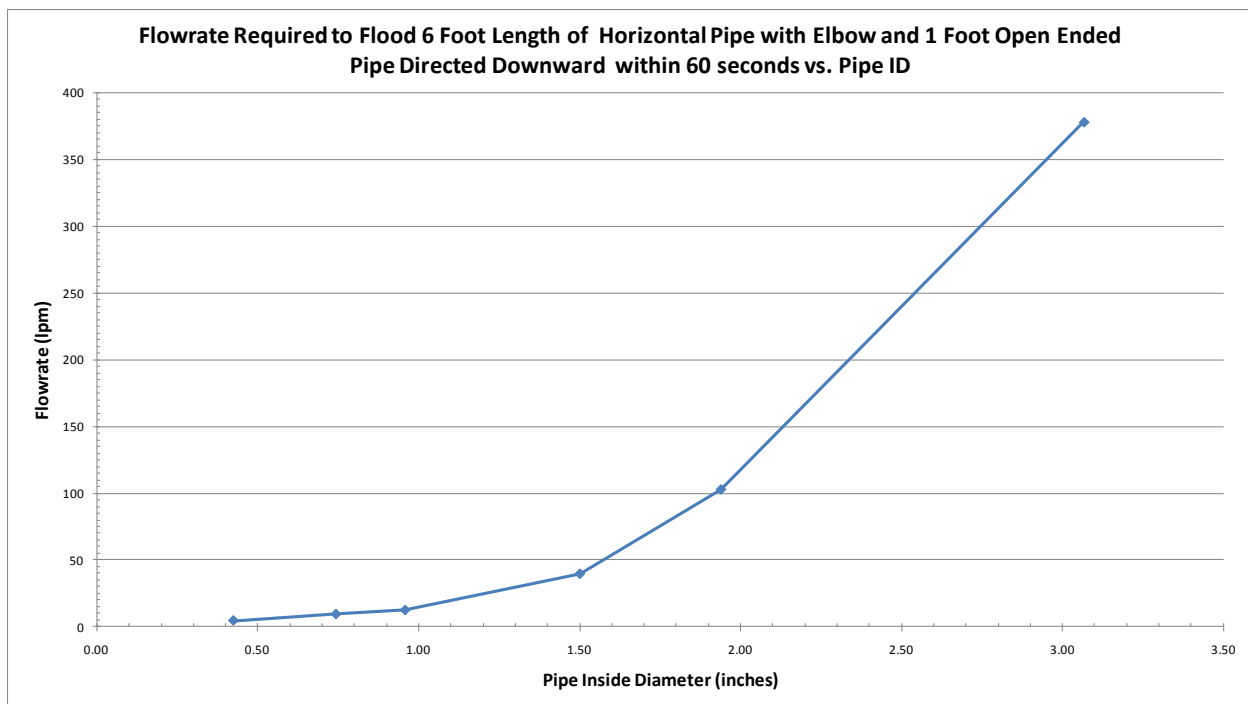
A common observation made in several instances is that once the vertical pipe was flooded, the flowrate could be reduced significantly while maintaining the vertical pipe in a flooded state. For example, after flooding the nominal 2" vertical piping, the flowrate was slowly reduced to as low as 34 lpm (less than half of the original flowrate required to flood the system) while still maintaining the system flooded. When the flowrate was reduced to 30 lpm, air entered into the system and the piping no longer remained flooded.

Due to the low operating speed of the centrifugal pump (controlled via the VFD) and the hydraulics of the system at the lower flowrates, the flooding flowrate values for the smaller 3/8"

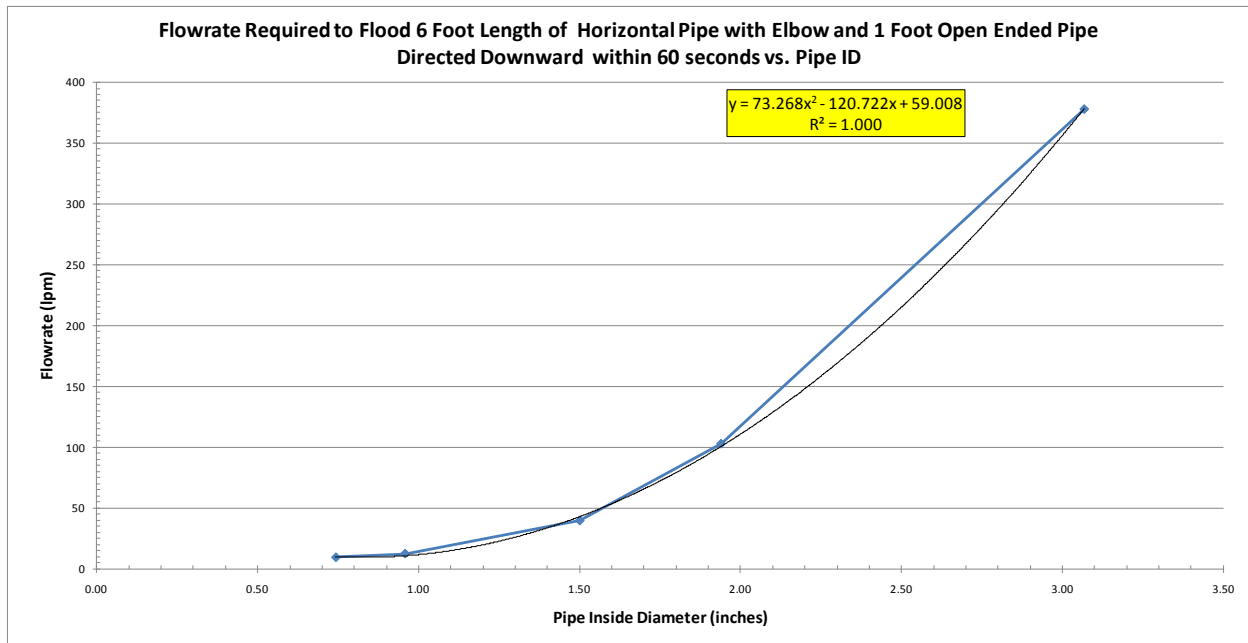
nominal piping were more erratic. The testing was performed in triplicate and the highest value was listed in Table 4. It is expected that the listed value represents a worse case flowrate for the nominal 3/8" piping. If additional testing is performed on smaller diameter piping, it may be beneficial to use a positive displacement style pump (eg. rotary lobe) with a smaller capacity so that the flow is not impacted as much by hydraulic changes.

Graph 9 is a plot of the flowrate required to flood piping with diameters ranging from a nominal 3/8" to 3".

Graph 10 is a similar plot, but the 3/8" data has been excluded (due to the more erratic flooding flowrates observed). A second order polynomial trend line has been added to this plot (second order polynomial chosen because second order provided the best fit for the data). The listed R^2 value for the trendline indicates that the trendline is a good fit of the data.



Graph 9 - Flowrate required to flood vertical piping open on end directed downward versus pipe ID



Graph 10 - Flowrate required to flood vertical piping open on end directed downward versus pipe ID with trendline

3.6. DISCUSSION OF DETERMINATION OF FLOWRATE REQUIRED TO FLOOD A 6 FOOT HORIZONTAL PIPE WITH A ONE FOOT OPEN ENDED VERTICAL PIPE DIRECTED DOWNWARD

As defined previously, the horizontal pipe with a 1 foot vertical open ended pipe directed downward was defined as “flooded” when all of the air was displaced from the horizontal pipe, the 90° elbow, and the vertical pipe directed downward within 60 seconds from the start of the pump.

At the flooding flowrate, the horizontal pipe would flood first, then the air would be displaced from the 90° elbow, and then the vertical pipe directed downward would become liquid filled.

More variability was observed in the time required for the open ended vertical pipe to become liquid filled as compared to the other tests that were performed. It was not uncommon for liquid to be flowing through the vertical pipe at the desired flowrate for more than 30 seconds before suddenly becoming liquid filled. Testing was performed in triplicate for each pipe size listed and in each case all piping was flooded an average of less than 60 seconds from starting the pump.

Once any portion of the vertical pipe became liquid filled, the whole line quickly became liquid filled (in approximately a second). Because of this observation, it is expected that little additional time would be required to flood a vertical pipe longer than the 1 foot spool piece evaluated in the testing at the flooding flowrate.

The equation of the trendline from Graph 10 can be used to estimate the flowrate required to flood a vertical open ended pipe within the range of inside diameters of approximately 0.75-3 inches. This is listed as Equation 2.

Equation 2

Legend:

- Open Ended Vertical Pipe Flooding Flowrate = flowrate required to flood a vertical pipe open on end directed downward (lpm)
- x = pipe inside diameter (inches)

3.7. RESULTS OF DETERMINATION OF FLOWRATE REQUIRED TO FLOOD A 6 FOOT HORIZONTAL PIPE WITH A TWO FOOT VERTICAL PIPE DIRECTED DOWNWARD THAT IS SEALED ON THE END

Testing was performed with piping that ranged from 3/8" – 4" nominal pipe diameter.

The test skid was unable to deliver a flowrate high enough to completely flood the 90° elbow in the test with the 4" pipe directed downward (the highest flowrate tested was 405 lpm). In the 4" test case, after 60 seconds both the horizontal pipe and vertical pipe were flooded, but an air bubble remained in the elbow.

In all cases testing began with the transparent piping drained and the pump off. When the pump started, water supplied to the system began to displace the air in the pipe. Because the end of the diptube was submersed 6 inches, bubbles from the displaced air were discharged into the water. With the pipe outlet submersed, there was no means for displaced air to be re-introduced back into the piping system. This was a significant difference between the open ended outlet and the sealed outlet.

As stated previously, the vertical pipe was defined as “flooded” when all of the air was displaced from the horizontal pipe, the 90° clear PVC elbow, and the vertical pipe. The testing determined the flowrate required to flood the system within 60 seconds of starting the pump. At the flowrates required to flood the piping in a 60 second time period, the horizontal portion of the piping flooded first, then the vertical piping flooded (liquid level started at the bottom of the vertical pipe and the liquid level increased from the bottom up), and then the last amount of air was displaced from the 90° clear PVC elbow.

When the liquid flowrate was sufficient to displace air from the vertical pipe, the volume of air displaced was replaced with water. This caused the liquid level in the submersed pipe to build up starting from the bottom of the pipe. As additional air was displaced, the liquid level in the vertical pipe continued to rise. The change in the vertical pipe liquid level impacted the hydraulics of the system which caused the flowrate to increase slowly (centrifugal pump running at a fixed speed throughout the test) as the vertical pipe became liquid filled. When the vertical portion of the pipe became completely liquid filled, but before the air was displaced from the 90° clear PVC elbow, the flowrate jumped up significantly (eg. when testing the 1" nominal pipe size, the flowrate immediately jumped from 6.0 lpm to 25.1 lpm) due to the hydraulics.

After the vertical portion of the pipe became liquid filled, a pocket of air remained at the top of the transparent 90° elbow. This remaining air was removed in small bubbles by the liquid flowing by. These bubbles were carried down the vertical pipe and discharged into the drum. This occurred until the last of the air was displaced from the 90° clear PVC elbow. As stated previously, the flowrate increased significantly when the last amount of air was displaced from the vertical portion of the pipe, but before the air was displaced from the 90° elbow. The air that remained in the 90° elbow after the vertical pipe was flooded was removed from liquid flowing

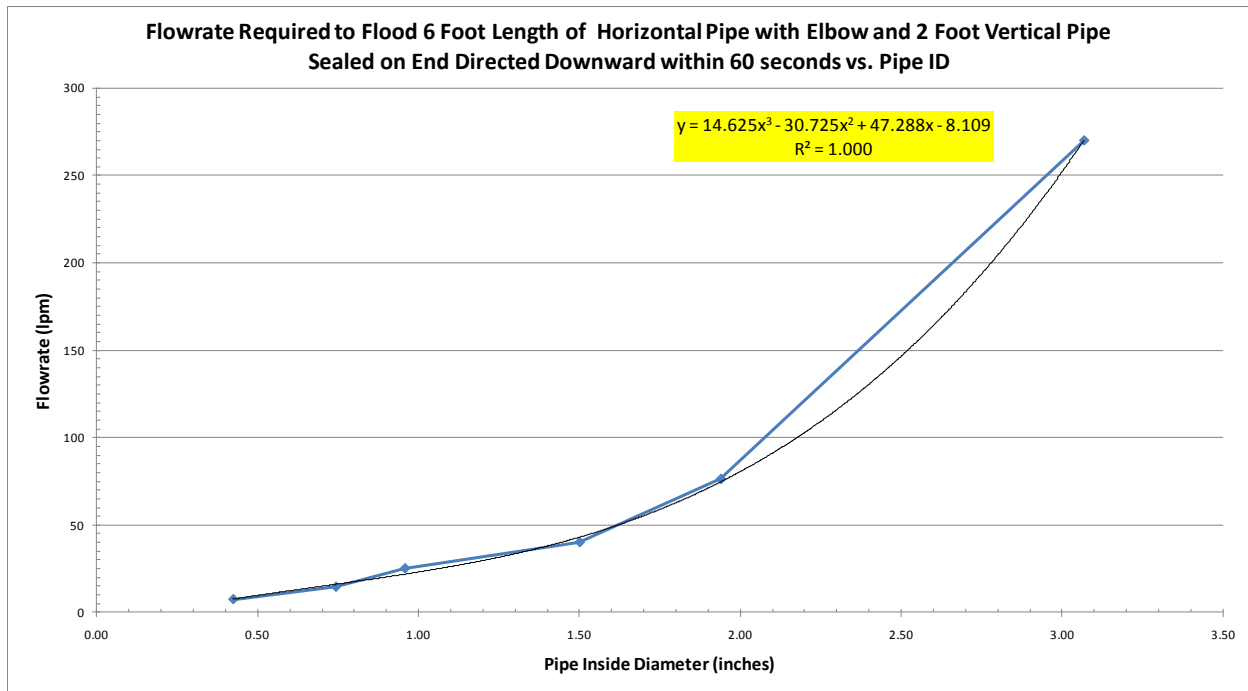
at the increased flowrate, therefore the liquid flowrate values recorded as the flooding flowrate were the highest flow values observed during the test. The flowrate observed just prior to the vertical portion of the piping becoming liquid filled was also recorded (listed as initial flowrate). This test data is included in Table 5.

As would be expected, once all air was displaced from the piping system and it became flooded, the piping remained flooded – even when the pump was turned off. When the pipe outlet is sealed by being submersed in water, there is no way for air to enter into the system.

Unique #'ers for Test Result	Nominal Pipe Size (inch)	Horizontal and Vertical Pipe			90 Degree Elbow			Water Temp (°C)	Initial Flowrate - prior to vertical pipe being liquid filled (lpm)	Flooding Flowrate - after vertical pipe became liquid filled (lpm)
		Pipe Schedule	ID (inch)	ID (mm)	Pipe Schedule	ID (inch)	ID (mm)			
181-183	0.38	80	0.42	10.74	40	0.49	12.52	22	4.0	7.4
168-170	0.75	80	0.74	18.85	40	0.82	20.93	22	8.2	14.5
126-128	1.00	80	0.96	24.31	40	1.05	26.64	23	6.0	25.1
104-106	1.50	80	1.50	38.10	40	1.61	40.89	23	26.0	40.0
35-37	2.00	80	1.94	49.25	40	2.07	52.50	25	72.0	76.2
204-206	3.00	40	3.07	77.93	40	3.07	77.93	26	not recorded	270.0

Table 5 - Test results of flowrate required to flood vertical pipe directed downward sealed on end

Graph 11 is a plot of this data which indicates the flowrate required to flood the piping with diameters ranging from a nominal 3/8" to 3". A third order polynomial trend line has been added to this plot (third order polynomial chosen because third order provided the best fit for the data). The listed R² value for the trendline indicates that the trendline is a good fit of the data.



Graph 11 - Flowrate required to flood vertical piping sealed on end directed downward versus pipe ID with trendline

3.8. DISCUSSION OF DETERMINATION OF FLOWRATE REQUIRED TO FLOOD A 6 FOOT HORIZONTAL PIPE WITH A TWO FOOT VERTICAL PIPE DIRECTED DOWNWARD THAT IS SEALED ON THE END

As defined previously, the horizontal pipe with a 2 foot vertical pipe directed downward sealed on the end was defined as “flooded” when all of the air was displaced from the horizontal pipe, the 90° elbow, and the vertical pipe directed downward within 60 seconds from the start of the pump.

The flowrates listed in Table 5 are the flowrates observed after the system was completely flooded. Due to the time component in the definition for achieving a flooding flowrate (all air had to be displaced from the system within 60 seconds), the length of the vertical pipe would impact the flooding flowrate. A two foot vertical spool piece was used in all test cases, but if a longer spool piece were used, a higher flowrate would be required to flood the piping within the allotted 60 seconds because it would take longer for the liquid level to build up to flood the vertical pipe.

In defining the “flooding flowrate” as the flowrate required to completely flood the foot of vertical piping within 60 seconds, the minimum velocity at which the liquid level builds up in the pipe is at least 2 ft/min. The time required to build up the liquid level in the vertical line should be considered when determining the time required to completely flood a longer vertical line.

Because a source of schedule 80 clear PVC 90° elbows could not be easily identified, schedule 40 clear PVC 90° elbows were purchased for the testing. For the schedule 40, 3" and 4" piping tested, the diameter of the piping tested matched that of the 90° elbow. For the schedule 80, 3/8", 3/4", 1", 1.5", and 2" piping tested, there was a difference between the ID of the piping and the

ID of the 90° elbow. The ID of the thicker walled schedule 80 piping was smaller than the thinner schedule 40 90° elbow. This difference resulted in a small step change in the pipe diameter at the glued interface between the elbow and the pipe. It is expected that this slightly larger diameter elbow made it more difficult to displace the air from the elbow, which caused the flooding flowrate to be slightly higher than what would have occurred if schedule 80 90° elbows were used for the 3/8, 3/4, 1, 1.5, and 2" test cases.

The equation of the trendline from Graph 11 can be used to estimate the flowrate required to flood a vertical pipe sealed on the end within the range of inside diameters of approximately 0.5-3". This is listed as Equation 3.

Equation 3

Legend:

- Sealed End Vertical Pipe Flooding Flowrate = flowrate required to flood a vertical pipe submersed on end (lpm)
- x = pipe inside diameter (inches)

Note: Before applying this equation, the user should consider their application and take the following into consideration:

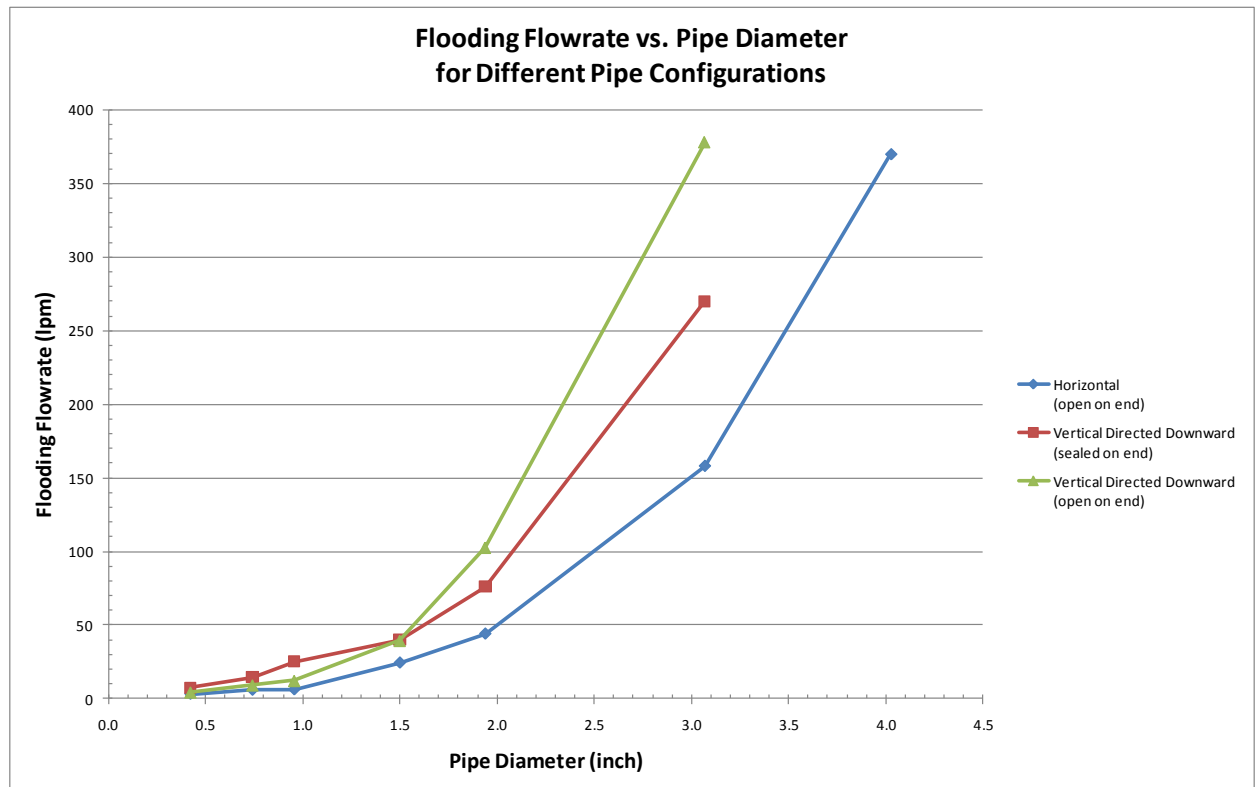
- The flowrate listed as the flooding flowrate is the highest flowrate in the range of flowrates observed over the approximate 60 second time period required for flooding.
- This testing was performed using a two foot long vertical pipe. If a longer vertical pipe is used, the time required to flood the piping and elbow may be longer than 60 seconds.

3.9. RESULTS AND DISCUSSION OF OVERALL IMPACT OF OUTLET CONDITION ON FLOODING FLOWRATE:

Table 6 indicates the cumulative data from the flooding flowrate testing performed using ambient water with various outlet conditions. This data is plotted in Graph 12. Note: as described previously, the data plotted for the flooding flowrate for the vertical pipe directed downward that was sealed on the end was the flowrate after the vertical pipe became liquid filled.

Nominal Pipe Size (inch)	Pipe Schedule	Pipe ID (inch)	Pipe ID (mm)	Flowrate Required to Flood Piping (lpm)			
				Horizontal (open on end)	Vertical Directed Downward (sealed on end)		Vertical Directed Downward (open on end)
					Initial Flowrate - prior to vertical pipe being liquid filled	Flooding Flowrate - after vertical pipe became liquid filled	
0.38	80	0.42	10.74	3.0	4.0	7.4	4.5
0.75	80	0.74	18.85	5.7	8.2	14.5	9.3
1.00	80	0.96	24.31	6.0	6.0	25.1	12.3
1.50	80	1.50	38.10	24.2	26.0	40.0	39.5
2.00	80	1.94	49.25	43.9	72.0	76.2	102.7
3.00	40	3.07	77.93	158.0	not recorded	270.0	378.0
4.00	40	4.03	102.26	370.0	n/a	n/a	n/a

Table 6 - Test results of flooding flowrates under different outlet conditions at ambient temperature.



Graph 12 -Test results of flooding flowrates under different outlet conditions at ambient temperature.

A general observation from Graph 12 is that of the three pipe configurations tested, the horizontal pipe open on the end flooded at the lowest flowrate, followed by the vertical pipe directed downward that was liquid sealed on the end. The vertical pipe directed downward that was open on the end required the highest flowrate to flood.

Note: at nominal pipe sizes below 1", in some cases, the recorded flowrate values required to flood a vertical pipe directed downward that was sealed on the end were slightly higher than that required to flood a vertical pipe directed downward that was open on the end. It is believed that these higher flowrate values for the vertical pipe sealed on the end are a result of the testing equipment and methodology used (eg. due to hydraulic effects of using the centrifugal pump). It is believed that the highest flowrate required to flood a pipe is that required to flood a vertical pipe directed downward with an open end.

3.10. RESULTS AND DISCUSSION OF IMPACT OF INCREASED 60° C TEMPERATURE ON LIQUID HEIGHTS AND FLOODING FLOWRATES ON 2" PIPING.

Testing was performed on nominal 2" piping to understand the impact that temperature has on both liquid heights and flooding flowrates with a variety of outlet conditions. Water at 60° C was used for the elevated temperature testing.

3.10.1. Impact of increased 60° C temperature on liquid height of 2" piping.

Table 7 lists the liquid height measurements taken at three different distances from the outlet of the 6 foot horizontal pipe for nominal 2" pipe at 6 different flowrates. Each flowrate tested was performed with both ambient (26° C) water and hot (60° C) water.

The liquid height was measured from the outside bottom of the transparent pipe. The wall thickness of the piping was then subtracted from these measured values to determine the actual height of liquid inside the piping (these values were recorded in Table 7 and plotted in Graph 13).

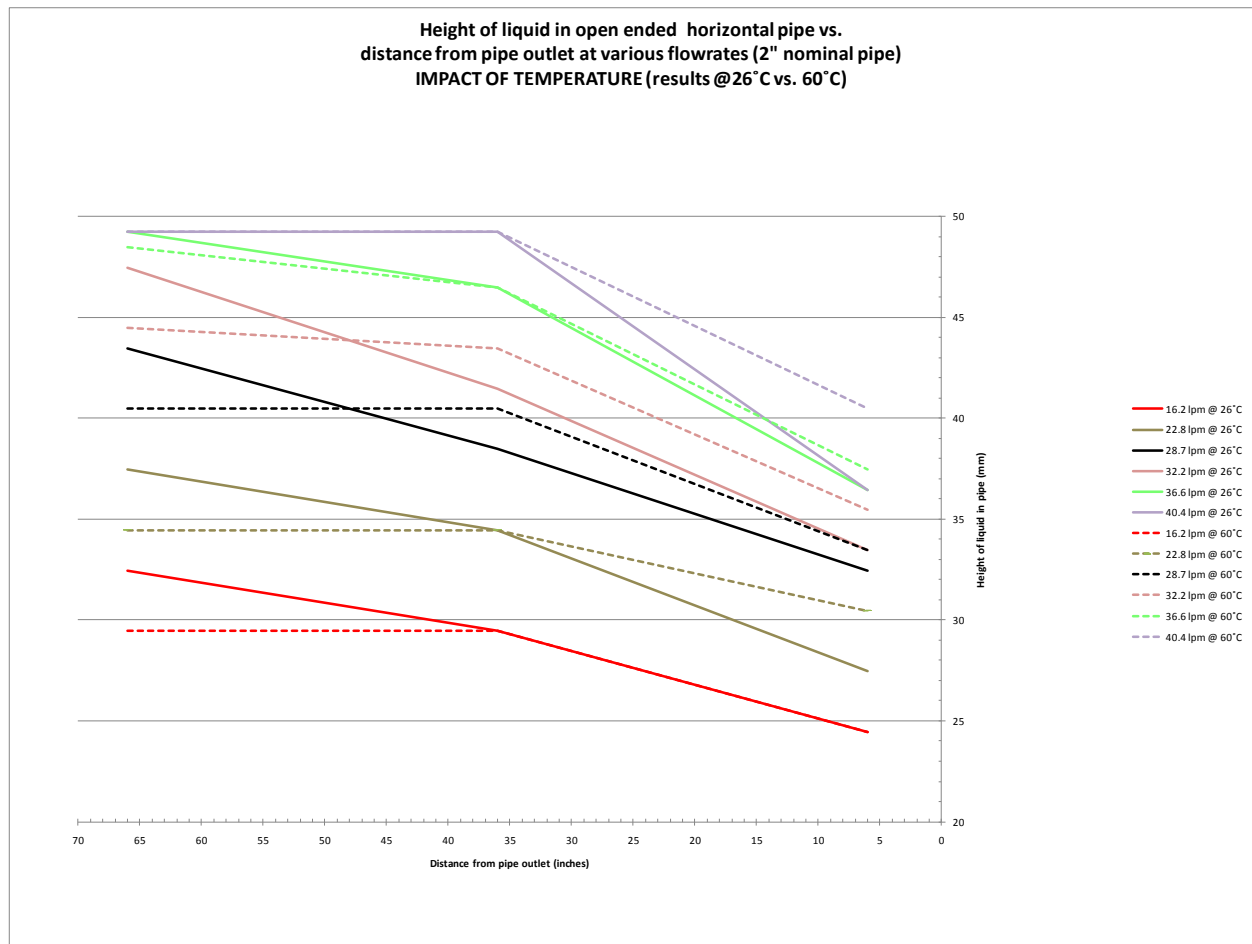
Graph 13 indicates the impact that temperature has on liquid height at the various flowrates. For this graph, each color represents a different flowrate, and for each flowrate, the solid line represents the liquid height at 26° C and the dashed line represents the liquid height at 60° C.

As indicated in Graph 13, the impact of temperature on liquid height is dependent on the distance from the outlet where the measurement was taken. For the 6 flowrates evaluated, the liquid height of 26° C water was always greater than or equal to the liquid height of the 60° C water at the location 66 inches from the outlet. At the location just 6 inches from the outlet, the opposite was true: the measured liquid height of 26° C water was always less than or equal to the height of the 60° C water.

The cause for this observed height difference has not been thoroughly investigated. One hypothesis is that the liquid height may be impacted by the viscosity of the solution. The viscosity of water at 26° C is 0.8708 centipoise and the viscosity at 60° C is approximately 1.9 times less at .4665 centipoise [1].

Unique # for Test Result	Nominal Pipe Size (in)	Pipe Schedule	Pipe ID (mm)	Pipe Wall Thickness (mm)	Water Temp (°C)	Flowrate (lpm)	Height from Outside Bottom of Pipe (mm)			Height from Inside Bottom of Pipe (mm)			Height from Outside Bottom of Pipe when Flooded (mm)
							66" from Outlet	36" from Outlet	6" from Outlet	66" from Outlet	36" from Outlet	6" from Outlet	
20	2.00	80	49.25	5.54	26	16.2	38	35	30	32	29	24	55
21	2.00	80	49.25	5.54	26	22.8	43	40	33	37	34	27	55
22	2.00	80	49.25	5.54	26	28.7	49	44	38	43	38	32	55
23	2.00	80	49.25	5.54	26	32.2	53	47	39	47	41	33	55
24	2.00	80	49.25	5.54	26	36.6	55	52	42	49	46	36	55
25	2.00	80	49.25	5.54	26	40.4	55	55	43	49	49	37	55
38	2.00	80	49.25	5.54	60	16.2	35	35	30	29	29	24	55
39	2.00	80	49.25	5.54	60	22.8	40	40	36	34	34	30	55
40	2.00	80	49.25	5.54	60	28.7	46	46	39	40	40	33	55
41	2.00	80	49.25	5.54	60	32.2	50	49	41	44	43	35	55
42	2.00	80	49.25	5.54	60	36.6	54	52	43	48	46	37	55
43	2.00	80	49.25	5.54	60	40.4	55	55	46	49	49	40	55

Table 7 - Test results of liquid heights at 26 and 60° C at various flowrates



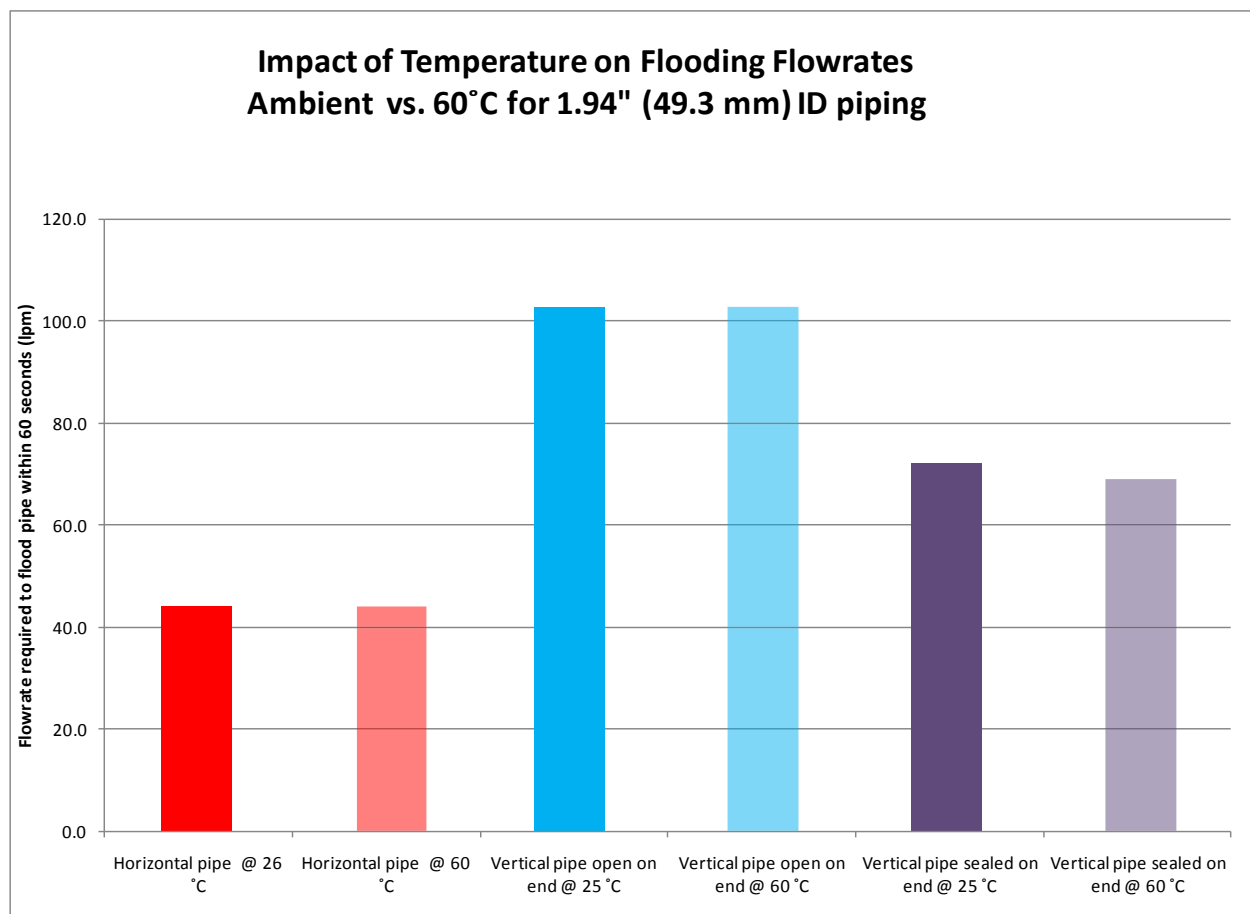
Graph 13 - Test results of liquid heights at 26 and 60° C at various flowrates

The impact that increasing the water temperature to 60° C has on the flooding flowrate for each of the three pipe configurations previously tested with ambient water was also evaluated.

The test results are listed in Table 8 and indicated in Graph 14.

Unique # for test result	Nominal pipe size (in)	Schedule	Pipe ID (inch)	Pipe ID (mm)	Temperature (°C)	Flowrate required to flood pipe configuration (lpm)					
						Horizontal pipe @ 26 °C	Horizontal pipe @ 60 °C	Vertical pipe open on end @ 25 °C	Vertical pipe open on end @ 60 °C	Vertical pipe sealed on end @ 25 °C	Vertical pipe sealed on end @ 60 °C
32-34	2.0	80	1.94	49.25	25.0			102.7			
35-37	2.0	80	1.94	49.25	25.0					72.0	
26	2.0	80	1.94	49.25	26.0	43.9					
48-50	2.0	80	1.94	49.25	60.0				102.7		
51-53	2.0	80	1.94	49.25	60.0						69.0
44	2.0	80	1.94	49.25	60.0		43.9				

Table 8 - Test results of flooding flowrates of nominal 2" horizontal piping at 26 and 60 ° C



Graph 14 - Test results of flooding flowrates of nominal 2" piping in various orientations at 26 and 60 ° C

3.10.2. Impact of 60°C temperature on flooding 2" horizontal pipe open on end

As indicated in Table 8 and Graph 14, the increased temperature had essentially no impact on the flowrate required to flood a nominal 2" horizontal pipe that is open on the end. In both tests, the pipe was flooded at 43.9 lpm.

3.10.3. Impact of 60°C temperature on flooding 2" vertical pipe open on end

As indicated in Table 8 and Graph 14, the increased temperature had essentially no impact on the flowrate required to flood a nominal 2" vertical pipe that is open on the end. In both tests, the pipe was flooded at 102.7 lpm.

3.10.4. Impact of 60°C temperature on flooding 2" pipe sealed on end

As indicated in Table 8 and Graph 14, the increased temperature had a minimal impact on the flowrate required to flood a nominal 2" vertical pipe that is sealed on the end. With ambient water the flooding flowrate was 72.0 lpm and at 60°C the flooding flowrate was 69.0 lpm.

3.11. RESULTS AND DISCUSSION OF IMPACT OF INCREASED 70°C TEMPERATURE ON FLOODING FLOWRATES ON PIPING.

Although the initial testing performed on nominal 2" piping with 60°C water indicated that the increased temperature did not cause a significant change in the flowrate required to flood piping under a variety of outlet conditions, additional testing was performed at an elevated temperature of approximately 70 C for a variety of piping sizes to better understand the impact that temperature has on flooding flowrates. This testing was performed on all outlet conditions described previously (horizontal open on end, vertical open on end, and vertical sealed on end).

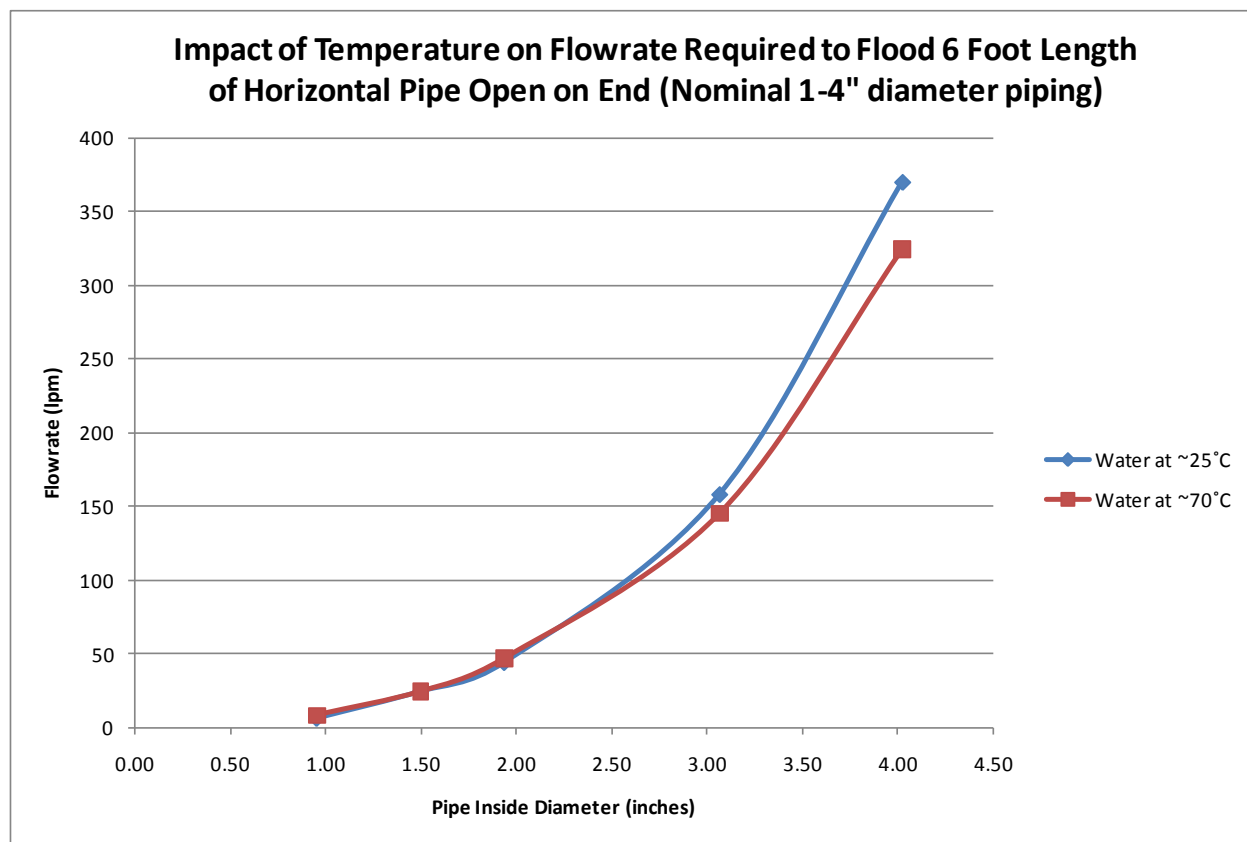
3.11.1. Impact of 70°C temperature on flowrate required to flood a horizontal pipe open on the end

Testing was performed on piping ranging in size from a nominal 1" to 4" in diameter. The testing was conducted in the same manner previously described for determining the flowrate required to flood a horizontal pipe open on the end with the only difference being that, instead of being performed at ambient temperature, the testing was performed at approximately 70°C. The test results listed along with the previously reported test results at ambient conditions are included in Table 9.

A graph of the flooding flowrates at approximately 70°C versus those at ambient temperature is included in Graph 15. As indicated by this graph, the flowrate required to flood a horizontal pipe open on the end at approximately 70°C is very similar to the flowrate required at ambient temperature.

Unique #'ers for Test Result	Nominal Pipe Size (inch)	Pipe Schedule	Pipe ID (inch)	Pipe ID (mm)	Water Temp (°C)	Flowrate Required to Flood Horizontal Piping (lpm)
112-114	1.00	80	0.96	24.31	23	6.0
81-83	1.50	80	1.50	38.10	22	24.2
26	2.00	80	1.94	49.25	26	43.9
187-189	3.00	40	3.07	77.93	23	158.0
143-145	4.00	40	4.03	102.26	28	370.0
<hr/>						
257-259	1.00	80	0.96	24.31	72	8.2
266-268	1.50	80	1.50	38.10	71	24.2
275-277	2.00	80	1.94	49.25	71	46.7
284-286	3.00	40	3.07	77.93	70	145.0
293-295	4.00	40	4.03	102.26	70	324.3

Table 9 – Test results of flooding flowrates of horizontal piping at ambient temperature and 70°C



Graph 15 - Flooding flowrates of horizontal piping versus pipe diameter at ambient temperature and 70°C

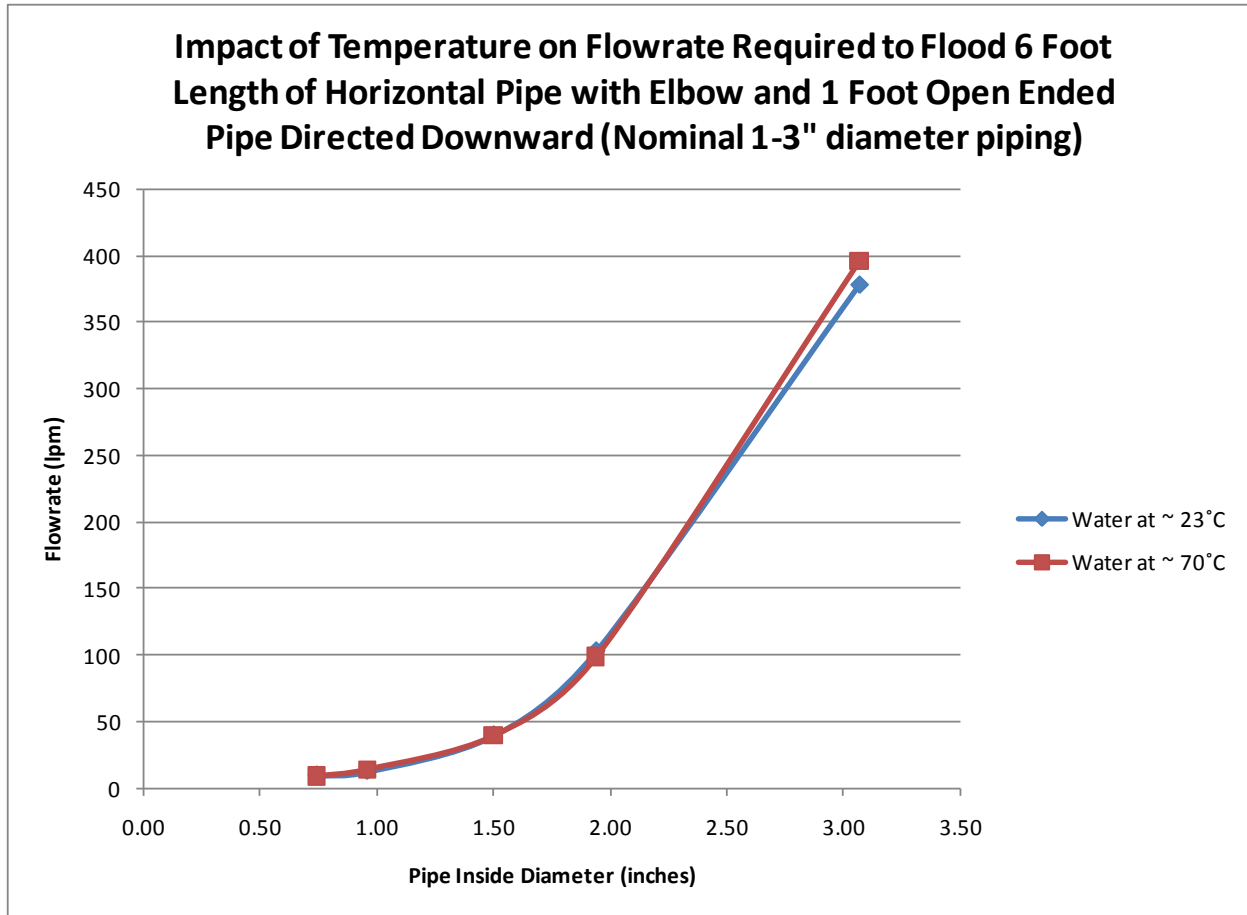
3.11.2. Impact of 70°C temperature on flowrate required to flood a vertical pipe open on the end

Testing was performed on piping ranging in size from a nominal 1" to 3" in diameter. The testing was performed in the same manner previously described for determining the flowrate required to flood a 6 foot horizontal pipe with a 1 foot open ended vertical pipe directed downward with the only difference being that, instead of being performed at ambient temperature, the testing was performed at approximately 70°C. The test results, listed along with the previously reported test results at ambient conditions, are included in Table 10.

A graph of the flooding flowrates at approximately 70°C versus those at ambient temperature is included in Graph 16. As indicated by this graph, the flowrate required to flood a 6 foot horizontal pipe with a 1 foot open ended vertical pipe directed downward at approximately 70°C is very similar to the flowrate required at ambient temperature.

Unique #ers for Test Result	Nominal Pipe Size (inch)	Piping			90° Elbow			Water Temp (°C)	Flowrate Required to Flood 1 Foot Vertical Pipe Directed Downward Open on End (lpm)
		Pipe Schedule	ID (inch)	ID (mm)	Pipe Schedule	ID (inch)	ID (mm)		
165-167	0.75	80	0.74	18.85	40	0.82	20.93	22	9.3
119-121	1.00	80	0.96	24.31	40	1.05	26.64	23	12.3
93-95	1.50	80	1.50	38.10	40	1.61	40.89	22	39.5
32-34	2.00	80	1.94	49.25	40	2.07	52.50	25	102.7
194-198	3.00	40	3.07	77.93	40	3.07	77.93	24	378.0
251-253	0.75	80	0.74	18.85	40	0.82	20.93	72	9.1
260-262	1.00	80	0.96	24.31	40	1.05	26.64	69	14.1
269-271	1.50	80	1.50	38.10	40	1.61	40.89	69	39.5
278-280	2.00	80	1.94	49.25	40	2.07	52.50	70	98.6
287-289	3.00	40	3.07	77.93	40	3.07	77.93	70	396.0

Table 10 - Test results of flowrate required to flood vertical pipe directed downward open on end at ambient temperature and 70°C



Graph 16 - Flooding flowrates of vertical pipe directed downward – open on end versus pipe diameter at ambient temperature and 70°C

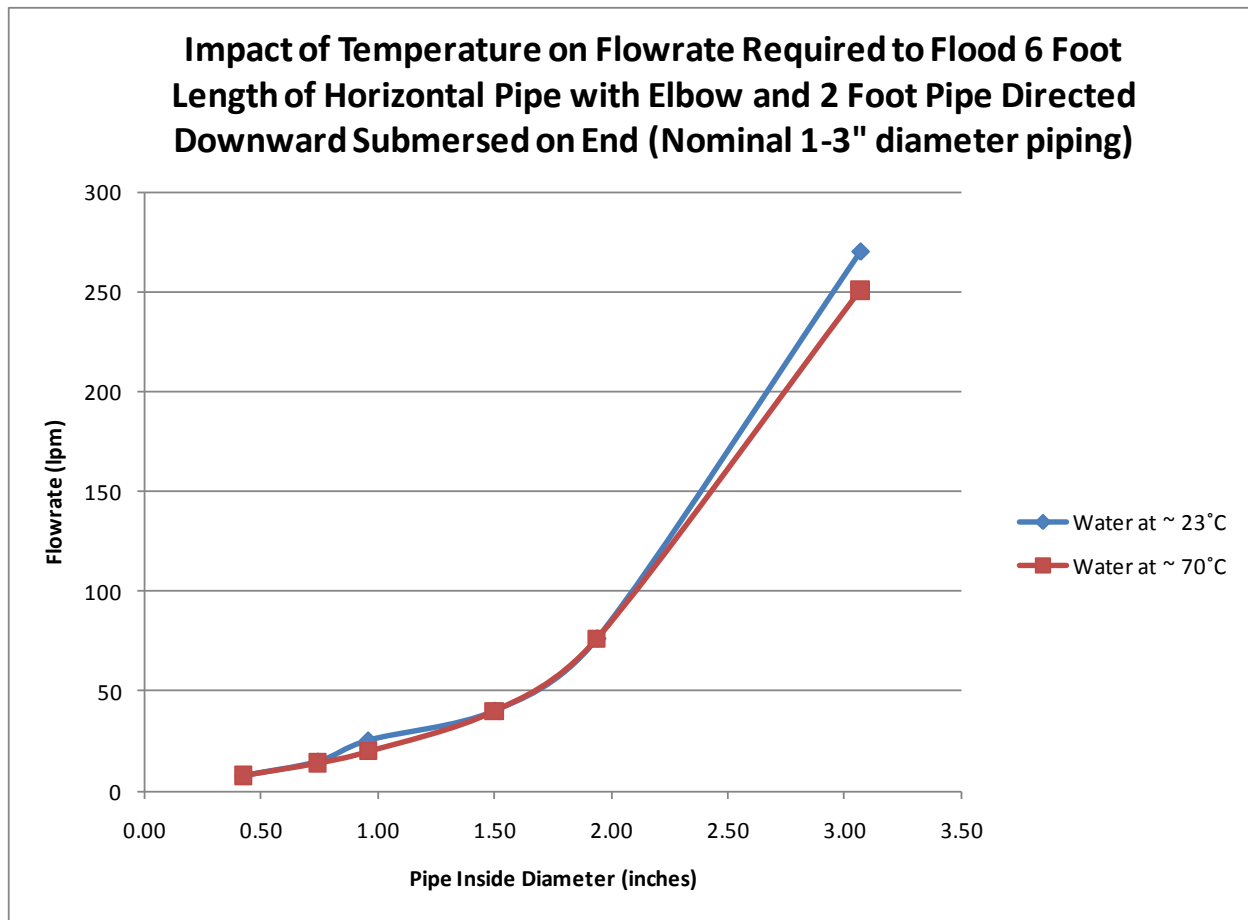
3.11.3. Impact of 70°C temperature on flowrate required to flood a vertical pipe sealed on the end

Testing was performed on piping ranging in size from a nominal 1" to 3" in diameter. The testing was performed in the same manner previously described for determining the flowrate required to flood a 6 foot horizontal pipe with a 2 foot vertical pipe directed downward that is sealed on the end with the only difference being that, instead of being performed at ambient temperature, the testing was performed at approximately 70°C. The results of this testing, listed along with the previously reported test results at ambient conditions, are included in Table 11.

A graph of the flooding flowrates at approximately 70°C versus those at ambient temperature is included in Graph 17. As indicated by this graph, the flowrate required to flood a 6 foot horizontal pipe with a 2 foot vertical pipe directed downward sealed on the end at approximately 70°C is very similar to the flowrate required at ambient temperature.

Unique #ers for Test Result	Nominal Pipe Size (inch)	Piping			90° Elbow			Water Temp (°C)	Initial Flowrate - prior to vertical pipe being liquid filled (lpm)	Flooding Flowrate - after vertical pipe became liquid filled (lpm)
		Pipe Schedule	ID (inch)	ID (mm)	Pipe Schedule	ID (inch)	ID (mm)			
181-183	0.38	80	0.42	10.74	40	0.49	12.52	22	4.0	7.4
168-170	0.75	80	0.74	18.85	40	0.82	20.93	22	8.2	14.5
126-128	1.00	80	0.96	24.31	40	1.05	26.64	23	6.0	25.1
104-106	1.50	80	1.50	38.10	40	1.61	40.89	23	26.0	40.0
35-37	2.00	80	1.94	49.25	40	2.07	52.50	25	72.0	76.2
204-206	3.00	40	3.07	77.93	40	3.07	77.93	26	not recorded	270.0
248-250	0.38	80	0.42	10.74	40	0.49	12.52	70	3.9	7.8
254-256	0.75	80	0.74	18.85	40	0.82	20.93	69	6.7	14.0
263-265	1.00	80	0.96	24.31	40	1.05	26.64	69	8.9	19.8
272-274	1.50	80	1.50	38.10	40	1.61	40.89	70	36.1	40.2
281-283	2.00	80	1.94	49.25	40	2.07	52.50	70	74.4	76.5
290-292	3.00	40	3.07	77.93	40	3.07	77.93	70	241.7	251.0

Table 11 -Test results of flowrate required to flood vertical pipe directed downward sealed on end at ambient temperature and 70°C



Graph 17- Flooding flowrates of vertical pipe directed downward – submersed on end versus pipe diameter at ambient temperature and 70°C

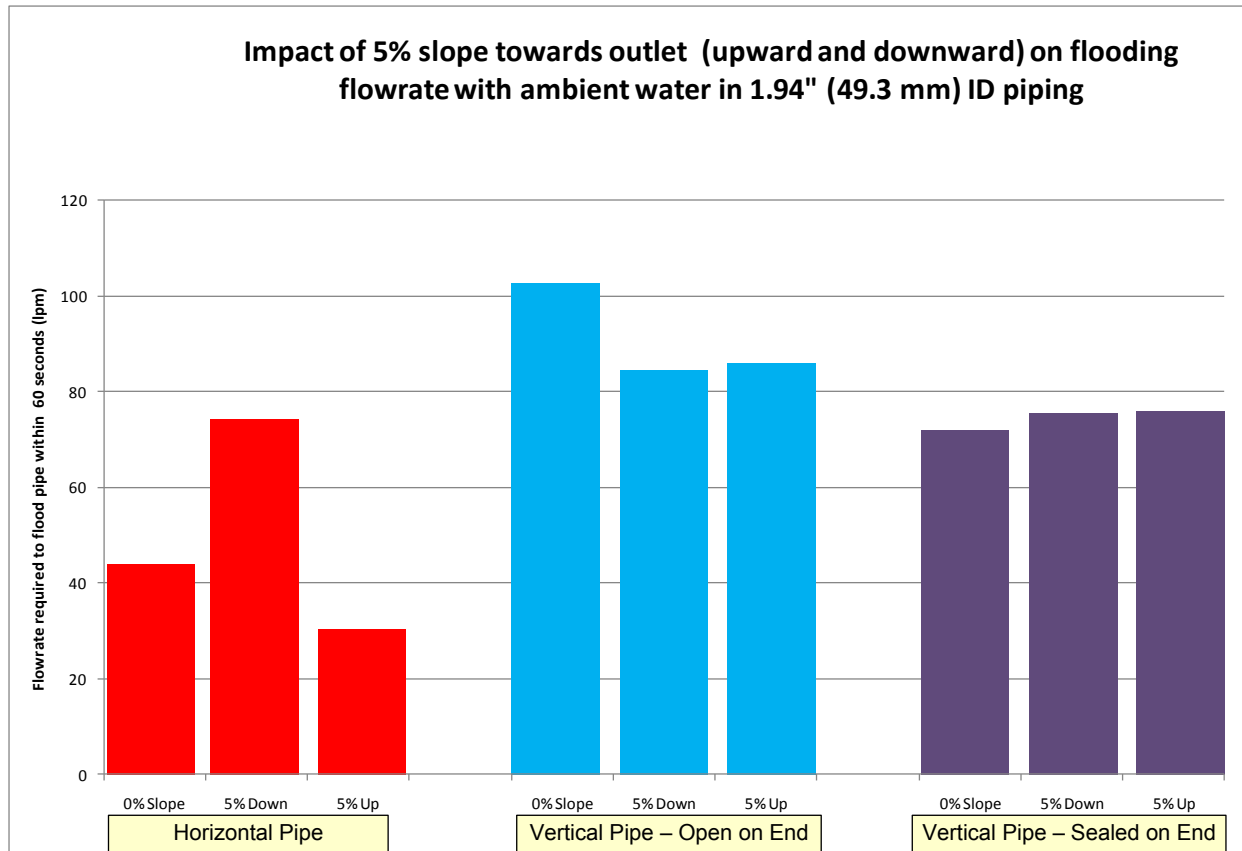
3.12. RESULTS AND DISCUSSION OF IMPACT OF PIPE SLOPE ON FLOODING FLOWRATES.

3.12.1. Pipe slope

In addition to testing the flooding flowrates of the three outlet conditions described previously (horizontal pipe open on end, vertical pipe sealed on end, and vertical pipe open on end) with the 6 foot horizontal spool piece being installed completely horizontal (0% slope), testing was also performed with both a 5% upward, and 5% downward slope on the 6 foot spool piece of transparent piping mounted in the horizontal plane. The test results are listed in Table 12 and plotted in Graph 18.

Unique # for test result	Nominal pipe size (in)	Pipe Schedule	Pipe ID (inch)	Pipe ID (mm)	Temperature (°C)	Slope of horizontal pipe (% towards outlet)	Flowrate required to flood pipe in various orientations (lpm)		
							Horizontal pipe open on end	Vertical pipe sealed on end	Vertical pipe open on end
26	2.0	80	1.94	49.25	26	0%	43.9		
35-37	2.0	80	1.94	49.25	25	0%		72.0	
32-34	2.0	80	1.94	49.25	25	0%			102.7
4	2.0	80	1.94	49.25	24	5% downward	74.2		
6	2.0	80	1.94	49.25	24	5% downward		75.5	
5	2.0	80	1.94	49.25	24	5% downward			84.5
7	2.0	80	1.94	49.25	22	5% upward	30.4		
9	2.0	80	1.94	49.25	22	5% upward		75.9	
8	2.0	80	1.94	49.25	22	5% upward			86.0

Table 12 - Test results of flooding flowrates of nominal 2" horizontal piping at varying angles



Graph 18 - Test results of flooding flowrates of nominal 2" horizontal piping at varying angles

This testing was performed using the test arrangements previously described (for schematics see Figure 3, Figure 7, and Figure 8). Where slope was applied, the slope was applied to the horizontal pipe using a calibrated level (which in turn applied the slope to the vertical pipe). The same definition of flooding previously described was used for the various outlet conditions.

Impact of slope on flooding flowrate of horizontal pipe open on end

As indicated from Graph 18, slope had a significant impact on the flowrate required to flood the horizontal pipe open on end.

As one would expect, sloping the horizontal pipe upwards reduced the flowrate required to flood the pipe. With the 5% upward slope towards the outlet, the majority of the horizontal pipe is naturally flooded at a very small flowrate (eg. 1 lpm) due to the orientation. A flowrate of 30.4 lpm was required to flood the pipe to a point 6 inches from the outlet.

This testing also indicated that sloping the horizontal pipe downward towards the outlet caused the flooding flowrate to increase. A flowrate of 74.2 lpm was required to flood the pipe with a 5% downward slope as compared to 43.9 lpm with a flat pipe (0% slope).

Impact of slope on flooding flowrate of vertical pipe sealed on end

As indicated from Graph 18, the flowrate required to flood a vertical pipe sealed on the end increased a small amount when the piping was sloped (both sloped 5% downward and 5% upward) compared to that of the flat pipe with 0% slope.

Impact of slope on flooding flowrate of vertical pipe open on end

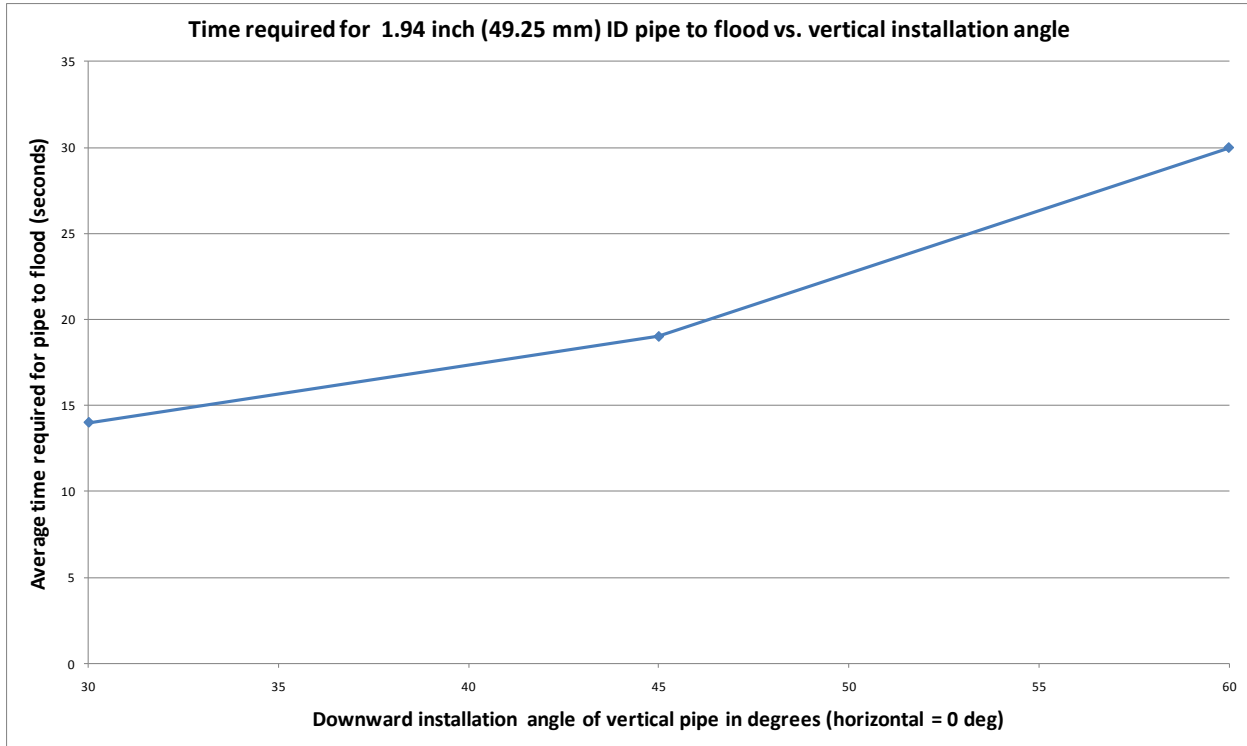
The flowrate required to flood a vertical pipe open on the end decreased approximately 15% when the horizontal pipe rigidly connected to the vertical pipe at a 90° angle was sloped (both sloped 5% downward and 5% upward) when compared to the flooding flowrate of the same piping arrangement with the horizontal pipe installed flat (0% slope). These results indicate that a vertical pipe oriented straight up and down (90° from horizontal) may be more difficult to flood than a vertical pipe installed on an angle.

To further test this, additional testing was performed on nominal 2" piping. The pipe configuration for this testing involved a 6 foot horizontal pipe with a 90° elbow directed downward connected to a 12 inch open ended spool piece. However for this testing, the 6 foot horizontal pipe was installed completely flat (0% slope) and the 90° elbow was rotated to provide different downward angles on the 12 inch open ended spool piece. The downward angles evaluated were 30°, 45°, and 60° (with the horizontal plane being a reference of 0°).

Instead of determining the flooding flowrate at each vertical angle, testing was performed at a fixed initial flowrate of 64.1 lpm and the time required to flood the pipe in the various orientations was recorded. Testing was performed a minimum of three times at each flowrate and the average time required to flood the pipe was recorded. The test results are indicated in Table 13, and the average times required to flood the piping at the various angles are plotted on Graph 19.

Unique # for test result	Nominal pipe size (in)	Pipe Schedule	Pipe ID (inch)	Pipe ID (mm)	Temperature (°C)	Flowrate (lpm)	Downward slope of vertical pipe (deg)	Average time required to flood (sec)	Comment
216-218	2.0	80	1.94	49.25	20	64.1-68.8	30	14	Vertical pipe flooded at time listed. Flowrate jumped from first value to second value listed when pipe flooded.
212-215	2.0	80	1.94	49.25	20	64.1-71.2	45	19	Vertical pipe flooded at time listed. Flowrate jumped from first value to second value listed when pipe flooded.
219-221	2.0	80	1.94	49.25	20	64.1-73.2	60	30	Vertical pipe flooded at time listed. Flowrate jumped from first value to second value listed when pipe flooded.
222-224	2.0	80	1.94	49.25	20	64	90	N/A	Piping did not flood within 120 seconds at this flowrate.

Table 13 - Test results of flooding flowrates of nominal 2" vertical piping open on end at varying angles



Graph 19 - Test results of flooding flowrates of nominal 2" vertical piping open on end at varying angles

As indicated by Graph 19, as the 90° elbow was rotated to become more vertical (more straight up and down), the average time required to flood the pipe increased. This indicates that it is more difficult to flood the open end pipe as it becomes more vertical. At the fixed 64.1 lpm flowrate, the vertical pipe installed straight up and down did not flood in any of the three tests performed (each test was allowed to run for a minimum of 120 seconds).

Based on both results of this testing and the previous testing with the 5% upward and downward slope, the most difficult to flood open ended vertical pipe configuration is when the vertical pipe is orientated straight up and down.

As indicated in Graph 18, the highest flowrate required to flood the nominal 2" pipe occurred with a vertical pipe with an open end that was oriented straight up and down.

3.13. RESULTS AND DISCUSSION OF IMPACT OF PUMP TYPE ON FLOODING FLOWRATES.

In addition to testing with a centrifugal pump, testing was also performed using an air operated diaphragm pump to better understand the impact that the pulsating flow supplied by the diaphragm pump has on the height of liquid in the pipe tested as compared to the consistent flow supplied by the centrifugal pump. This testing was completed on a 6 foot length of nominal 2" piping installed horizontally.

The impact that using an air operated diaphragm pump has on the manner that the flow is delivered is dependent on the size of the pump, the air pressure supplied to the pump, and the backpressure the pump is working against.

The size of the pump determines the volume of liquid delivered per pump stroke.

The difference between the air pressure supplied to the pump and the backpressure the pump is working against impacts the stroke frequency of the pump (as the differential pressure increases, the stroke frequency increases).

During testing, two different extremes in air pressure were evaluated. In one case, the air pressure supplied to the pump was regulated to 10 psig. With this low supply pressure, the pump frequency was low enough to where the flowrate during a stroke cycle could be monitored from the flowmeter. Under this condition, the measured flowrate supplied to a nominal 2" pipe varied from 4 to 41 lpm based on where the pump was in its stroke cycle. Under this condition, the liquid height at the point 66 inches from the pipe outlet varied as much as 20 millimeters depending on where the pump was in the discharge cycle.

In the second case, the air supply was set to 90 psig (this created a high pressure difference between the air supply pressure and the pressure of the liquid being pumped). In this case the pump stroke frequency was much higher and it was not possible to monitor the quickly changing flowrate via the flowmeter. Although difficult to quantify, it was clear that the pulsed flow provided additional turbulence which assisted in air removal.

Due to variations in both pump size and pump stroke frequency and the fact that the flowrate is varying throughout the pump stroke, it is very difficult to determine the exact impact that using an air operated diaphragm pump has on the flooding flowrate. However, for the same average flowrate (totalized flow divided by volume), it is clear that a diaphragm pump is able to flood a line as well as, if not better than, a centrifugal pump. During the displacement stroke of the diaphragm pump, the flowrate is significantly higher than the average flowrate, and the amount of air displaced from the piping during this pulse of higher flowrate is greater than the amount removed at the average flowrate. The turbulence created as a result of the pulsating flow produced by the diaphragm pump also helps to keep the trapped air moving which facilitates its removal.

3.14. RESULTS AND DISCUSSION OF IMPACT OF BACKPRESSURE ON FLOODING FLOWRATES.

The impact that increasing the backpressure has on the flooding flowrate was evaluated. Testing was performed with approximately 30 psig backpressure in addition to the routine testing that was performed with essentially 0 psig backpressure.

Testing previously performed on a horizontal 6 foot length of 2" schedule 80 clear piping (1.94" ID) that was open on end indicated a flooding flowrate of 43.9 lpm. The backpressure when performing this test was essentially zero.

This test was replicated with a backpressure of approximately 30 psig. To perform this test, a flexhose with a diaphragm valve on the end of it was connected to the end of the horizontal 6 foot length of nominal 2" piping. The flexhose and manual valve were installed so that the horizontal 6 foot length of piping was the high point of the system.

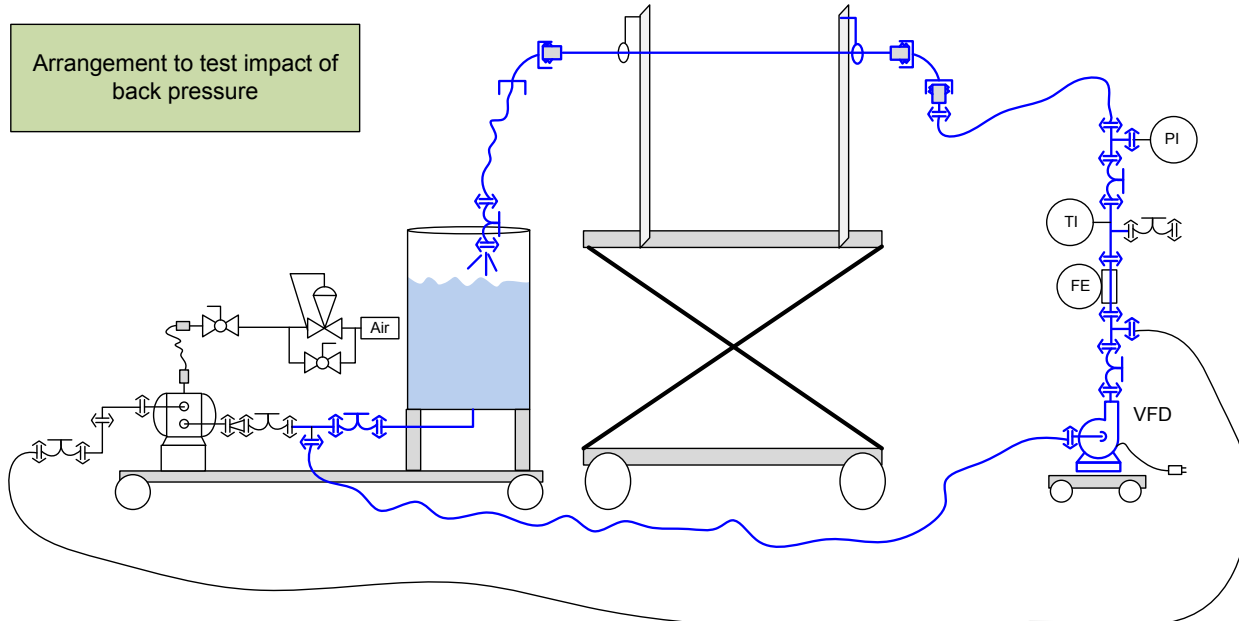


Figure 10 – Schematic of arrangement to test the impact of backpressure on the flooding flowrate

Trial and error was used to determine the pump speed and the manual diaphragm valve position that would result in a flowrate of approximately 40 lpm with a supply pressure (which is essentially equivalent to the back pressure on the horizontal pipe at this low flowrate) of 30 psig.

The pump was turned off, the system drained, and then the pump started with the manual valve set at the required position. With an inlet pressure of 30 psig and a flowrate of 40 lpm, the 6 foot horizontal pipe flooded within 15 seconds. Without backpressure (open on end), as described previously, the same horizontal pipe configuration flooded at a flowrate of 43.9 lpm in 19 seconds. The flooding flowrate with and without the backpressure were similar.

Observations from both the test just described and additional piping configurations that included the installation of tees pointed vertically upward in the horizontal piping indicated that the addition of backpressure simply compresses the initial mass of air present into a smaller volume as would be expected from the ideal gas law. Although the starting volume of air present is reduced with the additional backpressure, it appears that it still requires approximately the same flowrate to displace the smaller volume of compressed air from the piping system

4. CONCLUSIONS

A listing of variables evaluated along with the impact on the flooding flowrate follows in Table 14.

Variable evaluated	Additional details/ variations in what was tested	Results of testing
Inside diameter of piping	Tested piping from nominal 3/8" piping to nominal 4" piping.	As expected, the diameter of the pipe played a significant role in the flowrate required for flooding. Larger pipes required larger flowrates for flooding.
Piping orientation and outlet type	<ol style="list-style-type: none"> 1) Horizontal pipe - open on end 2) Vertical pipe directed downward - sealed on end 3) Vertical pipe directed downward - open on end 	The outlet orientation and type play a significant role in the flowrate required for flooding. Highest flowrate required to flood vertical piping directed downward that is open on end, smaller flowrate required to flood vertical piping directed downward that is sealed on end, and smallest flowrate required to flood horizontal piping that is open on end.
Slope of piping	<ol style="list-style-type: none"> 1) 0% slope (horizontal) 2) 5% upward slope 3) 5% downward slope 4) 30° downward slope 5) 45° downward slope 6) 60° downward slope 7) 90° downward slope (vertical) 	As pipes are orientated more vertical (straight up and down), the flowrate required for flooding increased. The highest flowrate required for flooding occurred when the pipe is oriented straight up and down.
Temperature of water	<ol style="list-style-type: none"> 1) Ambient temperature 2) 60 °C 3) 70 °C 	Between ambient temperature and 70 °C, the temperature of the water does not have a significant impact on the flowrate required to flood a pipe.
Backpressure of piping	<ol style="list-style-type: none"> 1) Essentially zero backpressure 2) 30 psig backpressure 	While not tested in great detail, it appears that adding backpressure compresses the air present in the piping system, but it does not reduce the flowrate required to flood the pipe.
Pump type supplying water	<ol style="list-style-type: none"> 1) Centrifugal pump 2) Positive displacement diaphragm pump 	Difficult to determine the exact impact of the pump type supplying flow on the flowrate required to flood a pipe due to many variations in operation of positive displacement pumps, however for the same average flowrate (flowrate/time) - the pulsating flow generated by a diaphragm pump will flood a pipe as easily or more easily than a non-pulsating centrifugal pump.

Table 14 – Summary of variables evaluated

As a result of this testing, there is a better understanding of the impact that the many variables that were evaluated have on the flowrate required to flood piping. Equations 1-3, derived from the test results, can be used to determine the flowrates required to flood piping in a variety of sizes and installations.

The test results indicate that the most difficult piping installation/outlet configuration to flood (i.e. that requiring the highest flowrate based on the inside diameter of the pipe) is a pipe installed vertically with the flow going downward that is open on the end. If the flowrate supplied is sufficient to flood the piping under these conditions, the same diameter piping installed with any other orientation/outlet condition will be flooded. For this reason, Equation 2, which was generated from the test results obtained under the most difficult conditions for flooding, can be used to conservatively determine the flowrate required to flood piping regardless of installation or outlet type. Equation 2 is applicable to piping with inside diameters ranging from 0.74-3.07" when pumping water with temperatures ranging from 20°C to 70°C.

Note: the information and the associated equations documented in this technical report are all based on empirical test data. In the future it would be beneficial to improve the understanding of flooding from a first principles perspective, possibly by performing a momentum balance and evaluating physical properties of the liquid stream (eg. viscosity, surface tension etc.).

5. REFERENCES

[1] CRC Handbook of Chemistry and Physics, 66th Edition, CRC Press Inc., pg F-37.

M. A. Habib · H. M. Badr · S. A. M. Said
E. M. A. Mokheimer · I. Hussaini · M. Al-Sanaa

Characteristics of flow field and water concentration in a horizontal deadleg

Received: 2 July 2003 / Published online: 16 September 2004
© Springer-Verlag 2004

Abstract Deadlegs are defined as the inactive portion of the pipe where the flow is stagnant. Corrosion in deadlegs occurs as a result of water separation due to the very low flow velocity. The present work provides an investigation of the effect of deadleg geometry and average flow velocity on flow field and oil/water separation in deadlegs. The investigation is based on the solution of the mass and momentum conservation equations of an oil/water mixture together with the volume fraction equation for the secondary phase. A fluid flow model based on the time-averaged governing equations of 3-D turbulent flow has been developed. An algebraic slip mixture model is utilized for the calculation of the two immiscible fluids (water and crude oil). The model solves the continuity and momentum equations for the mixture, and the volume fraction equation for the secondary phase utilizing an algebraic expression for the relative velocity. Flow visualization experiments were conducted in order to validate the numerical procedure. Good agreement was obtained between the calculated and measured flow patterns. Results are obtained for different lengths of the deadleg. The considered fluid mixture contains 90% oil and 10% water (by volume). The inlet flow velocity ranges from 0.2 to 10 m/s and the deadleg length to diameter ratio (L/D) ranges from 1 to 10. The results showed that the size of the stagnant fluid region increases with the increase of L/D and decreases with the increase of inlet velocity. The results also indicated that the water volumetric concentration increases with the increase of L/D and influenced by the deadleg geometry.

List of Symbols

C	inlet concentration
D_B	diameter of the branch
D, D_H	diameter of the header (main tube)
L	length of the deadleg
l	length scale
U	inlet axial (horizontal) velocity component
V	inlet (vertical) velocity component
W	velocity component perpendicular to the plane of the deadleg
C_μ	constant defined in Eq. 4
C_1	constant defined in Eq. 11
C_2	constant defined in Eq. 11
G_k	generation of turbulent kinetic energy
g	gravitational acceleration
k	turbulent kinetic energy
p	pressure
\bar{U}_j	average velocity component
u_j	fluctuating velocity component
x_j	space coordinate

Greek letters

α	volume fraction
ϵ	dissipation rate of turbulent kinetic energy
μ	dynamic viscosity
ρ	density
σ_k	effective Prandtl number for k
σ_ϵ	effective Prandtl number for ϵ

Superscripts

–	time average
---	--------------

Subscripts

D	drift
eff	effective
f	fluid
m	mixture

M. A. Habib (✉) · H. M. Badr · S. A. M. Said
E. M. A. Mokheimer · I. Hussaini
Mechanical Engineering Department,
King Fahd University of Petroleum and Minerals,
Dhahran, 31261, Saudi Arabia
E-mail: mahabib@kfupm.edu.sa

M. Al-Sanaa
Saudi Aramco, Saudi Arabia

1 Introduction

In oil piping systems, the inactive portion of the pipe, where the fluid is stagnant or having a very low velocity, is called deadleg. This inactive pipe is normally connected to an active pipe that carries the main stream. Deadlegs represent regions prone to corrosion due to stagnant or low velocity flow that causes emulsified water precipitation out of the crude oil. In addition, solid deposits and replenishment of corrosive species support microbial and under-deposit corrosion. In order to maintain the integrity of the connecting main pipe, internal corrosion of deadlegs must be prevented, since it is very difficult to control and usually requires a major shut down in order solve this major problem. In the oil and gas industry, deadleg corrosion presents the highest percentage of internal damage to pipelines or in-plant piping systems that are normally considered to be in a non-corrosive service. Deadlegs should be avoided whenever possible in design of piping for fluids containing or likely to contain corrosive substances. When deadlegs are unavoidable, the length of the inactive pipe must be as short as possible to avoid stagnant or low velocity flows.

The literature review shows that there is no criterion/standard to be adopted for the design of deadlegs in order to avoid or minimize corrosion. In addition, there is no research published on the effect of deadleg geometry and flow velocity on the concentration of water or other corrosive agents in deadlegs. Most of the relevant published work was focused on the effect of oil to water ratio on the flow pattern and pressure drop in straight pipes. Amongst that published research is the work by Charles et al. [8] who conducted an experimental investigation on the effect of oil-water ratio on the pressure gradient in a horizontal pipe. They found that at high oil-water ratio, oil formed the continuous phase and a water-drops-in-oil regime was observed. As the oil-water ratio was decreased, the flow patterns changed to concentric oil in water, oil-slugs-in-water, oil-bubbles-in-water and finally oil-drops-in-water. The measured pressure gradient was found to decrease by adding water to the oil that was originally in laminar flow ($Re < 1,500$) until reaching a minimum after which the addition of more water increases the pressure gradient. The reduction in the pressure gradient was found to depend on the oil viscosity as well as the oil-water ratio. In another paper, Charles and Lilleleht [9] presented the pressure gradient data obtained from three different sets of experiments for stratified flow of two immiscible liquids in the laminar-turbulent flow regime using the parameters introduced by Lockhart and Martinelli [15]. The Lockhart and Martinelli [15] parameters were used for correlating the pressure gradient data for gas-liquid mixture flows. It was found that these parameters represent the data with a maximum deviation of approximately 24%. However, the resulting curves were significantly displaced from the Lockhart-Martinelli

curves for gas-liquid systems. Barnea [3] presented unified models that incorporated the effect of the angle of inclination on the transition from annular flow to intermittent flow and from dispersed bubble flow. The models showed a smooth change in mechanisms, as the pipe inclination varies, over the whole range of upward and downward inclinations.

The stability of stratified liquid-liquid two-phase system was investigated by Brauner and Maron [5]. They found that sub zones of stratified-dispersed patterns may appear in regions where stable stratification was expected. The reduction of density differential, as the case in liquid-liquid systems, tended to extend the regions of dispersed flow patterns on the account of the range of the continuous stratified patterns. The formation of a stratified-dispersed/stratified pattern was attributed to the moderate buoyancy forces in the case of reduced density differential. A criterion was proposed for predicting whether the lighter phase may form a continuous upper layer or remain above the dense layer as a swarm of drops. It was shown that the departure from the stratified configuration to other patterns was associated with the existence of a buffer zone between the lower bound obtained from stability analysis and the upper bound obtained from conditions for reality of characteristics. Due to the limited available experimental data, the model was not fully validated. Schmidt and Loth [22] provided a practical and sufficiently accurate method for calculating the pressure drop in a tee junction with combining conduits using a semi-empirical approach. In their work, three basic models, termed the "loss coefficient model", "contraction coefficient model" and "momentum coefficient model" were derived. The experiments covered a flow ratio in the range of 0.15–0.75 and a reduced pressure range of 0.2–0.75 for the fluid R12. A formula based on the comparison between the measured and predicted pressure changes was recommended.

A computational study on the effect of fluid compressibility on the total pressure losses in three-leg branched ducts was conducted by Haidar [12]. A fully-elliptic, control volume model was presented for the simulation of subsonic steady flow under combining conditions in 30–150° sharp-cornered tee-junctions, in 30° increments. The $k-\epsilon$ turbulence model was adopted for the main flow while wall functions were employed in the near wall region. The Mach number of the average flow ranged between 0.2 and 0.6 in 0.1 increments. The study indicated that the popular practice of interfacial wall functions with two-dimensional, two-equation eddy viscosity model was not that accurate for compressible flows when $M > 0.5$. Rubel et al. [20] presented experimental data for the phase distribution of high-pressure steam-water mixtures in horizontal equal-sided dividing tee junctions of two different sizes. These data correspond to wide ranges of inlet vapor qualities, inlet superficial vapor velocities and extraction rates. For the reported test conditions, it was shown that an increase in phase separation resulted from a decrease in vapor

quality, a decrease in pressure or an increase in mass flux.

Plaxton [18] conducted an experimental investigation into the effect of influx in a two-phase, liquid-liquid flow systems on the pressure drop behavior. He found that the Brill and Beggs [6] correlation method could provide adequate pressure gradient predictions for oil-water flow. On the other hand, the acceleration confluence model reported by Asheim et al. [2] was found to be inadequate in predicting the pressure drops. Bates et al. [4] presented an experimental and numerical investigation for the flow in a 90° tee junction using LDA for flow velocity measurements and FLUENT software for modeling the 3-D velocity field. The static pressure distribution around the branch outlet, coupled with the swirling nature of the flow, was observed using laser sheet visualization and provided clear evidence of the necessity to computationally model these flows using fully 3-D grids coupled with realistic pressure boundary conditions at each outlet. Angeli and Hewitt [1] reported their experimental results on the effect of the water volume fraction in an oil-water system on the pressure gradient in pipe flow. The water volume fraction ranged from 5 to 85% and the phase inversion point (the volume fraction of the dispersed phase above which this phase becomes continuous) appeared between 37 and 40% in both pipes. The pressure gradient measurements showed that the liquid-liquid dispersions exhibited a flow behavior that diverged from a single-phase flow, which was represented by a homogeneous model using linearly averaged properties of the mixture. The homogeneous model not only failed to predict the sudden increase in the pressure gradient at the point of phase inversion, but also failed to estimate the measured pressure gradients. The measured values of the pressure gradient in both pipes were much lower than those predicted from the homogeneous model. The experimental friction factors, especially in the oil continuous phase, appeared to be lower than the predictions of the homogeneous model and sometimes even lower than the single phase of either oil flow or water flow friction factors. Similar studies for pressure losses in other pipe fittings were carried out by Hwang and Pal [13] for both sudden pipe expansion and sudden contraction and by Schabacker et al. [21] for a sharp 180° bend.

An experimental study of oil-water flow patterns in horizontal pipes was conducted by Trallero et al. [24] with emphasis on transition from one pattern to another. These flow patterns were classified into two main categories, namely, segregated flow and dispersed flow. The segregated flow included two patterns, namely, stratified flow pattern and stratified with some mixing at the interface while the dispersed flow included four patterns, two patterns were water dominated and the other two were oil dominated. A model was also proposed for predicting flow pattern transition in the case of using light oils. The model was based on a combination of the two-fluid model and the balance between gravity forces and the turbulent fluctuations normal to the main

flow. Other models were used for the stratified and dispersed flow patterns.

A new mathematical model for oil/water separation in pipes and tanks has been proposed by Hafskjold et al. [11]. The model describes the process of water separation in oil systems based on the two mechanisms of coalescence and settling. The model was validated against experimental data and the comparison was satisfactory. The separation of oil and water can be considered as a combination of emulsification and separation. The former dominates in chokes, valves and other regions with high shear rates. The latter can be further split into two: drop growth by coalescence, which dominates in pipes and other regions of moderate energy dissipation, and settling or creaming of the dispersed phase, which dominates in tanks and other regions of low energy dissipation. Celius and Aamo [7] observed that the separation rate for water in oil systems increases with the increase in water cut, and that some water remains in the oil even after long settling times. These features may be qualitatively understood by a combination of coalescence and settling. Celius and Aamo [7] developed a mathematical-numerical model that described these mechanisms qualitatively. This model calculates the quality of the output oil as function of system dimensions, flow rates, fluid physical properties, fluid quality and drop size distribution at the inlet.

Based on the above literature search, it is clear that no research has been published on the effect of various fluid and flow parameters on water separation in deadleg regions that are widely used in oil piping systems. This study investigates the effect of deadleg geometry, inlet flow velocity and fluid properties on the velocity field and water separation in deadlegs.

2 Problem statement

The problem considered is that of flow of an oil/water mixture having 90% crude oil and 10% water (by volume) in a tee junction with the deadleg forming one branch, Fig. 1. The deadleg is horizontal. The calculations were carried out for various lengths of the deadleg where the length to diameter ratio ranged from $L/D = 1$ to 10 with the objective of obtaining the details of the

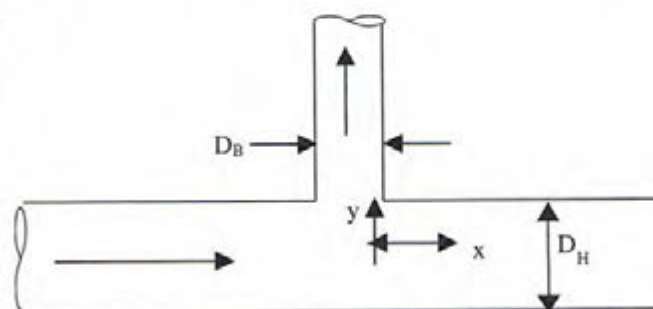


Fig. 1 The geometry of the deadleg configuration.

flow velocity field as well as the changes in the water volumetric concentration. This water concentration is important for corrosion prediction. The average inlet flow velocity is 1 m/s in most cases. However, the influence of the inlet flow velocity is considered.

2.1 Mathematical formulation

The mathematical formulation for the calculation of the fluid flow field has been established. The fluid is a mixture of water and crude oil. The fluid flow model has been based on the time-averaged governing equations of 3-D turbulent flow. The algebraic slip mixture model [16] has been utilized for the calculation of the two immiscible fluids (water and crude oil). The model solves the continuity equation for the mixture, the momentum equation for the mixture, and the volume fraction equation for the secondary phase, as well as an algebraic expression for the relative velocity.

2.2 The continuity and momentum equations

Mass conservation The steady state time-averaged equation for conservation of mass of the mixture can be written as

$$\frac{\partial}{\partial x_j} (\rho \bar{U}_{m,j}) = 0 \quad (1)$$

Momentum conservation The steady-state time-averaged equation for the conservation of momentum of the mixture in the i direction can be obtained by summing the individual momentum equations for both phases. It can be expressed as

$$\frac{\partial}{\partial x_j} (\rho \bar{U}_{m,i} \bar{U}_{m,j}) = -\frac{\partial p}{\partial x_i} + \frac{\partial}{\partial x_j} \left(\mu_m \frac{\partial \bar{U}_{m,i}}{\partial x_j} \right) - \frac{\partial}{\partial x_j} (\rho \overline{u_{m,i} u_{m,j}}) + \rho_m g + \sum_{k=1}^2 \alpha_k \rho_k u_{DK,i} u_{DK,j} \quad (2)$$

where p is the static pressure and the stress tensor $\rho \overline{u_{m,i} u_{m,j}}$ is given by

$$-\rho \overline{u_{m,i} u_{m,j}} = \left[\mu_{\text{eff}} \left(\frac{\partial \bar{U}_{m,i}}{\partial x_j} + \frac{\partial \bar{U}_{m,j}}{\partial x_i} \right) \right] - \frac{2}{3} \rho_m k_m \delta_{ij} \quad (3)$$

where δ_{ij} is the Kronecker delta which is equal to 1 for $i=j$ and equals 0 for $i \neq j$ and $\mu_{\text{eff}} = \mu_t + \mu$ is the effective viscosity. The turbulent viscosity, μ_t , is calculated using the high-Reynolds number form as

$$\mu_t = \rho_m C_\mu \frac{k_m^2}{\epsilon_m} \quad (4)$$

with $C_\mu = 0.0845$ [25], k_m and ϵ_m are the kinetic energy of turbulence of the mixture and its dissipation rate. These

are obtained by solving their conservation equations as given below.

ρ_m and μ_m in Eq. 2 are the density and viscosity of the mixture that can be obtained from:

$$\rho_m = \sum_{k=1}^n \alpha_k \rho_k \quad (5)$$

$$\mu_m = \sum_{k=1}^n \alpha_k \mu_k \quad (6)$$

\bar{U}_m is the mass-averaged velocity:

$$\bar{U}_m = \frac{\sum_{k=1}^n \alpha_k \rho_k \bar{U}_k}{\rho_m} \quad (7)$$

and \bar{U}_{Dk} are the drift velocities:

$$\bar{U}_{Dk} = \bar{U}_k - \bar{U}_m \quad (8)$$

2.3 The volume fraction equation for the secondary phase

From the continuity equation for the secondary phase, the volume fraction equation for the secondary phase can be written as:

$$\frac{\partial}{\partial x_j} (\alpha_p \rho_p \bar{U}_{m,j}) = -\frac{\partial}{\partial x_j} (\alpha_p \rho_p \bar{U}_{p,j}) \quad (9)$$

2.4 Conservation equations for the turbulence model

The conservation equations of the turbulence model [19, 23] are given as follows.

The kinetic energy of turbulence

$$\frac{\partial}{\partial x_j} (\rho \bar{U}_j k) = \frac{\partial}{\partial x_j} \left(\frac{\mu_{\text{eff}}}{\sigma_k} \frac{\partial k}{\partial x_j} \right) + G_k - \rho \epsilon \quad (10)$$

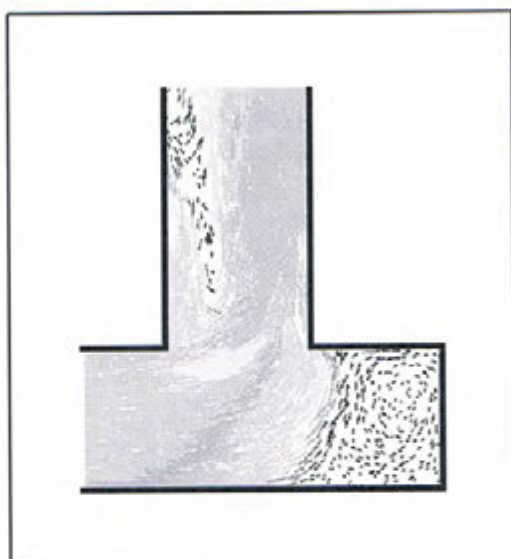
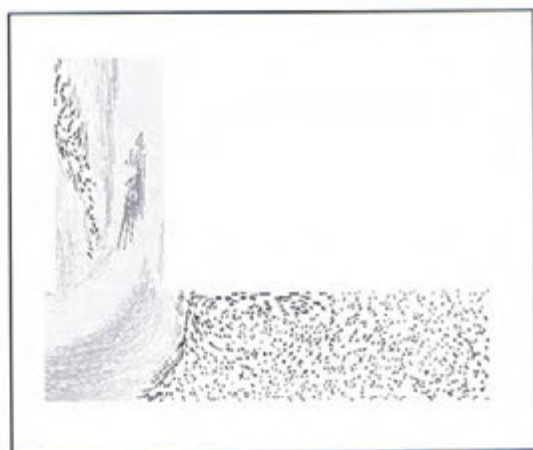
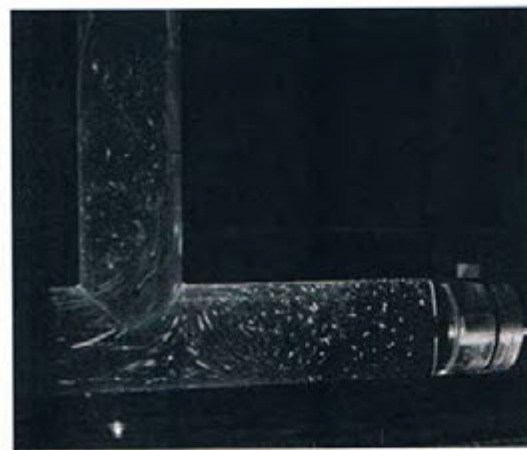
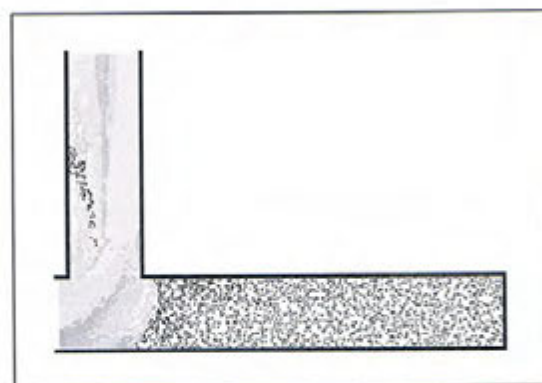
The rate of dissipation of the kinetic energy of turbulence

$$\frac{\partial}{\partial x_j} (\rho \bar{U}_j \epsilon) = \frac{\partial}{\partial x_j} \left(\frac{\mu_{\text{eff}}}{\sigma_\epsilon} \frac{\partial \epsilon}{\partial x_j} \right) + C_1 G_k \frac{\epsilon}{k} - C_2 \rho \frac{\epsilon^2}{k} \quad (11)$$

where G_k represents the generation of turbulent kinetic energy due to the mean velocity gradients and is given by

$$G_k = -\rho \overline{u_i u_j} \frac{\partial \bar{U}_j}{\partial x_i} \quad (12)$$

The quantities σ_k and σ_ϵ are the effective Prandtl numbers for k and ϵ , respectively and C_2 is given by Shih et al. [23] as a function of the term k/ϵ and, therefore, the model is responsive to the effects of rapid strain and

(a) Calculations; $L/D = 1$ (b) Flow visualizations; $L/D = 1$ (c) Calculations; $L/D = 3$ (d) Flow visualizations; $L/D = 3$ (e) Calculations; $L/D = 5$ (f) Flow visualizations; $L/D = 5$

streamline curvature and is suitable for the present calculations. The model constants C_1 and C_2 have the values; $C_1 = 1.42$ and $C_2 = 1.68$.

The wall functions establish the link between the field variables at the near-wall cells and the corresponding

Fig. 2 Flow visualization and calculation velocity vector results. **a** Calculations; $L/D = 1$, **b** Flow visualizations; $L/D = 1$, **c** Calculations; $L/D = 3$, **d** Flow visualizations; $L/D = 3$, **e** Calculations; $L/D = 5$, **f** Flow visualizations; $L/D = 5$

quantities at the wall. These are based on the assumptions introduced by Launder and Spalding [14] and have been most widely used for industrial flow modeling. The details of the wall functions are provided by the law-of-the-wall for the mean velocity as given by Habib et al. [10].

2.5 Boundary conditions

The velocity distribution has been considered to be uniform at the inlet section. This assumption is justified by the considerable length (15 times the diameter) upstream of the deadleg. Also this condition was fixed for all the cases studied in the present paper. The kinetic energy of turbulence at inlet is assigned through a specified value of \sqrt{k}/U^2 equal to 0.1, thus representing an average value for a fully developed flow. The dissipation rate of the turbulent kinetic energy is specified through a length scale (l) equal to the diameter of the inlet section. The boundary condition applied at the exit section is that of fully developed flow. At the wall boundaries, all velocity components are set to zero in accordance with the no-slip conditions. Kinetic energy of turbulence and its dissipation rate are determined from the equations of the turbulence model. The secondary-phase volume fraction is specified at flow boundaries of inlet and exit sections.

2.6 Solution procedure

The conservation equations are integrated over a typical volume that is formed by division of the flow field into a number of control volumes, to yield the solution. The equations are solved simultaneously using the solution procedure described by Patankar [17]. Calculations were performed with at least 300,000 volumes. Convergence was considered when the maximum of the summation of the residuals of all the elements for U , V and W and the pressure correction equations was less than 0.1%.

3 Validation

In order to validate the calculation procedure, flow visualization experiments were carried out using a laser sheet. An experimental setup which is composed of two main parts, namely, the flow loop and the test section, was designed and constructed to carry out the flow visualization experiments. The flow loop, which is a closed-type loop, consists of a pump, a piping system and two reservoirs. The lower reservoir is made of fiberglass and has a total volume of 1 m^3 . The upper reservoir is made out of Plexiglas and is used as a settling chamber that is utilized to minimize the lateral flow fluctuations and unsteady flow oscillations in order to provide a steady uniform flow at the inlet of the header tube. Water is pumped from the lower reservoir to the settling chamber and back to the lower reservoir through

the test section. The pump delivery valve together with the ball valve (installed downstream of the test section) are used to control the volume flow rate in the test section. The test section that simulates the flow process in the deadleg region is designed to provide flexibility for the variation of the deadleg length. The test section consisted of an inlet section, an outlet section and the deadleg region. The deadleg region contains a piston that can be moved in or out to provide a mechanism for varying the deadleg length. All the components of the test section are made out of plexiglas.

The flow visualization experiments were performed utilizing a two-dimensional laser light sheet to illuminate the middle section (plane of symmetry) of the deadleg region. The flow visualization was accomplished by utilizing a 200 mW argon laser source. The laser beam

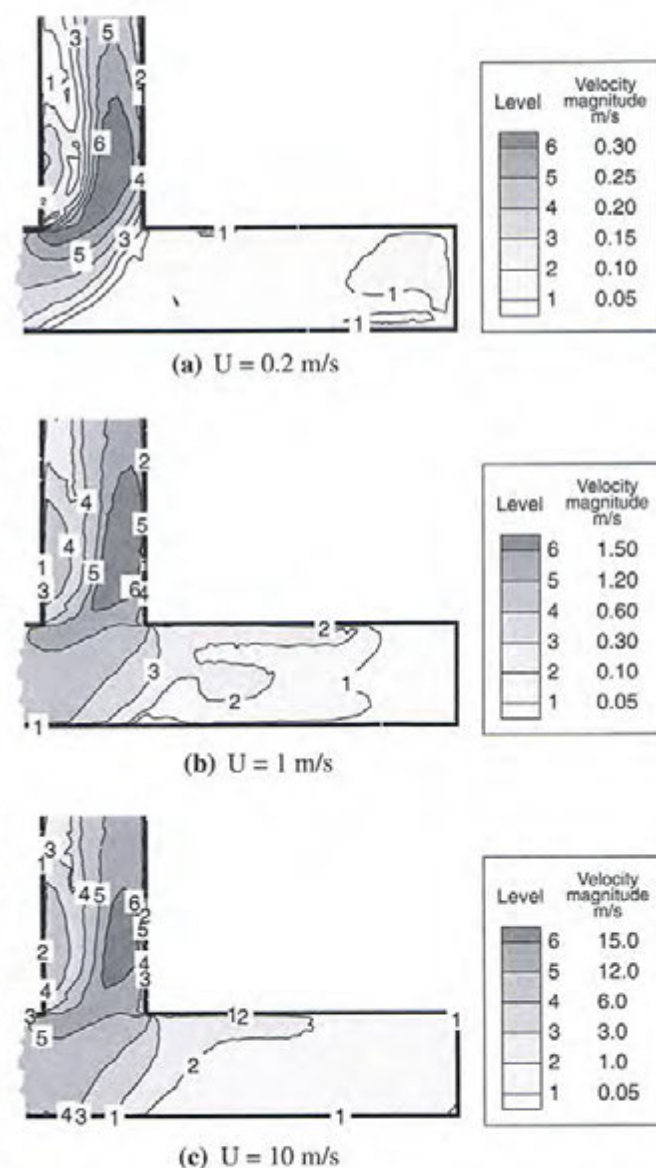


Fig. 3 Contours of velocity magnitude in the horizontal deadleg for the case of $L/D = 3$

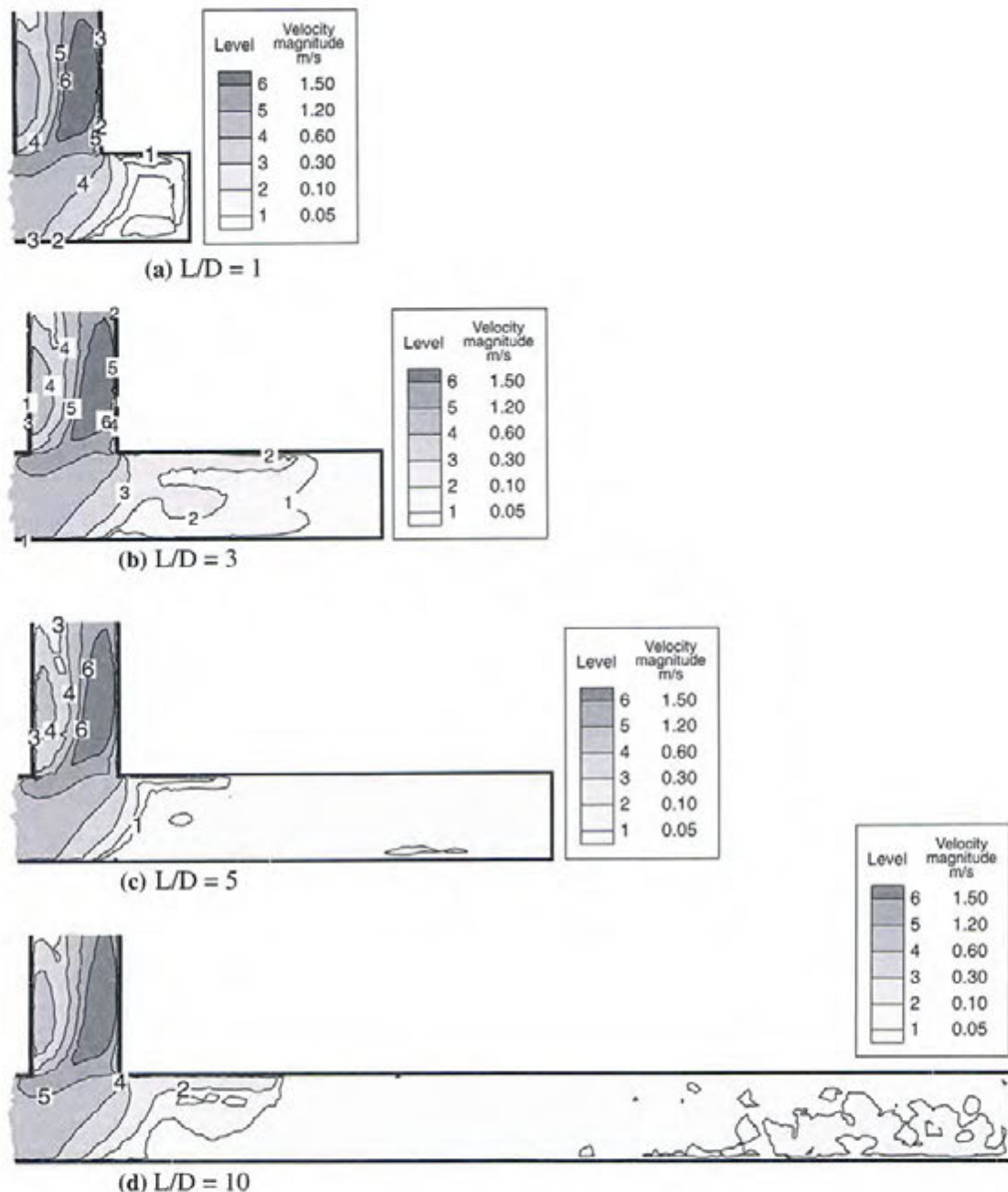


Fig. 4 Contours of velocity magnitude in the horizontal deadleg for the case of $U = 1$ m/s

was forced to pass through a vertical cylindrical glass rod of 8 mm diameter to produce a two-dimensional laser-light sheet. The horizontal laser sheet was diverted to the vertical plane using a 45° mirror. The laser sheet was aligned to pass through the plane of symmetry of the tube and deadleg region. The seeding particles used in the flow visualization experiments were small wooden particles that are almost of neutral buoyancy. The particle trajectory traces were photographed using a high-speed digital camera.

The details of the flow velocity field were visualized and photographed for the vertical deadleg geometry

with different deadleg lengths (L/D equal to 1, 3 and 5) and are shown in Fig. 2. The deadleg has equal header and branch diameters of $D = 0.0889$ m. The details of the flow calculated flow field for the case of $L/D = 1$ is shown in Fig. 2a. The visualized velocity vectors for the same case are shown in Fig. 2b. A very similar trend of flow pattern is observed between the flow visualization and calculated results. Figure 2c shows the calculated velocity field for the case of $L/D = 3$. It is clear from the figure that the circulating flow zone extends over most of the entire length of the deadleg, however, with low velocity in the upstream portion. This is in good agreement with the visualized velocity vectors for the same case as shown in Fig. 2d. The

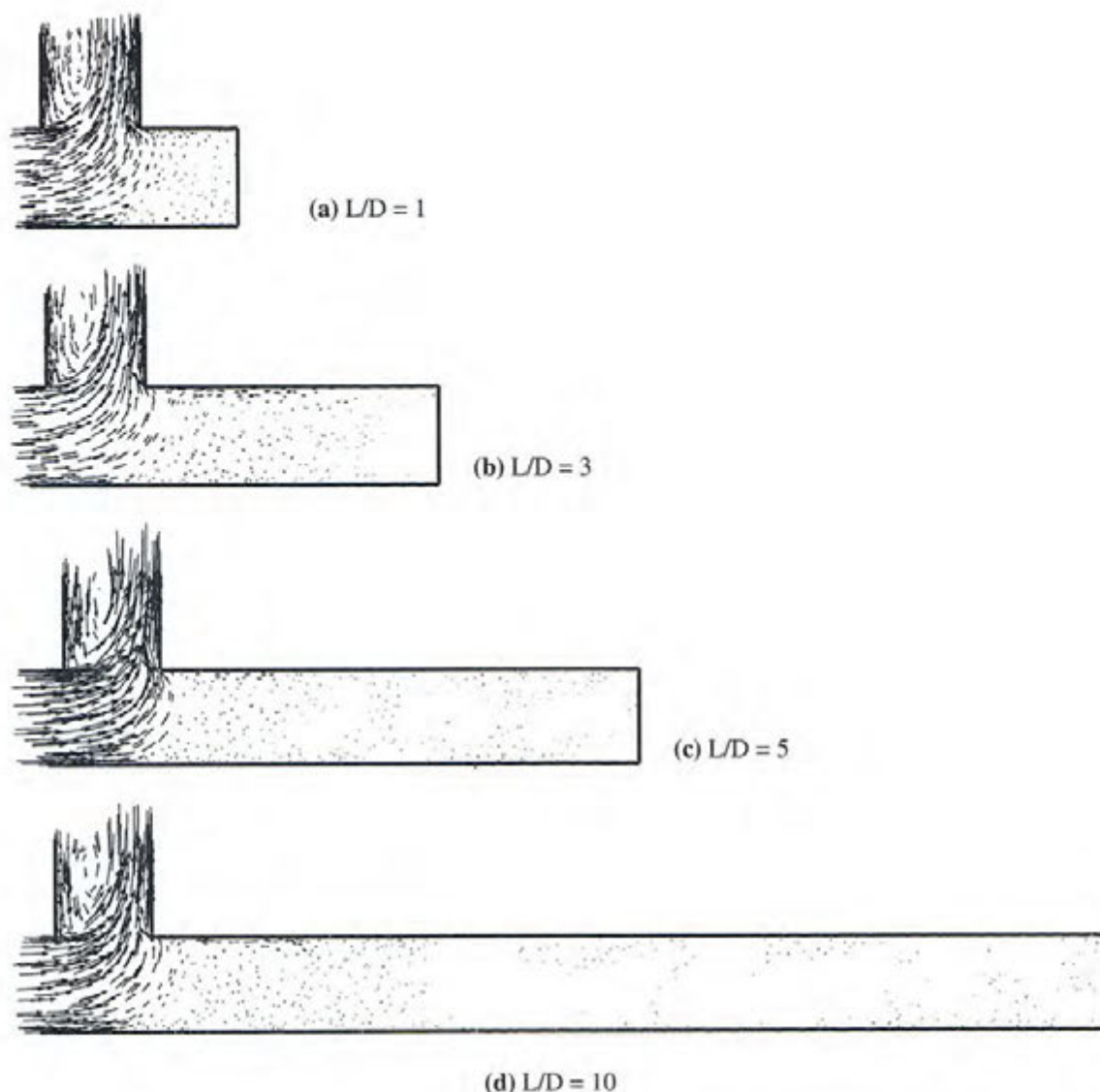


Fig. 5 Velocity vectors of velocity magnitude in the horizontal deadleg for the case of $U=1$ m/s

velocity flow field for $L/D=5$ is shown in Fig. 2e, f for the computed and visualized velocity vectors and very similar flow patterns are observed in both figures. The good comparison between the computed and visualized flow patterns provides verification of the accuracy of the computational model.

4 Results and discussion

The details of the flow velocity field were obtained for different deadleg geometries and different inlet flow velocities. The fluid at the inlet section in all of the considered cases was a homogeneous mixture containing 90% crude oil, by volume, and 10% water. Figure 3a–c show the contours of velocity magnitude for three inlet velocities (0.2, 1 and 10 m/s) for a horizontal deadleg with

equal header and branch diameters, $D_H = D_B = 0.3$ m. For simplicity, D_H will be referred to as D in the following. It is clear from the figure that the stagnant fluid region inside the deadleg gets smaller with the increase of the inlet velocity (note the difference in the velocity scale in the three figures). This is quite expected since higher velocity in the inlet section creates higher inertia force causing more flow penetration in the deadleg. The figures also show that the flow velocity in the deadleg outflow branch has a high degree of non-uniformity with higher velocity on the right side and much lower velocity on the left side. The low velocity region is clearly a separated flow region that gets longer with the increase of the inlet flow velocity. The effect of deadleg length on the velocity field is shown in Fig. 4 for the same case of $D_H = D_B = 0.3$ m when the inlet velocity is 1 m/s and for four values of the length to diameter ratio ($L/D = 1, 3, 5, 10$). Although the stagnant fluid region in the deadleg gets bigger with the increase of L/D , the fluid flow field in the tee junction region (upstream and downstream of the

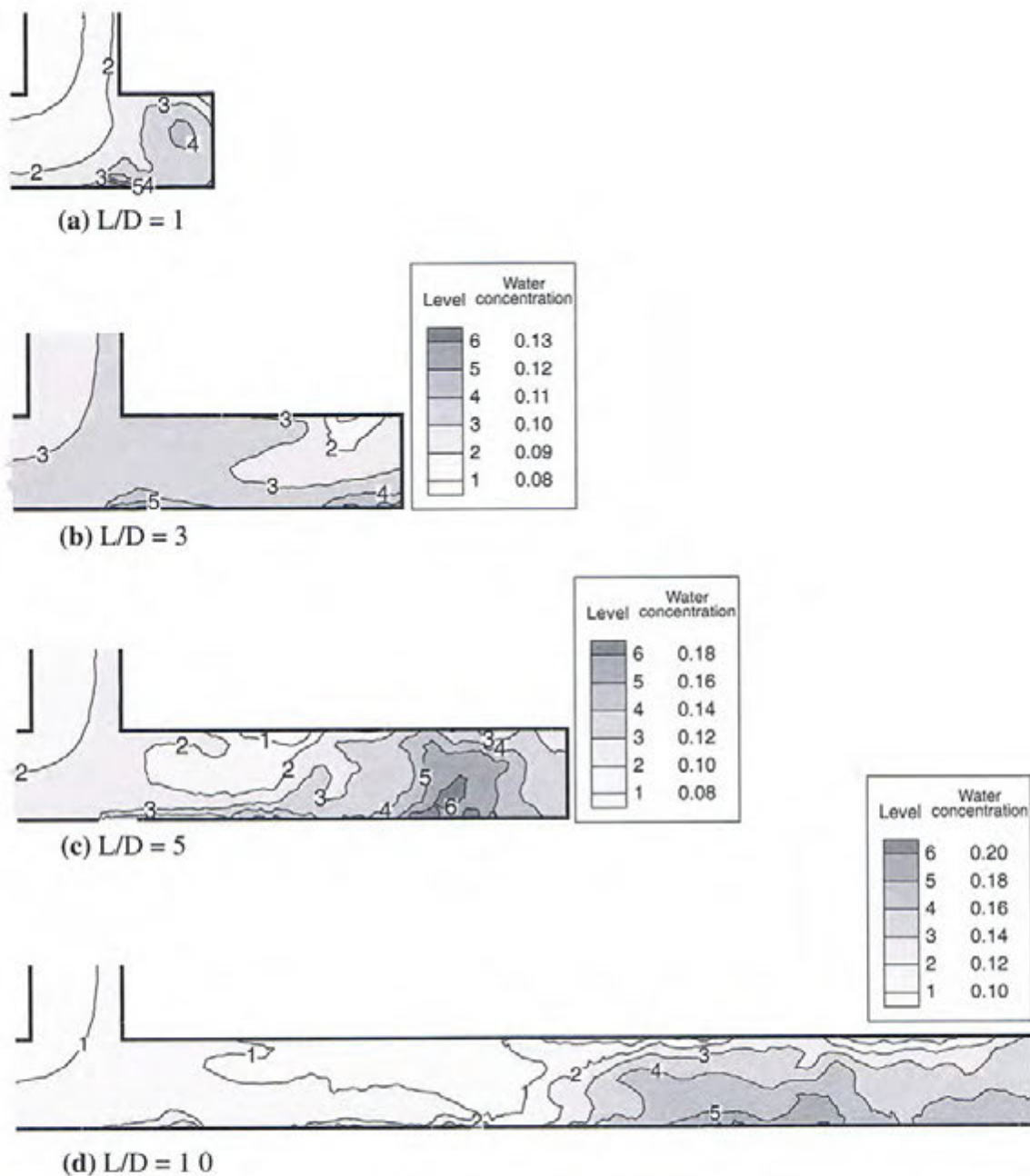


Fig. 6 Contours of water volumetric concentration in the horizontal deadleg for the case of $U = 1$ m/s

junction and the deadleg inlet region) is almost the same in all cases. In order to provide a better understanding of the flow features along the deadleg, the velocity vectors of the velocity magnitudes are shown in Fig. 5a–d. The velocity vectors are plotted for $U = 1$ m/s and show high velocity values at the tee junction with a recirculation zone in the exit pipe at the left side of the pipe. Low velocity values appear in the deadleg of $L/D = 1$ and most of the length of $L/D = 3$ case. The figures show very low velocity values in regions of x/D of more than three in the cases of $L/D = 5$ and 10. In general, it can be concluded that the whole length of the leg shows low velocity with

almost stagnant flow beyond a length of $2D$ to $3D$ downstream of inlet to deadleg inlet section in all the cases of L/D ratios.

The effect of deadleg length on the variation of the local water concentration is shown in Fig. 6 for the same case of $D_H = D_B = 0.3$ m when the inlet velocity is 1 m/s and for four values of length to diameter ratio ($L/D = 1, 3, 5, 10$). For a deadleg of small length ($L/D = 1$), the local water concentration is slightly higher than 10% (about 10.5%) over most of the deadleg and reaches a maximum of 11.7% in a small area (of length less than $0.2L$) on the lower surface as shown in Fig. 6a. The area of the deadleg subjected to higher water concentration increases with the increase of the deadleg length as shown in Fig. 6b–d. Figure 6b shows a water concen-

Table 1 Range of local water concentration in the horizontal deadleg with $D_H = D_B = 0.3$ m and $U = 1$ m/s for different length-to-diameter ratios

L/D	Range of water concentration (%)
1	10.5 – 11.7
3	9.5 – 12.8
5	7.2 – 21.0
10	6.2 – 21.6

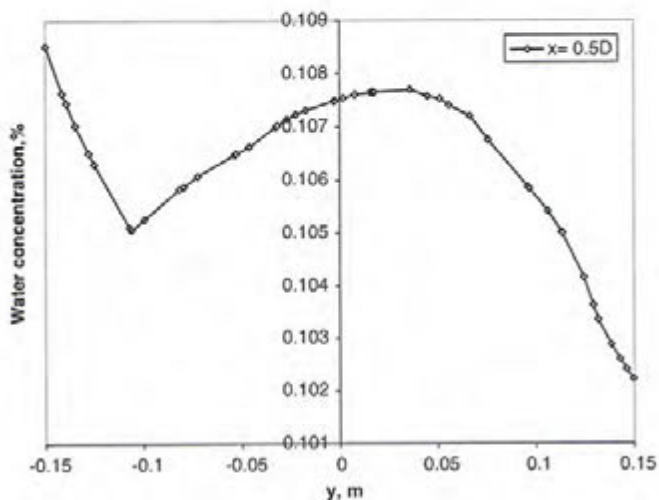


Fig. 7 Distribution of water volumetric concentration in the horizontal deadleg; $L/D=1$, $U=1$ m/s

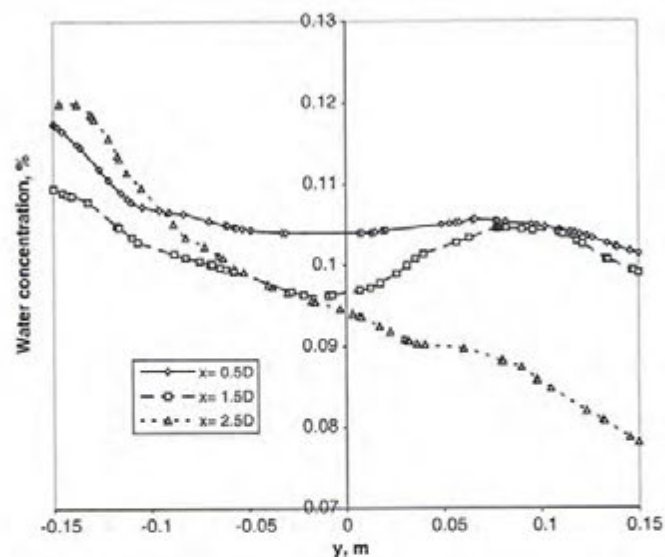


Fig. 8 Distribution of water volumetric concentration in the horizontal deadleg; $L/D=3$, $U=1$ m/s

tration of about 11% over most of the lower part of the deadleg and reaching a maximum of 12.8% over a length of about $0.3L$ on the lower surface. The same trend continues with the increase of the deadleg length

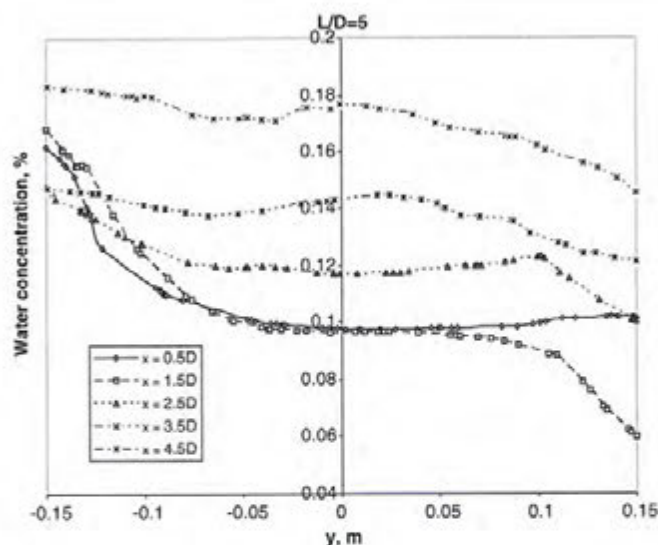


Fig. 9 Distribution of water volumetric concentration in the horizontal deadleg; $L/D=5$, $U=1$ m/s

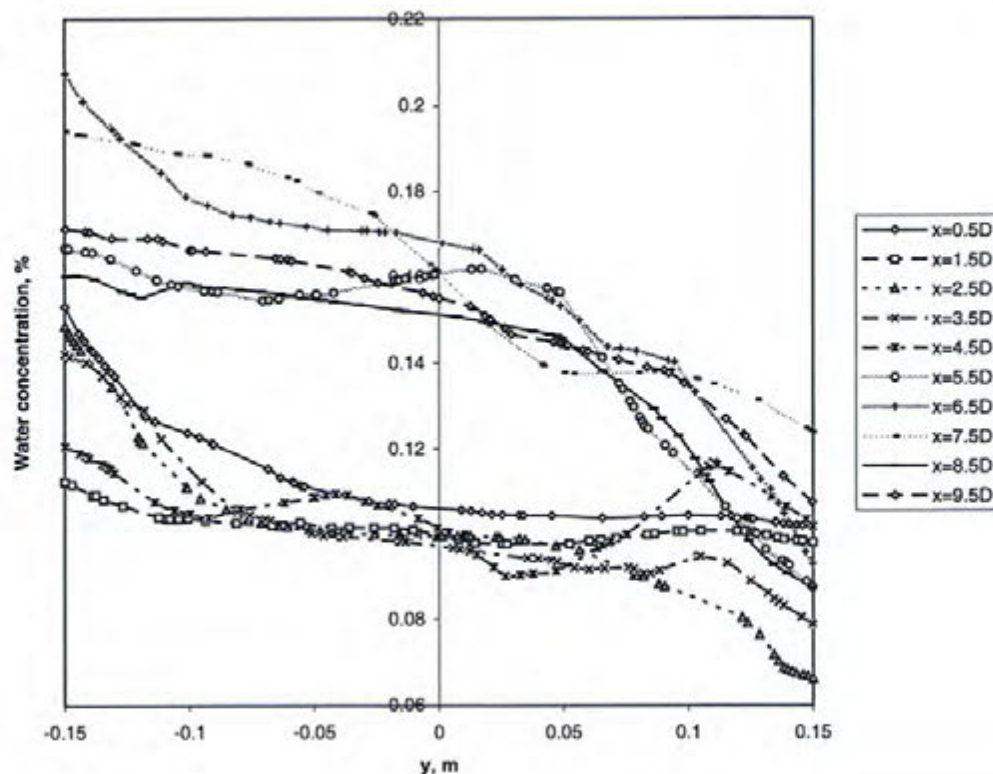
until reaching $L/D=10$ at which about 92% of the deadleg length is subjected to a local water concentration in the range 16–20% and reaches over 20% on the remaining length. That represents a maximum increase in local water concentration over 100% of its value at the inlet section in the case of $L/D=10$. Table 1 shows the range of water concentration for every length-to-diameter ratio in this case.

In order to provide an explanation for the deadleg phenomenon, profiles of the water concentration at different sections along the deadleg length are shown in Figs. 7, 8, 9 and 10. Figure 7 shows the concentration profile at a distance x of $0.5D_H$ for the case of $L/D=1$. It is shown that the concentration decreases from 0.11 at the bottom wall of the deadleg to a minimum of 0.105, then, increases to 0.108 at $y=0.04$ m and decreases monotonically to 0.102 at $y=0.15$ m (the upper surface). The water concentration profiles at different x -locations for the cases of $L/D=3$ and 5 are shown in Figs. 8 and 9. In Fig. 8, the radial profiles of the water concentration exhibit a variation of range of 0.11–0.12 at the bottom wall to a range of 0.08–0.11 at the upper wall. Figure 9 shows a spectrum of water concentration generally of increasing values from 0.1 to 0.18 as x/D increases. As L/D increases to $10D$, Fig. 10, two distinct groups of water concentration are shown. The region of $x/D=0.5$ – 4.5 has a low water concentration and the region of $x/D=5.5$ – 9.5 has higher concentration. Thus, the figures indicate a length of $x/D=5$ where the concentration remains relatively low.

5 Conclusions

The effect of deadleg geometry on oil/water separation has been investigated. The investigation is based on the

Fig. 10 Distribution of water volumetric concentration in the horizontal deadleg; $L/D=10$, $U=1$ m/s



solution of the mass and momentum conservation equations of an oil/water mixture together with the volume fraction equation for the secondary phase. A fluid flow model based on the time-averaged governing equations of 3-D turbulent flow has been developed. An algebraic slip mixture model is utilized for the calculation of the two immiscible fluids (water and crude oil). The model solves the continuity and momentum equations for the mixture, and the volume fraction equation for the secondary phase utilizing an algebraic expression for the relative velocity. Flow visualization experiments were conducted in order to validate the numerical procedure. Good agreement was obtained between the calculated and measured flow patterns. Results are obtained for different length to diameter ratios ranging from 1 to 10. The considered fluid mixture contains 90% oil and 10% water (by volume). The results show that the size of the stagnant fluid region increases with the increase of L/D . It is found that, for all the cases of L/D ratios, the whole region of the deadleg is occupied by a low velocity fluid. The calculated velocity vectors indicate two regions of low velocity (occupying 2–3 D of the deadleg length) and very low velocity regions (occupying the rest of the deadleg). The results also indicate that the water volumetric concentration increases with the increase of L/D . Maximum value of the water concentration increases from 11.4% in the case of $L/D=1$ to more than 20% in the case of $L/D=10$.

Acknowledgements The authors wish to acknowledge the support received from King Fahd University of Petroleum & Minerals and Saudi Aramco during the course of this study.

References

1. Angeli P, Hewitt GF (1996) Pressure gradient phenomena during horizontal oil-water flow, 1996 OMAE, Vol. V. Pipeline technology. ASME 1996, pp 287–295
2. Asheim H, Kolnes J, Oudeman P (1992) A flow resistance correlation for completed wellbore. *J Petrol Sci Eng* 8(2): pp 97–104
3. Barnea D (1986) Transition from annular flow and from dispersed bubble flow-unified models for the whole range of pipe inclinations". *International Journal of Multiphase Phase Flow*, Vol. 12, No. 5, pp 733–744
4. Bates CJ, Zonuzi F, Faram MG, O'Doherty T (1995) Experimental and numerical comparison of the flow in a 90° tee junction. Separated and complex flows. *ASME Fluid Eng Division FED 217*: 43–50
5. Brauner N, Maron DM (1992) Stability analysis of stratified liquid-liquid flow. *Int J Multiphase Flow* 18(1):103–121
6. Brill J, Beggs H (1994) Two-phase flow in pipes. 6th Ed. University of Tulsa Press
7. Celius HK, Aamo OM (1999) A new mathematical model for oil/water separation in pipes and tanks. *SPE Production and Facilities*, 14(1):30
8. Charles ME, Govier GW, Hodgson GW (1961) The horizontal pipeline flow of equal density oil-water mixture. *Can J of Chem Eng* 27–36
9. Charles ME, Lilleht LU (1966) Correlations of pressure gradients for the stratified laminar-turbulent pipeline flow of two immiscible liquids. *Can J Chem Eng* 47–49
10. Habib MA, Attya AM, McEligot DM (1989) Calculation of turbulent flow and heat transfer in channels with streamwise periodic flow. *ASME J Turbomachinery* 110:405–411
11. Hafskjold B, Celius HK, Aamo OM (1999) A new mathematical model for oil/water separation in pipes and tanks. *SPE Production and Facilities* 14(1):30–36
12. Haidar NIA (1994) Computational modeling of combining compressible flow through 30–150° tee junctions. *ASME Int Gas Turbine Inst COGEN-TURBO, IGTI* 9:141–150

13. Hwang CJ, Pal R (1997) Flow of two-phase oil/water mixtures through sudden expansions and contractions. *Chem Eng J* 68:157-163
14. Launder BE, Spalding DB (1974) The numerical computation of turbulent flows. *Computer Methods Appl Mech Eng* 3:269-289
15. Lockhart RW, Martinelli RC (1949) *Chem eng prog* 45:39
16. Manninen M, Taivassalo V, Kallio S (1996) On the mixture model for multiphase flow. VIT Publications, Finland
17. Patankar SV (1980) *Numerical heat transfer and fluid flow*, 1st edn. Taylor and Francis
18. Plaxton BL (1995) Pipeflow experiments for analysis of pressure drop in horizontal wells. SPE annual technical conference and exhibition, Dallas, pp 635-650, C22-25 October 1995
19. Reynolds WC (1987) Fundamentals of turbulence for turbulence modeling and simulation. Lecture Notes for Von Karman Institute, Agard Report No. 755
20. Rubel MT, Timmerman BD, Soliman HM, Sims GE, Ebadian MA (1994) Phase distribution of high pressure steam-water flow at large-diameter tee junctions. *ASME J Fluid Eng* 116:592-598
21. Schabacker J, Boles A, Johnson BV (1998) PIV investigation of the flow characteristics in an internal coolant passage with two ducts connected by a sharp 180° bend. *ASME (paper) n GT 1998*, Fairfield, 11 98:-GT-544.
22. Schmidt H, Loth R (1994) Predictive methods for two-phase flow pressure loss in tee junctions with combining ducts. *Int J Multiphase Flow*. 20(4):703-720
23. Shih TH, Liou WW, Shabbir A, Zhu J (1995) A new $k-\epsilon$ eddy-viscosity model for high Reynolds number turbulent flows—model development and validation. *Comput Fluids* 24(3):227-238
24. Trallero JL, Sarica C, Brill JP (1997) A study of oil/water flow patterns in horizontal pipes. In: *SPE Production and Facilities*, pp 165-172
25. Versteeg HK, Malalasekera W (1995) *An introduction to computational fluid dynamics; the finite volume method*. Longman Scientific and Technical

On the Development of Deadleg Criterion

M. A. Habib

Professor
email: mahabib@kfupm.edu.sa

H. M. Badr

Professor

S. A. M. Said

Professor

I. Hussaini

Lecturer

Mechanical Engineering Department, King Fahd
University of Petroleum & Minerals,
Dhahran 31261, Saudi Arabia

J. J. Al-Bagawi

Engineering Specialist,
Saudi Aramco, Saudi Arabia

Corrosion in deadlegs occurs as a result of water separation due to the very low flow velocity. This work aims to investigate the effect of geometry and orientation on flow field and oil/water separation in deadlegs in an attempt for the development of a deadleg criterion. The investigation is based on the solution of the mass and momentum conservation equations of an oil/water mixture together with the volume fraction equation for the secondary phase. Results are obtained for two main deadleg orientations and for different lengths of the deadleg in each orientation. The considered fluid mixture contains 90% oil and 10% water (by volume). The deadleg length to diameter ratio (L/D) ranges from 1 to 9. The results show that the size of the stagnant fluid region increases with the increase of L/D . For the case of a vertical deadleg, it is found that the region of the deadleg close to the header is characterized by circulating vortical motions for a length $l \approx 3D$ while the remaining part of the deadleg occupied by a stagnant fluid. In the case of a horizontal deadleg, the region of circulating flow extends to 3–5 D . The results also indicated that the water volumetric concentration increases with the increase of L/D and is influenced by the deadleg orientation. The streamline patterns for a number of cases were obtained from flow visualization experiments (using 200 mW Argon laser) with the objective of validating the computational model. [DOI: 10.1115/1.1852481]

1 Introduction

Deadleg is a term used to describe the inactive portion of a pipe, where the fluid is stagnant or having very low velocity, in various piping systems. This inactive pipe is normally connected to an active pipe that carries the main stream. Deadlegs represent regions prone to corrosion in oil piping systems due to stagnant or low velocity flow that causes emulsified water precipitation out of the crude. As described by Craig [1] and Lotz et al. [2], once water begins to drop out of solution onto the metal surface, wettability would become the controlling factor in corrosion. When metal becomes water wet, corrosion potential increases significantly. Internal corrosion was found to be predominant in low-velocity piping where emulsified water had precipitated out of the crude oil [3,4]. In order to maintain the integrity of the connecting main pipe, internal corrosion of deadlegs must be prevented, since it is very difficult to control and usually requires a major shut down to fix. In the oil and gas industry, deadleg corrosion presents the highest percentage of internal damage to pipelines or in-plant piping systems that are normally considered to operate in a non-corrosive environment. Deadlegs should be avoided whenever possible in the design of piping for fluids containing or likely to contain corrosive substances. When deadlegs are unavoidable, the length of the inactive pipe must be as short as possible to avoid stagnant or low velocity flows.

To date, there is no research published on the effect of deadleg geometry and flow velocity on the concentration of water or other corrosive agents in deadlegs. Most of the relevant published work focused on the effect of the oil-to-water ratio on the flow pattern and pressure drop in straight pipes. An experimental investigation [5] was conducted to study the effect of the oil-water ratio on the pressure gradient in a horizontal pipe. In this work, it was found that at a high oil-water ratio, oil formed the continuous phase and a water-drops-in-oil regime was observed. As the oil-water ratio was decreased, the flow patterns changed to concentric oil in water, oil-slugs-in-water, oil-bubbles-in-water, and finally oil-drops-in-water. The measured pressure gradient was found to be strongly dependent on the oil-water ratio. Pressure gradient data obtained

from three different sets of experiments for stratified flow of two immiscible liquids in laminar-turbulent regime was presented [6]. This investigation was based on the parameters introduced by Lockhart and Martinelli [7]. The Lockhart and Martinelli parameters were used [6] for correlating the pressure gradient data in case of gas-liquid mixture flows. Unified models that incorporate the effect of the angle of inclination on the transition from annular flow to intermittent flow and from dispersed bubble flow were presented [8]. The models showed a smooth change in mechanisms as the pipe inclination varies over the whole range of upward and downward inclinations.

The stability of a stratified liquid-liquid two-phase system was investigated [9] and it was found that subzones of stratified-dispersed patterns might appear in regions where stable stratification is expected. The reduction of density differential, as the case in liquid-liquid systems, tended to extend the regions of dispersed flow patterns on the account of the range of the continuous stratified patterns. The formation of a stratified-dispersed/stratified pattern was attributed to the moderate buoyancy forces in case of reduced density differential. Due to the limited available experimental data, the model was not fully validated. A practical and sufficiently accurate method for calculating the pressure drop in a tee junction with combining conduits using a semiempirical approach was provided [10].

The experimental investigation [11] on the effect of influx in a two-phase, liquid-liquid flow system on the pressure drop behavior proved that the Brill and Beggs correlation method [12] was able to provide adequate pressure gradient predictions for oil-water flow. On the other hand, the acceleration confluence model [13] was found to be inadequate in predicting the pressure drops. Experimental results on the effect of the water volume fraction in an oil-water system on the pressure gradient in pipe flow were reported [14]. The pressure gradient measurements showed that the liquid-liquid dispersions exhibited a flow behavior that diverged from a single-phase flow. The measured values of the pressure gradient were much lower than those predicted from the homogeneous model. Similar studies for pressure losses in other pipe fittings were carried out [15] for both sudden pipe expansion and sudden contraction and by Schabacker et al. [16] for a sharp 180 deg bend.

A mathematical model for oil/water separation in pipes and tanks was recently proposed [17]. The model describes the pro-

Contributed by the Fluids Engineering Division for publication on the JOURNAL OF FLUIDS ENGINEERING. Manuscript received by the Fluids Engineering Division June 2, 2003; revised manuscript received September 30, 2004. Review Conducted by: I. Celik.

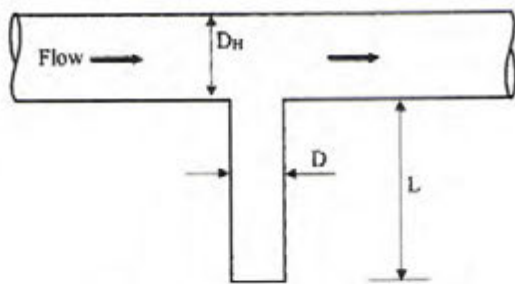


Fig. 1 The geometry of the deadleg configuration

cess of water separation in oil systems based on the two mechanisms of coalescence and settling. The separation of oil and water can be considered as a combination of emulsification and separation. It was observed [17] that the separation rate for water in oil systems increases with the increase in water cut, and that some water remains in the oil even after long settling times. These features may be qualitatively understood by a combination of coalescence and settling. A mathematical-numerical model that describes these mechanisms qualitatively was developed [17]. This model calculates the quality of the output oil as a function of system dimensions, flow rates, fluid physical properties, fluid quality, and drop size distribution at inlet. The computation of a continuous flow of a mixture of two immiscible fluids using the most general model for multiphase flows, the Eulerian approach, is difficult for large-scale industrial applications. On the other hand, the Lagrangian approach, which is used for continuous

phase (liquid or gas) and a discrete secondary phase (particles, drops or bubbles), is only suitable for low discrete phase concentrations. The algebraic slip mixture model [18–22], which is a simplified version of the Eulerian model, allows the phases to be interpenetrating and allows the volume fraction of the two fluids to be between 0 and 1.

After a comprehensive literature search, it was found, to the best of our knowledge that no research was published on the effect of deadleg length and orientation on water separation in deadleg regions that are widely used in oil piping systems. This study aims at investigating the effect of deadleg geometry and orientation on the velocity field and water separation in deadlegs. The present work also aims to establish a deadleg criterion based on deadleg orientation and length-to-diameter ratio.

2 Problem Statement and Formulation

The problem considered is that of flow of an oil/water mixture having 90% oil and 10% water (by volume) in a tee junction with the deadleg forming one branch. The configuration considered for the deadleg is shown in Fig. 1. In this configuration, the deadleg may take either a horizontal or vertical position. The calculations were carried out for various lengths of the deadleg where the length-to-diameter ratio ranged from $L/D=1$ to 9 with the objective of obtaining the details of the flow velocity field as well as the changes in the water volumetric concentration inside the deadleg. This water concentration is important for corrosion prediction [1–4]. The average inlet flow velocity is 1 m/s in all cases. The length of the main tube (header) upstream the deadleg is 4.5 m, thus a length of 15 header diameters developing region is considered to eliminate the effect of the inflow velocity profile. This has

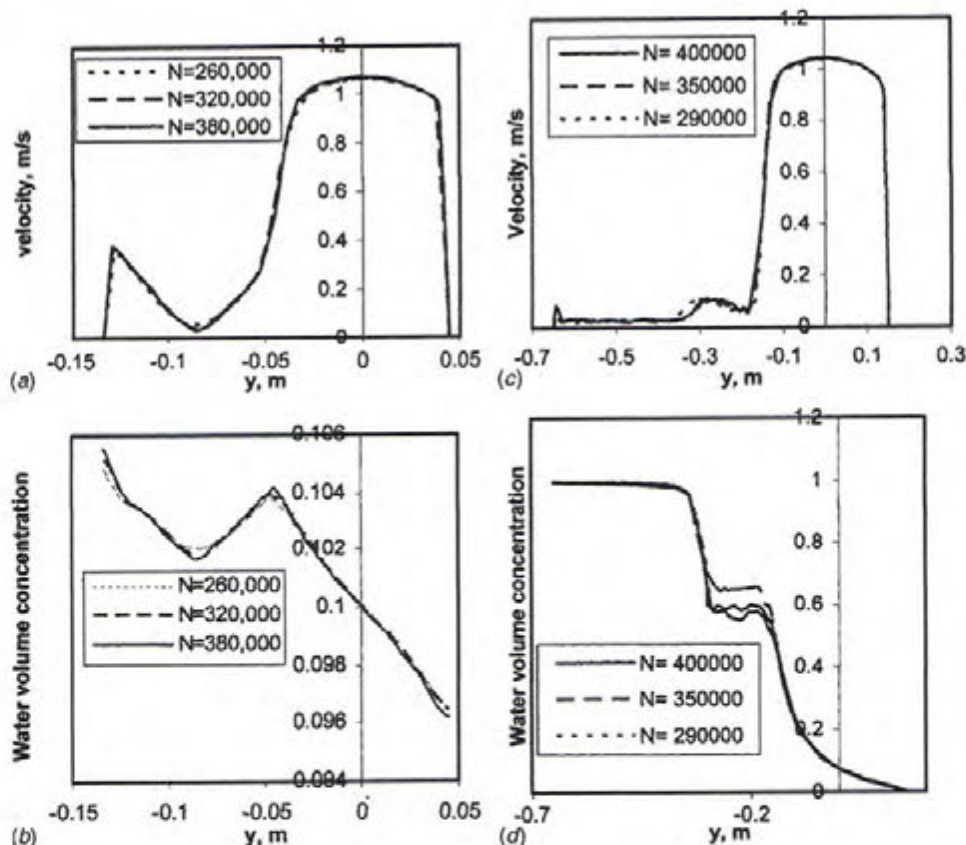


Fig. 2 The influence of mesh refinement on the velocity magnitude and volumetric water concentration along the axis of the deadleg, (a) Velocity magnitude $L/D=1$, $d=10^{-4}$ m (b) Volumetric water concentration $L/D=1$, $d=10^{-4}$ m (c) Velocity magnitude, $L/D=5$, $d=10^{-3}$ m (d) Volumetric water concentration $L/D=5$, $d=10^{-3}$ m

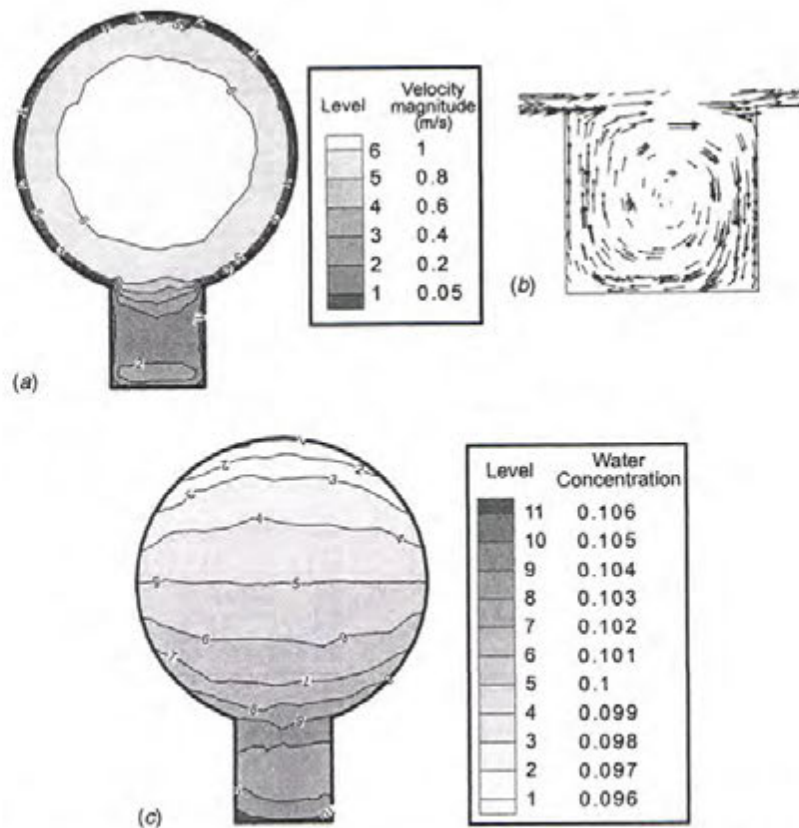


Fig. 3 Velocity contours, velocity vectors, and contours of the volumetric concentration of water for the vertical deadleg; $L/D=1$. (a) Velocity contours, (b) velocity vectors, and (c) Water concentration.

been justified by comparing profiles at different sections of the header tube upstream of the deadleg. The mathematical formulation for the calculation of the fluid flow field has been established. The fluid flow model is based on the time-averaged governing equations of three-dimensional (3D) turbulent flow. The algebraic slip mixture model [15] is utilized for the calculation of the two immiscible fluids (water and crude oil). The model solves the continuity equation for the mixture, the momentum equation for the mixture, and the volume fraction equation for the secondary phase (water), as well as an algebraic expression for the relative velocity. The slip mixture model [18,23] allows the phases to be interpenetrating. Therefore, the volume fraction of the primary and secondary flows for a control volume can take any value between 0 and 1. The model is based on the assumption of local momentum equilibrium. This occurs when the relative velocity between phases is small and the inertia associated with the drift is insignificant.

2.1 Continuity and Momentum Equations. The continuity and momentum equations [24–26] are described in the following.

2.1.1 Mass Conservation. The steady-state time-averaged equation for conservation of mass of the mixture can be written as

$$\frac{\partial}{\partial x_j} (\rho \bar{U}_{m,j}) = 0 \quad (1)$$

2.1.2 Momentum Conservation. The equation of momentum involves terms representing convection, diffusion, pressure gradient, body force, and frictional drag force. The drag force is given in terms of density and drift velocity. The steady-state time-averaged equation for the conservation of momentum of the mixture in the i direction can be obtained by summing the individual momentum equations for both phases. It can be expressed as

$$\begin{aligned} \frac{\partial}{\partial x_j} (\rho_m \bar{U}_{m,i} \bar{U}_{m,j}) = & -\frac{\partial p}{\partial x_i} + \frac{\partial}{\partial x_j} \left(\mu_m \frac{\partial \bar{U}_{m,i}}{\partial x_j} \right) - \frac{\partial}{\partial x_j} (\overline{\rho u_{m,i} u_{m,j}}) \\ & + \rho_m g + \frac{\partial}{\partial x_j} \sum_{k=1}^2 \alpha_k \rho_k u_{DK,i} u_{DK,j} \end{aligned} \quad (2)$$

where p is the static pressure and the stress tensor $\overline{\rho u_{m,i} u_{m,j}}$ is given by

$$-\overline{\rho u_{m,i} u_{m,j}} = \left[\mu_{eff} \left(\frac{\partial \bar{U}_{m,i}}{\partial x_j} + \frac{\partial \bar{U}_{m,j}}{\partial x_i} \right) \right] - \frac{2}{3} \rho_m k_m \delta_{ij} \quad (3)$$

where δ_{ij} is the Kronecker delta which is equal to 1 for $i=j$ and equals 0 for $i \neq j$ and $\mu_{eff} = \mu_t + \mu_l$ is the effective viscosity. The turbulent viscosity μ_t is calculated using the high-Reynolds number form as

$$\mu_t = \rho_m C_\mu \frac{k_m^2}{\varepsilon_m} \quad (4)$$

with $C_\mu = 0.0845$ [16], and k_m and ε_m are the kinetic energy of turbulence of the mixture and its dissipation rate, respectively. These are obtained by solving their conservation equations as given below.

ρ_m and μ_m in Eq. (2) are the density and viscosity of the mixture that can be obtained from

$$\rho_m = \sum_{k=1}^n \alpha_k \rho_k \quad (5)$$

$$\mu_m = \sum_{k=1}^n \alpha_k \mu_k \quad (6)$$

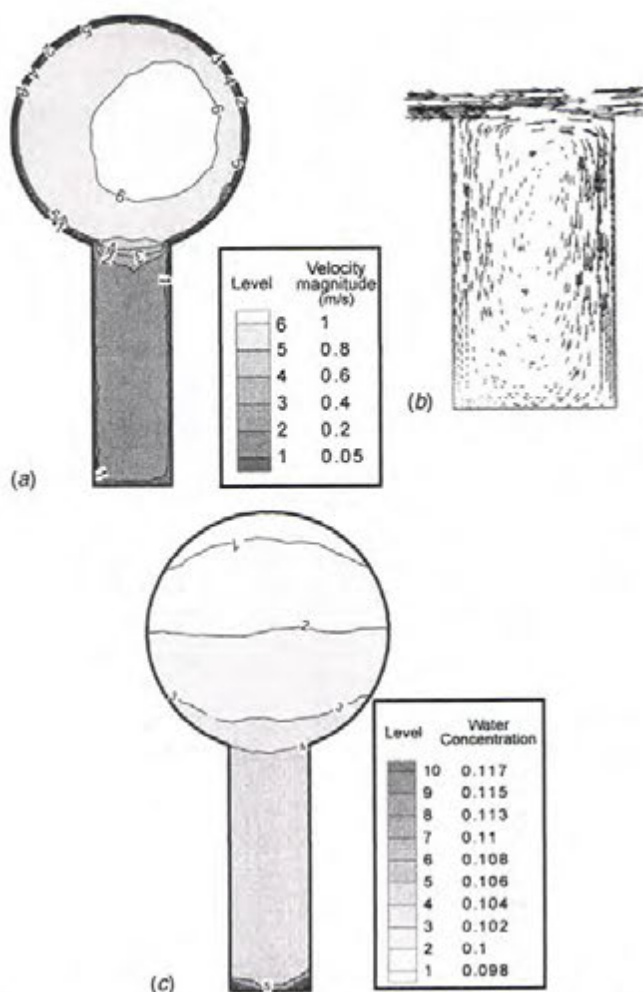


Fig. 4 Velocity contours, velocity vectors, and contours of the volumetric concentration of water for the vertical deadleg; $L/D=3$. (a) Velocity contours, (b) velocity vectors, and (c) water concentration.

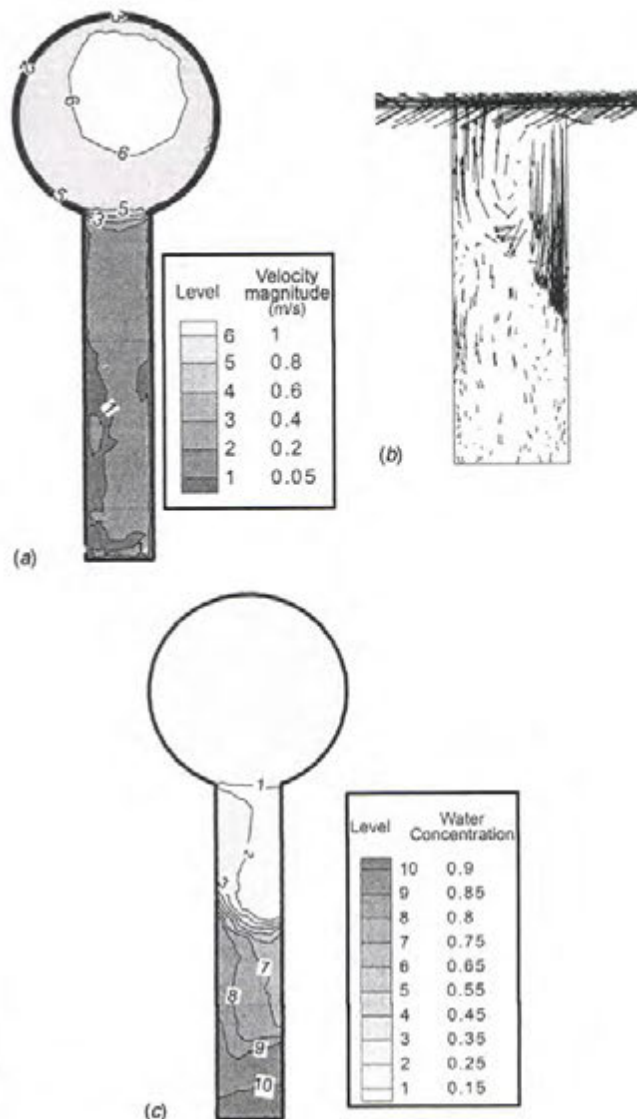


Fig. 5 Velocity contours, velocity vectors, and contours of the volumetric concentration of water for the vertical deadleg; $L/D=5$. (a) Velocity contours, (b) velocity vectors, and (c) water concentration.

\bar{U}_m is the mass-averaged velocity

$$\bar{U}_m = \frac{\sum_{k=1}^n \alpha_k \rho_k \bar{U}_k}{\rho_m} \quad (7)$$

and \bar{U}_{Dk} are the drift velocities and are given by

$$\bar{U}_{Dk} = \bar{U}_k - \bar{U}_m \quad (8)$$

The drift velocity is related to the relative (slip) velocity \bar{U}_{ps} as

$$\bar{U}_{Ds} = \bar{U}_{ps} - \sum_{k=1}^n \frac{\alpha_k \rho_k}{\rho_m} \bar{U}_{pk} \quad (9)$$

with \bar{U}_{ps} is given by

$$\bar{U}_{ps} = \bar{U}_s - \bar{U}_p \quad (10)$$

The slip velocity is a function of the density difference, droplet diameter, body force per density, and droplet Reynolds number. The body force includes gravitational and rotational forces. The slip velocity is expressed [18,23] as

$$\bar{U}_{ps} = \frac{(\rho_m - \rho_s) d_s^2}{18 \mu_p f_{drag}} \left[g - \bar{U}_m \frac{\partial}{\partial x_j} \bar{U}_{m,j} \right] \quad (11)$$

The drag function f_{drag} in the above equation is given by

$$f_{drag} = 1 + 0.15 \text{Re}_d^{0.687} \quad \text{for } \text{Re}_d \leq 1000$$

and

$$f_{drag} = 0.0183 \text{Re}_d \quad \text{for } \text{Re}_d > 1000 \quad (12)$$

The droplet Reynolds number

$$\text{Re}_d = \frac{\rho_p \bar{U}_{ps} d_s}{\mu_p} \quad (13)$$

2.2 Volume Fraction Equation for the Secondary Phase

From the continuity equation for the secondary phase, the volume fraction equation for the secondary phase can be written as

$$\frac{\partial}{\partial x_j} (\alpha_s \rho_s \bar{U}_{m,j}) = - \frac{\partial}{\partial x_j} (\alpha_s \rho_s \bar{U}_{Ds}) \quad (14)$$

2.3 Conservation Equations for the Turbulence Model

The conservation equations of the turbulence model [[17] and [18]] are given as follows.

2.3.1 Kinetic Energy of Turbulence.

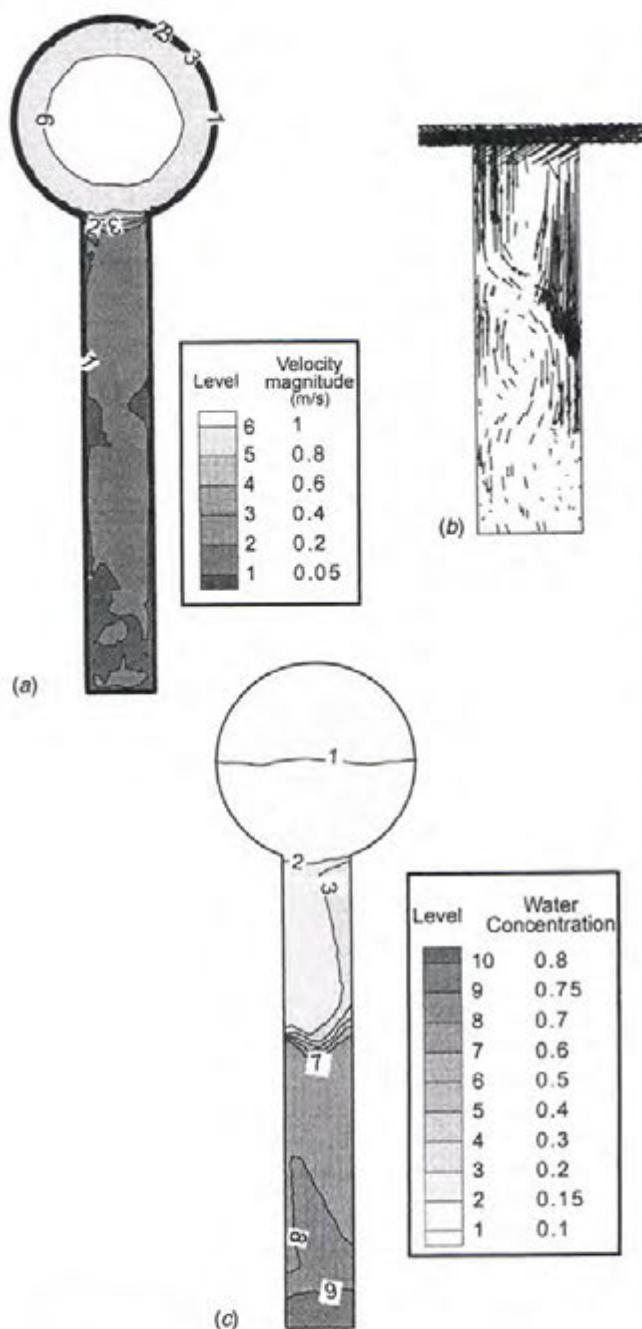


Fig. 6 Velocity contours, velocity vectors, and contours of the volumetric concentration of water for the vertical deadleg; $L/D=7$. (a) Velocity contours, (b) velocity vectors, and (c) water concentration.

$$\frac{\partial}{\partial x_j} (\rho \bar{U}_j k) = \frac{\partial}{\partial x_j} \left(\frac{\mu_{eff}}{\sigma_k} \frac{\partial k}{\partial x_i} \right) + G_k - \rho \epsilon \quad (15)$$

2.3.2 Rate of Dissipation of the Kinetic Energy of Turbulence

$$\frac{\partial}{\partial x_j} (\rho \bar{U}_j \epsilon) = \frac{\partial}{\partial x_j} \left(\frac{\mu_{eff}}{\sigma_\epsilon} \frac{\partial \epsilon}{\partial x_i} \right) + C_1 G_k \frac{\epsilon}{k} - C_2 \rho \frac{\epsilon^2}{k} \quad (16)$$

where G_k represents the generation of turbulent kinetic energy due to the mean velocity gradients and is given by

$$G_k = -\rho \overline{u_m u_{mj}} \frac{\partial \bar{U}_m}{\partial x_j} \quad (17)$$

The quantities σ_k and σ_ϵ are the effective Prandtl numbers for k and ϵ , respectively, and C_2 is given [27] as a function of the term k/ϵ and, therefore, the model is responsive to the effects of rapid strain and streamline curvature and is suitable for the present calculations. The model constants C_1 and C_2 have the values; $C_1 = 1.42$ and $C_2 = 1.68$.

The wall functions establish the link between the field variables at the near-wall cells and the corresponding quantities at the wall. These are based on the assumptions introduced [28] and have been most widely used for industrial flow modeling. The details of the wall functions are provided by the law-of-the-wall for the mean velocity [29].

2.4 Boundary Conditions. The velocity distribution is considered uniform at the inlet section. Kinetic energy and its dissipation rate are assigned through a specified value of \sqrt{k}/U^2 equal to 0.1 and a length scale L equal to the diameter of the inlet section. The boundary condition applied at the exit section (outlet of the heat exchanger tubes) is that of fully developed flow. At the wall boundaries, all velocity components are set to zero in accordance with the no-slip and impermeability conditions. Kinetic energy of turbulence and its dissipation rate are determined from the equations of the turbulence model. The secondary-phase volume fraction is specified at the inlet and exit sections of the flow domain.

2.5 Solution Procedure. The calculations were obtained using the FLUENT CFD-5.5 package. The conservation equations are integrated over a typical volume that is formed by dividing the flow field into a number of control volumes, to yield the solution. The equations are solved simultaneously using the solution procedure described by Patankar [30]. Calculations are performed with at least 300,000 finite volumes. Convergence is considered when the maximum of the summation of the residuals of all the elements for U , V , W and pressure correction equations is less than 0.01%. The grid independence tests were performed by increasing the number of control volumes from 260,000 to 380,000 ($h_{min} = 0.16$ to 0.18 cm and $h_{max} = 0.46$ to 0.51 cm) for the case of $L/D=1$ and from 290,000 to 400,000 ($h_{min} = 0.27$ to 0.32 cm and $h_{max} = 1.7$ to 2.0 cm) for a case of $L/D=5$ in two steps for each case. Figures 2(a) and 2(b) show the effect of mesh refinement on the variation of the velocity and volumetric water concentration along the axis of the deadleg. The influence of refining the grid on the velocity is very negligible. The grid independence test resulted in a maximum difference of less than 2.5% in the volumetric water concentration as the number of finite volumes increased from 260,000 to 320,000 and less than 0.8% as the number of volumes further increased from 320,000 to 380,000. Similar results are shown in Figs. 2(c) and 2(d) for the case of $L/D=5$ where the change of the number of control volumes from 350,000 to 400,000 has a negligible influence on both the velocity and the water volumetric concentration and has a maximum influence of 3% on the volumetric water concentration in a limited region of

Table 1 Range of local water concentration and length of regions with circulating flow for different orientations and length-to-diameter ratios

Deadleg orientation	L/D	Range of water concentration	Length of regions with circulating flow
Vertical	1	10.2%–10.4%	None
	3	10.2%–11.7%	2.8 D
	5	14.0%–86.7%	2.3 D
	7	13.2%–82.2%	2.8 D
Horizontal	1	9.0%–11.0%	Whole region, 1D
	3	8.2%–11.6%	Whole region, 3D
	5	6.5%–12.9%	3.3–4.5 D
	7	4.7%–16.0%	3.5–4.5 D
	9	4.2%–17.7%	4–5 D

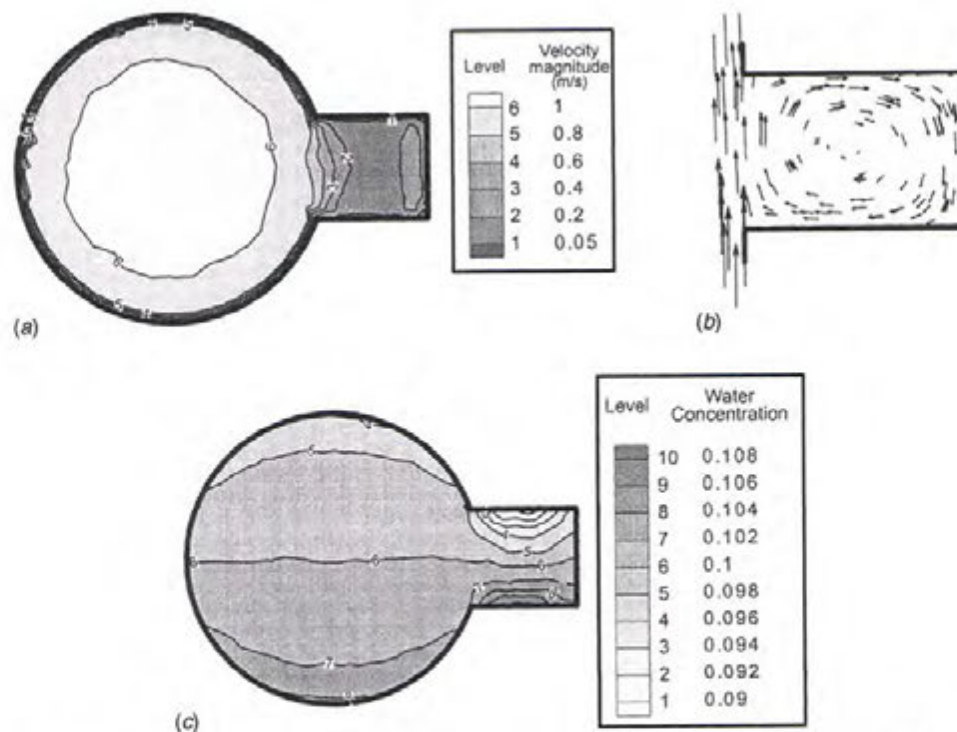


Fig. 7 Velocity contours, velocity vectors, and contours of the volumetric concentration of water for the horizontal deadleg; $L/D=1$. (a) Velocity contours, (b) velocity vectors, and (c) water concentration.

the deadleg. The abovementioned figures and percentage differences indicate that more mesh refinement will result in negligible changes in the accuracy of the computational model.

3 Results and Discussion

The details of the flow velocity field were obtained for different deadleg geometries and two orientations. The fluid at the inlet section in all of the considered cases is a homogeneous mixture containing 90% crude oil, by volume, and 10% water and the average flow velocity at inlet is 1 m/s. This concentration ratio represents a typical value in most of the crude oil wells. The header and branch diameters are $D_H=0.3$ and $D=0.1$ m for all cases. The deadleg length L is defined as the distance from the header to the end of the branch tube. Hafskjold et al. [17] show that, for a fully developed flow of two immiscible fluids, the droplet size ranges from 20 and 300 μm . The model is found to be only sensitive to droplets of diameters in the range of 10–25 μm and is less sensitive at larger droplet sizes. Therefore, the droplet size was taken to be 10^{-4} m for the cases considered in the present study.

The results are presented in terms of velocity contours, velocity vectors, and contours of water concentration. The velocity and water concentration contours are presented for a section in the deadleg that includes the branch (deadleg) tube centerline and is perpendicular to the header axis. The velocity vectors are presented for a section of the deadleg that contains the centerlines of the branch and header tubes. The first case is that of a vertical deadleg where four values of the lengths to diameter ratios ($L/D=1, 3, 5,$ and 7) are considered. The contours of velocity magnitude and velocity vectors in addition to the volumetric water concentration are presented for each L/D ratio. Figure 3(a) shows the contours of velocity magnitude for the case of $L/D=1$. In this case, the core region of the main pipe has an almost uniform velocity distribution with a large velocity gradient near the wall as what one would expect in the case of a fully developed turbulent flow in a pipe. The velocity is high at the top and bottom regions

of the deadleg (about 0.2 m/s) while low velocity exists at the middle. This distribution suggests the existence of a circulating flow zone similar to that occurring in a rectangular cavity with an upper moving boundary [31]. The velocity vectors in the deadleg (viewed from the side) are shown in Fig. 3(b). It is clear from the figure that a circulating flow zone exists in the deadleg that acted as a cylindrical cavity with its upper boundary open to the main stream. Such a circulating flow pattern tended to eliminate the stagnant fluid zone in the vertical deadleg. The effect of deadleg length on the variation of local water concentration in the vertical deadleg is shown in Fig. 3(c) for the same case of $L/D=1$. The local water concentration is found to be slightly higher than 10% (ranging between 10.2% and 10.5%) with the maximum concentration at the top and bottom regions of the deadleg as shown in Fig. 3(c). Having this maximum water concentration at the bottom is quite expected because of gravity effects but having the same value at the top may create some confusion. Actually, the maximum water concentration should occur at the bottom of the deadleg in the case of a stagnant fluid, however, because of the strong vortical motion [see Fig. 3(b)], the same concentration reaches the top region.

Figure 4(a) shows the contours of velocity magnitude in the case of $L/D=3$ and the corresponding velocity vectors for the same case are shown in Fig. 4(b). Figure 4(c) shows the contours of the water volumetric percentage for the same case. It is clear from these figures that the circulating flow zone extends over most of the entire length of the deadleg, however, with low velocity in the lower portion (about 0.05 m/s). Figure 4(a) also shows an asymmetric velocity profile in the main pipe as a result of the deadleg. Figure 4(c) shows that the water concentration varies from 10.2% to 11.7% with the maximum occurring in a very small region at the bottom of the deadleg.

The contours of velocity magnitude and velocity vectors as well as the water concentration for $L/D>3$ are shown in Figs. 5 and 6. The asymmetry of the velocity in the main pipe exists for $L/D=5$. Similar to the case of $L/D=1$, a circulating flow region occurs in

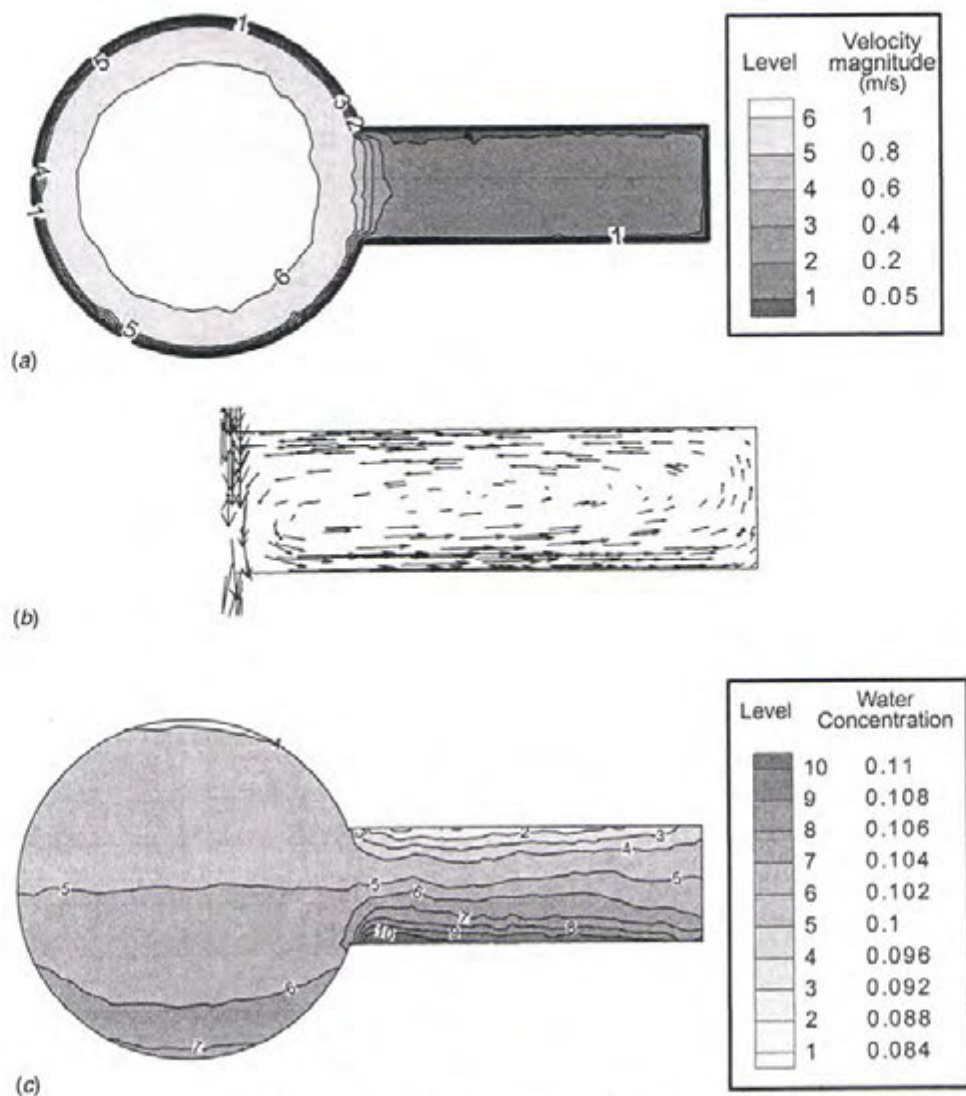


Fig. 8 Velocity contours, velocity vectors, and contours of the volumetric concentration of water for the horizontal deadleg; $L/D=3$. (a) Velocity contours, (b) velocity vectors, and (c) water concentration.

the upper part of the deadleg. The length of this part is equal to $2.3 D$. A stagnant fluid zone appears in the middle and lower portions of the deadleg in cases of $L/D > 3$ as shown in Figs. 5 and 6. Figure 5(a) shows a stagnant fluid region appearing near the wall in the case of $L/D=5$. That region extends, in a scattered fashion, in the lower part of the deadleg. The size of that region is found to increase with increasing L/D as can be seen in Figs. 5(a) and 6(a). Figure 6(a) shows an interesting flow pattern in which the upper section of the deadleg ($0 < y < 2.8 D$) is characterized by a circulating flow zone similar to that found in the case of $L/D=3$. This is followed by the middle section ($2.8 D < y < 5.2 D$) that is occupied by some counter-rotating vortices. The lower section ($5.2 D < y < 7 D$) is occupied by a stagnant fluid. The total length of the deadleg occupied by a stagnant fluid is $4.2 D$ that corresponds to 60% of the deadleg length. Considering the fact that the vortices in the middle region are too weak with negligible velocity magnitudes, it can be concluded that almost 70% of the deadleg is occupied by stagnant fluid.

Increasing L/D from 3 to 5 is found to create very high values of water concentration that reaches 86.7% at the bottom region as shown in Fig. 5(c). In this case, the upper half of the deadleg has a water concentration in the range from 14% to 39% while the lower half has a concentration in the range from 40% to 86.7%

with maximum value at the bottom of the deadleg. The part of the deadleg that has high water concentration of more than 20% is about 46% of the deadleg length (about $2.3 D$). The situation is almost the same in the case of $L/D=7$ [see Fig. 6(c)], however, the region of high water concentration (more than 20%) occupies about 40% of the deadleg length (about $2.8 D$). Table 1 shows the range of local water concentration in the deadleg for different values of length-to-diameter ratios. Thus, for the case of vertical deadleg, it is clear that there is no stagnant fluid zone in all cases so long as $L/D < 3$. For the cases of $L/D > 3$, it is also clear that the region of the deadleg close to the header is characterized by circulating vortical motions for a length $l \approx 3 D$ while the remaining part of the deadleg occupied by stagnant fluid.

The case of a horizontal deadleg was investigated for the same geometry of the vertical deadleg ($D_H=0.3$, $D=0.1$ m) but with different orientation. The problem was solved for five length-to-diameter ratios ($L/D=1, 3, 5, 7$, and 9) and the obtained contours of velocity magnitude, velocity vectors and concentration of liquid water are shown in Figs. 7–11. The only difference between this case and the one presented in Figs. 3–6 is the direction of gravity forces. In the previous case the gravity was acting in line with the deadleg axis while perpendicular to it in the present case. Figure 7(a) shows the velocity contours in case of $L/D=1$. The

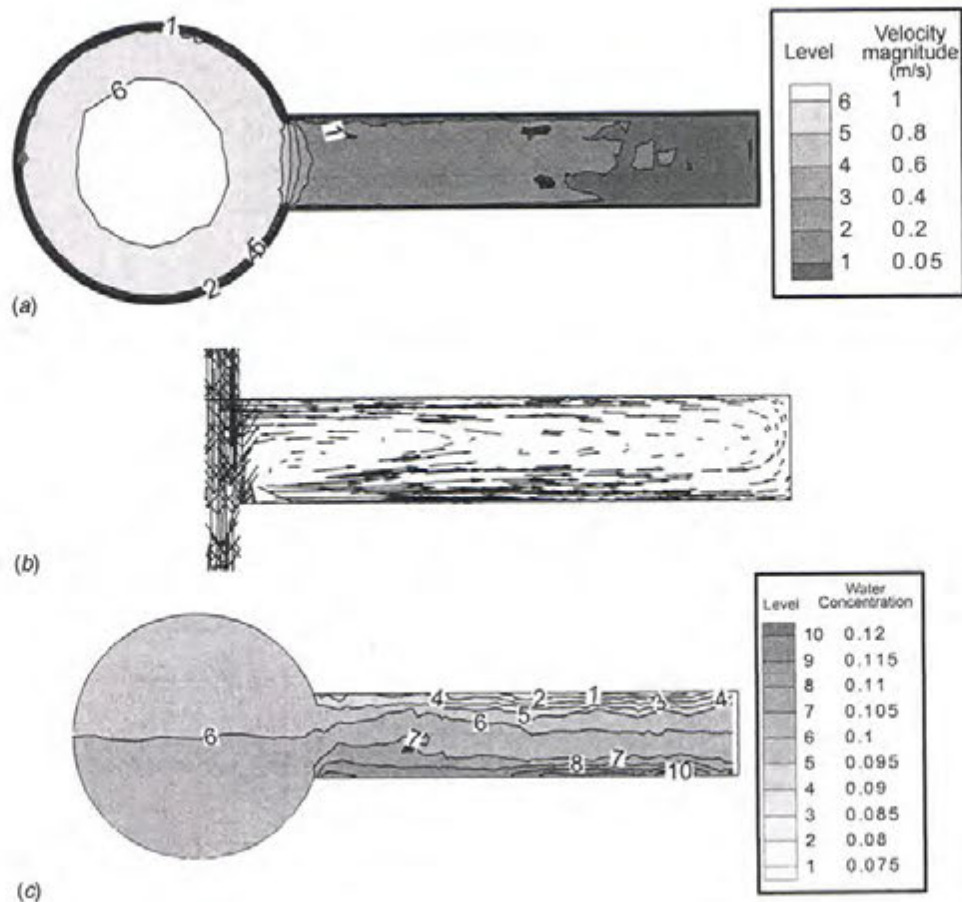


Fig. 9 Velocity contours, velocity vectors, and contours of the volumetric concentration of water for the horizontal deadleg; $L/D=5$. (a) Velocity contours, (b) velocity vectors, and (c) Water concentration.

fluid is stagnant only at the deadleg walls (the no-slip condition) while a circulating vortical motion occupies the entire deadleg region similar to that presented in Fig. 3(a). The outer and inner regions of the deadleg have higher velocity (≈ 0.2 m/s) with the lowest velocity in the central part (≈ 0.05 m/s). The velocity vectors for the same case are shown in Fig. 7(b). It is shown that the entire region is occupied by a recirculating flow region and confirms the contours of the velocity vectors in Fig. 7(a). Figure 8(a) shows the contours of velocity magnitude for the case of $L/D=3$. The velocity in the deadleg ranges from 0.01 m/s in the central region to about 0.05 m/s in the inner region (close to the header) with the stagnant fluid zones limited to the deadleg walls. The velocity vectors are shown in Fig. 8(b) and indicate circulating vortical flow with the vortex center at the pipe center line. As the length-to-diameter ratio increases to $L/D=5$, the circulating flow zone is found to occupy about 65%–80% of the deadleg length (about 3.2 D) leaving the remaining 20%–35% as stagnant fluid as shown in Fig. 9(a). As L/D increases further to $L/D=7$ and $L/D=9$, the length of the stagnant fluid zone increases as shown in Figs. 10(a) and 11(a). The figures show a stagnant fluid zone of length 3–3.5 D in the case of $L/D=7$ and of length 4–5 D in the case of $L/D=9$. Based on the obtained results, it is quite clear that there is no stagnant fluid zone in all cases of this orientation (horizontal deadleg configuration) so long as $L/D < 5$. For the cases of $L/D > 5$, it is also clear that the region of the deadleg close to the header is characterized by circulating vortical motions for a length $L = 3-5$ D while the remaining part of the deadleg occupied by stagnant fluid.

To show the effect of deadleg orientation on the water concentration fields, we now compare the water concentration contours

for a vertical deadleg presented in Figs. 3–6 with those of a horizontal deadleg presented in Figs. 7–11. For a horizontal deadleg of $L/D=1$, the water concentration varies from 9% in the upper region to 11% in the lower region as shown in Fig. 7(c). Although the range is very much the same as in the case of a vertical deadleg having the same geometry, the distribution is quite different [see Fig. 3(c) for comparison] due to the change of direction of gravity forces. In the horizontal deadleg case, the water concentration increases from top to bottom with an approximate symmetry about a vertical axis due to the circulating vortical fluid motion. As L/D increases to 3, the range of water concentration in the horizontal deadleg becomes slightly wider (from 8.2% to 11.6%) with a low concentration at the top and a high concentration at the bottom as can be seen in Fig. 8(c). For the cases of $L/D=5, 7$, and 9, the water concentration contours follow the same pattern as that of $L/D=3$, however with a wider range as L/D increases as shown in Table 1. The water concentration varies in the range 6.5% to 12.9% in the case of $L/D=5$ and becomes 4.7% to 16% in the case of $L/D=7$ and finally attains the range 4.2% to 17.7% in the extreme case of $L/D=9$.

4 Flow Visualization Procedure and Results

4.1 Experimental Setup. The experimental setup which is composed of two main parts, namely, the flow loop and the test section, is designed and constructed to carry out the flow visualization experiments. Descriptions of the two parts are given in the following subsections.

4.2 Flow Loop. The flow loop, which is a closed-type loop,

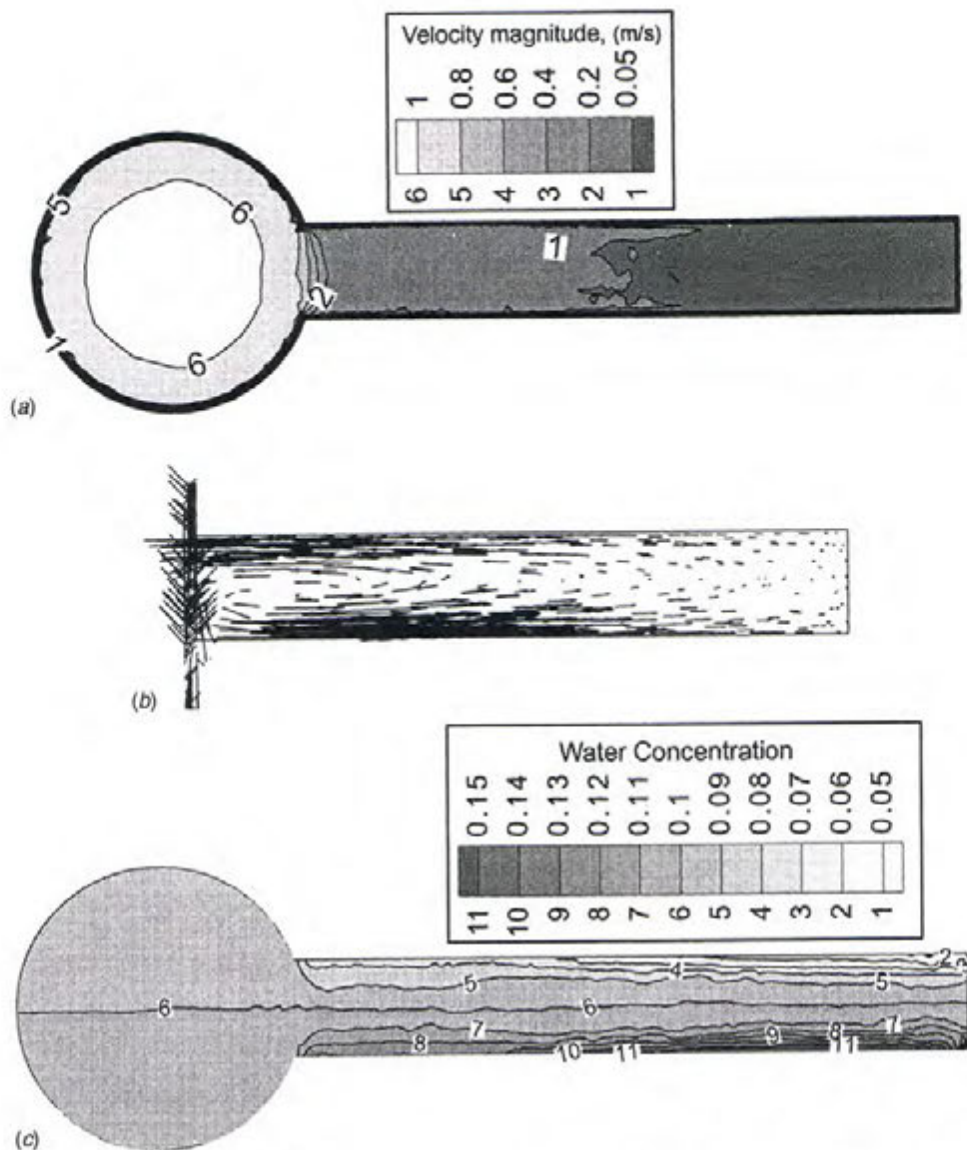


Fig. 10 Velocity contours, velocity vectors, and contours of the volumetric concentration of water for the horizontal deadleg; $L/D=7$. (a) Velocity contours, (b) velocity vectors, and (c) water concentration.

consists of a pump, a piping system, and two reservoirs. The lower reservoir has a total volume of 1 m^3 . The upper reservoir is used as a settling chamber that is utilized to minimize the lateral flow fluctuations and unsteady flow oscillations in order to provide a steady uniform flow at the inlet of the header tube. The pump is a centrifugal-type water pump that has a rated power of 5 hp. The piping system is made of 2-in. PVC pipes and is equipped with three valves and a number of 90° bends. The two gate valves are used as pump suction and delivery valves and the ball valve is installed downstream of the deadleg. Water is pumped from the lower reservoir to the settling chamber and back to the lower reservoir through the test section. The pump delivery valve together with the ball valve (installed downstream of the test section) are used to control the volume flow rate in the test section.

4.3 Test Section. The test section that simulates the flow process in the deadleg region is designed to provide flexibility for the variation of the deadleg length. The detailed design drawings of the test section including construction details are shown in Fig. 12. The test section consists of an inlet section, an outlet section, and the deadleg region. The deadleg region contains a piston that

can be moved in or out to provide a mechanism for varying the deadleg length. All the components of the test section are made out of plexiglas. It should be noted that the deadleg region is the main region of interest in this study. The deadleg geometry can be changed by installing the piston at the end of the header tube or the branch tube.

4.4 Instrumentation. The flow visualization experiments were performed utilizing a two-dimensional laser light sheet to illuminate the middle section (plane of symmetry) of the deadleg region. The flow visualization was accomplished by utilizing a 200 mW argon laser source. The laser beam was forced to pass through a vertical cylindrical glass rod of 8 mm diameter to produce a two-dimensional laser-light sheet. The horizontal laser sheet was diverted to the vertical plane using a 45° mirror. The laser sheet was aligned to pass through the plane of symmetry of the tube and deadleg region. The seeding particles used in the flow visualization experiments were small wooden particles that are almost of neutral buoyancy. The particle trajectory traces were photographed using a high-speed digital camera.

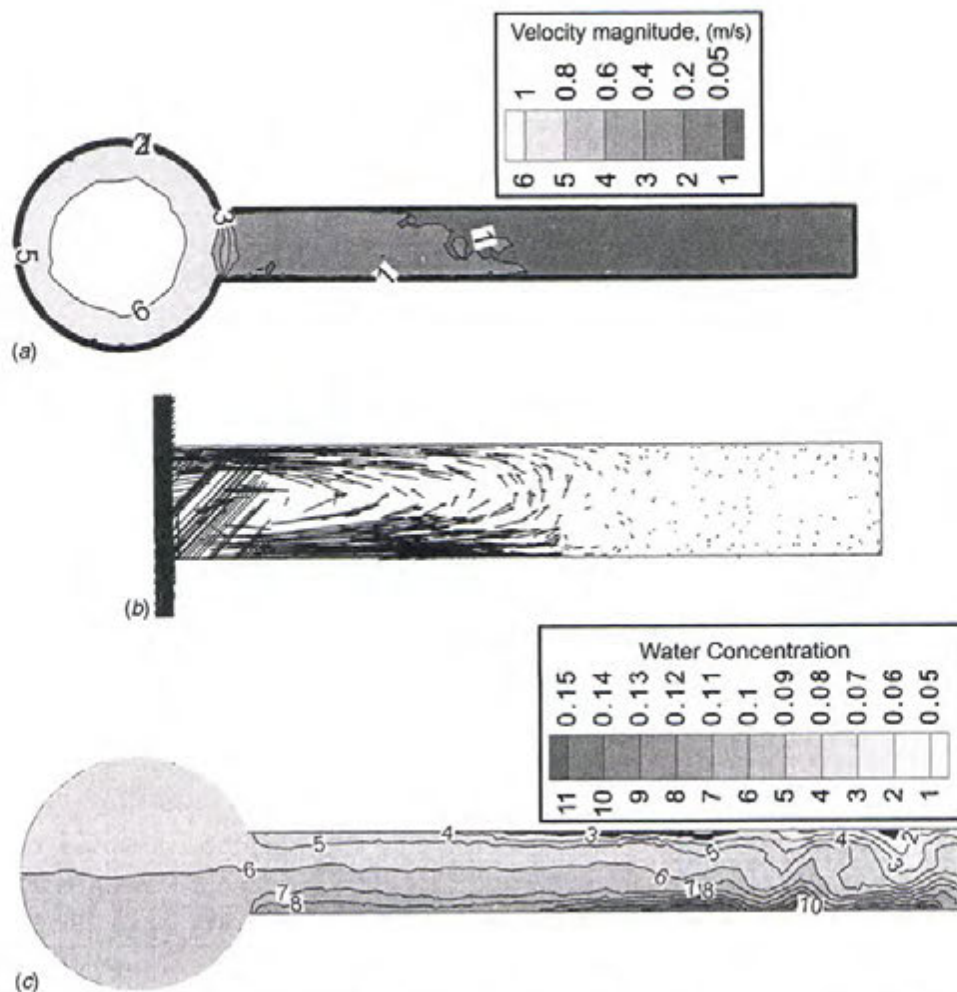


Fig. 11 Velocity contours, velocity vectors, and contours of the volumetric concentration of water for the horizontal deadleg; $L/D=9$. (a) Velocity contours, (b) velocity vectors, and (c) water concentration.

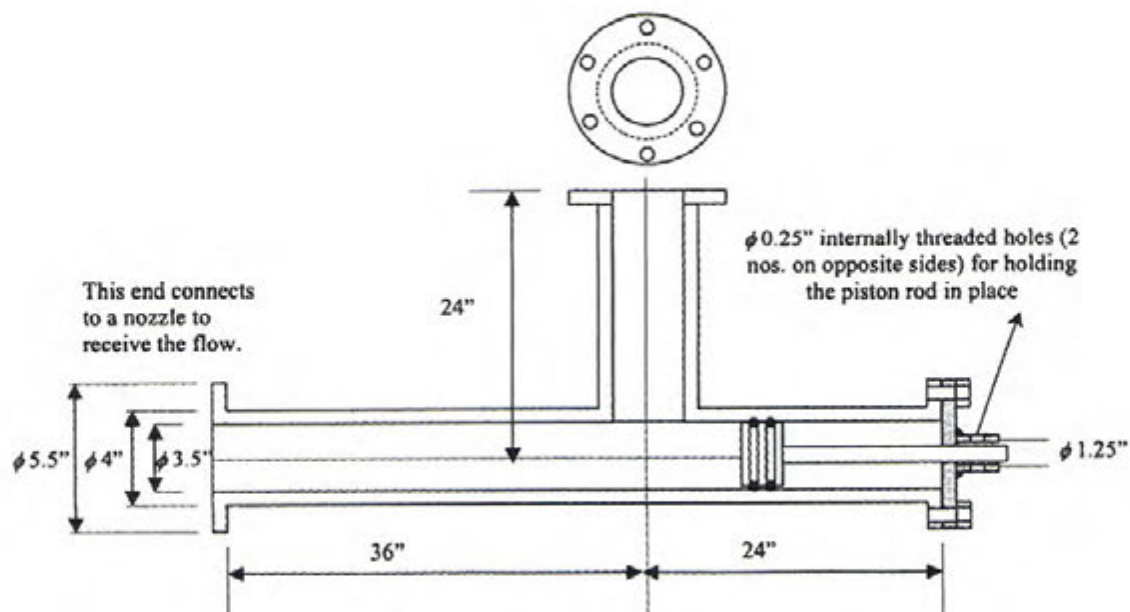


Fig. 12 Detailed construction of the test section

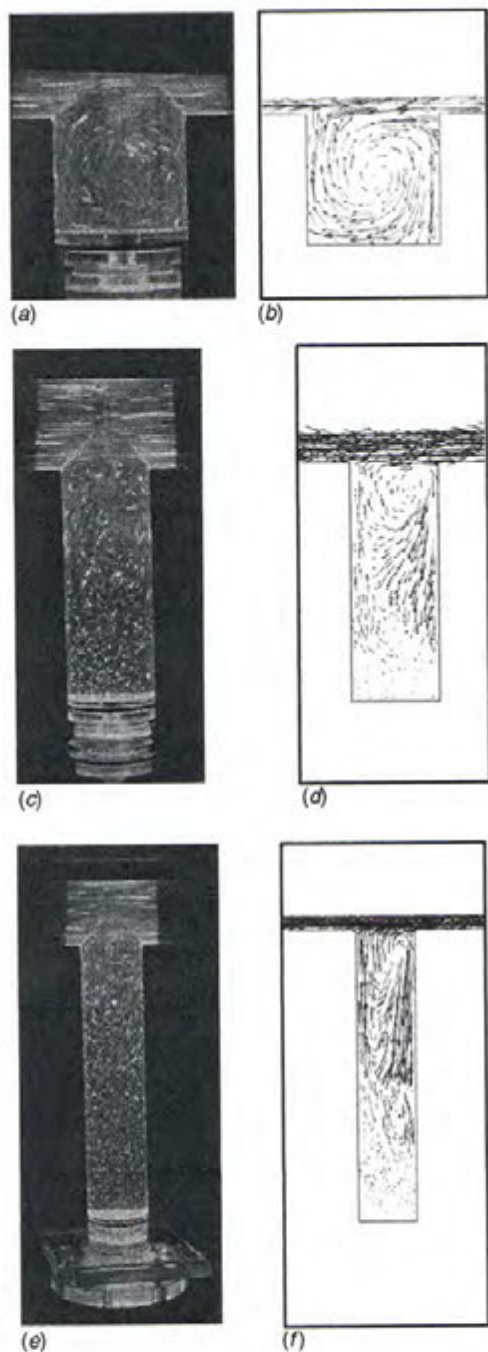


Fig. 13 Calculated and measured velocity vectors inside the deadleg. (a) Flow visualization results $L/D=1$, (b) calculated results $L/D=1$, (c) flow visualization results $L/D=3$, (d) calculated results $L/D=3$, (e) flow visualization results $L/D=5$, and (f) Calculated results $L/D=5$.

4.5 Flow Visualization Results. The details of the flow velocity field were visualized and photographed for the vertical deadleg geometry with different deadleg lengths (L/D equal to 1, 3, and 5) and are shown in Fig. 13. The case considered is that of a vertical deadleg with equal header and branch diameters of $D = 0.0889$ m. The details of the flow field for the case of $L/D=1$ are shown in Fig. 13(a). The computed velocity vectors for the same case are shown in Fig. 13(b). A very similar trend of flow pattern is observed between the flow visualization and calculated results. Figure 13(c) shows the velocity field for the case of $L/D=3$. It is clear from the figure that the circulating flow zone

extends over most of the entire length of the deadleg, however, with low velocity in the lower portion. This is in good agreement with the computed velocity vectors for the same case as shown in Fig. 13(d). The velocity flow field for $L/D=5$ is shown in Figs. 13(e) and 13(f) for the computed and visualized velocity vectors and very similar flow patterns are observed in both figures. The good comparison between the computed and visualized flow patterns provide another verification of the accuracy of the computational model.

5 Conclusions

The effect of deadleg geometry and orientation on oil/water separation is investigated. The investigation is based on the solution of the mass and momentum conservation equations of an oil/water mixture together with the volume fraction equation for the secondary phase. Results are obtained for two main deadleg orientations and for length-to-diameter ratios ranging from 1 to 9 in each orientation. The considered fluid mixture contains 90% oil and 10% water (by volume) and the inlet flow velocity is kept constant (1 m/s). The results show that the size of the stagnant fluid region increases with the increase of L/D . For the case of a vertical deadleg, it is found that the region of the deadleg close to the header is characterized by circulating vortical motions for a length $l \approx 3D$ while the remaining part of the deadleg occupied by a stagnant fluid. The results also indicated that the water volumetric concentration increases with the increase of L/D and influenced by the deadleg orientation. Maximum value of the water concentration increases from 10.4% in the case of $L/D=1$ to more than 80% in the case of $L/D=7$ for the vertical deadleg orientation. In the case of a horizontal deadleg, the region of circulating flow extends to 3–5 D and the maximum concentration increases from 11% in the case of $L/D=1$ to 17.7% in the case $L/D=9$. The flow visualization experiments for the case of the vertical deadleg were carried out using a laser sheet. The visualized flow patterns provide an important verification of the accuracy of the calculated velocity field and also validate the present calculation procedure.

Acknowledgments

The authors wish to acknowledge the support received from King Fahd University of Petroleum & Minerals and Saudi Aramco during the course of this study.

Nomenclature

- C = inlet concentration of water liquid
- D = diameter of the deadleg (branch tube)
- D_H = diameter of the header (main tube)
- d = droplet diameter
- L = Length of the deadleg
- V = Inlet mixture velocity
- C_μ = constant defined in Eq. (4)
- C_1 = constant defined in Eq. (16)
- C_2 = constant defined in Eq. (16)
- \tilde{G}_k = generation of turbulent kinetic energy
- g = gravitational acceleration
- h = representative grid size, ($h = \text{cell_volume}^{1/3}$)
- k = turbulent kinetic energy
- N = number of control volumes
- p = pressure
- Re = Reynolds number
- \bar{U}_j = mass-average velocity component
- u_j = fluctuating velocity component
- x_j = space coordinate
- y = vertical distance, measured from the header tube center

Greek letters

- α = volume fraction
- ϵ = dissipation rate of turbulent kinetic energy

μ = dynamic viscosity
 ρ = density
 σ_k = effective Prandtl number for k
 σ_ε = effective Prandtl number for ε

Superscripts

— = time average

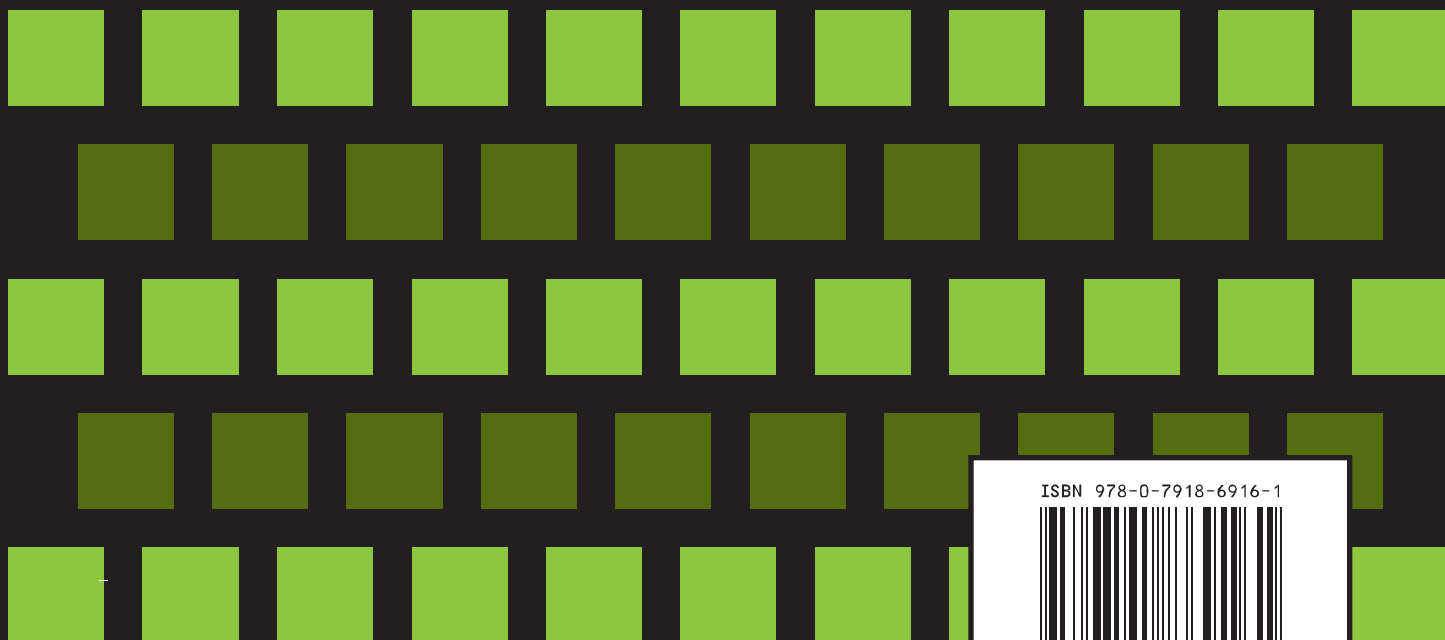
Subscripts

D = drift
 d = droplet
 eff = effective
 k = species
 l = laminar
 p = primary flow
 max = maximum
 min = minimum
 m = mixture
 s = secondary flow
 t = turbulent

References

- [1] Craig, B. C., 1996, "Corrosion in Oil/Water Systems," Mater. Selection Design, Aug.
- [2] Lotz, U., Van Bodegom, L., and Ouweland, C., 1990, "Effect of Type of Oil or Gas Condensate on Carbon Acid Corrosion," *Corrosion/90*, Paper no. 41, NACE, Houston TX.
- [3] Ricca, P. M., 1991a, "Ultrasonic Inspection Prompts Chemical Inhibitor Program," *Oil & Gas Journal*, **22**, pp. 73–82.
- [4] Ricca, P. M., 1991b, "Control of Deadleg Corrosion in a Crude Oil Pipeline," PD-Vol. 34, *Pipeline Engineering*, ASME, pp. 34–39.
- [5] Charles, M. E., Govier, G. W., and Hodgson, G. W., 1961, "The Horizontal Pipeline Flow of Equal Density Oil-Water Mixture," *Can. J. Chem. Eng.*, **39**(1), pp. 27–36.
- [6] Charles, M. E., and Lilleleht, L. U., 1966, "Correlations of Pressure Gradients for the Stratified Laminar-Turbulent Pipeline Flow of Two Immiscible Liquids," *Can. J. Chem. Eng.*, **44**(1), pp. 47–49.
- [7] Lockhart, R. W., and Martinelli, R. C., 1949, *Chem. Eng. Prog.*, **45**, pp. 39–48.
- [8] Barnea, D., 1986, "Transition From Annular Flow and From Dispersed Bubble Flow—Unified Models for the Whole Range of Pipe Inclinations," *Int. J. Multiphase Flow*, **12**, 5, pp. 733–744.
- [9] Brauner, N., and Maron, D. M., 1992, "Stability Analysis of Stratified Liquid-Liquid Flow," *Int. J. Multiphase Flow*, **18**, 1, pp. 103–121.
- [10] Schmidt, H., and Loth, R., 1994, "Predictive Methods for Two-Phase Flow Pressure Loss in Tee Junctions With Combining Ducts," *Int. J. Multiphase Flow*, **20**, 4, pp. 703–720.
- [11] Plaxton, B. L., 1995, "Pipeflow Experiments for Analysis of Pressure Drop in Horizontal Wells," *SPE Annual Technical Conference and Exhibition*, October 22–25, Dallas, TX, SPE Int. L. Stdnt. Pap. Cntst., pp. 635–650.
- [12] Brill, J., and Beggs, H., 1994, *Two-Phase Flow in Pipes*, University of Tulsa Press, Tulsa, OK.
- [13] Asheim, H., Kolnes, J., and Oudeman, P., 1992, "A Flow Resistance Correlation for Completed Wellbore," *J. Pet. Sci. Eng.*, **8**, 2, pp. 97–104.
- [14] Angeli, P., and Hewitt, G. F., 1996, "Pressure Gradient Phenomena During Horizontal Oil-Water Flow," 1996 OMAE—*Pipeline Technology*, Vol. V, ASME, pp. 287–295.
- [15] Hwang, C. J., and Pal, R., 1997, "Flow of Two-Phase Oil/Water Mixtures Through Sudden Expansions and Contractions," *Chem. Eng. J.*, **68**, pp. 157–163.
- [16] Schabacker, J., Boles, A., and Johnson, B. V., 1998, "PIV Investigation of the Flow Characteristics in an Internal Coolant Passage With Two Ducts Connected by a Sharp 180° Bend," ASME Paper No. 98-GT-544, Fairfield, NJ.
- [17] Hafskjold, B., Celius, H. K., and Aamo, O. M., 1999, "A New Mathematical Model for Oil/Water Separation in Pipes and Tanks," *SPE Prod. Facil.*, **14**, 1, pp. 30–36.
- [18] Fluent, 1988, *CD-Rom Fluent 5, User's Guide*, section 14.2.
- [19] Wilson, W., 1999, "The Development of a Droplet Formation and Entrainment Model for Simulations of Immiscible Liquid-Liquid Flows," MS thesis, West Virginia University.
- [20] Celik, I. B., Badeau, A. E., Burt, A., and Kandil, S., 2001, "A Single Fluid Transport Model for Computation of Stratified Immiscible Liquid-Liquid Flows," *Proceedings of the XXIX IAHR Congress*, Sep., Beijing, China, pp. 1–18.
- [21] Dluska, E., Wronski, S., and Rudnaik, L., 2001, "Two-Phase Gas-Liquid Couette-Taylor Eccentric Reactor. Computational Calculation of Reactor Hydrodynamics," *Proceedings of the 2nd International Conference on Computational Heat and Mass Transfer COPPE/UFRRJ*, Federal University of Rio de Janeiro, Brazil, Oct. 22–26.
- [22] Vigil, R. D., and Zhu, X., 2001, "Banded Liquid-Liquid Taylor-Couette-Posuille Flow," *AIChE J.*, **47**(9), pp. 1932–1940.
- [23] Manninen, M., Taivassalo V., and Kallio, S., 1996, *On the Mixture Model for Multiphase Flow*, Technical Research Center of Finland, VTT Publication No. 288.
- [24] Maron, D. M., 1992, "Flow Pattern Transitions in Two-Phase Liq-Liq Flow in Horizontal Tubes," *Int. J. Multiphase Flow*, **18**, 1, pp. 123–140.
- [25] Versteeg, H. K., and Malalasekera, W., 1995, *An Introduction to Computational Fluid Dynamics: The Finite Volume Method*, Longman Scientific and Technical, Essex, England.
- [26] Reynolds, W. C., 1987, "Fundamentals of Turbulence for Turbulence Modeling and Simulation," Lecture Notes for Von Karman Institute, Agard Report No. 755, pp. 1–11.
- [27] Shih, T. H., Liou, W. W., Shabbir, A., and Zhu, J., 1995, "A New $k-\varepsilon$ Eddy-Viscosity Model for High Reynolds Number Turbulent Flows—Model Development and Validation," *Comput. Fluids*, **24**, 3, pp. 227–238.
- [28] Launder, B. E., and Spalding, D. B., 1974, "The Numerical Computation of Turbulent Flows," *Comput. Methods Appl. Mech. Eng.*, **3**, pp. 269–289.
- [29] Habib, M. A., Attya, A. M., and McEligot, D. M., 1989, "Calculation of Turbulent Flow and Heat Transfer in Channels With Streamwise Periodic Flow," *ASME J. Turbomach.*, **110**, pp. 405–411.
- [30] Patankar, S. V., 1980, *Numerical Heat Transfer and Fluid Flow*, Hemisphere Publishing Corporation, New York.
- [31] Chiang, T. P., Sheu, W. H., and Hwang, R. R., 1998, "Effect of Reynolds Number on the Eddy Structure in a Lid-Driven Cavity," *Int. J. Numer. Methods Fluids*, **26**, pp. 557–579.

STP-PT-065



ISBN 978-0-7918-6916-1



9 780791 869161



A2521Q